Dissertation zur Erlangung des Doktorgrades

der Fakultät für Chemie und Pharmazie

der Ludwig-Maximilians-Universität München

Investigation of Organic Peroxides and their Properties as Energetic Materials

Benedikt Wolfgang Werner Stiasny

aus

Fürth

2016

Erklärung:

Diese Dissertation wurde im Sinne von § 7 der Promotionsordnung vom 28. November 2011 von Herrn Prof. Dr. Thomas M. Klapötke betreut.

Eidesstattliche Versicherung:

Diese Dissertation wurde eigenständig und ohne unerlaubte Hilfe erarbeitet.

München, ……. ….. …….

Benedikt Stiasny

Dissertation eingereicht am:	8.11.2016
1. Gutachter:	Prof. Dr. Thomas M. Klapötke
2. Gutachter:	Prof. Dr. Konstantin Karaghiosoff
Mündliche Prüfung am:	16.12.2016

Danksagung

Mein erster Dank gilt meinem Doktorvater Prof. Dr. Thomas M. Klapötke dafür, dass er mir nach dem Masterabschluss die Möglichkeit gab in seiner Arbeitsgruppe auch die Dissertation anzufertigen. Des Weiteren möchte ich ihm dafür danken, dass er mir die allermeiste Zeit durch einen Hilfskraftvertrag auch eine gewisse finanzielle Unterstützung zukommen ließ. Der größte Dank gebührt ihm dafür, dass er meine Arbeitszeiten geduldet hat.

An zweiter Stelle muss ich Herrn Prof. Dr. Konstantin Karaghiosoff danken, dass er freundlicherweise das Zweitgutachten dieser Arbeit übernommen hat. Außerdem für seine freundliche Art und seinen guten Kern.

Ferner möchte ich den weiteren Mitgliedern der Prüfungskomission Prof. Dr. Manfred Heuschmann, Prof. Dr. Ingo-Peter Lorenz, Prof. Dr. Wolfgang Beck und Prof. Dr. Jürgen Evers danken, dass sie sich die Zeit genommen haben als Prüfer zu fungieren.

Darüber hinaus möchte ich Herrn Dr. Jörg Stierstorfer danken, dass er stets ein offenes Ohr für meine Probleme und Nöte hatte. Außerdem für das Lösen der Kristallstrukturen und die auch ansonsten meiner Meinung nach hervorragende Zusammenarbeit im Publikationsprozess.

Herrn Dr. Burkhard Krumm danke ich für die Duldung meiner Arbeitszeiten. Außerdem möchte ich ihm und seinem Nachfolger im ACI Praktikum Dr. Stierstofer dafür danken, dass sie mich durch die dreimalige Vergabe der Mixerstelle finanziell unterstützt haben.

Frau Irene Scheckenbach gilt mein besonderer Dank dafür, dass sie mich bei bürokratischen Hürden vor allem im Zusammenhang mit den Hilfskraftverträgen unterstützt hat.

Herrn Prof. Dr. Charles H. Winter und Frau Dr. Nipuni-Dhanesha Gamage danke ich für die sehr erfolgreiche, angenehme und schöne Kooperation im Rahmen einiger gemeinsamer Publikationen.

Herrn Dr. Dennis Fischer danke ich dafür, dass er vor allem in den frühen Morgenstunden ein treuer Kamerad war und wir nicht nur über Chemie, sondern auch über diverse andere naturwissenschaftliche Phänomene und die Gesellschaftsordnung sowie das Leben an sich diskutieren konnten. Auch auf diesem Wege möchte ich ihm viel Glück für seine Zukunft wünschen.

Herrn Thomasz Witkowski möchte ich ebenfalls für eine Vielzahl von Hilfestellungen danken. Vor allem sein theoretisches Wissen über Explosivstoffe, das Berechnen der Leistungsdaten und Computersoftware haben mir stets weitergeholfen. Außerdem gilt ihm herzlichster Dank dafür, dass er sich trotz des immensen Arbeitspensums, das er sich auferlegt die Zeit genommen hat, Teile dieser Arbeit zu korrigieren. Ich würde mir wünschen, dass sein Arbeitseifer von wirklich allen Leuten am Lehrstuhl geschätzt wird und ihm mit dem Respekt entgegengetreten wird, den er verdient. Es war mir mehr als eine Ehre mit ihm zusammen promovieren zu dürfen.

Unserer Putzfrau Katharina möchte ich für viele schöne Gespräche in der Früh und auch für ihren Fleiß und ihre Aufopferung danken. Wenn alle Deutschen so wären wie sie als Kroatin, dann würde unser Land einer goldenen Zukunft entgegengehen. Außerdem gilt ihr mein Dank für die Tatsache, dass Sie stets loyal war und ich freue mich darüber, dass wir in vielerlei Hinsicht das gleiche Weltbild haben. Ich hoffe sie kann ihren Ruhestand nun genießen.

Herrn Stefan Huber danke ich für das gemeinsame bestimmen der Sensitivitäten und das Bestellen von Chemikalien. Mehr jedoch muss ich ihm aber für die vielen Gespräche, meist lustiger aber teils auch ernster sowie wissenschaftlicher Natur danken, die wir miteinander führen durften. Ich wünsche mir, er bleibt auch in Zukunft wie er ist und damit ein wichtiger Bestandteil der guten Stimmung im Arbeitskreis. Außerdem wünsche ich ihm für die Zukunft, dass auch er Englisch lernt.

Ansonsten bleibt mir noch mich bei allen (und zwar ausnahmslos allen) jetzigen und ehemaligen Mitarbeitern der Arbeitsgruppen Klapötke und Karaghiosoff zu bedanken. In meiner ganzen Zeit hier habe ich nicht eine Person kennengelernt, mit der ich persönlich nicht zurechtkam und die mir nicht hilfsbereit entgegengetreten ist. Ich hoffe ich konnte all denjenigen, die mir geholfen haben auch etwas zurückgeben und, dass sie mich in eben so guter Erinnerung behalten werden, wie ich mich erinnern werde.

Table of contents

1 Preliminary goals of this thesis

During the last centuries, the interest in new energetic materials varied. The first investigations were made in search for better performing substances, then reduced sensitivity was a concern that had to be taken into account. High performing and acceptably sensitive substances have been found in molecules that are still applied today. However, environmental concerns have risen and research for new, more environmentally benign substances is currently under way, focusing primarily on the synthesis of heterocyclic compounds. In times were research for energetic materials was still pretty basic, acetone peroxide was discovered by chance. In 1895 its inventor, Richard Wolffenstein, wanted to oxidize Coniin with hydrogen peroxide and used acetone as solvent. Although the synthesis is easy and it was discovered in the same period as other energetic materials (e. g. trinitrotoluene (TNT), pentaerythritol tetranitrate (PETN) and hexogen (RDX)), acetone peroxide was not applied due to its high sensitivity and more important high volatility resulting in an unpredictable behavior. Another explosive peroxide that was discovered in the same time by German chemist Ludwig Leger is hexamethylene triperoxide diamine (HMTD). But beside the two mentioned compounds and methyl ethyl ketone peroxide, the substance class of organic peroxides, was only relatively poorly investigated during the last century with respect to new energetic molecules. Even less effort was put into a detailed investigation of the energetic properties like impact-, friction-, ESD-sensitivity and thermal stability as well as performance values, for example detonation velocity and detonation pressure.

This thesis was started with the intention of synthesizing a number of energetic organic peroxides form different subclasses, to investigate them with respect to their energetic behavior and to compare them among each other and with already investigated molecules in order to gain a deeper knowledge about the different peroxide subclasses with respect to sensitivity, thermal stability, ease of preparation and differences in performance. Moreover investigations were performed whether the sensitivity of peroxides can significantly be varied by different substituents. A further question studied in this thesis is if peroxides can find practical application as energetic materials. The subclasses of the organic peroxides investigated with respect to their synthesis, sensitivities towards impact, friction and electrostatic discharge, heat resistance and performance properties within this thesis are displayed in figure 1.

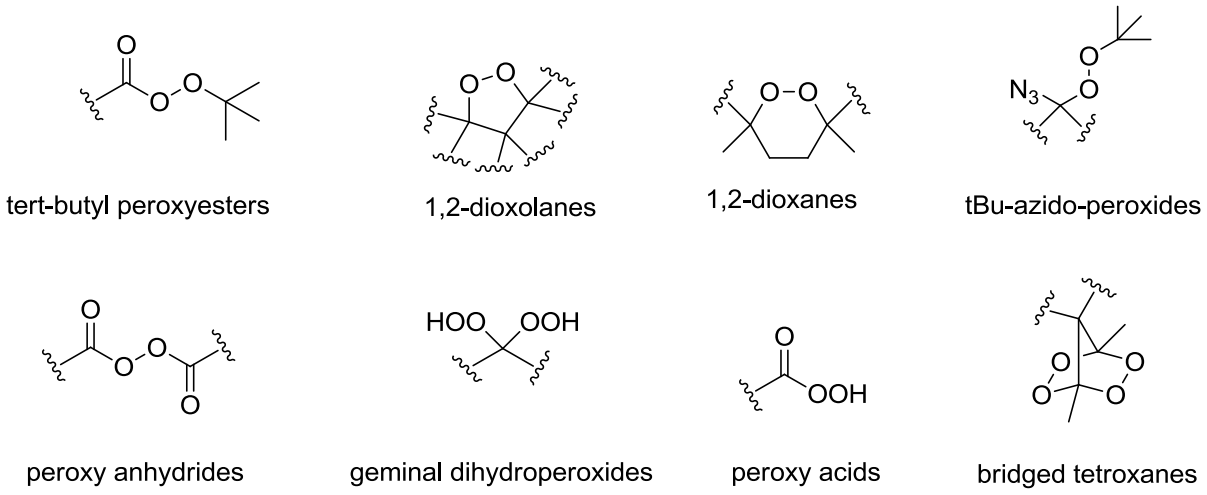

Figure 1: Subclasses of the investigated organic peroxides.

2 Preface about energetic materials

2.1 General classification

The ASTM (American Society of Testing and Materials) definition defines an energetic material as a substance or a mixture of substances which contains the oxidizer and the fuel at the same time and is therefore capable to react readily under the liberation of large amounts of heat and gaseous reaction products without any external reaction partner [1]. However, this definition neglects some compounds and formulations which definitely have energetic properties. For example, pyrotechnical formulations used for delayed ignition in hand grenades do designedly not form gaseous reaction products in order to prevent unwanted pressure increase. An example for those formulations is a mixture of the two fuels Boron and Silicon, combined with potassium dichromate as oxidizer [2]. Moreover nitrogen only compounds, although not synthesized until now, would definitely be potential explosives with extreme power since the very stable N≡N- triple bond would be formed multiple times with gaseous dinitrogen being the reaction product after detonation, but they carry neither fuel nor oxidizing groups in them [3].

In general energetic materials can be divided into the following different subclasses: Propellants (which react slowest among all energetic materials), Pyrotechnics (who´s reaction kinetics is in between) and Explosives (who react fastest among all energetic materials). Explosives can to be further divided into low explosives (normally subsonic propagation of reaction front, particle to particle propagation) and high explosives (normally supersonic propagation of reaction front, propagation by a shock wave). The resulting main difference between those two is the performance [4]. High explosives can again be divided into primary explosives and secondary explosives [2].

Primary explosives show a rapid deflagration to detonation transition and most often can easily be set off by outer stimuli like heat, impact, friction and electric sparks. A qualitative rule states, that every compound, that is more sensitive than pentaerithrytole tetranitrate (PETN) has to be classified as a primary explosive (border values: impact sensitivity 3 J, friction sensitivity 60 N [5]). In contrast to their high sensitivity, their performance values (energy release per time) are relatively low. They are therefore exclusively used for the initiation of a secondary main charge. Most of the primary explosives of the past and also the ones in application today are using heavy metals, mainly lead, copper and mercury. The heavy metal is beneficial for the desired high sensitivity. Until of today´s knowledge, this cannot fully be explained. A qualitative trend states, that it is connected to the covalence of the metal-anion bond and the ionization potential of the metal cation [6]. Figure 2 shows the structures of lead styphnate, lead azide and mercury fulminate, the most commonly used primary explosives of the past and today. Among them, mercury fulminate sees decreasing application nowadays, but was one of the first primaries ever applied. Lead azide is mainly used as initiation charge for a secondary high explosive whereas lead styphnate is still the most commonly used primer in ammunition to ignite the propellant.

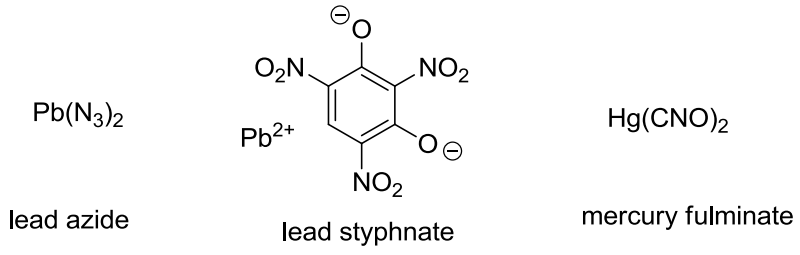

Figure 2: Structural formulas of lead azide, lead styphnate and mercury fulminate.

However, strong research interests are under way to synthesize new, more environmentally benign primary explosives, which feature either no metals or mainly not harmful alkaline metals. Two substances are diazo-dinitro-phenol (DDNP) [7], which is actually known since the middle of the 19th century [8] and Potassium 1,1′-Dinitramino-5,5′-bistetrazolate K_2DNABT [9] which was developed recently. Figure 3 displays the structures of those compounds.

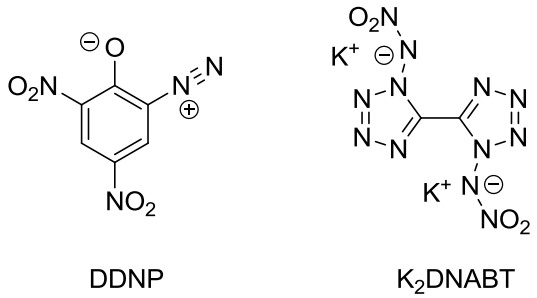

Figure 3: Structural formulas of DDNP and K_2DNABT.

Secondary explosives are in contrast to primary explosives characterized by lower sensitivities, but their performance values exceed those of primary explosives [2]. Secondary explosives are used for many kinds of applications ranging from mining over construction works to the application in bombs and grenades. With respect to the many explosives with potential application, the number of explosives which are actually used is comparably low. Nowadays in the civil sector, these are still mostly explosives basing on ammonium nitrate. In the military sector compounds like ammonal have been replaced by TNT and the more potent RDX and HMX are both still the standard. However for more specialized applications they are sometimes replaced by PETN. PETN is also the most often applied secondary explosive in detonators [2]. It has to be mentioned, that all of this compounds are dangerous for the environment. This is the reason why research for new, more environmentally benign explosives is currently under way. Today, the general trend is to incorporate nitrogen rich heterocycles, because during detonation, the unusually stable N≡N- triple bond is formed. Salt formation with nitrogen rich cations is an established way of reducing the sensitivity and increasing the thermal stability. Figure 4 shows the molecular structures of the molecules mentioned above.

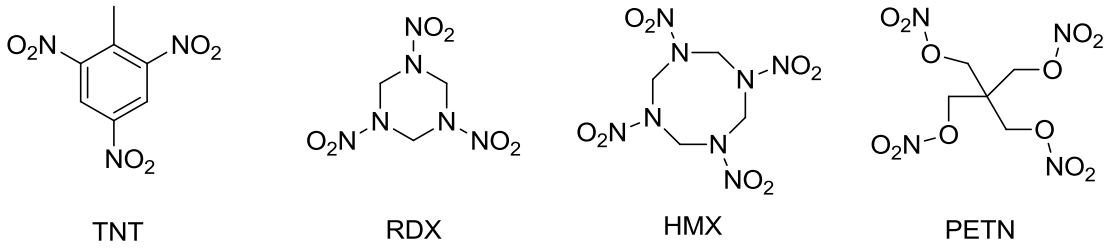

Figure 4: Structural formulas of TNT, RDX, HMX and PETN.

Propellants can be divided into gun propellants and rocket propellants. The gun propellant with the widest application diversity today is still Nitrocellulose. Normally it is not used as neat compound but in mixtures, for example in cordite, which consist of nitrocellulose, nitroglycerine and Vaseline [10] and was already in use in WW I, or the modern IMR-series [11]. An additional, but today outdated, mixture is ballistite, which consist of camphor, nitroglycerine and collodion [12]. Rocket propellants are used in rocket motors and can be divided into solid and liquid propellants. Solid propellants can be divided into double based propellants and composite propellants. Composite propellants are in terms of application the more important subclass. They consist of a defined mixture of a fuel and an oxidizer, which are glued by a binder. Regardless of the long service time the today most commonly applied composite propellant mixture uses aluminum as fuel, hydroxyl terminated poly butadiene (HTPB) as binder and ammonium perchlorate as oxidizer. The perchlorate anion has almost the same size as the iodide ion and therefore competes with it in the thyroid gland which makes it toxic to animals and humans [13]. This is why strong research activities are under way to find a suitable replacement. Liquid propellants can be divided into monopropellants and bipropellants [2]. Suitable molecules for the use as monopropellants decompose readily and exothermically [14] on the surface of a catalyst under the liberation of gaseous reaction products. (Hypergolic) bipropellants in contrast consist of a strong reducing agent and a strong oxidizing agent, which react violently together under the libation of heat, gases and commonly also under the evolvement of fire. Hypergolic mixtures in application use monomehtyl-hydrazine and red- or white-fuming nitric acid as the two components [2]. However, alternatives basing on highly concentrated hydrogen peroxide are desired today.

Pyrotechnic formulations are used in numerous fields ranging from colored flames to decoy flares and smoke compositions [2] for the visible and infrared range. The formulations for colored flames still use heavy metals like barium (green) and strontium (red) as colorants today and therefore have negative effects on the environment. Currently strong efforts are

made in research for more environmentally benign formulations, especially to replace barium in green and strontium in red burning formulations [15], [16]. Particularly for green colored pyrotechnics, some successes have already been achieved in the form of nitrogen rich boric acid esters [17], [18].

2.2 Possible ways for an energetic material to release its energy

In general, there are three main ways in which an energetic material can react and release its energy. The one with the least energy output per time is the simple combustion, the reaction of a fuel and an oxidizer under the formation of a flame. No shock wave is formed during this process. A more rapid process is the so called deflagration. Deflagrating materials react under the formation of a flame, which proceeds slower than sonic velocity, however, a considerable noise can be heard. Materials that deflagrate after ignition mainly consist of mixtures of fuel and oxidizers. During the reaction a considerable pressure is created. Pyrotechnical formulations and also some propellants are typical representatives. Under certain conditions, most important confinement, deflagrating compounds can undergo deflagration to detonation transition (DDT). This happens when a shock wave reaches sonic velocity and then propagates faster than sonic velocity into the zone with the unreacted explosive. Consequently a detonation is characterized by a shock wave which propagates self-preservative through the explosive material with a velocity higher than sonic velocity inside the corresponding material.

2.3 Properties of Energetic Materials

There are several properties and characteristics that are important for energetic materials. One of them is the oxygen balance. Basically, two different oxygen balances for CHNO explosives exist, depending on the assumed products formed after detonation. One oxygen balance is based on the formation of nitrogen, water and carbon dioxide, the other is valid for the formation of nitrogen, water and carbon monoxide. In the following the respective formulas

(1 and 2) for both oxygen balances for compounds with the general sum formula $C_aH_bN_cO_d$ are given.

$$\Omega_{CO_2} = \frac{\left[d - (2a) - \frac{b}{2}\right] \cdot 16.00 \frac{g}{mol} \cdot 100}{M} \quad (1) \qquad \Omega_{CO} = \frac{\left[d - a - \frac{b}{2}\right] \cdot 16.00 \frac{g}{mol} \cdot 100}{M} \quad (2)$$

Other characteristic figures that have to be taken into account are

- The heat of detonation Q [kJ kg^{-1}]
- The detonation velocity v_{det} [m s^{-1}]
- The detonation pressure p_{CJ} [GPa]
- The volume of gaseous products formed per kg of explosive [l kg^{-1}]
- The temperature of explosion [K]

Depending on the planned field of application, the emphasize on the different properties varies.

In this thesis the numerical values for those data have been calculated using the EXPLO5 thermochemical computer code. The two most important performance characteristics of an explosive are its detonation velocity and its detonation pressure. The detonation velocity can be calculated and determined experimentally. On the other hand it is not possible to determine the detonation pressure via an experiment directly. A qualitative way to recalculate the detonation pressure from the brisance (see below) exists (Kamlet Jacobs equation) [2], but normally it is determined with relatively complicated computer codes under Chapman-Jouguet conditions. Those conditions can be found in a thin surface between the free detonation products and the chemical reaction zone which itself is upstream off the shock front growing from the unreacted explosive material. Figure 5 gives a graphical overview for better visualization.

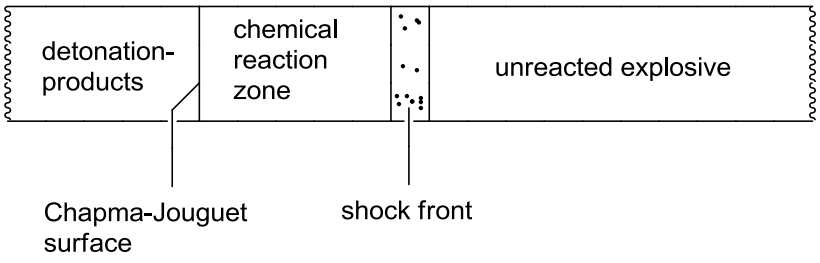

Figure 5: Graphical overview for the visualization of the different zones at a fixed point during a detonation.

Another feature of great importance is the brisance of the explosive. Qualitatively it is a measure for the shattering power of the energetic material. The brisance B [kg s^{-3}] can be calculated by a simple formula and is directly dependent on the density of the explosive ρ, the specific energy F and the detonation velocity v_{det}. Formula 3 displays the linear correlation between the parameters.

$$B = \rho \cdot F \cdot v_{det} \quad (3)$$

The specific energy F can be calculated from the ideal gas law by applying formula (4).

$$F = p_{ex} \cdot V = n \cdot R \cdot T \quad (4)$$

In this formula p_{ex} is the pressure of the detonation products, V the volume of gaseous reaction products, n the amount of substance of detonation products, R the ideal gas constant and T the temperature of explosion.

3 History of Energetic Materials

The first known example for an energetic material is black powder [2]. It consists of a mixture of charcoal, potassium nitrate and sulfur [19]. The combination of these three ingredients varied during time since its first accidental invention in China around 220 BC and also adapted to the specific applications. The first investigations which resulted in a deeper knowledge of the optimum mixture were performed by two monks [2]. The first one was Englishman Roger Bacon in 1249 followed by German Berthold Schwarz around seventy years later. However it lasted another seventy years until black powder was really used practically, first in the military sector [4]. But black powder is only a poorly performing mixture and if today´s standards are applied it has be classified as a low explosive [2]. Concerning gunpowder, black powder was the standard formulation in use for a couple of centuries. However it had some striking disadvantages. The most important one is the production of large amounts of smoke during combustion which leads to limited visibility on the battle field and makes it also impossible to cover the own position. With the primitive and

only low precision weapons and the military tactics of the time of its use it might have been of lower concern but nevertheless black powder produces large quantities of solid combustion products which settle in the mechanic of the bolt and can therefore lead to jams. It was the French army which first experimented with nitro based powders, namely nitrocellulose (poudre B, B in this case stands for *blanc*), and introduced them as their standard propulsion formulation [20], [21]. Nitrocellulose was invented in the middle of the 1840s like many other energetic materials by three independent scientists [22]. Because of its unbeaten properties Nitrocellulose is still today´s standard in ammunition. In the first decades after its invention the compound was also used as ingredient in film rolls. However it was replaced by other substances rather quickly because of its high flammability in an attempt to make cinemas safer. While Nitrocellulose replaced black powder as propellant charge, picric acid did so in the fields of explosives. Picric acid as a neat substance is a relatively harmless compound which can be handled safely. A great disadvantage is the comparably high acidity of the OH-proton, because it can react with metal containments and form much more sensitive metal picrates [2]. This is why research for different explosives went on. Italian chemist Ascanio Sobrero synthesized Nitroglycerin during experiments with nitrocellulose. Even Sobrero mentioned the extremely dangerous nature of Nitroglycerin from the beginning and suffered severe face injuries during his research. He therefore neglected, that his invention can be used commercially [23]. However the industrial revolution and the desire for coal, steel and railway tunnels kept the demand for explosives on an extremely high level. Therefore Alfred Nobel, who knew Sobrero personally, searched for a way to reduce the sensitivity of Nitroglycerin and found one by adsorbing it on the surface of diatomaceous earth [2]. His invention was named Dynamite and made him a rich man. After seeing the brutal results of actions his invention can also be used for in the many conflicts during this time, he decided to endow a price for the people, who have helped mankind the most in the previous year which is named after him- the Nobel price. Investigations for new and better explosives were performed and resulted in the development of molecules that are still in use today. 1880 2,4,6-Trinitrotoluene (TNT) was firstly synthesized [2]. The compound gained importance quickly until it made its way into grenades and mortar shells of all participating nations of World War 1. TNT has advantages over the materials used previously. It is indefinitely stable and melt-castable. Mostly because of this last property, it was not only used in T-ammonal in World War 1 but also in the more advanced T-ammonals of World War 2 and amatol, the explosive used in the V1-rocket [24]. However TNT lacks explosive performance and more investigations were undertaken for better performing compounds. One was found in Hexogen

(RDX) which was first synthesized in 1899 [25] and became a second standard secondary explosives, mainly as a intermixture to TNT, of all armies during the second world war and is still in use today. In the time of World War 2, two main processes were used by the different parties. The German Reich used the so called Bachmann-process, which delivered good yields for RDX. However the product of this process is always polluted by a varying amount of HMX (around 10%). The western allies applied the Brockman-process, which delivers pure RDX [2].

Good thermal stability is an important property for energetic materials, especially for those applied deep under the surface. In the second half of the 20th century hexanitrostilbene (HNS), triaminotrinitrobenzene (TATB) and 2,6-bis(picrylamino)-3,5-dinitro-pyridine (PYX) were investigated [2] and were found to be suitable for applications in high temperature environments. Figure 6 shows the structures of a selection of commonly used explosives.

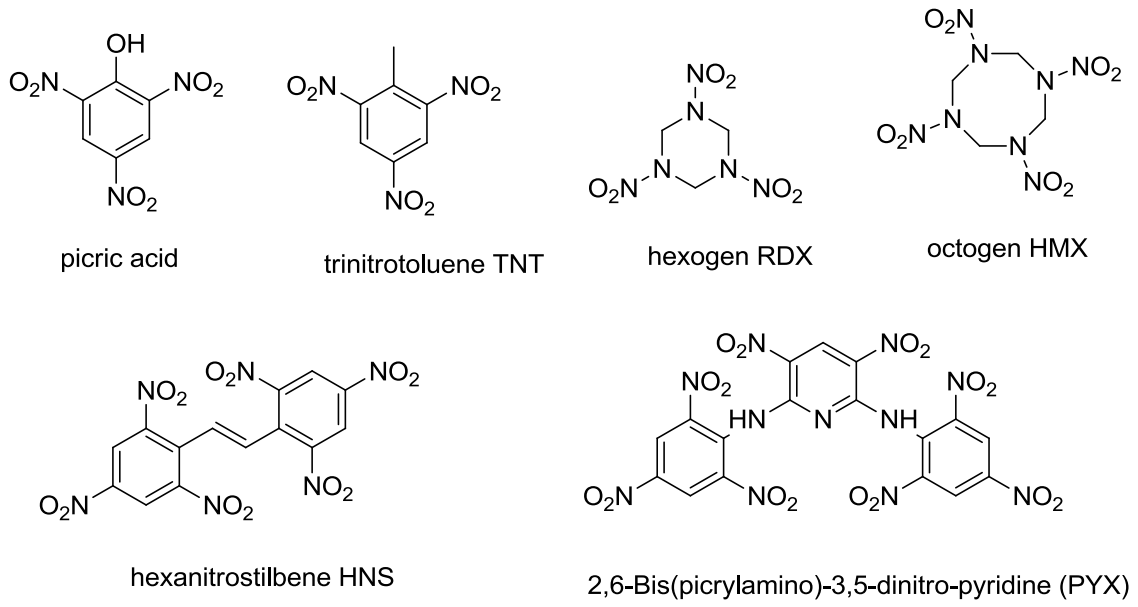

Figure 6: Structural formulas of picric acid, TNT, RDX, HMX, HNS and PYX.

In addition to the secondary explosives discussed in the upper section of the history part, some more modern approaches were made to find better performing and less sensitive energetic materials. For a better performance, the introduction of cage like structures is beneficial since the additional strain brings more energy to the molecule. On the other hand planned synthesis of cage structures is a challenging task. The two most prominent examples are octanitrocubane [26] and CL-20 [27], which has a remarkable high density of around

2 g cm^{-3}. A similar, but easier to synthesize and therefore also more cost efficient compound is TEX [28]. Figure 7 displays the molecular structures.

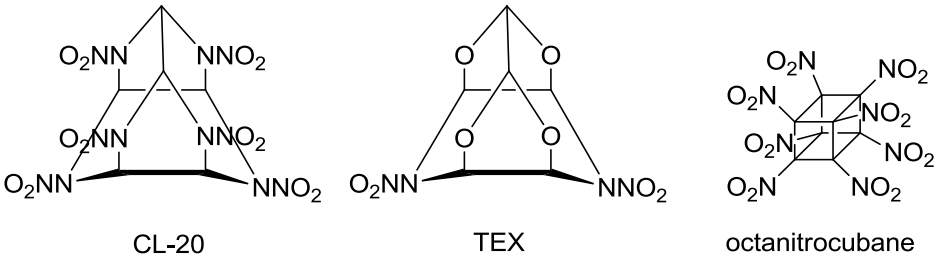

Figure 7: Structural formulas of CL-20, TEX and octanitrocubane.

Two compounds which performance values are not terrific, but that have very low sensitivities towards outer stimuli are FOX-7 [29] and FOX-12 [30]. They can find application as insensitive munitions. Figure 8 displays the molecular structures.

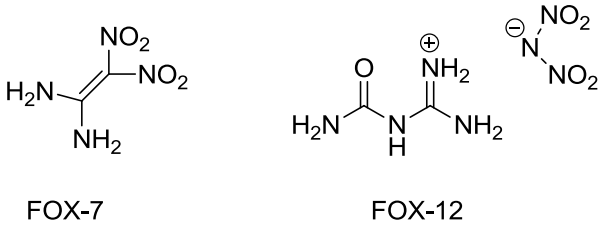

Figure 8: Structural formulas of FOX-7 and FOX-12.

As good as the secondary explosives used today are with respect to their performance and sensitivity as well as thermal stability values, they are all more or less toxic and therefore dangerous for the environment. Research for modern energetic materials therefore focuses on substances which in addition to their improved energetic properties are also more environmentally benign. In research for those compounds nitrogen rich heterocycles turned out to be a possible class of molecules. The chemical requirements for new energetic materials are: oxygen balance of ideally 0%, high density and high heat of formation. Moreover they should have low sensitivities towards outer stimuli and should show compatibility with different substances most important metals. The trend for new explosives therefore goes in the direction of compounds which have a heterocyclic, nitrogen rich core structure. A major achievement is the hydroxylammonium salt of 1,1´-bistetrazolyl-1*N*-oxide (TKX 50) [31]. Another important molecule which features high thermal stability and good

performance values is 5,5'-bis(2,4,6-trinitrophenyl)-2,2'-bi(1,3,4-oxadiazole) (TKX 55) [32]. The molecular structures of the two mentioned compounds are displayed in figure 9.

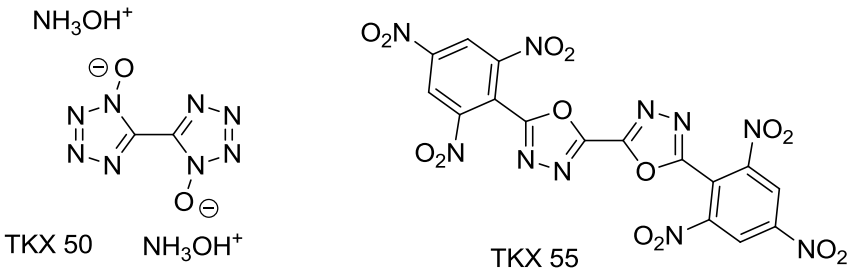

Figure 9: Structural formulas of TKX 50 and TKX 55.

4 Organic Peroxides

4.1 Energetic Organic Peroxides

Peroxides are a class of substances which is characterized by an O-O single bond. They can be divided into the subclasses of inorganic and organic peroxides. Known inorganic peroxides are metal salts which feature the peroxide anion O_2^{2-}, for example BaO_2 or Na_2O_2, salts of Caro´s acid H_2SO_5 and hydrogen peroxide.

Barium peroxide was important for the industrial preparation of oxygen and also hydrogen peroxide about 100 years ago. However it is no longer used for those purposes since better ways of preparation have been found in the Linde process for oxygen [19] respectively the antrachinone process for hydrogen peroxide production [33]. In combination with magnesium, it was also used in ignition pellets for thermite mixtures [19]. In pyrotechnical formulations BaO_2 is used as oxygen delivery agent and, like the other barium salts, produces a green flame color. Sodium peroxide was used as bleaching agent in detergents and can also be used to bind released carbon dioxide and in turn release oxygen. Li_2O_2 was used for the same purpose on submarines because of its lower molecular weight [19]. However, on German submarines of World War 2, in emergency situations CO_2 was only filtered from the

air by reacting it with CaO. No peroxide was used to replace the consumed oxygen, most likely because of the hazard of accidental fire. Hydrogen peroxide itself found application in the Aggregat 4 (V2)-rocket as steam producing agent to run the fuel pump of the rocket engine [34] and as the so called *T-Stoff* [35], [36] in combination with *Z-Stoff* (a solution of calcium permanganate or potassium permanganate in water) [36] for start assistance devices of the Fieseler Fi 103 (V1) missile, the Messerschmitt Me 321 glider and the Arador AR 234 operational bomber [37]. Moreover it was again used as *T-Stoff* in the Messerschmitt Me 163 [37], the first plane to exceed Mach 1, this time in combination with *C-Stoff*, a mixture of methanol, hydrazine-hydrate and water [35]. Other applications are bleaching and disinfection [19].

In this thesis however, those substances were not investigated and the research was limited to organic C, H, N, O- peroxides. This is why in the following sections of the thesis the term "peroxide" always means "organic peroxide". The way how the two remaining valences of the O-O building block are substituted varies. Figure 10 shows the main subclasses of organic peroxides.

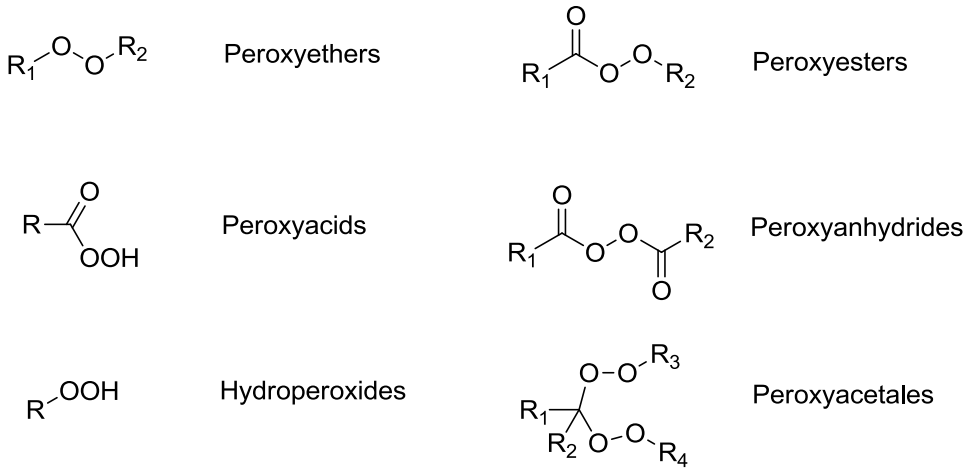

Figure 10: Main subclasses of organic peroxides.

With respect to their energetic properties, peroxides are a relatively unexplored class of substances. The most prominent example for an explosive organic peroxide today is acetone peroxide which was synthesized for the first time by the German chemist Richard Wolffenstein in 1895 [38]. Originally he wanted to oxidize Coniin with hydrogen peroxide and used acetone as solvent. The white precipitate formed turned out to have explosive

properties. Detailed investigations concerning the composition of the product were performed later and it was found that the main fraction is a trimeric molecule (triacetone tri peroxide, TATP), what was also suggested by Wolffenstein in the beginning basing on his experimental observations. The trimer is accompanied by a dimer (diacetone di peroxide, DADP) [39]. The ratio in which the two possible products are formed depends on the reaction conditions, mostly the concentration of the acid used during the reaction. Generally concentrated and strong acids favor the formation of DADP whereas lower acid concentrations or acid free conditions lead to the formation of TATP. Under the catalysis of tin (IV), a tetrameric form can be isolated [40]. Wolffenstein also patented his invention [41] and tried to sell it to the German army, but the high sensitivity and especially the high volatility of the compound prohibited a use. However the starting materials are relatively easy to buy or to produce and the synthesis is straightforward. It can successfully be performed by people without excessive preparative chemical training and is therefore very popular among terrorists. In recent years, cocrystallization with trinitro-trihalogeno-benzenes was found to be an effective way to reduce the sensitivity of DADP. For TATP however, this strategy turned out not successful, because the O-atoms are not accessible in the trimeric structure [42], [43]. Hexamethylene triperoxide diamine (HMTD) was discovered in the same period as acetone peroxide by Ludwig Leger from the reaction of ammonia and *Lampensäure* [44]. This compound is also sensitive towards shock and friction and shows a fast DDT which means it can be used as a primary explosive. Additionally it showed less sensitivity than the primary explosives used before and therefore found a short period of application in initiation charges for mining operations [45]. Like acetone peroxide it is prepared in a straightforward way today by reacting hydrogen peroxide with hexamine and citric acid [46]. The ingredients are again easy to procure and the compound is not volatile. The unpredictable behavior due to the, for modern standards, too high sensitivity to all external stimuli is again the most significant drawback of HMTD. A liquid peroxide is methyl ethyl ketone peroxide which is similarly prepared from the ketone and hydrogen peroxide under acidic conditions [47]. It consists of a mixture of several different molecules, but an open chain dimer is the main product. Figure 11 shows the molecular structures of DADP, TATP, TrATrP, HMTD and MEKP.

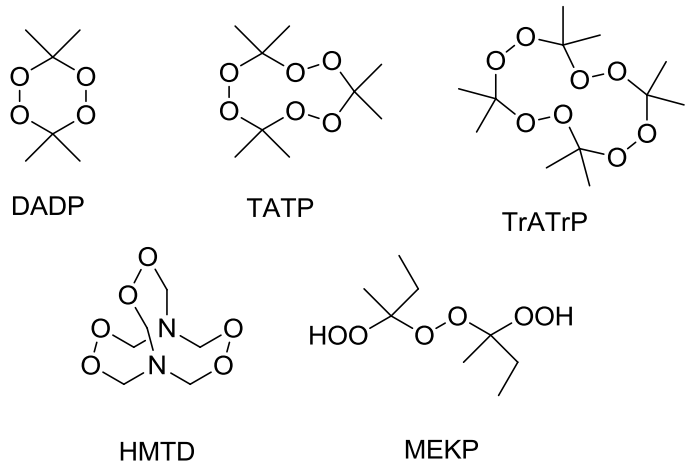

Figure 11: Structural formulas of DADP, TATP, TrATrP, HMTD and MEKP.

Most of the energetic materials in application today gain their explosive power from the oxidation of a carbon backbone or from the release of heat and gaseous reaction products [2]. For most peroxides, the general decomposition mechanism is not investigated in detail until now. Only for acetone peroxide deeper studies have been performed. In this case, the main reaction products are carbon dioxide, methane, ethane, ethylene and acetone and no significant amount of heat is released [48]. In addition, the fire ball which can be observed during the combustion of acetone peroxide is a secondary effect resulting from the oxidation of the flammable reaction products with surrounding oxygen and not from a self illumination like in normal detonation processes, which are auto-luminous. Under a nitrogen atmosphere, no flame can be observed [48]. This kind of detonation is called entropic detonation. It is not unlikely, that the other peroxides feature a comparable decomposition pathway. Figure 12 displays a series of photos made during decomposition of a TATP sample initiated with a smoldering wooden stick. It can clearly be observed, that the combustion takes place after the initial decomposition reaction.

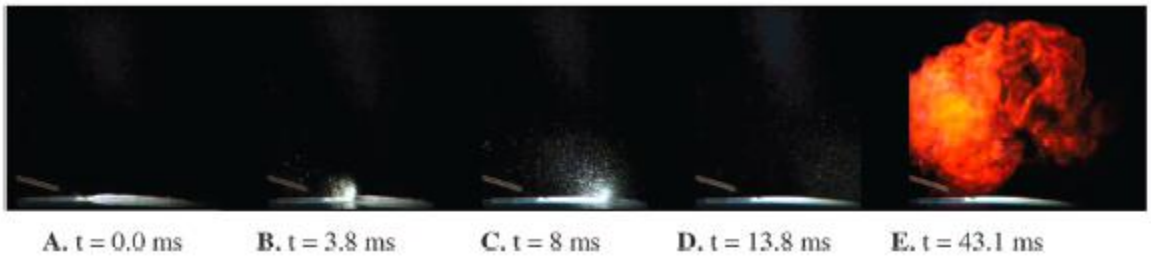

Figure 12: Time resolved decomposition and secondary combustion with surrounding oxygen [48].

Since the acetone peroxides, HMTD and MEKP as the in terms of energetic properties deeper investigated peroxides belong to the subclasses of peroxy ethers and acetals, and because this subclasses form the backbone of most other organic peroxides, they shall be presented with a little bit more detail. By and large all known compounds are cyclic basing on a five- or six-membered ring. Figure 13 shows the six main structures.

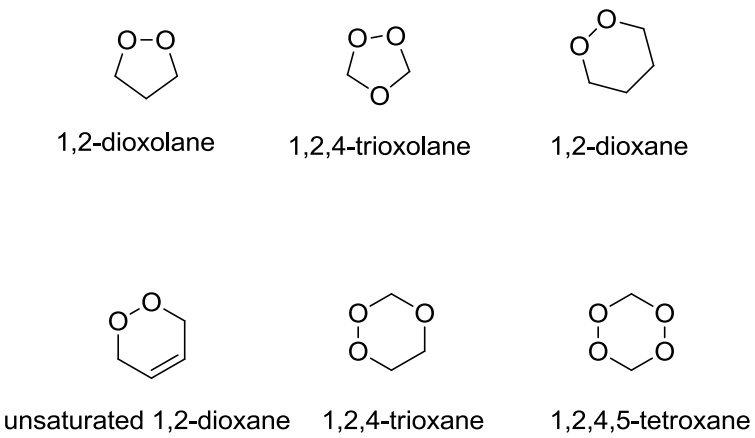

Figure 13: Main structures of cyclic peroxy ethers.

In all these examples, the valences of the O-O-bond are substituted by C-atoms, but this does not necessarily has to be the case. The substitution by one carbon and one silicon atom is also known [49], [50].

A further peroxide subclass of higher importance, because the molecules can be used for the synthesis of other peroxides, is the one of geminal dihydroperoxides. In contrast to geminal dioles, those molecules are stable and do not decompose into the ketone under the elimination of water. Figure 14 displays a general structure.

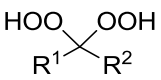

Figure 14: General structural formula of a geminal dihydroperoxide.

Geminal dihydro peroxides are very weak acids. However it is possible to deprotonate them in a tert.-BuOK/ 18-crown-6 system and trap the resulting anion in consecutive reactions [51].

4.2 Practical applications of peroxides

Even though peroxides do not find application as energetic materials today, they are of great importance in different and also diverse fields. The most prominent one is by far the use of dibenzoyl peroxide as initiation reagent in radical polymerization reactions [52]. Of minor importance for industrial processes but a valuable reagent in organic synthesis is meta-Chloroperbenzoic acid (mCPBA). Its main application is the epoxidation of double bonds. This reaction is known as the Prileschajew reaction [53]. Moreover m-CPBA can be used in the synthesis of energetic materials as source for N-oxides [54] and for different oxidation reactions [55]. Other peroxide based N-oxidation reagents are monoperphthalic acid [56], monopermaleic acid [57] and perbenzoic acid [58].

Peroxides are also used in less obvious fields especially as important building block in pharmaceutical substances. The greatest interest in this field focuses on anti-malaria drugs inspired by the naturally occurring peroxide Artemisinin which can be isolated from blossoms and leaves of sweet wormwood (*Artemisia annua*) [59]. Figure 15 displays the structures of Dibenzoyl peroxide, meta-Chloroperpenzoic acid and Artemisinin.

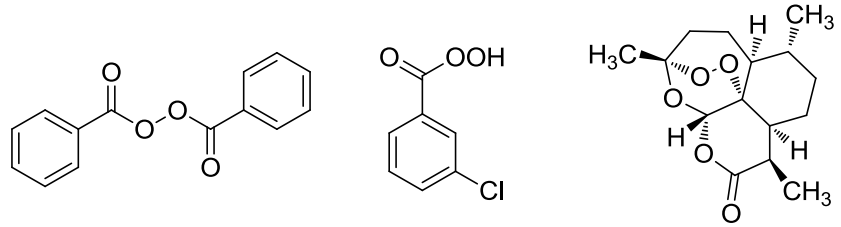

Figure 15: Structural formulas of Dibenzoyl peroxide, meta- Chloroperbenzoic acid and Artemisinin.

Currently different synthetic and semi-synthetic Artemisinin analogs are under investigation [60], [61]. The most commonly accepted mode of action for this compounds says, that the enclosed peroxide bond gets cleaved when exposed to high concentrations of Fe(III)-ions. Those high concentrations are found in the human blood. The created radicals then destroy the plasmodii responsible for the disease [62]. 1, 3, 4, 5- Tetroxanes were also tested with respect to their antimalarial activities [63]. Other important endo- peroxides which were tested against

cancer were synthesized by Zhu and coworkers [64]. Two structures are given as examples in figure 16.

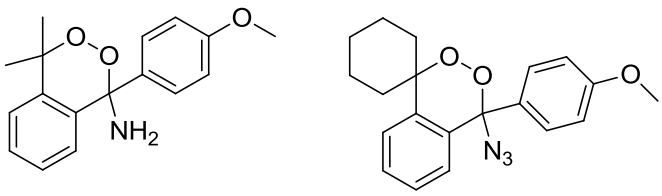

Figure 16: Structural formulas of two endoperoxides, which were tested against cancer.

The examined molecules proved more or less valuable in *in vitro* tests which shows, that peroxides can be an important part of new generation anti-cancer drugs [64].

Another class of peroxides important in pharmaceutically active compounds are bridged tetroxanes. The simplest representative was synthesized by Milas in the early 1960s [65]. Other molecules containing this moiety were prepared by the Terentev group and investigated against schistosomiasis [66], [67], [68]. Figure 17 shows the general structure, the simplest example and one of the compounds prepared and tested by Terentev and coworkers.

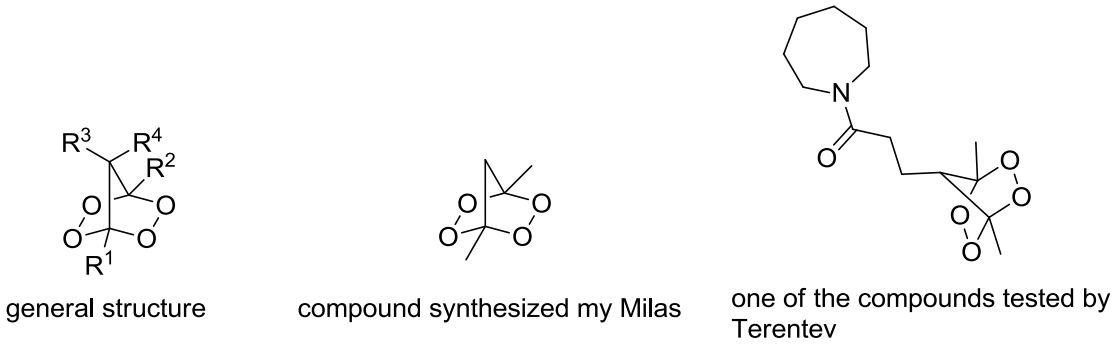

Figure 17: Structural formulas of different bridged tetroxanes, R1, R2, R3 and R4 can be varied over a relatively large range.

In contrast to the chemical intuition, the bridged tetroxane moiety is relatively stable towards some selected standard chemical reactions like epoxidations and the bromination of enclosed double bonds [67].

4.3 Reactions for the preparation of organic peroxides

Peroxides are a more or less exotic class of compounds which is commonly not discussed in detail during studies and reactions for their preparation are normally not performed in laboratory courses. Therefore only little knowledge about peroxide synthesis is spread under chemists. Because of this a short overview over the general reagents and reactions and also some more curious reactions will be given in the following part of the thesis.

4.3.1 General reactions

In general mainly three different reagents can be used for the synthesis of organic peroxides. Other sources for the O-O building block are only used in niche applications and are not enclosed in this thesis. Those main reagents are hydrogen peroxide (most often dissolved in appropriate solvents), singlet oxygen and ozone. The reaction mechanisms in this context differ from molecule to molecule. The most prominent reaction to gain peroxides is the reaction of hydrogen peroxide with carbonyl compounds to get hydroperoxides, peroxy acetals and peroxy ethers, or activated carbonyl derivatives mostly carbonic acid chlorides for the synthesis of peroxy acids. For carbonyl compounds, this reaction is an addition, in case of carbonic acid chlorides, the reaction is a substitution. Especially if the carbonyl is sterically hindered or if reaction times should be shortened, different activating reagents like acids [69], iodine [70] or metal salts [71], [72] are used to perform the reaction. Activation can also be achieved by using heterogeneous catalysts, for example silica supported sodium bisulfate [73] or Wells-Dawson heteropolyacids [74]. Hydrogen peroxide is in the far most cases dissolved in water. However solutions in different solvents like acetonitrile sometimes also find application [75]. The second key reagent is singlet oxygen which reacts with alkenes in a [2+2]-cycloaddition-reaction [76], as dienophile in [4+2]-cycloaddition reactions with 1,3-dienes [77], [78] or as reaction partner in ene- reactions [79]. Singlet oxygen itself is most commonly prepared via a photochemical reaction of triplet oxygen under the presence of photosensitizers like rubrene or perylene [80]. Chemical ways for its preparation are the reaction of hydrogen peroxide with sodium hypochlorite under alkaline reaction conditions [81] and the reaction of alkyl-phosphines with ozone [82]. The third widely used reagent for the synthesis of organic peroxides is ozone, which yields 1,2,4-trioxolanes when it is reacted

with alkenes via an initial 1,3-dipolar cycloaddition and a subsequent rearrangement of the intermediate [83], [84], [85]. Scheme 1 displays the reagent and the possible reaction products.

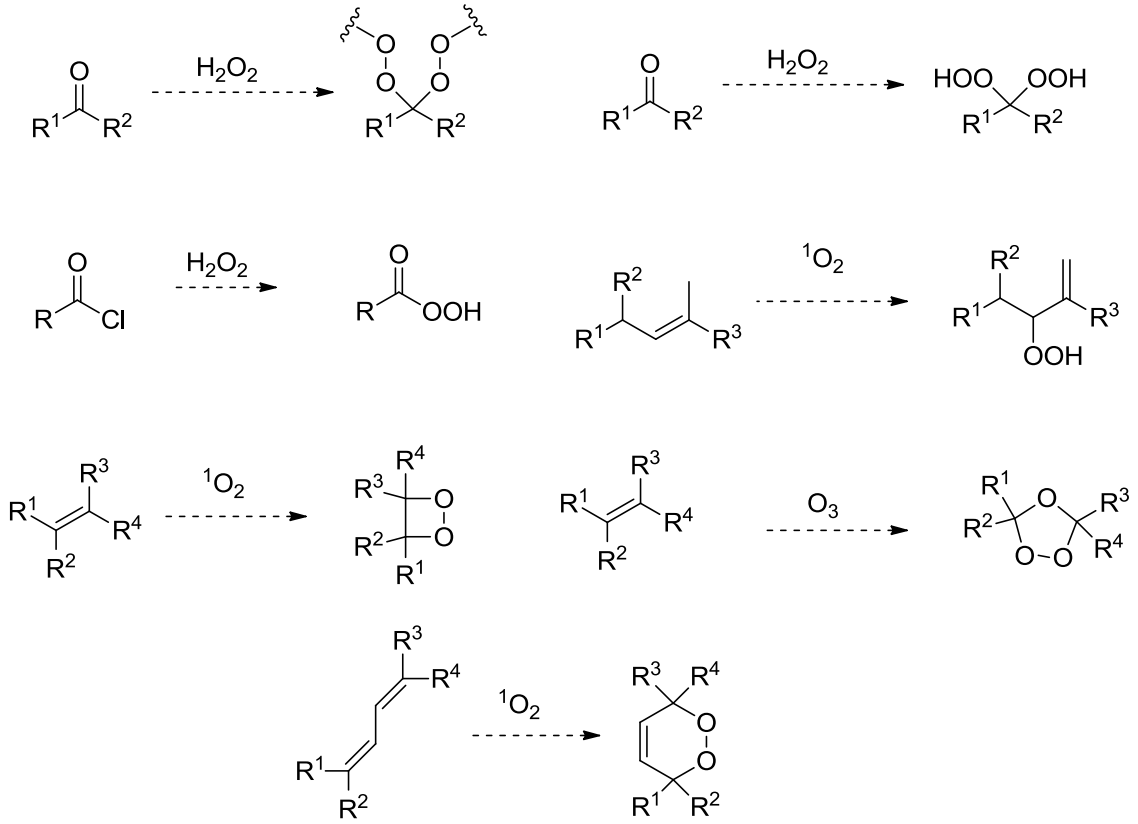

Scheme 1: The three key reagents for peroxide synthesis, the corresponding starting materials and products.

4.3.2 More curious reactions

A synthetic procedure of minor importance which can be applied for the synthesis of linear peroxy ethers is the reaction of dialkylsulfates with alkaline hydrogen peroxide solution [86]. When treated with the same reaction conditions alkyldisulfates yield the corresponding cyclic peroxides [87]. Scheme 2 displays the corresponding reaction equations.

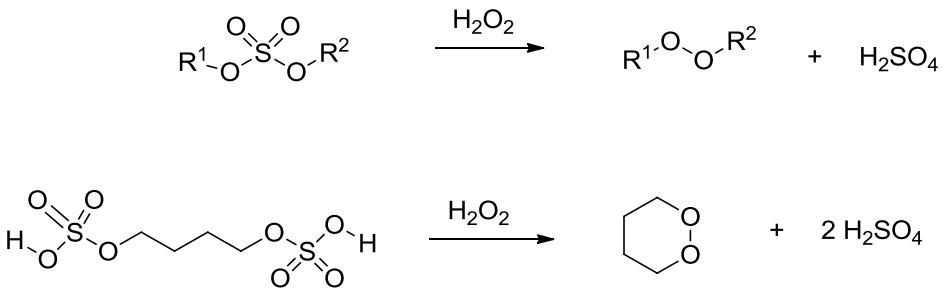

Scheme 2: reaction equations for the preparation of dialkylperoxides via dialkylsulfonates.

In addition to the direct reaction of ketones and hydrogen peroxide (DADP-formation), cyclic tetroxanes can be created by some alternative methods. Very interesting in this context is the treatment of geminal dihydroperoxides with ketones to form tetroxanes [88]. Scheme 3 shows the reaction pathway for the synthesis of geminal dihydroperoxides and for the possible tetroxane formation thereafter. The biggest advantage of this approach is, that unsymmetrically substituted 1,2,4,5- tetroxanes can be prepared specifically.

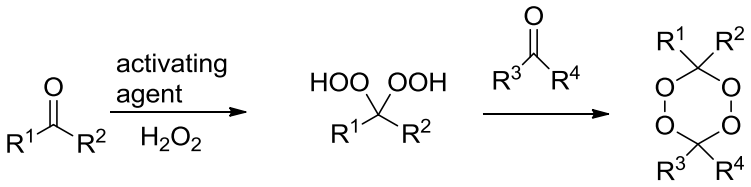

Scheme 3: Synthesis of geminal dihydroperoxides and subsequent tetroxane formation.

Tetroxanes with a symmetrical substitution pattern can also be synthesized from ozonides via the recombination of zwitter ions (scheme 4) [89].

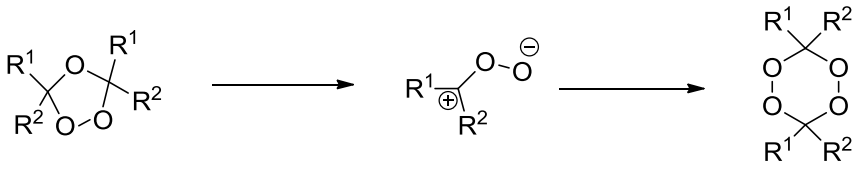

Scheme 4: Tetroxane formation via combination of zwitter ions.

A not very common way for the synthesis of 1,2,4,5-tetroxanes is the ozonolysis of O-methyloximes (see scheme 5) [90], [91]. However this synthesis is limited to only a few appropriate substrates and only gives the products with poor yields.

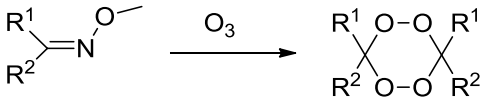

Scheme 5: Tetroxane synthesis form O-methyloximes.

1,2-Dioxanes can be formed via the Isayama-Mukaiyama reaction. Triethylsilane and oxygen are reacted under the catalysis of Co(II) with 1,5-dienes to form the corresponding structure (Scheme 6) [92].

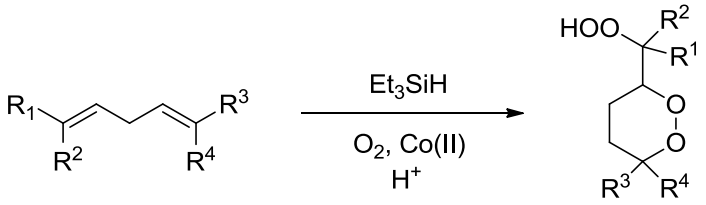

Scheme 6: Display of the Isayama-Mukaiyama reaction.

1,2,4-Triooxolanes (secondary ozonides) can in addition to the reaction of a double bond and ozone also be synthesized via the so called Griesbaum reaction. Methyloximes are reacted with ozone to form instable 1,2,3-trioxa-4-azacyclopentanes, that decompose into zwitter ions. The O-O-containing zwitterionic structure then reacts with an additional ketone to form the desired products (scheme 7) [93].

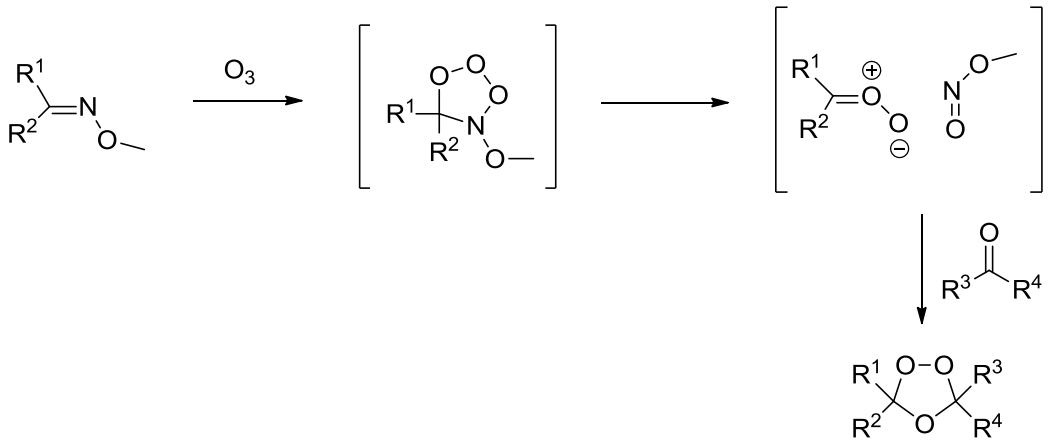

Scheme 7: Reaction pathway for the preparation of 1,2,4-trioxolanes form O-methyloximes (Griesbaum reaction).

A very interesting synthetic pathway to produce 1,2-dioxolanes photochemically starts from cyclopropanes. Various sensitizers like 1,2,4,5-tetracyanobenzene can be used and the reactions are normally performed in acetonitrile. The yields are quantitative in most of the investigated reactions [94]. Scheme 8 gives a graphical insight in the reaction pathway.

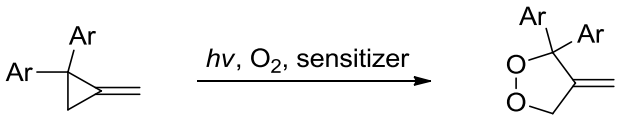

Scheme 8: Reaction equation for the photo induced synthesis of 1,2-dioxolanes.

Peroxy acetals can be prepared from the reaction of carbonyl compounds with hydroperoxides [95] or from the reaction of hydroperoxides with alkylhalogenides, mainly methyl iodide [96], [97]. Scheme 9 displays the corresponding reaction equations.

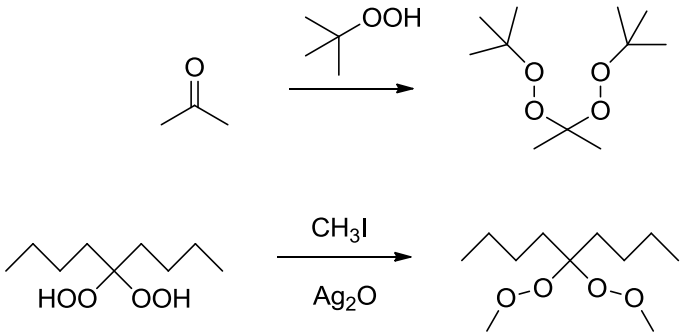

Scheme 9: Two examples for alternative possibilities for the synthesis of peroxy acetals.

A further method is the reaction of acid chlorides with hydroperoxides in alkaline medium (Scheme 10) [98].

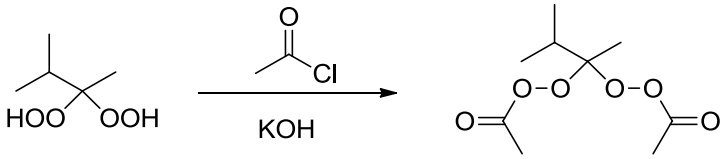

Scheme 10: A further possibility to synthesize peroxy acetals.

5 Sensitivity Classification

The sensitivities of the synthesized compounds within this thesis towards impact and friction were determined by standardized methods of the Bundesanstalt für Materialprüfung (BAM) [99] on a drop hammer and a friction tester. Electrostatic discharge (ESD) values were determined on an ESD testing device, but for ESD sensitivity no internationally standardized sensitivity range was applied. The following tables 1 and 2 reflect the sensitivity ranges for impact sensitivity respectively friction sensitivity. The BAM uses the one out of six method, which means, that a sensitivity value is valid, when one out of a total of six tests turns out positive.

Table 1: Sensitivity classification for impact sensitivity.

range of values	sensitivity classification
40 J	insensitive
40 J – 35 J	less sensitive
≥ 4 J	sensitive
≤ 3 J	very sensitive

Table 2: Sensitivity classification for friction sensitivity.

range of values	sensitivity classification
> 360 N	insensitive
= 360 N	less sensitive
< 360 N – 80 N	sensitive
< 80 N – 10 N	very sensitive
≤ 10 N	extremely sensitive

The maximum electrostatic charge, that can be created by the human body is 20 mJ [2]. Therefore it is possible to predict, if accidental ignition by ESD of the respective substance is possible or not. The decomposition points in this thesis are all determined at a heating rate of 5 °C min^{-1}, which is the internationally accepted standard and onset temperatures are taken.

6 Summary of the different chapters of this thesis

The following sequence will give a short summary of the thesis going through the different investigated compound classes and putting emphasize on the achieved results. Moreover a generalized reaction equation and a figure of the synthesized compounds are displayed for better visualization of the performed reactions and the shape of the products. Molecular structures of selected compounds are pictured for the same purpose. The respective original scientific papers are part of the appendix together with the corresponding supporting information.

6.1 Aromatic peroxy acids

The first paper which is part of this thesis deals with the synthesis of aromatic peroxy acids and their investigation towards application as energetic materials. The compounds were synthesized form the corresponding carbonic acid chlorides resp. carbonic acids via reaction with highly concentrated hydrogen peroxide and methansulfonic acid in high yields over 90%. Most of the examined compounds have impact sensitivities around 10 J and friction sensitivities up to 360 N what would categorize them as suitable for a number of applications like secondary explosives and reagents for organic synthesis. However per-trimesic acid is extremely sensitive with an impact sensitivity of 1 J and a friction sensitivity of 5 N. In this context, calculations concerning the surprising insensitivity of most studied compounds were performed resulting in a new concept of atom close contacts for stabilization of energetic molecules similar to the close contacts suggested by Matzger in tri-halogeno-trinitro benzene DADP co crystals [60], [61]. The investigated compounds have calculated detonation velocities in the rage of commonly used secondary explosives (v_{det} = 5262 to 7217 ms^{-1}) like TNT (6950 ms^{-1} [83]) and calculated detonation pressures between 88 and 213 kbar. Decomposition temperatures are between 132 and 160 °C. The best performing substance is 3,5-Dinitroperbenzoic acid. The results were published in *Chemistry-A European Journal* **2015**, *22*, 2582-2585, DOI: 10.1002/chem.201502989.

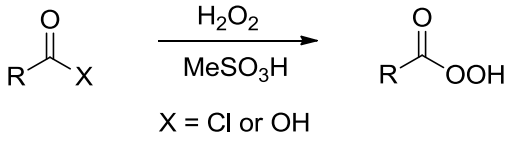

Scheme 11: General reaction equation for the synthesis of peroxy acids.

The following figure 18 gives an overview over the synthesized compounds.

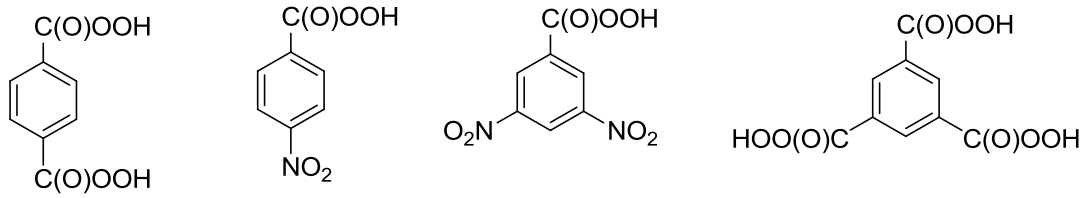

Figure 18: Structural formulas of the peroxy acids synthesized in the course of this thesis.

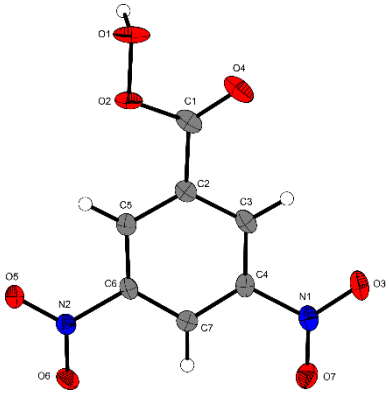

Figure 19: Representative molecular structure of a peroxy acid.

6.2 Geminal dihydroperoxides

The second paper deals with the synthesis of new difunctional geminal dihydroperoxides. The compounds were synthesized from ketones and hydrogen peroxide under the catalysis of acid or iodine and were isolated in 21 to 93% yield. Most of them are very sensitive to outer stimuli with impact sensitivity values around 1 J and friction sensitivity values around 5 N, but 1,4-bis(dihydroperoxymethyl)benzene has an impact sensitivity of 3 J and is therefore insensitive enough to find possible application as a primary explosive (impact sensitivity of

PbN_3: 3 J [83]). A possible explanation for this can again be found in the concept of atom close contacts. The calculated detonation velocities of the investigated compounds are in a range between 6150 and 7130 ms^{-1} and the calculated detonation pressures are between 126 and 195 kbar. In addition, four of the five studied molecules could be crystallized and therefore the number of crystalline gem. dihydroperoxides, which are still few in number, could be increased. The results were published in *Chemical Communications* **2015**, *51*, 13298-13230, DOI: 10.1039/c5cc05015d.

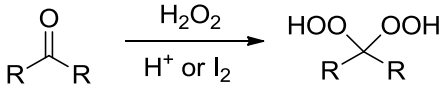

Scheme 12: General reaction equation for the synthesis of geminal dihydroperoxides.

The following figure 20 gives an overview over the synthesized compounds.

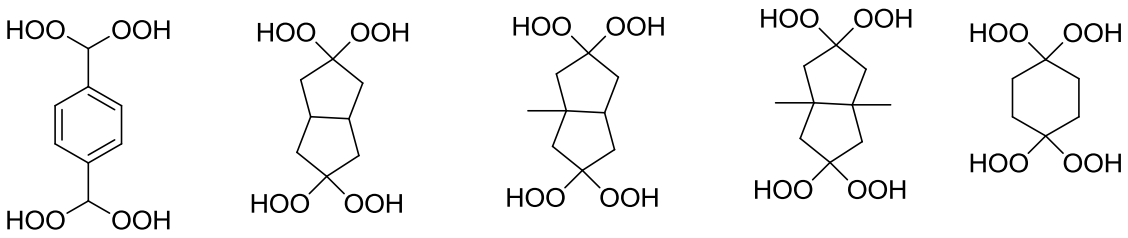

Figure 20: Structural formulas of the geminal dihydroperoxides synthesized within this thesis.

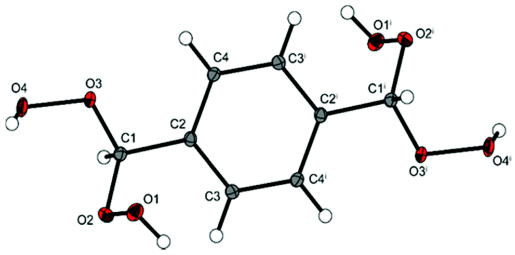

Figure 21: Representative molecular structure of a geminal dihydroperoxide.

6.3 Bridged 1,2,4,5-tetroxanes

The third paper of the thesis deals with the synthesis of bridged tetroxanes from alkylated acetyl acetone derivatives and hydrogen peroxide under the catalysis of hydrochloric acid respectively by the elimination of water through P_4O_{10} form the corresponding hydroxyl-hydroperoxy-dioxolanes. The yields obtained were between 10% and 73%. The investigated moiety is spread in pharmaceutical substances, but with respect to energetic materials research no deeper investigations were performed. Moreover only very few molecules with an embodied bridged tetroxane have been crystallized until now. In the course of this work, a total of six additional crystal structures could be determined which considerably increased the knowledge of bond angles and bond distances for bridged tetroxanes. With respect to their energetic properties, all of the compounds have to be classified as extremely sensitive toward impact (1.5 J as highest determined value) and friction (< 5 N for all investigated compounds). The calculated detonation velocities of the compounds are in a range between 6048 and 6343 ms^{-1}. Calculated detonation pressures are between 97 and 133 kbar. Additionally all examined substances are volatile compounds. Therefore a practical application in the energetic sector seems to be limited. The results were published in *European Journal of Organic Chemistry* **2015**, *28*, 6237-6242, DOI: 10.1002/ejoc.201500919.

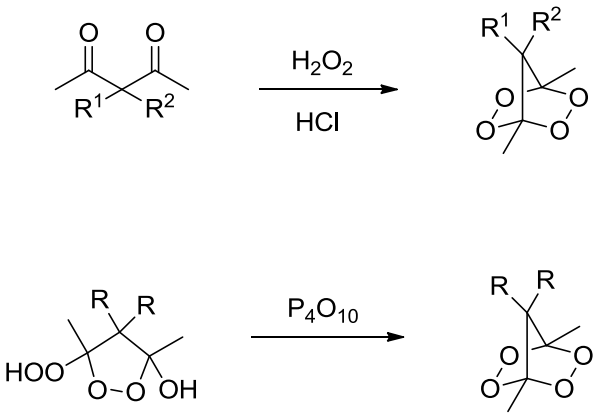

Scheme 13: The two general reaction equations for the synthesis of bridged tetroxanes.

Figure 22 gives an overview over the synthesized compounds.

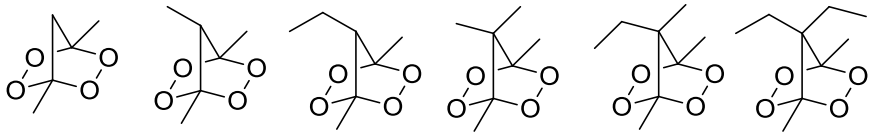

Figure 22: Structural formulas of the bridged tetroxanes synthesized within this thesis.

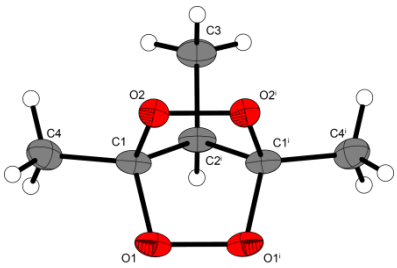

Figure 23: Representative molecular structure of a bridged tetroxane.

6.4 Aromatic peroxy esters

The fourth paper of the thesis deals with the synthesis of polyfunctional peroxy esters. They were prepared from tert-butyl hydroperoxide and carbonic acid chlorides under the presence of pyridine. The yields obtained are between 7% and 77%. Crystal structures for all compounds were determined. The densities however are only low with values between 1.161 and 1.460 gcm^{-3} (room temperature densities). Concerning their properties as energetic materials, they show low sensitivities towards outer stimuli compared to other peroxides with values for impact sensitivity up to 40 J and values for friction sensitivity up to 360 N. However the sensitivity increases with increasing content of embodied peroxidic groups and therefore the compounds with the highest peroxide content are also the most sensitive ones. The nitroaromatic compounds however show a good compromise between density, peroxide content and accompanied sensitivity. Curiously, aromatic compounds are in general much less sensitive than non aromatic compounds (sensitivity values of di-tert-butylperoxolate: IS 1 J, FS: 5 N, ESD: 15 mJ). The calculated performance values of the studied compounds are lower than that of TNT (highest calculated value for detonation velocity: 6003 ms^{-1}) which may prevent any application as secondary explosives. The calculated detonation pressures are in a range between 56 and 118 kbar. However it was possible to show, that compounds with

peroxo groups participating in electron delocalization are in general less sensitive than their analogs, which also is in good accordance with the results of paper 1 and paper 7. The results are submitted for publication to *Chemistry Select*.

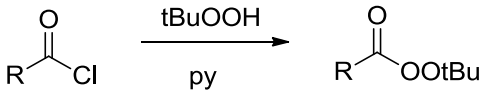

Scheme 14: General reaction equation for the synthesis of tert-butyl peroxy esters.

Figure 24 gives an overview over the synthesized compounds.

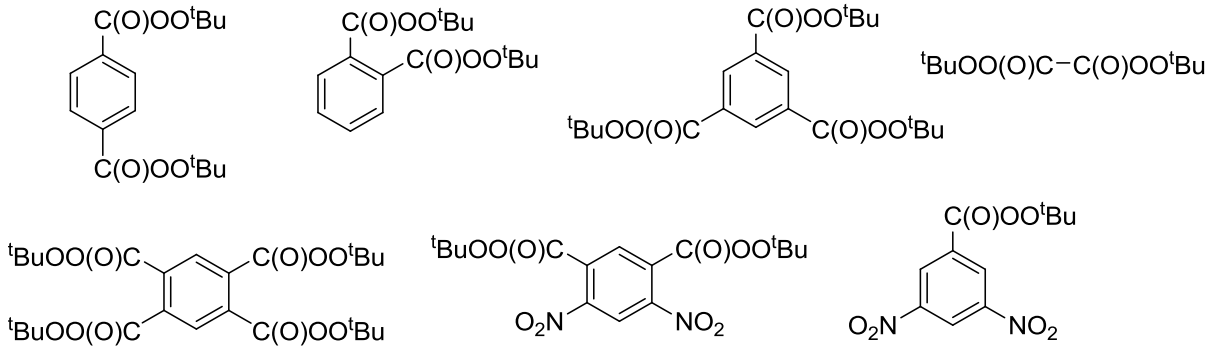

Figure 24: Structural formulas of the tert-butyl peroxy esters synthesized within this thesis.

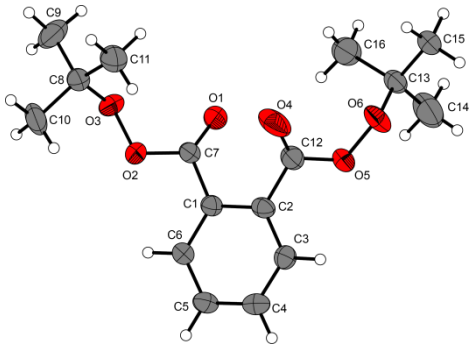

Figure 25: Representative molecular structure of a tert-butyl peroxy ester.

6.5 1,2-Endoperoxides

The fifth paper of this thesis deals with the synthesis of hydroperoxide substituted 1,2-endoperoxides derived from acetyl acetone, 3,5-heptadione and acetonyl acetone. The studies

were focused on the synthesis of compounds that were substituted either by two hydroperoxides or by a hydroperoxy group and a hydroxyl group and thus containing two different groups of organic peroxides. Compounds which are substituted by two hydroxyl groups were excluded in this study due to their lower energy content, but could be worth a study in the future. Different 1,3-diketones and a 1,4-diketone were used as starting materials and were reacted with hydrogen peroxide under the presence of different catalysts (acid or iodine). The hydroxy-hydroperoxy and dihydroperoxy compounds were obtained from the same reactions and were separated by column chromatography. The yields obtained are between 15% and 62%. Significant differences concerning the sensitivity values of the different compounds could be observed with impact sensitivity values varying from < 1 J to 3 J and friction sensitivity values varying from < 5 N to 40 N. The unsymmetrically substituted compounds are in general less sensitive. Variations in the alkylation degree instead seem to have no significant influence on the sensitivity. Calculations were performed which resulted in the discovery of O-O close contacts, that might have a stabilizing effect on some of the studied compounds and result in a reduced sensitivity. The calculated detonation velocities of the compounds are in a range between 5954 and 6694 ms^{-1}, calculated detonation pressures are between 98 and 154 kbar. The dihydroperoxy substituted molecules in all cases perform better than their hydroxy-hydroperoxy substituted analogs. The results are accepted for publication in *European Journal of Inorganic Chemistry*, DOI: 10.1002/ejic.201600767.

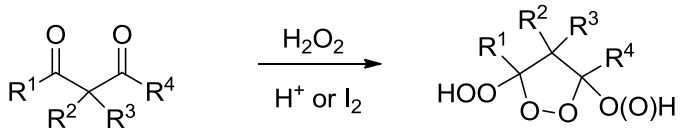

Scheme 15: General reaction equation for the synthesis of 1,2-dioxolanes.

Figure 26 gives an overview over the synthesized compounds.

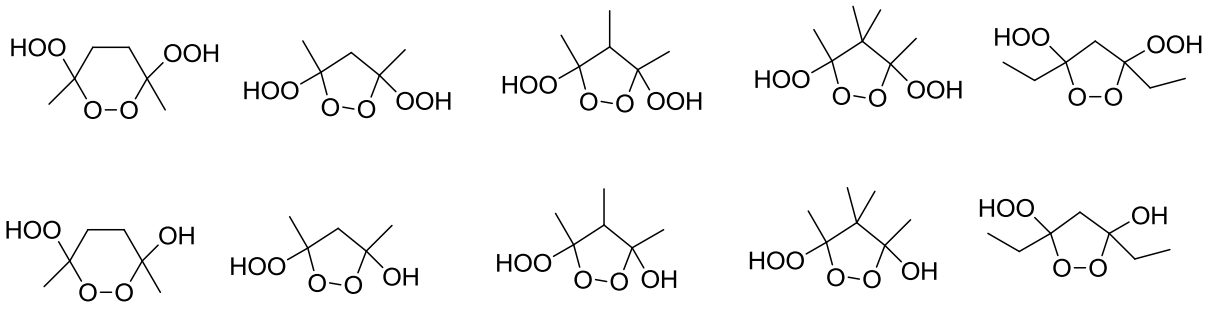

Figure 26: Structural formulas of the 1,2-dioxolanes synthesized within this thesis.

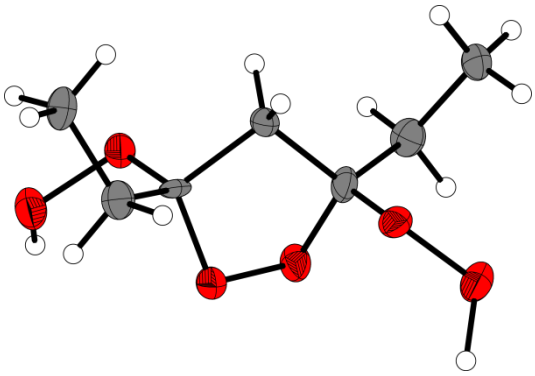

Figure 27: Representative molecular structure of a 1,2-dioxolane.

6.6 Tert-butyl azido-peroxides

The sixth paper which is part of this thesis deals with the synthesis tert-butyl azido-peroxides. These compounds were discovered only quiet recently and are therefore an almost uninvestigated class of substances, but on the other hand very interesting since a peroxide group is combined with a further energetic group, in this context an azide. Combinations of peroxides with other energetic moieties, especially on the same carbon atom, are only barely known. Moreover all compounds of this substance class synthesized so far were liquids and only mono functional. It was possible to synthesize the first solid and also difunctional compounds via a Fe(III) catalyzed reaction of carbonyl compounds with trimethyl silyl azide and tert-butyl hydroperoxide. The yields obtained are between 1% and 60%. In addition it was possible to determine the first crystal structure for compounds with the examined functional group and thereby achieving fundamental results for further investigations. Moreover for the first time sensitivities for such compounds were determined and therefore other scientists who use those substances in further reactions get a feeling for how to work with the compounds. However all synthesized substances were too sensitive for a possible large scale application as energetic material with impact sensitivity values of not more than 2 J and friction sensitivity values for the solid compounds of 5 N. The calculated detonation velocities are in a range between 5989 and 6435 ms^{-1} and therefore similar to commonly used secondary explosives. The calculated detonation pressures are between 90 and 110 kbar. Curiously, the non aromatic compounds perform slightly better than the aromatic ones. The results were published in

European Journal of Organic Chemistry **2016**, *25*, 4382-4386, DOI: 10.1002/ejoc.201600717.

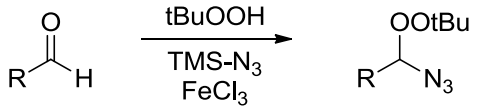

Scheme 16: General reaction equation for the synthesis of tert-butyl azido peroxides.

Figure 28 gives an overview over the synthesized compounds.

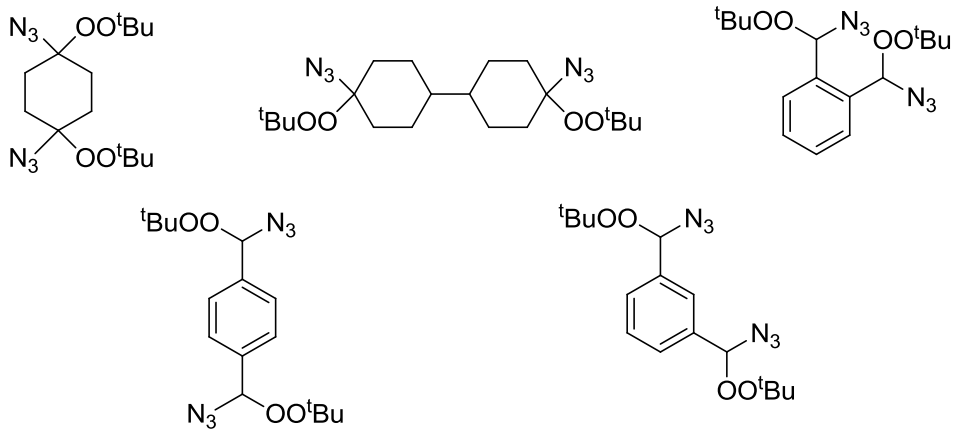

Figure 28: Structural formulas of the tert-butyl azido peroxides synthesized within this thesis.

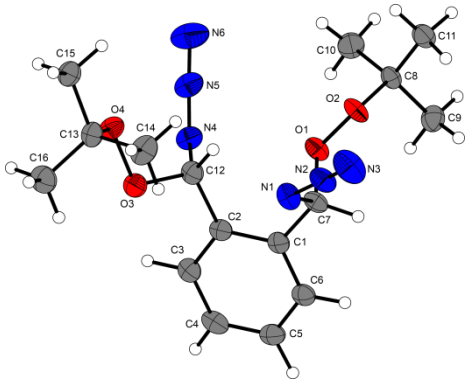

Figure 29: Representative molecular structure of a tert-butyl azido peroxide.

6.7 Aromatic peroxy anhydrides

The seventh paper contributing to this thesis deals with the synthesis of mono and difunctional aromatic peroxy anhydrides. The respective compounds were synthesized form

carbonic acid chlorides and hydrogen peroxide or peroxy acids under the influence of sodium hydroxide. The obtained yields are between 13% and 61%. Peroxy anhydrides are a unique class of small organic peroxides since they show relatively high densities up to over 1.7 gcm^{-1} and thermal stabilities higher than 160 °C. Moreover, in contrast to other small organic peroxides like hydroperoxides, they are inevitably stable at room temperature. The sensitivities of the examined compounds towards outer stimuli are still acceptable with impact sensitivity values up to 5 J and friction sensitivity values up to 360 N. A possible explanation for this might be the participation of the peroxy group in a π-conjugation. This is in accordance with the results of papers 1 and 4. The calculated performance values of some compounds exceed those of TNT (calculated detonation velocities up to over 7000 ms^{-1} for peroxy anhydrides, 6950 ms^{-1} for TNT [83]). The calculated detonation pressure is in a range between 210 and 250 kbar. Nitrated compounds perform better than non nitrated compounds. Difunctional molecules are in the context of performance inferior to the monofunctional what can be explained by the lower density. The results were published in *Chemistry Select* **2016**, *1*, 4057-4061, DOI: 10.1002/slct.201601114.

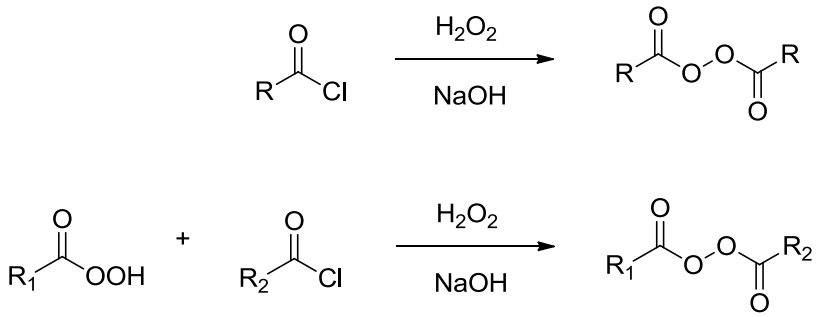

Scheme 17: General reaction equations for the synthesis of peroxy anhydrides.

Figure 30 gives an overview over the synthesized compounds.

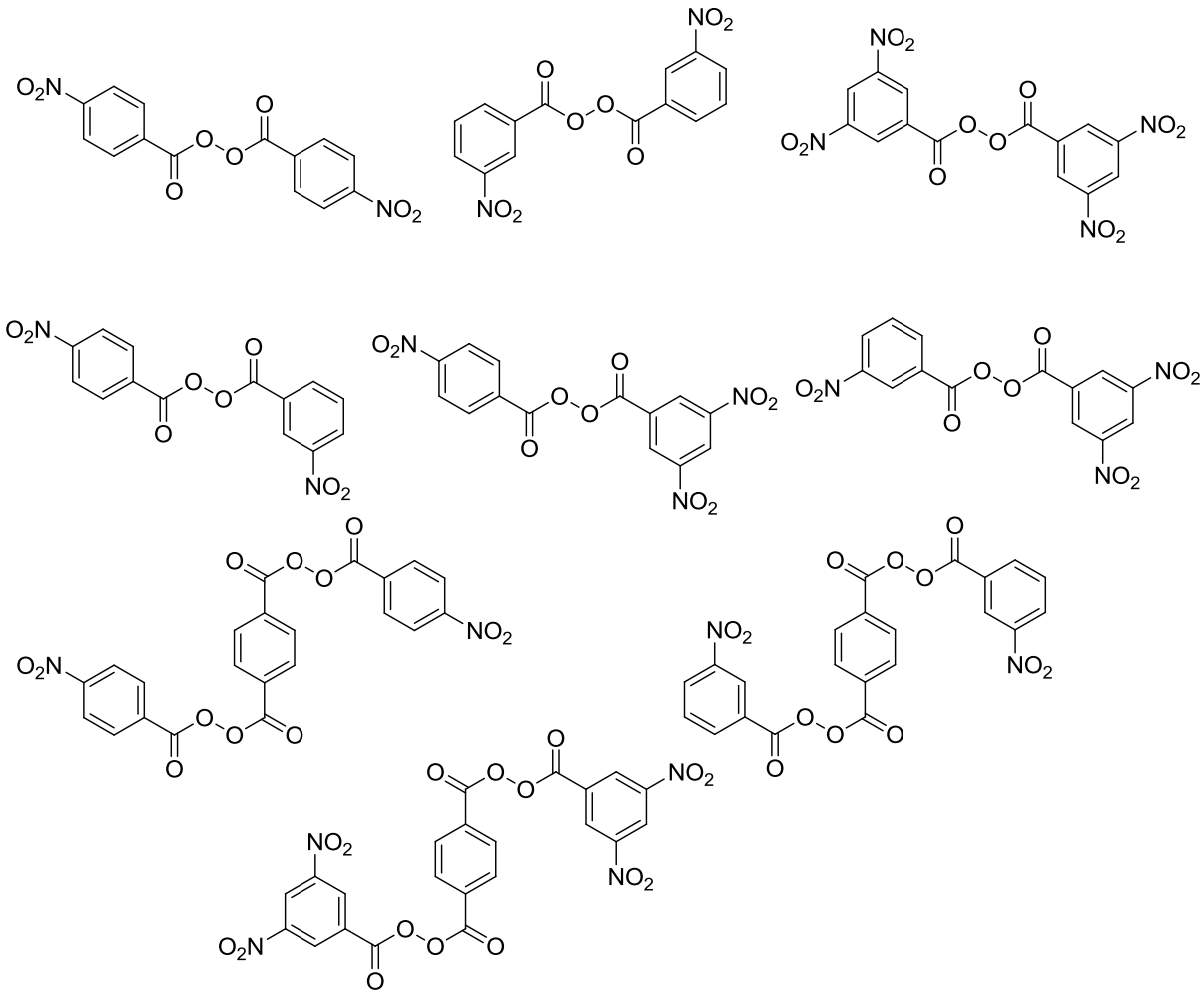

Figure 30: Structural formulas of the peroxy anhydrides synthesized within this thesis.

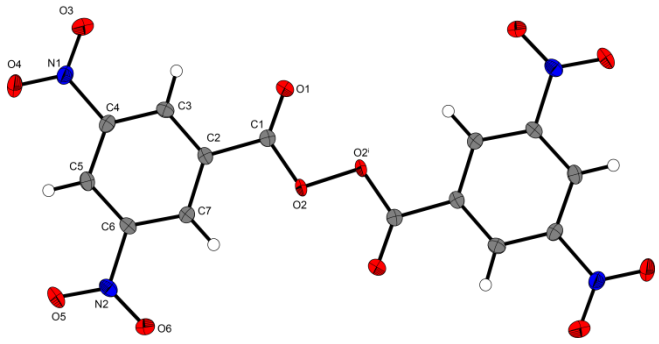

Figure 31: Representative molecular structure of a peroxy anhydride.

6.8 1,3-Di(5-nitraminotetrazol-1-yl)-propan-2-ole and its Salts

The eighth paper contributing to this thesis deals with the synthesis of 1,3-di(5-nitraminotetrazol-1-yl)-propan-2-ole and selected salts of it. The metal and nitrogen-rich salts were prepared from simple acid base chemistry by reacting the neutral compound with the corresponding hydroxides, carbonates or neutral N-bases. The neutral molecule is one of the rare examples of heterocyclic compounds which carry a hydroxyl group and a nitrimino group at the same time. Calculated performance values exceed those of TNT (calculated detonation velocities 8024 to 8462 ms^{-1}, calculated detonation pressures between 210 and 250 kbar) and the thermal decomposition points of the salts are all higher than 200 °C. Moreover the ionic derivatives are in contrast to the neutral molecule insensitive towards external stimuli with impact sensitivity values > 40 J and friction sensitivity values > 360 N. The results are published in *Zeitschrift für Anorganische und Allgemeine Chemie*, DOI: 10.1002/zaac.201600389

.

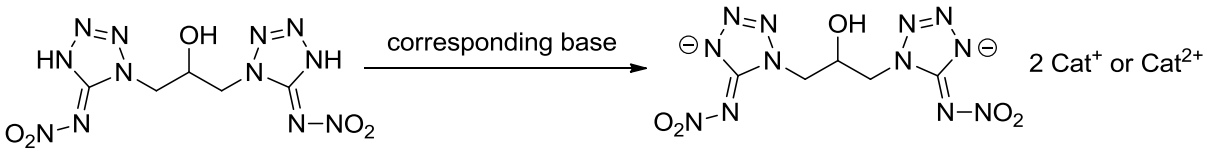

Scheme 18: General reaction equation for the salt formation.

Figure 32 gives an overview over the synthesized compounds.

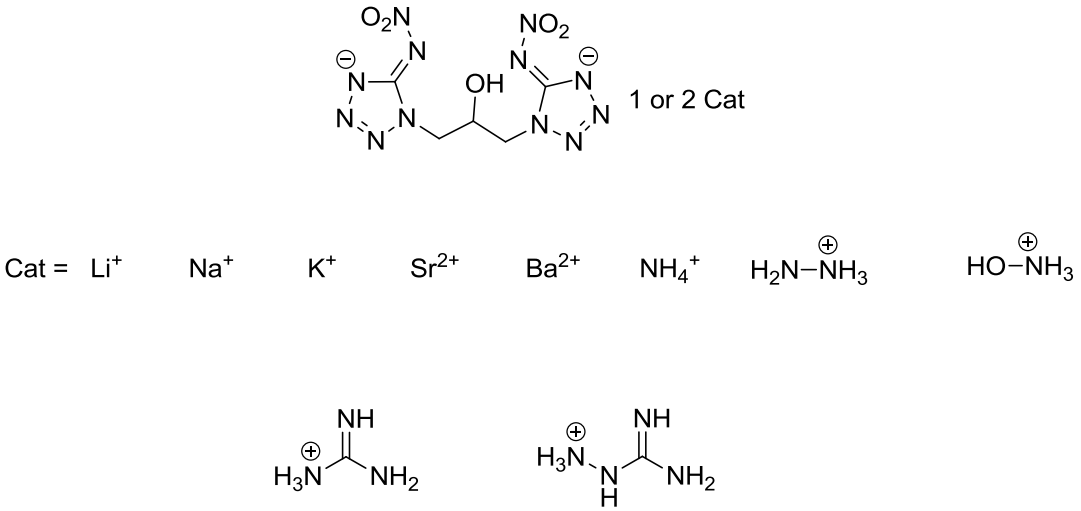

Figure 32: Metal- and nitrogen-rich salts synthesized within this thesis.

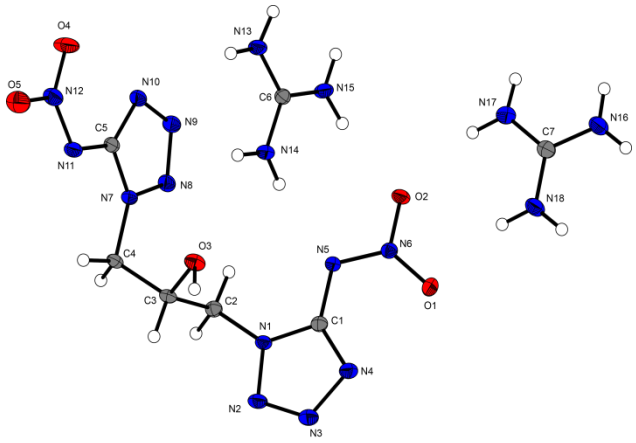

Figure 33: Representative molecular structure of one nitrogen-rich salt.

6.9 Gas-phase concentration determination of DADP and TATP

The ninth paper contributing to this thesis deals with the determination of the gas-phase concentrations of DADP and TATP by transpiration method. Gas-phase concentrations and vapor pressures for DADP and TATP are well known and different determination methods along with the corresponding values are published. However since those substances gain more and more prominence today in times of growing terrorism and because the literature values for TATP scatter vastly, there is always a need to determine the gas phase concentration by new ways and to put emphasize on new not investigated details. One of those details is polymorphism of the cyclic compounds. In this study, it was possible to show, that for DADP the determined values correlate well with the ones published in literature. However for TATP quite strong deviations from literature values can be observed showing that polymorphism plays an important role in gas-phase studies of TATP. The results are not submitted or published yet. Publication is planned in *Propellants Explosives Pyrotechnics.*

7 General summary of this thesis

Within this thesis it was possible to prepare a number of new energetic organic peroxides of different subclasses namely peroxy esters, peroxy acids, geminal dihydroperoxides, peroxy anhydrides and different cyclic peroxy acetals, and investigate them with respect to their energetic properties especially the sensitivities towards impact, friction, electrostatic discharge and heat as well as their calculated performance values consisting of detonation velocity, detonation pressure, heat of explosion, temperature of explosion and volume of detonation products. This alone is remarkable since until today only very few peroxides are investigated in terms of their energetic performances and thus this thesis gives a hitherto unknown insight in the energetic materials properties of organic peroxides. By taking all results obtained during this study into account it can be shown, that there are significant differences between the subgroups of organic peroxides with respect to their energetic properties. The examined organic peroxo-acetals and (di)hydroperoxides are all very sensitive (IS around 1.5 J, FS around 6 N) and thermally instable compounds (decomposition point around 120 °C). However different subclasses aromatic like peroxy acids, aromatic tert- butyl peroxy esters and aromatic peroxy anhydrides show reduced sensitivity, which can result from an electron delocalization, and from this point of view can possibly find application as additional energetic groups in modern energetic materials. Also the aromatic core structures seem to decrease the sensitivity. The most promising class of peroxo based molecules for a possible application in the design of modern energetic materials is the one of aromatic peroxy anhydrides. They feature relatively high thermal decomposition points, sometimes even above 160 °C, and their sensitivity is still acceptable. Also the performance values are in the range of commonly used secondary explosives. In addition their density is remarkable high (up to around 1.7 g cm^{-3}) in comparison with other organic peroxides and they are inevitably stable at room temperature. Moreover some other peroxidic compounds synthesized within this thesis show calculated performance values, which are in the range of commonly used secondary explosives. By and large the calculated detonation velocity seems to be independent form the examined peroxide class since all compound families show values in the same range. Grounding on the achieved results, it might be possible to add organic peroxides to the modern design of energetic materials, especially in the oxidizer sector where oxygen rich substances are needed, but where the requirements towards thermal stability are not extreme.

8 References

[1] ASTM International, http://www.astm.org, accessed May 24, 2015.

[2] T. M. Klapötke *Chemie der Hochenergetischen Materialien*, 1. Auflage, de Gruyter, Berlin **2009**.

[3] T. M. Klapötke, T. G. Witkowski, *Propellants Explos. Pyrotech.* **2015**, *40*, 366-373.

[4] T. G. Witkowski, *private communication*.

[5] J. Köhler, R. Meyer, A. Homburg: *Explosivstoffe*, 10. , vollständig überarbeitete Auflage, Wiley-VCH Weinheim **2008**.

[6] C. M. Traver, T. C. Goodale, M. Coperthwaite, M. E. Hill, Structure/Property correlations in primary explosives **1977**, found on www.researchgate.net, accessed June 3, 2016.

[7] F. M. Garfield, H. W. Dreher *US patent*, **1946**, No 2 408 059.

[8] P. Greifs, *Annal. D. Chem.* **1858**, *106*, 123-125.

[9] D. Fischer, T. M. Klapötke, J. Stierstorfer, *Angew. Chem.* **2014**, *53*, 8172-8175.

[10] S. Rose, *The Navel Miscellany*, volume VII, Ashgate **2008**.

[11] www.imrpowder.com , accessed June 21, 2016.

[12] H. Schück, R. Sohlman, W. v. d. Mülbe, *Alfred Nobel*, 2. Auflage, P. List, Leipzig **1933**.

[13] R. E. Tarone, L. Lipworth, J. K. McLaughlin, *Journal of occupational and environmental Medicine* **2010**, *6*, 653.

[14] G. P. Sutton, *Rocket Propulsion Elements*, 7th edition, Wiley and sons **2001**.

[15] J. Glück, T. M. Klapötke, M. Rusan, J. Stierstorfer, *Chem. Eur. J.* **2014**, *20*, 15947-15960.

[16] E. C. Koch, C. Jennings-White, *Proceedings of the International Pyrotechnics* Seminar **2009**, *36*, 105-110.

[17] T. M. Klapötke, M. Rusan, V. Sproll, *Z. Anorg. Allg. Chem.* **2013**, *14*, 2433-2443.

[18] T. M. Klapötke, B. Krumm, M. Rusan, J. J. Sabatini, *Chem. Commun.* **2014**, *50*, 9581-9583.

[19] A. F. Holleman, E. Wiberg, *Lehrbuch der Anorganischen Chemie*, 102. Auflage, DeGryter, Berlin, New York, **2007**.

[20] T. L. Davis, *The Chemistry of Powder and Explosives*, volume 2, 1st edition, **1943**.

[21] W. Finze, J. Görtz, *Fremde Gewehre in Deutschen Diensten 1914-1918*, Books on Demand GmbH, **2003**.

[22] J. Gratz, *Vom Griechischen Feuer zum Dynamit-eine Kulturgeschichte der Explosivstoffe*, 1. Auflage, E. S. Mittler & Sohn, Hamburg, Berlin, Bonn **2007**.

[23] Giovanni Boaga, *Storia di Scienza*, Friday, January 10th **2014**, www.giovanniboaga.blogsport.de, accessed May 25, **2015**.

[24] R. Haas, *Lexikon der Deutschen Explosivstoffmischungen*, www.r-haas.de, accessed August 4, 2016.

[25] W. E. Bachmann, J. C. Sheenan, *J. Am. Chem. Soc.* **1949**, *71*, 1842-1845.

[26] M.-X. Zhang, P. E. Eaton, R. Gilardi, *Angew. Chem.* **2000**, *112*, 422-426.

[27] A. T. Nielsen, R. A: Nissan, D. J. Vanderah, C. L. Coon, R. D. Gilardi, C. F. George, J. Flippen-Anderson, *J. Org. Chem.* **1990**, *55*,1459-1466.

[28] J. H. Boyer, T. V. Ramakrishnan, M. Vedachalam, *Heterocycles* **1990**, *31*, 479-480.

[29] N. Latypov, A. Langlet, U. Wellmar, *WO 9903818 A1*, **1999**.

[30] N. Latypov, A. Langlet, *WO 9946202 A1*, **1999**.

[31] N. Fischer, D. Fischer, T. M. Klapötke, D. G. Piercey, J. Stierstorfer, *J. Mater. Chem.* **2012**, *38*, 20418-20422.

[32] T. M. Klapötke, T. G. Witkowski, *ChemPlusChem* **2016**, *4*, 357-360.

[33] E. Riedel, Ch. Janiak, *Anorganische Chemie*, 7. Auflage, Walter de Gruyter, Berlin, **2007**.

[34] G. P. Kennedy, Vengeance Weapon 2: The V-2 Guided Missile. Washington DC: Smithsonian Institution Press, **1983**.

[35] B. Stüwe, *Peenemünde West*, Weltbild **1998**.

[36] B. J. Ford, *Secret Weapons*, Osprey Publishing, **2011**.

[37] J. Christpher, *The Race for Hitler´s X-Planes*, The Mill, Gloucestershire: History Press, **2013**.

[38] R. Wolffenstein, *Ber. Dtsch. Chem. Ges.* **1895**, *28*, 2265-2269.

[39] R. Matyas, J. Pachman, *Propellants Explos. Pyrotech.* **2010**, *35*, 31-37.

[40] H. Jiang, G. Chu, H. Gong, Q. Qiao, *J. Chem. Res.* **1999**, *28* (4), 288-289.

[41] R. Wolffenstein, *Deutsches Reichspatent* **1895**, *84*, 953.

[42] K. B. Landenberger, O. Bolton, A. J. Matzger, *Angew. Chem. Int. Ed.* **2013**, *52*, 6468-6471.

[43] K. B. Landenberger, O. Bolton, A. J. Matzger, *J. Am. Chem. Soc.* **2015**, *137*, 5074–5079.

[44] L. Leger, *Eur. J. Inorg. Chem.* **1885**, *18*, 3343-3351.

[45] C. A. Taylor, W. H. Rinkenbach, *Army Ordnance* **1924**, *5*, 463–466.

[46] A. Wierzbicki, E. A. Slater, E. A. Cioffi, E. D: Stevens, *J. Phys. Chem. A* **2001**, *105*, 8763-8768.

[47] N. Milas, A. Golubovic, *J. Am. Chem. Soc.* **1959**, *21*, 5824-5826.

[48] V. Bulatov, O. Reany, R. Grinko, I. Schechter, E. Keinan, *Phys. Chem. Chem. Phys.* **2013**, *15*, 6041-6048.

[49] M. R. Miner, K. A. Woerpel, *Eur. J. Org. Chem.* **2016**, *10*, 1860-1866.

[50] M. Trommer, W. Sander, *Organometallics* **1996**, *15*, 189-193.

[51] H. Ikeda, Y. Hoshi, T. Miyashi, *Tetrahedron Lett.* **2001,** *42*, 8485-8488.

[52] H. Klenk, P. H. Götz, R. Siegmeier, W. Mayr, *Ullmann´s Encyclopedia of Industrial Chemistry*.

[53] Baeyer, Walter, *Lehrbuch der Organischen Chemie*, 23. Auflage, S. Hirzel Verlag Stuttgart **1998**.

[54] O. E. Edwards, D. C: Gillespie, *Tetrahedron Lett.* **1966**, *40*, 4867-4870.

[55] J. M. Fukuto, D. J. Stuehr, P. L. Feldman, M. P Bova, P. Wong, *J. Med. Chem.* **1993**, *36*, 2666-2670.

[56] B. Brobanski, L. Kochanska, A. Kowalewska, *Ber. Dtsch. Chem. Ges.* **1938**, *71*, 2385-2388.

[57] M. A. Weiner, *J. Organomet. Chem.* **1970**, *23*, C20-C22.

[58] J. Meisenheimer, *Ber. Dtsch. Chem. Ges.* **1926**, *59*, 1848-1853.

[59] L.H. Miller, X. Su, Cell **2011**, *146*, 855-858.

[60] L. H. Binh, N. T. T. Van, V. T. Kien, N. T. T. My, L. V. Chinh, N. T. Nga, H. X. Tien, D. T. Thao, T. K. Vu, *Med. Chem. Res.* **2016**, *25*, 738-750.

[61] N. Surineni, P. Buragohain, N. C. Barua, *Mol. Divers.* **2015**, *19*, 717-724.

[62] P. Cravo, H. Napolitano, R. Culleton, *Acta Tropica* **2015**, *148*, 1–7.

[63] K. Zmitek, St. Stavber, M. Zupan, D. Bonnet-Delpon, S. Charneau, P. Grellier, J. Iskra, *Bioorg. Med. Chem.* **2006**, *14*, 7790-7795.

[64] P. Zhu, B. MK. Tong, R. Wang, J. P. Chen, S. Foo, H. C. Chong, X. L. Wang, G. Y. Ang, S. Chiba, N. S. Tan, *Cell Death Dis.* **2013**, *4*

[65] N. A. Milas, O. L. Magelli, A. Golubovic, R. W. Arndt, J. C. J. Ho, *J. Am. Chem. Soc.* **1963**, *24*, 222–226.

[66] A. O. Terent'ev, I. A. Yaremenko, V. A. Vil, I. K. Moiseev, S. A. Kon'kov, V. M. Dembitsky, D. O. Levitska, G. I. Nikishin, *Org. Biomol. Chem.* **2013**, *11*, 2613–2623.

[67] A. O. Terent'ev, D. A. Borisov, V. V. Chernyshev, G. I. Nikishin, *J. Org. Chem.* **2009**, *74*, 3335–3340.

[68] K. Ingarm, I. A. Yaremenko, I. B. Krylov, L. Hofer, A. O. Terent'ev, J. Keiser, *J. Med. Chem.* **2012**, *55*, 8700–8711.

[69] T. M. Klapötke, B. Stiasny, J. Stierstorfer, C. H. Winter, *Eur. J. Org. Chem.* **2015**, *28*, 6237-6242.

[70] K. Žmitek, M. Zupan, S. Stavber, J. Iskara *J. Org. Chem.* **2007,** *72*, 6534–6540.

[71] B. Das, M. Krishnaiah, B. Veeranjaneyulu, B. Ravikanth, *Tetrahedron Letters* **2007**, *48*, 6286-6289.

[72] D. Azarifar, K. Khosravi, F. Soleimanei, *Synthesis* **2009**, No15, 2553-2556.

[73] B. Das, B. Veeranjaneyulu, M. Krishnaiah, B. Balasubramanyam, *Journal of molecular catalysis A: chemical* **2008**, *284*, 116-119.

[74] G. P. Romanelli, A. G. Sthicq, J. C. Autino, H. J. Thomas, T. G. Baronetti, *Afinidad* **2007**, *64*, 535-537.

[75] J. C. Oxley, *private communication*.

[76] H. Becker, K. Schwetlick, *Organikum*, 21. Auflage, Wiley-VCH, **2001**

[77] W. J. Baader, E. L. Bastos, *Science of Snythesis* **2009**, *38*, 323-344.

[78] T. V. Robinson, D. S. Pedersen, D. K. Taylor, E. R. T. Tiekink, *J. Org. Chem.* **2009**, *74*, 5093-5096.

[79] K. Yamaguchi, T. Fueno, I. Saito, T. Matsuura, K. N. Houk, *Tetrahedron Lett.* **1981**, *22*, 749-752.

[80] C. Schweitzer, R. Schmidt, *Chem. Rev.* **2003**, *103*, 1685-1757.

[81] A. Greer, *Acc. Chem. Res.* **2006**, *39*, 797-804.

[82] N. Milas, A. Golubovic *J. Am. Chem. Soc.* **1959**, *21*, 5824-5826.

[83] F. Cataldo, *Tetrahedron Lett.* **2015**, *56*, 994-998.

[84] H. Keul, R. L Kuczkowski, *J. Org. Chem.* **1985**, *50*, 3371-3376.

[85] A. J. Kendall, J. T. Barry, D. T. Seidenkranz, A. Ryerson, C. Hiatt, C. A. Salazar, D. J. Bryant, D. R. Tyle, *Tetrahedron Lett.* **2016**, *57*, 1342-1345.

[86] S. S. Medwedew, E. N. Alexejewa, *Chem. Ber.* **1932**, *65*, 137–142.

[87] R. Criegee, G. Müller, *Chem. Ber.* **1956**, *89*, 238–240.

[88] R. Amewu, A. V. Stachulski, S. A. Ward, N. G. Berry, P. G. Bray, J. Davies, G. Labat, L. Vivas, P. M. O'Neill, *Org. Biomol. Chem.* **2006**, *4*, 4431-4436.

[89] O. S. Kukovinets, T. I. Zvereva, N. N. Kabalnova, V. G. Kasradze, E: V. Salimova, L.

R. Khalitova, M. I. Abdullin, L. V. Spirikhin, *Mendeleev Commun.* **2009**, *19*, 106-107.

[90] Y. Dong, J. L. Vennerstrom, *J. Heterocycl. Chem.* **2001**, *38*, 463-466.

[91] Y. Dong, J. L. Vennerstrom, *J. Org. Chem.* **1998**, *63*, 8582-8585.

[92] T. Tokuyasu, S. Kunikawa, K. J. McCullough, A. Masuyama, M. Nojima, *J. Org. Chem.* **2005,** *70*, 251-260.

[93] K. Griesbaum, Ö. Bikem, T. S. Huh, Y. Dong, *Liebigs Ann.* **1995**, 1571-1574.

[94] H. Ikeda, K. Akiyama, Y. Takahashi, T. Nakamura, S. Ishizaki, Y. Shiratori, H. Ohaku, J. L. Goodman, A. Houmam, D. D. M. Wayner, S. Tero-Kubota, T. Miyashi, *J. Am. Chem. Soc.* **2003**, *125*, 9147-9157.

[95] L. B. Berehevich et al., Vestsi Akademii Navuk BSSR, Seryya Khimichnykh Navuk **1991**, (1), 116-118.

[96] G. Vassilikogiannakis, T. Montagnon, *Science of Synthesis* **2009**, *38*, 179-204.

[97] Y. Hamada, H. Tokuhara, A. Masuyama, M. Nojima, H.-S. Kim, K. Ono, N. Ogura, Y. Wataya, *J. Med. Chem.* **2002**, *6*, 1374-1378.

[98] A. G. van de Bovenkamp-Bouwman, J. W. J. van Gendt, J. Meijer, A. H. Hogt, A. P. van Swieten, From PCT Int. Appl. **1999**, WO 9932442 A1 19990701.

[99] Bundesanstalt für Materialforschung und -prüfung, http://www.bam.de, accessed December 31, 2012.

9 Appendix

Most results contributing to this thesis are published in peer reviewed journals or submitted to publication. Permissions for using the results within this thesis were obtained from the respective publishing companies and licenses for the individual journals were provided by the University of Munich. The permissions of the publishing companies Wiley VCH and RSC are highly acknowledged. In cases where manuscripts are still in the review process, the most recent draft is used. This is also true for not published results.

ChemPubSoc Europe

DOI: 10.1002/chem.201502989

CHEMISTRY
A European Journal
Communication

Peroxides

Highly Energetic, Low Sensitivity Aromatic Peroxy Acids

Nipuni-Dhanesha H. Gamage,[a] Benedikt Stiasny,[b] Jörg Stierstorfer,[b] Philip D. Martin,[a] Thomas M. Klapötke,*[b] and Charles H. Winter*[a]

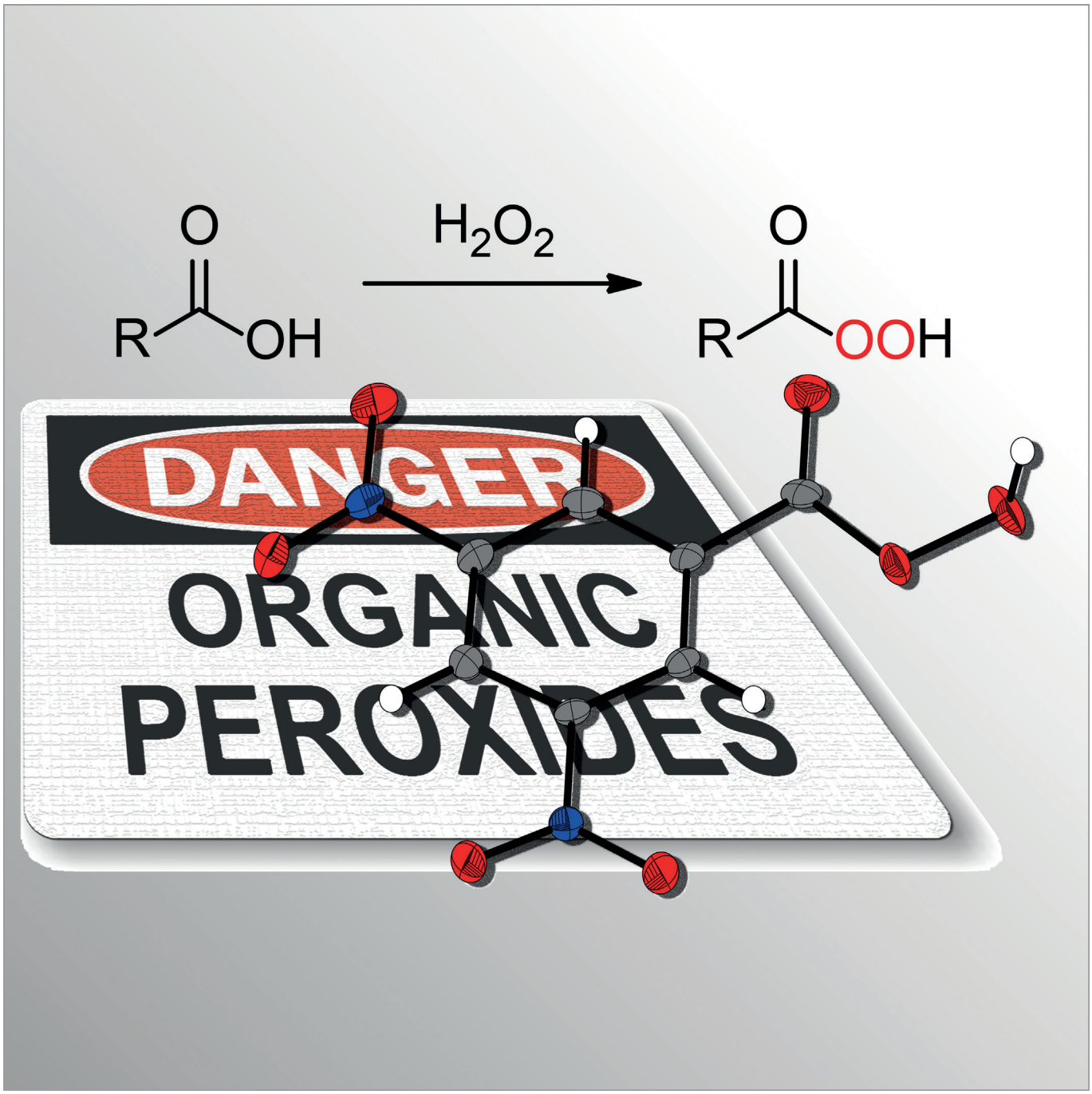

Abstract: The synthesis, structure, and energetic materials properties of a series of aromatic peroxy acid compounds are described. Benzene-1,3,5-tris(carboperoxoic) acid is a highly sensitive primary energetic material, with impact and friction sensitivities similar to those of triacetone triperoxide. By contrast, benzene-1,4-bis(carboperoxoic) acid, 4-nitrobenzoperoxoic acid, and 3,5-dinitrobenzoperoxoic acid are much less sensitive, with impact and friction sensitivities close to those of the secondary energetic material 2,4,6-trinitrotoluene. Additionally, the calculated detonation velocities of 3,5-dinitrobenzoperoxoic acid and 2,4,6-trinitrobenzoperoxoic acid exceed that of 2,4,6-trinitrotoluene. The solid-state structure of 3,5-dinitrobenzoperoxoic acid contains intermolecular O-H···O hydrogen bonds and numerous N···O, C···O, and O···O close contacts. These attractive lattice interactions may account for the less sensitive nature of 3,5-dinitrobenzoperoxoic acid.

The compounds triacetone triperoxide (TATP), diacetone diperoxide (DADP), hexamethylene triperoxide diamine (HMTD), and methyl ethyl ketone peroxide (MEKP) are the only peroxides for which detailed energetic materials properties have been determined.[1–3] These peroxides are extremely sensitive to stimuli and are dangerous to handle.[1–3] Other issues include a low decomposition temperature for HMTD (75 °C),[1a] high volatilities for TATP and DADP,[1,2] and calculated detonation velocities for TATP (6168 m s^{-1}), DADP (6773 m s^{-1}), and MEKP (6191 m s^{-1}) that are much lower than those of high nitrogen explosives such as RDX (8750 m s^{-1}) and HMX (9100 m s^{-1}).[1a] These issues, particularly the high sensitivities, have prohibited military and civilian energetic materials applications of TATP, DADP, HMTD, and MEKP. Moreover, the high sensitivities have likely limited more extensive exploration of peroxo compounds as energetic materials. Peroxo-based compounds might serve as useful explosives if their sensitivities can be adjusted to optimum levels for specific applications and also to allow safe handling. A recent report demonstrated that co-crystals of DADP and 1,3,5-triiodo-2,4,6-trinitrobenzene (TITNB) have reduced impact sensitivity compared to both pure DADP and TITNB, because of I···O close contacts in the co-crystals.[4] We have also recently described the synthesis, structure, and energetic materials properties of oxygen-rich organic compounds containing bis(hydroperoxy)-methylene groups that are less sensitive than TATP, DADP, HTMD, and MEKP.[5] Herein, we report the synthesis, structure, and energetic materials properties of four aromatic peroxy acids. Remarkably, three of these compounds have low sensitivities, very high energy contents, and have properties appropriate for application as secondary energetic materials. These are the first peroxide-based compounds that can be classified as secondary explosives. Structural data point to stabilization of the labile oxygen–oxygen bonds through hydrogen bonding and intermolecular N···O, C···O, and O···O close contacts.

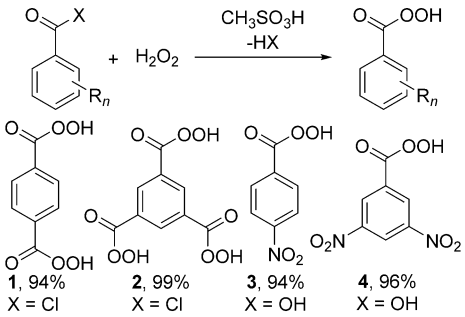

Scheme 1. Synthesis of **1**–**4**.

Peroxy acids **1**–**4** were prepared in high yields, as depicted in Scheme 1. Compounds **3** and **4** were prepared by literature procedures entailing treatment of the carboxylic acids with 84% H_2O_2 in the presence of methanesulfonic acid.[6] Compounds **1** and **2** were prepared under similar conditions from the acid chlorides and 84% H_2O_2.[7] Importantly, **1**–**4** precipitate from the reaction solutions upon cooling to near 0 °C and can be isolated as pure materials by filtration and subsequent air drying. Minimal synthetic manipulation is a great advantage in the synthesis of highly energetic compounds. Attempts to prepare peroxy acids using the acid chlorides derived from 1,2,4,5-benzene tetracarboxylic acid and mellitic acid led to violent reactions upon addition of H_2O_2, and the desired compounds could not be isolated. Compounds **1**–**4** were characterized with ^{1}H and ^{13}C NMR spectroscopy, infrared spectroscopy, and elemental analyses.[7] Additionally, the X-ray crystal structures of **1**·DMF and **4** were determined.[7] Crystals of **1**·DMF were used only for the X-ray experiment, whereas solvent-free **1** was used for all other measurements.

A perspective view of **4** is shown in Figure 1. The bond lengths in **4** are normal. The density of **4** is 1.748 g cm^{-3} at 100 K, which is higher than those of orthorhombic (1.704 g cm^{-3} at 123 K) and monoclinic (1.713 g cm^{-3} at 100 K) 2,4,6-trinitrotoluene (TNT).[8] Because the formula weights of **4** and TNT are almost identical, **4** packs more efficiently than TNT in the solid state. TNT does not contain any strong hydrogen bonds, and only van der Waals forces are present.[8] The asymmetric unit of **4** consists of two molecules situated in an edge-to-face fashion, with a close contact of 2.988 Å between an oxygen atom of a nitro group in one molecule and the π-face of a ring C–H carbon atom in the other molecule. The lattice contains intermolecular O-H···O hydrogen bonds, in addition to numerous N···O (2.993–3.054 Å), C···O (3.043–3.215 Å), and O···O (2.670–3.029 Å) close contacts that are within the van der Waals radii for N···O (3.07 Å), C···O (3.22 Å), and O···O (3.04 Å).[9]

[a] *N.-D. H. Gamage, Dr. P. D. Martin, Prof. Dr. C. H. Winter*
Department of Chemistry
Wayne State University, Detroit
Michigan 48202 (USA)
E-mail: chw@chem.wayne.edu

[b] *B. Stiasny, Dr. J. Stierstorfer, Prof. Dr. T. M. Klapötke*
Department of Chemistry
Ludwig-Maximilians University
Butenandtstr. 5–13 (D), 81377 München (Germany)
E-mail: tmk@cup.uni-muenchen.de

Supporting information for this article is available on the WWW under http://dx.doi.org/10.1002/chem.201502989.

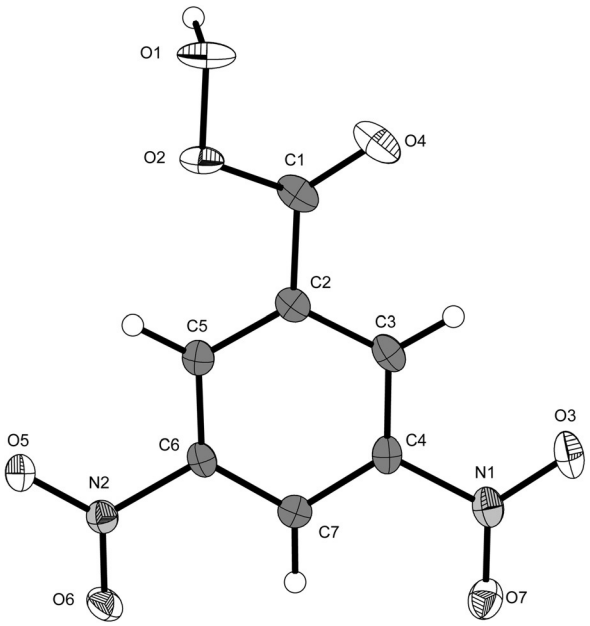

Figure 1. X-ray crystal structure of **4**. Selected bond lengths (Å): O1–O2 1.447(3), O2–C1 1.342(4), O4–C1 1.196(4).

Recent studies of energetic materials have shown that such close contacts are attractive because the dispersion forces are larger than the repulsive Coulombic forces.[10] Dissociation energies of O···O close contacts are similar to those of weak hydrogen bonds (3–13 kJ mol^{-1}).[10] Accordingly, much of the lattice energy in **4** arises from non-bonded interactions. Additionally, these non-bonded attractive interactions contribute to the high solid state density of **4**.

The thermal behaviour of **1**–**4** was studied using thermogravimetric analysis and differential thermal analysis. The compounds show decomposition onsets ranging from 132 to 160 °C (Table 1). A 200 mg sample of **4** was reported to explode just above its melting point of 112 °C.[6b] We observed no explosions with **4** up to 150 °C, but extreme care should be used when handling this compound. CBS-4M electronic enthalpies were calculated with the Gaussian 09 software package to obtain heats of formation values using the atomization equation.[11] The values are all exothermic, but **3** and **4** have the most positive heats of formation.

Table 1 gives detailed energetic test results for **1** and **3**–**5**. Impact, friction, and sensitivity toward electrostatic discharge were determined with a drop hammer, friction tester, and electrostatic discharge tester, respectively, using standard Bundesanstalt für Materialforschung und –prüfung (BAM) and electrostatic methods.[12] Sensitivity classifications are based on the "UN Recommendations on the Transport of Dangerous Goods".[13] Energetic performance was calculated using the EXPLO5 V6.02 software.[14] Compound **2** has an impact sensitivity of 1 J, a friction sensitivity of 5 N, and an electrostatic discharge of 0.025 J.[7] This electrostatic discharge value is close to what can be created by the human body ($\leq$0.02 J),[1b] so **2** must be handled with great care. Compounds **1**, **3**, and **4** have impact sensitivity values of 10 (**1**) and 9 (**3**, **4**) J and friction sensitivity values of 288 (**1**) and 360 (**3**, **4**) N. The calculated

Table 1. Sensitivities and energetic performance of **1** and **3**–**5**.

	1	**3**	**4**	**5**
Formula	$C_8H_6O_6$	$C_8H_6O_6$	$C_7H_4N_2O_7$	$C_7H_3N_3O_9$
FW [g mol^{-1}]	198.14	183.12	228.11	271.11
IS [J][a]	10	9	9	—
FS [N][b]	288	360	360	–
ESD [J][c]	0.1	0.1	0.1	–
Ω_{CO2} [%][d]	−105.0	−100.5	−63.13	−38.4
T_{Dec} [°C][e]	160	141	132	–
ρ [g cm^{-3}][f]	1.423	1.586[m]	1.748	1.80[n]
$\Delta_f H°$ [kJ mol^{-1}][g]	−584.1	−324.3	−310.9	−275.5
$\Delta_{Ex}U°$ [kJ kg^{-1}][h,i]	−3373	−3590	−4660	−5243
P_{CJ} [kbar][h,j]	88	133	213	269
V_{Det} [m s^{-1}][h,k]	5262	6176	7217	7885
V_o [L kg^{-1}][h,l]	598	628	596	619

[a] BAM drophammer. [b] BAM friction. [c] Electrostatic discharge sensitivity. [d] Oxygen balance for CO_2. [e] Decomposition temperature from DTA (5 °C min^{-1}). [f] Density from X-ray diffraction for **1**·DMF and **4** at −173 °C. [g] Calculated molar enthalpy of formation. [h] Calculated using EXPLO5V6.02. [i] Total energy of detonation. [j] Detonation pressure. [k] Detonation velocity. [l] Volume of detonation products. [m] Published crystal density.[14] [n] Estimated density at 25 °C.

detonation performance values increase in going from **1** to **4**. The calculated detonation pressure (P_{CJ}) range from 88 kbar for **1** to 213 kbar for **4**. The calculated detonation velocities increase from 5262 to 7217 m s^{-1} for **1** and **4**, respectively.

The extremely high performance values and low sensitivity of **4** prompted us to consider the more highly nitrated peroxy acid **5**. Synthetic approaches to **5** are ongoing, but the performance parameters were calculated using EXPLO5.[14] Using an estimated solid-state density of 1.80 g cm^{-3} based upon those of **3**[15] and **4**, the calculated detonation pressure of **5** is 269 kbar and the calculated detonation velocity is 7885 m s^{-1}.

The present work documents the energetic materials properties of peroxy acids **1**–**5**. Compound **2** is "very sensitive" and "extremely sensitive" to impact and friction, respectively, according to the UN recommendations,[13] with values that are in the same range as those of TATP.[1,2] By contrast, **1**, **3**, and **4** are much less sensitive than **2**, TATP, DADP, HMTD, and MEKP. According to the UN Recommendations,[13] **1**, **3**, and **4** are "sensitive" toward impact and "less sensitive" to "insensitive" toward friction. These impact and friction sensitivity values are very similar to those of TNT, which is a widely used secondary explosive.[1] Hence, **1**, **3**, and **4** can also be classified as secondary explosives. These are the first peroxide-based secondary explosives. Moreover, the detonation velocity of **4** (7217 m s^{-1}) exceeds that of TNT (6900 m s^{-1}). The detonation velocity of **5** (7885 m s^{-1}) is much higher than those of **4** and TNT, but is less than that of RDX (8750 m s^{-1}).[1] Hence, **4** and **5** are powerful explosives, which likely arises from higher solid-state densities compared to TATP, DADP, HMTD, and MEKP.[1–3]

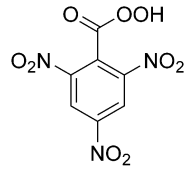

5

There is no single structural feature in **1**, **3**, and **4** that can explain their reduced sensitivities relative to **2**, TATP, DADP, HMTD, and MEKP. Low sensitivity, high energy explosives tend to pack

in layered structures with hydrogen bonds within each layer, but only weak van der Waals interactions between the layers.[10] These materials can absorb shocks by allowing interlayer sliding without covalent bond breaking.[10c] By contrast, high sensitivity, high energy explosives tend to have structures that do not allow facile dissipation of shocks, which leads to hot spots, covalent bond breaking, and explosions.[10b] Compound **3** contains a wave-like packing arrangement,[7,15] which has been previously proposed as a structural motif that allows shock dissipation in low sensitivity, high energy explosives.[10c] The lattice of **3** contains O-H···O hydrogen bonds, three O···O close contacts (2.740–2.965 Å), and one N···O close contact (3.063 Å).[7,15] Examination of the packing in **4** does not show a layered structure like those observed in low sensitivity, high energy explosives.[10c] The low sensitivity of **4** may arise from the presence of intermolecular O-H···O hydrogen bonds and the numerous N···O (5 interactions), C···O (5 interactions), and O···O (7 interactions) close contacts, which stabilize the lattice and could allow dissipation of shock without covalent bond breaking. In this vein, the reduced sensitivity of DADP/TITNB co-crystals was proposed to originate from attractive I···O close contacts that stabilize the covalent oxygen–oxygen and iodine–carbon bonds.[4] As comparisons, the solid-state structures of highly sensitive DADP and TATP have no O···O close contacts, and contain only very weak O···H and C···H interactions.[2b,7] Features in **3** and **4** that are lacking in DADP and TATP include the O-H···O hydrogen bonding and the N···O, C···O, and O···O close contacts. We propose that these structural motifs stabilize the lattices and contribute to the low sensitivities of **1**, **3**, and **4**. In particular, the O···O close contacts in **4** likely stabilize the labile oxygen–oxygen bonds and make bond cleavage less favorable. The sterically unconstrained nature of the oxygen and nitrogen atoms in peroxy acid and nitro groups allows more intermolecular close contacts, relative to the peroxo groups in DADP and TATP.

As a cautionary note, **4** has been suggested a "safe" oxygen transfer reagent for epoxidations and other oxygen transfer reactions.[6b] The highly energetic nature of **4** advises against its large-scale synthesis. Finally, there is significant interest in the development of high-energy dense oxidizers to replace ammonium perchlorate.[1] Though the oxygen balances of **1**–**5** are all negative (−105 to −38%) and ammonium perchlorate is positive (34%[1]), the present work suggests that incorporation of peroxy acid groups in energetic materials structures can make the oxygen balance more positive without increasing sensitivity and decreasing performance. It has been reported that the active oxygen content of **4** is reduced from 93.5% to 84.0% upon standing at ambient temperature for 80 days.[6b] Accordingly, further studies are needed to explore the thermal stability, sensitivity upon heating, and chemical compatibility of peroxy acid derivatives as potential explosives.

Acknowledgements

The authors acknowledge generous support from the Office of Naval Research (Grant No. N00014-12-1-0526 to C.H.W., Grant No. N00014-12-1-0538 to T.M.K.).

Keywords: explosives · hydrogen bonding · peroxides · sensitivities · structure elucidation

[1] a) T. M. Klapötke, T. Wloka in *Patai's Chemistry of Functional Groups*, (Ed.: S. Patai), Wiley, Chichester, **2014**, pp. 1–28; b) T. M. Klapötke, *Chemistry of High-Energy Materials, 2nd ed.*, de Gruyter, Berlin/Boston, **2012**.

[2] a) J. C. Oxley, J. L. Smith, H. Chen, *Propellants Explos. Pyrotech.* **2002**, *27*, 209–216; b) F. Dubnikova, R. Kosloff, J. Almog, Y. Zeiri, R. Boese, H. Itzhaky, A. Alt, E. Keinan, *J. Am. Chem. Soc.* **2005**, *127*, 1146–1159; c) C. Denekamp, L. Gottlieb, T. Tamiri, A. Tsoglin, R. Shilav, M. Kapon, *Org. Lett.* **2005**, *7*, 2461–2464; d) O. Reany, M. Kapon, M. Botoshansky, E. Keinan, *Cryst. Growth Des.* **2009**, *9*, 3661–3670; e) R. Matyáš, J. Šelešovský, *J. Hazard. Mater.* **2009**, *165*, 95–99; f) A. E. Contini, A. J. Bellamy, L. N. Ahad, *Propellants Explos. Pyrotech.* **2012**, *37*, 320–328; g) G. R. Peterson, W. P. Bassett, B. L. Weeks, L. J. Hope-Weeks, *Cryst. Growth Des.* **2013**, *13*, 2307–2311; h) J. C. Oxley, J. L. Smith, L. Steinkamp, G. Zhang, *Propellants Explos. Pyrotech.* **2013**, *38*, 841–851; i) V. P. Sinditskii, V. I. Kolesov, V. Y. Egorshev, D. I. Patrikeev, O. V. Dorofeeva, *Thermochim. Acta* **2014**, *585*, 10–15.

[3] J. C. Oxley, J. L. Smith, H. Chen, E. Cioffi, *Thermochim. Acta* **2002**, *388*, 215–225.

[4] K. B. Landenberger, O. Bolton, A. J. Matzger, *J. Am. Chem. Soc.* **2015**, *137*, 5074–5079.

[5] N.-D. H. Gamage, B. Stiasny, J. Stierstorfer, P. D. Martin, T. M. Klapötke, C. H. Winter, *Chem. Commun.* **2015**, *51*, 13298–13300.

[6] a) D. G. Harman, A. Ramachandran, M. Gracanin, S. Blanksby, *J. Org. Chem.* **2006**, *71*, 7996–8005; b) W. H. Rastetter, T. J. Richard, M. D. Lewis, *J. Org. Chem.* **1978**, *43*, 3163–3166.

[7] See the Supporting Information. CCDC 1407222 (**1**·DMF) and 1407223 (**4**) contain the supplementary crystallographic data for this paper. These data are provided free of charge by The Cambridge Crystallographic Data Centre.

[8] R. M. Vreclj, J. N. Sherwood, A. R. Kennedy, H. G. Gallagher, T. Gelbrich, *Cryst. Growth Des.* **2003**, *3*, 1027–1032.

[9] M. Mantina, A. C. Chamberlain, R. Valero, C. J. Cramer, D. G. Truhlar, *J. Phys. Chem. A* **2009**, *113*, 5806–5812.

[10] a) C. J. Eckhardt, A. Gavezzotti, *J. Phys. Chem. B* **2007**, *111*, 3430–3437; b) Y. Ma, A. Zhang, X. Zue, D. Jiang, Y. Zhu, C. Zhang, *Cryst. Growth Des.* **2014**, *14*, 6101–6114; c) Y. Ma, A. Zhang, C. Zhang, D. Jiang, Y. Zhu, C. Zhang, *Cryst. Growth Des.* **2014**, *14*, 4703–4713.

[11] Gaussian 09, Revision A.01, M. J. Frisch, G. W. Trucks, H. B. Schlegel, G. E. Scuseria, M. A. Robb, J. R. Cheeseman, G. Scalmani, V. Barone, B. Mennucci, G. A. Petersson, H. Nakatsuji, M. Caricato, X. Li, H. P. Hratchian, A. F. Izmaylov, J. Bloino, G. Zheng, J. L. Sonnenberg, M. Hada, M. Ehara, K. Toyota, R. Fukuda, J. Hasegawa, M. Ishida, T. Nakajima, Y. Honda, O. Kitao, H. Nakai, T. Vreven, J. A. Montgomery, Jr., J. E. Peralta, F. Ogliaro, M. Bearpark, J. J. Heyd, E. Brothers, K. N. Kudin, V. N. Staroverov, R. Kobayashi, J. Normand, K. Raghavachari, A. Rendell, J. C. Burant, S. S. Iyengar, J. Tomasi, M. Cossi, N. Rega, J. M. Millam, M. Klene, J. E. Knox, J. B. Cross, V. Bakken, C. Adamo, J. Jaramillo, R. Gomperts, R. E. Stratmann, O. Yazyev, A. J. Austin, R. Cammi, C. Pomelli, J. W. Ochterski, R. L. Martin, K. Morokuma, V. G. Zakrzewski, G. A. Voth, P. Salvador, J. J. Dannenberg, S. Dapprich, A. D. Daniels, Ö. Farkas, J. B. Foresman, J. V. Ortiz, J. Cioslowski, D. J. Fox, Gaussian, Inc. Wallingford CT, **2009**.

[12] a) NATO Standardization Agreement (STANAG) on Explosives, *Impact Sensitivity Tests*, No. 4489, 1st ed., Sept. 17, **1999**; b) WIWEB-Standardarbeitsanweisung 4–5.1.02, Ermittlung der Explosionsgefährlichkeit, hier der Schlagempfindlichkeit mit dem Fallhammer, Nov. 8, **2002**; c) http://www.bam.de; d) NATO Standardization Agreement (STANAG) on Explosives, *Friction Sensitivity Tests*, No. 4487, 1st ed., Aug. 22, **2002**.

[13] a) Test Methods According to the UN Manual of Tests and Criteria, Recommendations on the Transport of Dangerous Goods, United Nations Publications, New York, Geneva, 4th revised ed., **2003**; b) www.reichel-partner.de.

[14] M. Sućeska, *EXPLO5 V6.02 Program*, Brodarski Institute, Zagreb, Croatia, **2014**.

[15] H. S. Kim, S.-C. Chu, G. A. Jeffrey, *Acta Crystallogr. Sect. A* **1970**, *26*, 896–900.

Received: July 30, 2015
Published online on January 7, 2016

CHEMISTRY
A European Journal

Supporting Information

Highly Energetic, Low Sensitivity Aromatic Peroxy Acids

Nipuni-Dhanesha H. Gamage,[a] Benedikt Stiasny,[b] Jörg Stierstorfer,[b] Philip D. Martin,[a] Thomas M. Klapötke,*[b] and Charles H. Winter*[a]

chem_201502989_sm_miscellaneous_information.pdf

Supporting Information

Nipuni-Dhanesha H. Gamage,[a] Benedikt Stiasny,[b] Jörg Stierstorfer,[b] Philip D. Martin,[a] Thomas M. Klapötke,*[b] and Charles H. Winter*[a]

[a]Department of Chemistry, Wayne State University, Detroit, Michigan 48202, United States
[b]Department of Chemistry, Ludwigs-Maximilians University, Butenandtstr. 5-13 (D), 81377 München, Germany

1. Experimental Procedures

General Considerations

Chemicals were purchased from Sigma-Aldrich, Acros Organics, or Alfa Aesar and were used without further purification. ACS grade solvents were obtained from EMD and Fisher Scientific. Syntheses of **3** and **4** were carried out using published procedures.[1,2]

Hydrogen peroxide solution (50 wt. % in H_2O) was evacuated on a vacuum line (4-5 h per 5.0 mL) to obtain a concentrated hydrogen peroxide solution (84 wt. % in H_2O) for the syntheses of **1**-**4**. The final concentration of the hydrogen peroxide solution was analyzed by titrating with a solution of 0.176 M $KMnO_4$ under acidic conditions (H_2SO_4).

^1H and $^{13}C\{^1H\}$ NMR spectra were obtained at 400 MHz and 101 MHz, respectively, in $CDCl_3$, CD_3OD, or $(CD_3)_2NCOD$ as indicated and were referenced to the residual proton and carbon resonances of the solvents ($CDCl_3$, ^1H NMR δ 7.27; ^{13}C NMR 77.23 ppm. CD_3OD, ^1H NMR δ 3.31; ^{13}C NMR 49.00 ppm. $(CD_3)_2NCOD$, ^1H NMR δ 2.74; ^{13}C NMR 162.70 ppm). Infrared spectra were obtained with a Shimadzu MIRacle 10 IRAffinity-1 equipped with a single reflection ATR accessory. Melting points were determined on an Electrothermal IA 9300 melting point apparatus and are uncorrected. Thermogravimetric and differential thermal analysis (TGA/DTA) measurements to determine the decomposition temperatures of compounds **1**-**4** were performed at a heating rate of 5 °C min^{-1} with an OZM Research DTA 552-Ex instrument.

Caution. The H_2O_2 solutions are strong oxidizers that may cause explosions. All organic peroxides are explosive and require handling with extreme care. Compound **2** is very sensitive, and **1**-**4** are high explosives. Reactions and manipulations should be run in fume hoods behind blast shields. Personal safety gear should include a face shield, leather gloves, a leather apron, and hearing protection. Peroxide compounds should not come into contact with strong acids, metal salts, or easily oxidized species. All reactions should be performed on small scales.

Qualitative Energetic Properties. Qualitative sensitivities to heat, impact, and electrostatic discharge were determined to assess initial safety. Tests included burning about 3-5 mg of the compound in a Bunsen burner flame, striking 3-5 mg of the compound on a metal plate with a hammer, and passing an electrostatic discharge through 3-5 mg of the compound on a metal plate using an Electro Technic BD 10 Tesla coil (120 V, 0.35 A).

Benzene-1,4-bis(carboperoxoic) acid (1). A 100 mL round bottomed flask was charged with a magnetic stir bar and terephthaloyl chloride (0.105 g, 0.517 mmol). Then, methanesulfonic acid (0.4 mL, 5 mmol) was added and the reaction mixture was allowed to stir for 5-10 min at 50 °C. Afterwards, hydrogen peroxide solution (84 wt. % in H_2O, 0.25 mL, 4 mmol) was added dropwise and the reaction mixture was stirred for 1 h at 50 °C. The product mixture was cooled to 0 °C in an ice bath, and then crushed ice (0.5 g) was added to the reaction mixture. The resultant white precipitate was collected by suction filtration and was dried under reduced pressure to afford **1** (0.093 g, 94%) as a white solid: mp 165 °C, dec. (explodes); IR (ν, cm^{-1}) 3240 (m, broad), 3125 (w), 3107 (w), 3063 (w), 1715 (m), 1504 (w), 1414 (m), 1393 (m), 1304 (w), 1267 (m), 1250 (m), 1092 (m), 1015 (m), 895 (m), 866 (m), 845 (m), 714 (s); ^1H NMR (400 MHz, $(CD_3)_2NCOD$, 23 °C, δ) 14.18 (broad s, 1H, OO*H*), 8.06 (s, 4H, C*H*); $^{13}C\{^1H\}$

NMR (101 MHz, $(CD_3)_2NCOD$, 23 °C, ppm) 164.93 (peroxy *C*), 132.50 (*C*), 130.04 (*C*H). Anal. Calcd for $C_8H_6O_6$: C, 48.49; H, 3.06. Found: C, 48.10; H, 3.36. Sensitivity data: IS, 10 J; FS, 288 N; ESD, 0.1 J. Colorless needles of **1**•DMF suitable for X-ray crystallography were grown from DMF at -29 °C. The NMR spectra of **1**•DMF were identical to those of **1**, expect for the presence of DMF resonances.

Benzene-1,3,5-tris(carboperoxoic) acid (2). A dry 100 mL Schlenk flask was charged with a magnetic stir bar and benzene-1,3,5-tricarbonyl trichloride (0.105 g, 0.396 mmol). Then, methanesulfonic acid (0.5 mL, 6 mmol) was added and the reaction mixture was allowed to stir for 5-10 min at 50 °C. Afterwards, hydrogen peroxide solution (84 wt. % in H_2O, 0.30 mL, 4.8 mmol) was added dropwise and the reaction mixture was stirred for 30 min at 50 °C. The product mixture was cooled to 0 °C in an ice bath, and then crushed ice (0.5 g) was added into the reaction mixture. The white solid in the reaction mixture was collected by suction filtration and was dried under reduced pressure to afford **2** (0.101 g, 99%) as a white solid: mp not taken due to explosion hazard; IR (ν, cm^{-1}) 3226 (m, broad), 3087 (m), 1737 (s), 1608 (w), 1410 (m), 1326 (m), 1278 (m), 1224 (s), 1131 (m), 1115 (m), 1098 (m), 934 (w), 881 (m), 835 (w), 767 (w), 717 (s); ^{1}H NMR (400 MHz, CD_3OD, 23 °C, δ) OO*H* resonance not observed due to exchange with CD_3OD, 8.65 (s, 4H, C*H*); $^{13}C\{^1H\}$ NMR (101 MHz, CD_3OD, 23 °C, ppm) 164.95 (peroxy *C*), 134.52 (*C*), 130.51 (*C*H). Anal. Calcd for $C_9H_6O_9$: C, 41.87; H, 2.35. Found: C, 41.98; H, 2.36. Sensitivity data: IS, 1 J; FS, 5 N; ESD, 0.025 J.

4-Nitrobenzoperoxoic acid (3). Compound **3** was prepared in 94% yield as a pale yellow solid by a literature procedure[1] starting from 4-nitrobenzoic acid: mp 138-140 °C (lit[1] 139 °C); IR (ν, cm^{-1}) 3308 (broad, m), 3115 (w), 2986 (w), 1744 (m), 1718 (m), 1609 (m), 1541 (m), 1491 (w), 1414 (m), 1383 (m), 1348 (m), 1321 (m), 1302 (m), 1258 (m), 1242 (m), 1111 (w), 1074 (m), 1013 (w), 974 (w), 951 (w), 934 (w), 893 (m), 868 (m), 837 (s), 775 (w), 710 (s); ^{1}H NMR (400 MHz, $CDCl_3$, 23 °C, δ) 11.57 (broad s, 1H, OO*H*), 8.37 (dm, *J* = 8.4 Hz, 2H, C*H*), 8.21 (dm, *J* = 8.8 Hz, 2H, C*H*); $^{13}C\{^1H\}$ NMR (101 MHz, $CDCl_3$, 23 °C, ppm) 166.33 (peroxy *C*), 151.45 (*C*), 131.55 (*C*), 130.81 (*C*H), 124.26 (*C*H). Anal. Calcd for $C_7H_5NO_5$: C, 45.90; H, 2.76; N, 7.65. Found: C, 46.37; H, 3.00; N, 7.75. Sensitivity data: IS, 9 J; FS, 360 N; ESD, 0.1 J.

3,5-Dinitrobenzoperoxoic acid (4). Compound **4** was prepared in 96% yield as a pale yellow solid by a literature procedure[2] starting from 3,5-dinitrobenzoic acid: mp 113-115 °C (lit[2] 113-115 °C); IR (ν cm^{-1}) 3447 (broad, m), 3088 (m), 2883 (w), 1734 (m), 1717 (m), 1701 (m), 1628 (m), 1597 (w), 1541 (s), 1489 (w), 1458 (m), 1420 (w), 1348 (s), 1269 (m), 1179 (m), 1152 (s), 1094 (m), 1043 (m), 916 (m), 881 (w), 781 (m), 764 (w), 714 (s); ^{1}H NMR (400 MHz, CD_3OD, 23 °C, δ) OO*H* resonance not observed due to exchange with CD_3OD, 9.22 (t, *J* = 2.4 Hz, 1H, C*H*), 9.03 (d, *J* = 2.4 Hz, 2H, C*H*); $^{13}C\{^1H\}$ NMR (101 MHz, CD_3OD, 23 °C, ppm) 163.62 (peroxy *C*), 150.17 (*C*), 131.98 (*C*), 129.73 (*C*H), 123.83 (*C*H). Anal. Calcd for $C_7H_4N_2O_7$: C, 36.86; H, 1.77; N, 12.27. Found: C, 36.89; H, 1.90; N, 11.95. Sensitivity data: IS, 9 J; FS, 360 N; ESD, 0.1 J. Colorless thin needles suitable for X-ray crystallography were grown from 1:1 diethyl ether:pentane at -29 °C.

[1] D. G. Harman, A. Ramachandran, M. Gracanin, S. Blanksby, *J. Org. Chem.* **2006**, *71*, 7996-8005.
[2] W. H. Rastetter, T. J. Richard T. J.; Lewis, M. D. *J. Org. Chem.* **1978**, *43*, 3163-3166.

2. Energetic Materials Testing Procedures

References for the various techniques are given in the manuscript text.

Impact Tests



Impact sensitivity tests were carried out according to STANAG 4489 modified instructions using a BAM (Bundesanstalt für Materialforschung) drop hammer. Approximately 0.4 mL volume of a compound was placed in the sample holder (between two steel cylindrical blocks that are contained in a hollow steel cylinder) and a series of increasing weights was dropped from a fixed height or a fixed weight was dropped from varying heights. A test was considered positive when a sound (160 dB) was heard. Sensitivity was obtained when one out of six tests was positive.

Friction Tests

Friction sensitivity tests were carried out according to STANAG 4487 modified instruction using the BAM friction tester. A line of approximately 5 mg of a compound was laid on a ceramic plate and a ceramic peg was kept on it. The ceramic plate was then moved from side-to-side so that the ceramic peg was exerting force on the sample. The force exerted on the sample was regulated by the weight and distance of the weight. A test was considered positive when a detonation was observed. Sensitivity was obtained when one out of six tests was positive.

Electrostatic Discharge Tests


Compounds were tested for the sensitivity towards electrical discharge using an OZM Electric Spark Tester ESD 2010 EN according to STANAG 4515 instructions. Approximately 0.1 mL volume of a compound was incorporated in a plastic tube and a charge is exerted through a steel electrode. The test is positive when a small hole was observed after the electricity interacted with the compound.

Table 1. Sensitivities and energetic performance of **1-5**, TNT, RDX, and TATP.

	1	**2**	**3**	**4**	**5**	TNT	RDX	TATP
Formula	$C_8H_6O_6$	$C_9H_6O_9$	$C_7H_5NO_5$	$C_7H_4N_2O_7$	$C_7H_3N_3O_9$	$C_7H_5N_3O_6$	$C_3H_6N_6O_6$	$C_9H_{18}O_6$
FW (g/mol)	198.14	258.15	183.12	228.11	271.11	227.14	222.12	222.24
IS[a] (J)	10	1	9	9	---	15	7.5	0.3
FS[b] (N)	288	5	360	360	---	353	120	0.1
ESD[c] (J)	0.1	0.025	0.1	0.1	---	0.46-0.57	0.20	0.16
Ω_{CO_2}[d] (%)	-105.0	-74.38	-100.5	-63.13	-38.4	-74.0	-21.6	-151.3
T_{Dec}[e] (°C)	160	167	141	132	---	240	170	150-160
ρ[f] (g/cm³)	1.423	1.4[l]	1.586[m]	1.748	1.80[l]	1.60	1.76	1.272
$\Delta_fH°$[g] (kJ/mol)	-584.1	-846.6	-324.3	-310.9	-275.5	-50.6	70.3	-583.8
EXPLO5 V6.02								
$\Delta_{Ex}U°$[h](kJ/kg)	-3373	-3590	-3934	-4660	-5243	-2732	-5277	-4016
P_{CJ}[i] (kbar)	88	105	133	213	269	190	347	103
V_{Det}[j] (m/s)	5262	5588	6176	7217	7885	6900	8750	6168
V_o[k] (L/kg)	598	628	593	596	619	740	908	919

[a]BAM drophammer [b]BAM Impact [c]Electrostatic discharge sensitivity [d]Oxygen balance for CO_2 [e]Decomposition temperature from DTA (5 °C min^{-1}) [f]Density from X-ray diffraction for **1**•DMF and **4** at -173 °C [g]Calculated molar enthalpy of formation [h]Total energy of detonation [i]Detonation pressure [j]Detonation velocity [k]Volume of detonation products [l]Estimated density at 25 °C [m]Published crystalline density

3. Packing and Intermolecular Close Contacts for 3, 4, DADP, and TATP.

Figure 1. Packing diagram of **4** prepared using the program Mercury 3.5.

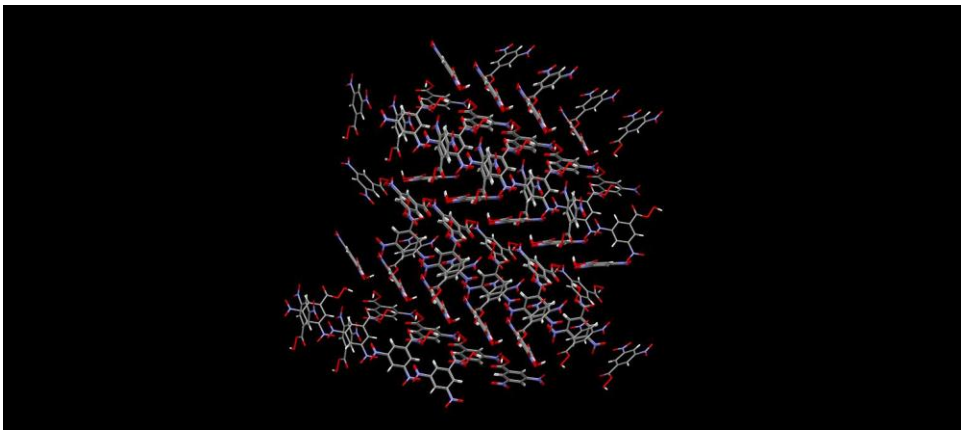

Figure 2. Packing diagram of **3** prepared using the program Mercury 3.5. Data are from ref. 14.

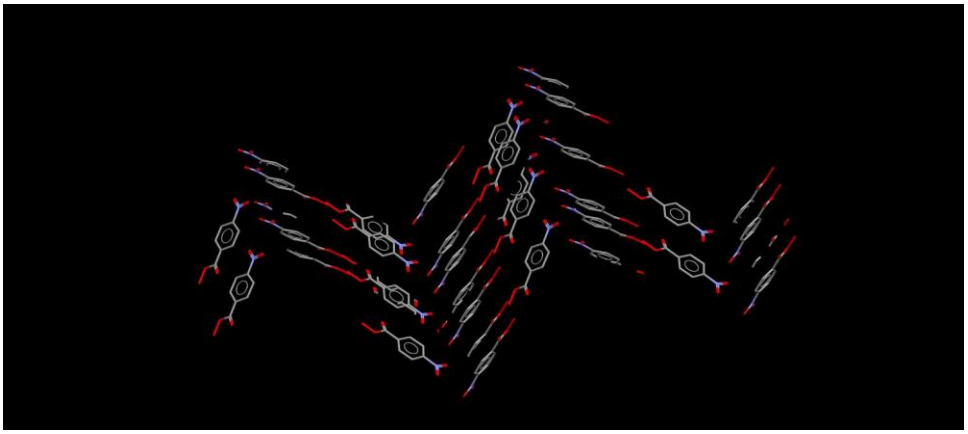

Figure 3. Asymmetric unit view of **4** emphasizing the intermolecular contacts, prepared using the program Mercury 3.5. Red = oxygen, blue = nitrogen, gray = carbon, white = hydrogen.

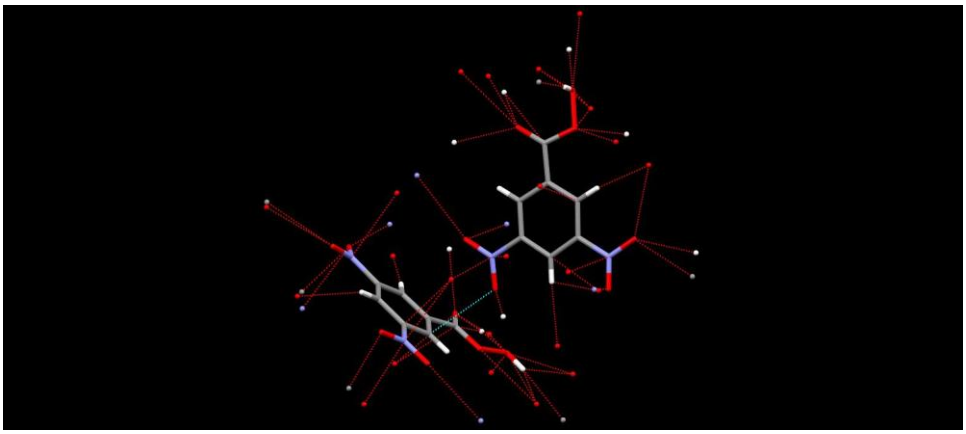

Table 1. Intermolecular close contacts for **4** prepared using the program Mercury 3.5.

Number	Atom1	Atom2	Length	Length-VdW
1	O6	N1	3.001	-0.069
2	N2	O3	3.054	-0.016
3	O5	C7	3.055	-0.165
4	O5	H5	2.712	-0.008
5	O5	O1	2.887	-0.153
6	H3	O1	2.343	-0.377
7	O7	H7	2.435	-0.285
8	N1	O8	2.993	-0.077
9	H5	O11	2.431	-0.289
10	O1	O10	3.017	-0.023
11	O1	O11	2.749	-0.291
12	H1	O10	2.365	-0.355
13	H1	O11	1.884	-0.836
14	H1	C11	2.747	-0.153
15	O2	O10	3.021	-0.019
16	O7	C12	3.048	-0.172
17	O4	O9	3.029	-0.011
18	O4	O10	2.670	-0.370
19	O4	H6	1.740	-0.980
20	C1	H6	2.758	-0.142
21	O2	H6	2.450	-0.270
22	C5	O13	3.142	-0.078
23	O3	N4	3.053	-0.017
24	O4	H8	2.534	-0.186
25	N4	O8	3.006	-0.064
26	C13	O8	3.215	-0.005
27	O12	N3	3.032	-0.038
28	O11	O14	2.978	-0.062
29	C11	O14	3.043	-0.177

Table 2. Intermolecular close contacts for **3** prepared using the program Mercury 3.5. Data are from ref. 14.

Number	Atom1	Atom2	Length	Length-VdW
1	O2	O3	2.966	-0.074
2	O3	O1	2.740	-0.300
3	O3	O3	2.965	-0.075
4	O4	N1	3.063	-0.007

Table 3. Intermolecular close contacts for DADP prepared using the program Mercury 3.5. Data are from ref. 2d.

Number	Atom1	Atom2	Length	Length-VdW
1	H2	O2	2.693	-0.027
2	O2B	H2B	2.693	-0.027
3	O1	H3B	2.707	-0.013
4	H3	O1B	2.707	-0.013

Table 4. Intermolecular close contacts for TATP (space group $P2_1/c$) prepared using the program Mercury 3.5. Data are from ref. 2d.

Number	Atom1	Atom2	Length	Length-VdW
1	O6	H13	2.521	-0.199
2	O3	H1	2.553	-0.167
3	C6	H33	2.850	-0.050
4	H17	C13	2.870	-0.030
5	O8	H28	2.667	-0.053
6	H36	O9	2.710	-0.010

Table 5. Intermolecular close contacts for TATP (space group P1bar) prepared using the program Mercury 3.5. Data are from ref. 2d.

Number	Atom1	Atom2	Length	Length-VdW
1	O3	H12	2.476	-0.244
2	H5	H9	2.224	-0.176
3	H3	C14	2.858	-0.042
4	H11	H23	2.353	-0.047
5	C8	H36	2.771	-0.129
6	C5	H30	2.831	-0.069
7	H6	O7	2.646	-0.074
8	H6	H30	2.321	-0.079
9	H15	H26	2.223	-0.177
10	H13	O9	2.679	-0.041
11	H20	H32	2.341	-0.059
12	O11	H33	2.506	-0.214

ChemComm

COMMUNICATION

View Article Online
View Journal | View Issue

Cite this: *Chem. Commun.*, 2015, 51, 13298

Received 17th June 2015,
Accepted 18th July 2015

DOI: 10.1039/c5cc05015d

www.rsc.org/chemcomm

Less sensitive oxygen-rich organic peroxides containing geminal hydroperoxy groups†

Nipuni-Dhanesha H. Gamage,[a] Benedikt Stiasny,[b] Jörg Stierstorfer,[b] Philip D. Martin,[a] Thomas M. Klapötke*[b] and Charles H. Winter*[a]

A series of oxygen-rich organic peroxide compounds each containing two bis(hydroperoxy)methylene groups is described. Energetic testing shows that these compounds are much less sensitive toward impact and friction than existing classes of organic peroxides. The compounds are highly energetic, which may lead to practical peroxide-based explosives.

Organic energetic materials usually contain carbon, hydrogen, nitrogen, and oxygen, and tend to be nitrogen rich to increase the energy content through formation of highly stable dinitrogen upon detonation.[1] While the explosive nature of organic peroxides is widely recognized, due to the presence of weak O–O bonds (45–50 kcal mol^{-1}),[2–5] detailed energetic materials properties have only been reported for triacetone triperoxide (TATP), diacetone diperoxide (DADP), hexamethylene triperoxide diamine (HMTD), and methyl ethyl ketone peroxide (MEKP).[2–4] The high sensitivities of TATP, DADP, HMTD, and MEKP toward impact, friction, and other stimuli have precluded civilian and military energetic materials applications due to safety concerns.[2] These high sensitivities, coupled with the widely publicized use of TATP by terrorists,[2] have likely discouraged broader exploration of organic peroxides as energetic materials. To allow practical applications, it will be necessary to identify organic peroxides that combine high energy contents with reduced sensitivities toward stimuli. In this direction, a recent report demonstrated that cocrystals of DADP and 1,3,5-triiodo-2,4,6-trinitrobenzene (TITNB) have reduced impact sensitivity compared to both pure DADP and TITNB, because of stabilizing I···O close contacts in the cocrystals.[6]

Herein, we describe the synthesis, structure, and energetic materials properties of five new organic compounds (**1–5**) that each contain two geminal methylene bis(hydroperoxy) moieties. These compounds have oxygen to carbon ratios ranging from 0.80 to 1.33. Four of the new compounds are significantly less sensitive toward impact and friction than TATP, and the detonation velocity and detonation pressure of one compound are higher than those of 2,4,6-trinitrotoluene.

Geminal hydroperoxides **1–5** were synthesized by treating the corresponding ketones or aldehyde with 30–50 wt% H_2O_2 in the presence of iodine (method A, **1**, **3–5**) or concentrated HCl (method B, **2**) as a catalyst using published general procedures for geminal hydroperoxides (Scheme 1).[7,8] Compounds **1–5** were characterized with ^{1}H and ^{13}C NMR spectroscopy, infrared spectroscopy, and elemental analyses. Additionally, X-ray crystal structures of **4** and **5**·H_2O were determined. A low resolution X-ray crystal structure of **1**·Et_2O confirmed the molecular structure. Solvates **1**·Et_2O and **5**·H_2O were used only for the crystallography experiments; unsolvated **1–5** were used for all other measurements. Attempts to prepare the geminal hydroperoxides derived from cyclohexane-1,3,5-trione, cyclohexane-1,2,3,4,5,6-hexaone, and benzene-1,3,5-tricarbaldehyde led to violent gas evolution, likely due to the instability of the products.

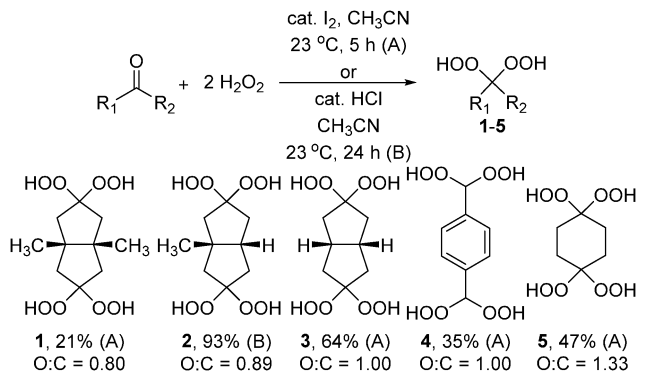

Scheme 1 Synthesis of **1–5**.

[a] *Department of Chemistry, Wayne State University, Detroit, Michigan 48202, USA. E-mail: chw@chem.wayne.edu*
[b] *Department of Chemistry, Ludwig-Maximilians University, Butenandtstr. 5-13 (D), 81377 München, Germany. E-mail: tmk@cup.uni-muenchen.de*

† Electronic supplementary information (ESI) available: Experimental details, structural figures, and crystallographic data. CCDC 1406377 and 1406378. For ESI and crystallographic data in CIF or other electronic format see DOI: 10.1039/c5cc05015d

The thermal behaviour was studied with thermogravimetry. Compounds **1–5** show onsets of thermal decomposition between 98 and 117 °C (Table 1). CBS-4M electronic enthalpies were calculated with the Gaussian09 software package to obtain heat of formation values.[9] The heat of formation values are all exothermic, ranging from −703.6 to −418.2 kJ mol^{-1}. Compound **4** has the most positive heat of formation.

A perspective view of **4** is shown in Fig. 1. This is the only compound among **1–5** for which unsolvated single crystals could be grown. Compound **4** has a crystalline density (1.648 g cm^{-3} at 100 K) that is slightly lower than those of orthorhombic (1.704 g cm^{-3} at 123 K) and monoclinic (1.713 g cm^{-3} at 100 K) 2,4,6-trinitrotoluene (TNT).[10] Since the formula weights of **4** and TNT are similar (Table 1), **4** packs nearly as efficiently as TNT in the solid state. TNT does not contain any strong hydrogen bonds, and only van der Waals forces are present.[10] By contrast, the lattice of **4** contains intermolecular O–H···O hydrogen bonds, where the hydrogen atom on O1 is donated to O4′ and the hydrogen atom on O4 is donated to O1′. The oxygen–oxygen distance in this interaction is 2.701 Å. This configuration results in O1 and O4 being both hydrogen bond donors and acceptors. Additionally, there are close contacts between O2 and O2′ (2.912 Å) and C3–H5′ (2.896 Å). These contacts are within or at the edge of the van der Waals radii for O···O (3.04 Å) and C···H (2.80 Å).[11] Recent studies of energetic materials have shown that such close contacts are attractive because the dispersion forces are larger than the repulsive Coulombic forces.[12] Dissociation energies of O···O close contacts are similar to those of weak hydrogen bonds (3–13 kJ mol^{-1}).[12]

Table 1 gives energetic test results for **1–5**, with TNT and TATP for comparison. Impact, friction, and electrostatic discharge sensitivities were determined with a BAM drop hammer, a BAM friction tester, and an electrostatic discharge tester using standard test methods.[13] Sensitivity classifications are based on the "UN Recommendations on the Transport of Dangerous Goods".[14] Energetic performance was calculated using the EXPLO5 V6.02 software.[15] Compounds **1–5** are "very sensitive" toward impact,[14] with values ranging from <1 to 3 J. They are "extremely sensitive" toward friction,[14] with values of 5 N for **1–3** and <5 N for **4** and **5**. The electrostatic discharge sensitivity values for **1–5** are much greater than electrical discharges that can be created by the human body (≤0.02 J[1]), so they can be safely handled.

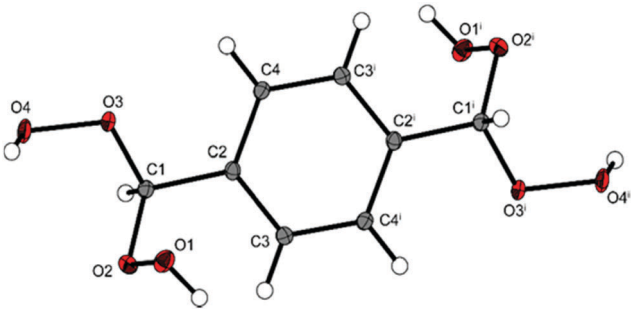

Fig. 1 Perspective view of **4**. Selected bond lengths (Å): O1–O2: 1.4714(7), O3–O4: 1. 4594(7).

The calculated detonation velocities of **1–5** range from 6150 to 7130 m s^{-1} (Table 1). The increase in detonation velocities in going from **1** to **3** parallels the increasing oxygen to carbon ratios and increasing crystalline density. Compound **4** has the highest detonation velocity (7130 m s^{-1}) and the highest crystalline density (1.648 g cm^{-3} at 100 K) among **1–5**.

This work demonstrates that **1–4** have impact and friction sensitivities that are much lower than those of the known peroxide explosives TATP, DADP, HMTD, and MEKP.[2–4] Compound **5** is much more sensitive than **1–4**, with values similar to those of TATP. The higher sensitivity of **5** may arise from its high oxygen to carbon ratio of 1.33. The calculated detonation velocities for **1–5** are much higher than that of TATP, most likely due to the higher crystalline densities and greater oxygen to carbon ratios. The calculated detonation velocity and detonation pressure of **4** are higher than those of TNT (Table 1). Thus, **4** is highly energetic. Typical primary energetic materials

Table 1 Sensitivities and energetic performance of **1–5**, TNT, and TATP

	1	**2**	**3**	**4**	**5**	TNT[l]	TATP[l]
Formula	$C_{10}H_{18}O_8$	$C_9H_{16}O_8$	$C_8H_{14}O_8$	$C_8H_{10}O_8$	$C_6H_{12}O_8$	$C_7H_5N_3O_6$	$C_9H_{18}O_6$
FW (g mol^{-1})	266.28	252.25	238.22	234.18	212.18	227.14	222.24
IS[a] (J)	2	1	2	3	<1	15	0.3
FS[b] (N)	5	5	5	<5	<5	353	0.1
ESD[c] (J)	0.2	0.5	0.1	0.25	0.6	0.57	0.16
Ω_{CO_2}[d] (%)	−126.20	−114.18	−100.76	−88.83	−75.41	−73.96	−151.19
T_{Dec}[e] (°C)	117	98	100	105	117	240	150–160
ρ[f] (g cm^{-3})	1.35	1.375	1.40	1.60	1.40	1.704, 1.713[m]	1.18
$\Delta_f H°$[g] (kJ mol^{-1})	−703.6	−660.8	−617.0	−418.2	−627.1	−70.6	−583.8
EXPLO5 V6.02							
$\Delta_{Ex}U°$[h] (kJ kg^{-1})	−4636	−4875	−5083	−5498	−5329	−2732	−2745
P_{CJ}[i] (kbar)	117	126	138	195	155	190	—
V_{Det}[j] (m s^{-1})	6150	6250	6428	7130	6700	6900	5300
V_o[k] (L kg^{-1})	829	831	808	688	847	825	855

[a] BAM drophammer. [b] BAM friction. [c] Electrostatic discharge sensitivity. [d] Oxygen balance for CO_2. [e] Decomposition temperature from DTA (5 °C min^{-1}). [f] Room temperature density estimation without solvent. [g] Calculated molar enthalpy of formation. [h] Total energy of detonation. [i] Detonation pressure. [j] Detonation velocity. [k] Volume of detonation products. [l] Values from ref. 3*h* and 16. [m] Values from ref. 10.

have impact and friction sensitivities of $\leq$4 J and $\leq$10 N, respectively, but must be safe enough to handle.[1] Compounds **1–4** have sensitivity values in this range, and are the first organic peroxides that might be safely used as primary explosives. For comparison, the impact and friction sensitivities of **5**, TATP, DADP, HMTD, and MEKP are too high for safe use.[2–4] Despite their less sensitive nature, the thermal decomposition temperatures of **1–4** will need to be increased to allow use as primary energetic materials. Interestingly, the impact (1–3 J) and friction ($\sim$5 N) sensitivity values for **1–4** are similar, and do not vary with the nature of the organic framework and increasing O : C ratios from **1–4**. This lack of a trend is consistent with the O–O linkages being the "trigger bonds" that initiate decomposition upon cleavage. The solid state structure of **4** reveals intermolecular O–H$\cdots$O hydrogen bonds, as well as several O$\cdots$O and C$\cdots$H close contacts. The hydrogen bonds and attractive close contacts may serve to stabilize the labile O–O bonds and buffer them toward shock, thereby reducing the sensitivities of **1–4**. Intermolecular I$\cdots$O close contacts also lead to reduced sensitivity in cocrystals of DADP and TITNB.[6] For comparison, the solid state structures of highly sensitive DADP and TATP lack O–H$\cdots$O hydrogen bonds and O$\cdots$O close contacts, and contain only very weak O$\cdots$H and C$\cdots$H interactions.[3b] The stronger hydrogen bonds and close contacts are likely important stabilizing features in **1–4**. Finally, this work demonstrates that careful manipulation of organic peroxide structures can lead to compounds with useful energetic materials properties.

The authors acknowledge generous support from the Office of Naval Research (Grant No. N00014-12-1-0526 to C.H.W., Grant No. N00014-12-1-0538 to T.M.K.).

Notes and references

1 T. M. Klapötke, *Chemistry of High-Energy Materials*, de Gruyter, Berlin/Boston, 2nd edn, 2012.
2 T. M. Klapötke and T. Wloka, *Peroxide Explosives, Patai's Chemistry of Functional Groups*, S. Patai Ed, Wiley, 2014, pp. 1–28.
3 (*a*) J. C. Oxley, J. L. Smith and H. Chen, *Propellants, Explos., Pyrotech.*, 2002, **27**, 209–216; (*b*) F. Dubnikova, R. Kosloff, J. Almog, Y. Zeiri, R. Boese, H. Itzhaky, A. Alt and E. Keinan, *J. Am. Chem. Soc.*, 2005, **127**, 1146–1159; (*c*) C. Denekamp, L. Gottlieb, T. Tamiri, A. Tsoglin, R. Shilav and M. Kapon, *Org. Lett.*, 2005, **7**, 2461–2464; (*d*) O. Reany, M. Kapon, M. Botoshansky and E. Keinan, *Cryst. Growth Des.*, 2009, **9**, 3661–3670; (*e*) R. Matyáš and J. Šelešovský, *J. Hazard. Mater.*, 2009, **165**, 95–99; (*f*) A. E. Contini, A. J. Bellamy and L. N. Ahad, *Propellants, Explos., Pyrotech.*, 2012, **37**, 320–328; (*g*) G. R. Peterson, W. P. Bassett, B. L. Weeks and L. J. Hope-Weeks, *Cryst. Growth Des.*, 2013, **13**, 2307–2311; (*h*) V. P. Sinditskii, V. I. Kolesov, V. Y. Egorshev, D. I. Patrikeev and O. V. Dorofeeva, *Thermochim. Acta*, 2014, **585**, 10–15.
4 J. C. Oxley, J. L. Smith, H. Chen and E. Cioffi, *Thermochim. Acta*, 2002, **388**, 215–225.
5 R. D. Bach, P. Y. Ayala and H. B. Schlegel, *J. Am. Chem. Soc.*, 1996, **118**, 12758–12765.
6 K. B. Landenberger, O. Bolton and A. Matzger, *J. Am. Chem. Soc.*, 2015, **137**, 5074–5079.
7 (*a*) V. I. Tropina, O. V. Krivykh, N. P. Sadchikova, A. O. Terent'ev and I. B. Krylov, *Pharm. Chem. J.*, 2010, **44**, 248–250; (*b*) K. Žmitek, M. Zupan, S. Stavber and J. Iskra, *Org. Lett.*, 2006, **8**, 2491–2494; (*c*) P. Ghorai and P. H. Dussault, *Org. Lett.*, 2008, **10**, 4577–4579.
8 K. Žmitek, M. Zupan, S. Stavber and J. Iskara, *J. Org. Chem.*, 2007, **72**, 6534–6540.
9 M. J. Frisch, *et al.*, *Gaussian 09, Revision A.1*, Gaussian, Inc., Wallingford CT, 2009.
10 R. M. Vreclj, J. N. Sherwood, A. R. Kennedy, H. G. Gallagher and T. Gelbrich, *Cryst. Growth Des.*, 2003, **3**, 1027–1032.
11 M. Mantina, A. C. Chamberlain, R. Valero, C. J. Cramer and D. G. Truhlar, *J. Phys. Chem. A*, 2009, **113**, 5806–5812.
12 (*a*) C. J. Eckhardt and A. Gavezzotti, *J. Phys. Chem. B*, 2007, **111**, 3430–3437; (*b*) Y. Ma, A. Zhang, X. Zue, D. Jiang, Y. Zhu and C. Zhang, *Cryst. Growth Des.*, 2014, **14**, 6101–6114; (*c*) Y. Ma, A. Zhang, C. Zhang, D. Jiang, Y. Zhu and C. Zhang, *Cryst. Growth Des.*, 2014, **14**, 4703–4713.
13 (*a*) NATO Standardization Agreement (STANAG) on Explosives, *Impact Sensitivity Tests*, No. 4489, 1st edn, Sept. 17, 1999; (*b*) WIWEB-Standardarbeitsanweisung 4-5.1.02, Ermittlung der Explosionsgefähr-lichkeit, hier der Schlagempfindlichkeit mit dem Fallhammer, Nov. 8, 2002; (*c*) http://www.bam.de; (*d*) NATO Standardization Agreement (STANAG) on Explosives, *Friction Sensitivity Tests*, No. 4487, 1st edn, Aug. 22, 2002.
14 (*a*) *Test Methods According to the UN Manual of Tests and Criteria, Recommendations on the Transport of Dangerous Goods*, United Nations Publications, New York, Geneva, 4th revised edn, 2003; (*b*) www.reichel-partner.de.
15 M. Sućeska, *EXPLO5 V6.02 Program*, Brodarski Institute, Zagreb, Croatia, 2014.
16 (*a*) R. Meyer, J. Kohler and A. Homburg, *Explosives*, Wiley-VCH, Weinheim, 6th edn, 2007; (*b*) D. Skinner, D. Olson and A. Block-Bolten, *Propellants, Explos., Pyrotech.*, 1998, **23**, 34–42; (*c*) V. S. Mishra, S. R. Vadali, R. K. Garg, V. S. Joshi, R. D. Wasnik and S. Asthana, *Cent. Eur. J. Energ. Mater.*, 2013, **10**, 569–580; (*d*) H. Muthurajan, R. Sivabalan, M. B. Talawar, M. Anniyappan and S. Venugopalan, *J. Hazard. Mater.*, 2006, **A133**, 30–45; (*e*) M. S. Keshavarz, *Indian J. Eng. Mater. Sci.*, 2007, **14**, 77–80; (*f*) R. Matyas and J. Pachman, *Primary Explosives*, Springer-Verlag, Berlin, 2013, vol. 10.

Supporting Information for:

Sensitivity Reduction in Oxygen-Rich Organic Peroxides Containing Geminal Hydroperoxy Groups

Nipuni-Dhanesha H. Gamage,[†] Benedikt Stiasny,[‡] Jörg Stierstorfer,[‡] Philip D. Martin,[†] Thomas M. Klapötke,*[,‡] and Charles H. Winter*[,†]

[†]Department of Chemistry, Wayne State University, Detroit, Michigan 48202, United States
[‡]Department of Chemistry, Ludwigs-Maximilians University, Butenandtstr. 5-13 (D), 81377 München, Germany

1. Experimental Procedures

General Considerations

Syntheses of all organic peroxides were carried at room temperature under ambient atmosphere. Chemicals were purchased from Sigma-Aldrich, Acros Organics, EMD, or Alfa Aesar and were used without further purification. ACS grade solvents were obtained from EMD and Fisher Scientific. Geminal hydroperoxides **1** and **3**–**5** were synthesized using a modified published general procedure for germinal hydroperoxides.[1] Compound **2** was obtained using concentrated HCl as the catalyst and no column purification was required.

Silica gel 60, 230–400 mesh (EMD Chemicals) was used to perform silica gel column chromatography.[2] ASTM TLC plates precoated with silica gel 60 F_{254} (250 μm layer thickness) were used for thin-layer chromatography (TLC). TLC spots were observed using a UV lamp and/or a potassium permanganate solution as a stain (3 g $KMnO_4$, 20 g K_2CO_3, 5 mL 5% w/v aqueous NaOH, 300 mL H_2O). The spots on the stained TLC plates were visualized after heating with a heat gun.

^1H and $^{13}C\{^1H\}$ NMR spectra were obtained at 400 MHz and 101 MHz, respectively, in CD_3OD as indicated and were referenced to the residual proton and carbon resonances of the solvent (^1H δ 3.31, ^{13}C 49.00 ppm). Infrared spectra were obtained from a Shimadzu MIRacle 10 IRAffinity-1 equipped with a single reflection ATR accessory (**1** and **3**–**5**) and a Perkin-Elmer One FT-IR Spectrum BXII instrument with a Smith ATR Dura Sample IRII accessory (**2**). Melting points were determined on an Electrothermal IA 9300 melting point apparatus and are uncorrected. Thermogravimetric (TGA/DTA) measurements to determine the decomposition temperatures of compounds **1**−**5** were performed at a heating rate of 5 °C min^{-1} with an OZM Research DTA 552-Ex instrument.

Caution: The H_2O_2 solutions are strong oxidizers that may cause explosions. All organic peroxides are potentially explosive and require handling with extreme care. Reactions and manipulations should be run in fume hoods behind blast shields. Personal safety gear should include a face shield, leather gloves, a leather apron, and hearing protection. Peroxide compounds should not come into contact with strong acids, metal salts, or easily oxidized species. All reactions should be run at or below room temperature and performed on small scales. Specifically, **3** exploded upon concentrating a solution containing ca. 30 mg of crystals on the walls of the flask, and shattered the flask and damaged the stir bar.

Qualitative Energetic Properties: Qualitative sensitivities to heat, impact, and electrostatic discharge were determined to assess initial safety issues. Tests included burning about

3-5 mg of the compound in the Bunsen burner flame, striking 3-5 mg of the compound on a metal plate with a hammer, and passing an electrostatic discharge through 3-5 mg of the compound on a metal plate using an Electro Technic BD 10 Tesla coil (120 V, 0.35 A).

2,2,5,5-tetrahydroperoxy-*cis*-3,6-dimethyloctahydropentalene (1).

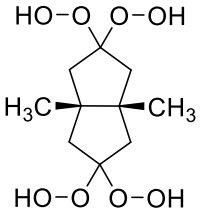

A 50-ml round bottomed flask was charged with a magnetic stir bar, I_2 (0.050 g, 0.2 mmol) in CH_3CN (3 mL), and then a 50 wt.% aqueous solution of H_2O_2 (0.5 mL, 9 mmol) was added. To this solution *cis*-1,5-dimethylbicyclo[3.3.0]octane-3,7-dione (0.166 g, 1.00 mmol) was added and the reaction was stirred at room temperature (23 °C) for 5 h. At this point, the reaction mixture was concentrated under reduced pressure, dissolved in 1 mL of DCM: CH_3OH (20:1) and the product was purified by silica gel column chromatography with CH_2Cl_2: CH_3OH = 20:1 to obtain **1** (0.061 g, 21%) as a white solid: mp not taken due to explosion hazard; IR (ν, cm^{-1}) 3365 (broad, m), 2965 (m), 2874 (m), 2808 (w), 1688 (w), 1452 (m), 1431 (m), 1380 (m), 1319 (m), 1274 (s), 1225 (m), 1189 (m), 1156 (m), 1125 (m), 1083 (m), 1045 (s), 1001, 993 (m), 982 (m), 945 (m), 901 (m), 866 (m), 826 (s), 798 (m), 732 (w); ^{1}H NMR (400 MHz, CD_3OD, 23 °C, δ) OO*H* resonances not observed due to exchange with CD_3OD, 2.18 (d, 4H, J = 14.8 Hz), 1.88 (d, 2H, J = 14.8 Hz), 1.01 (s, 6H, C*H*$_3$); ^{13}C{^{1}H} NMR (101 MHz, CD_3OD, 23 °C, ppm) 120.14 (peroxy *C*), 50.55 (C), 46.49 (*C*H_2), 22.27 (*C*H_3); Anal. Calcd for $C_{10}H_{18}O_8$: C, 45.11; H, 6.81. Found: C, 44.90; H, 6.90. Colorless, planar, hexagonal crystals of **1**·ether were obtained by slow evaporation from diethyl ether.

2,2,5,5-tetrahydroperoxy-3-methyloctahydropentalene (2).

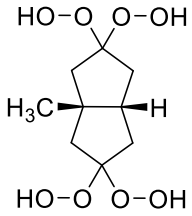

A 100-ml round bottomed flask was charged with a magnetic stir bar and CH_3CN (20 mL). Then, *cis*-1-methylbicyclo[3.3.0]octane-3,7-dione (0.280 g, 1.84 mmol) was added and the mixture was stirred at room temperature (23 °C) until the solid was completely dissolved. Afterwards, 30 wt.% aqueous solution of H_2O_2 (2.00 mL, 19.7 mmol) and concentrated HCl (4 drops/0.100 g, 1.01 mmol) were added and the resulting solution was stirred at room temperature (23 °C) for 24 h. The solvent was removed under reduced pressure to obtain **2** (0.46 g, 93 %) as a white solid: mp not taken due to explosion hazard; IR (ν, cm^{-1}) 3371 (broad, m), 2954 (m), 2872 (m), 2349 (w), 2280 (w), 1722 (m), 1712 (m), 1631 (w), 1433 (m), 1379 (s), 1311 (s), 1262 (m), 1227 (m), 1162 (m), 1136 (m), 1048 (m), 994 (m), 953 (m), 935 (w), 832 (m), 802 (w), 752 (w);

^{1}H NMR (400 MHz, CD_3OD, 25 °C, δ) OO*H* resonances not observed due to exchange with CD_3OD, 2.27–2.09 (m, 4H, C*H*$_2$), 1.99–1.82 (m, 4H, C*H*$_2$), 1.21–1.13 (m, 1H, C*H*), 1.17 (s; 3H, C*H*$_3$); ^{13}C{^{1}H} NMR (101 MHz, CD_3OD, 25 °C, ppm) 123.6 (peroxy *C*), 48.7 (*C*), 48.4 (*C*H) 46.8 (*C*H$_2$), 38.9 (*C*H$_2$), 28.1 (*C*H$_3$); Anal. Calcd for $C_9H_{16}O_8$: C, 42.84; H, 6.40. Found: C, 42.92; H, 6.17.

2,2,5,5-tetrahydroperoxyoctahydropentalene (3).

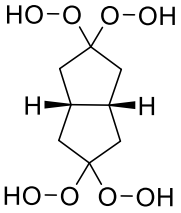

In a fashion similar to the preparation of **1**, treatment of I_2 (0.010 g, 0.040 mmol) in CH_3CN (1 mL) and a 50 wt.% aqueous solution of H_2O_2 (0.10 mL, 1.7 mmol) with *cis*-1,5-dimethylbicyclo[3.3.0]octane-3,7-dione (0.028 g, 0.20 mmol) afforded **3** (0.031 g, 64%) as a crude white solid. The product was purified by silica gel column chromatography with 4:1 CH_2Cl_2: EtOAc: mp not taken due to explosion hazard; ^{1}H NMR (400 MHz, CD_3OD, 23 °C, δ) OO*H* resonances not observed due to exchange with CD_3OD, 2.72-2.56 (m, 2H, C*H*), 2.18 (d of d, 4H, *J* = 14.4, 8.8 Hz), 1.86 (d of d, 4H, *J* = 14.4, 5.6 Hz); ^{13}C{^{1}H} NMR (101 MHz, CD_3OD, 23 °C, ppm) 122.10 (peroxy *C*), 40.54 (*C*H), 39.03 (*C*H$_2$); Anal. Calcd for $C_8H_{14}O_8$: C, 40.34; H, 5.92. Found: C, 39.98; H, 5.77.

1,4-bis(dihydroperoxymethyl)benzene (4).

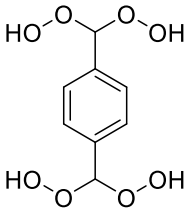

In a fashion similar to the preparation of **1**, treatment of I_2 (0.200 g, 0.800 mmol) in CH_3CN (10 mL) with a 50 wt.% aqueous solution of H_2O_2 (1.84 mL, 32.0 mmol) and 1,4-cyclohexanedione (0.536 g, 4.00 mmol) afforded a product mixture that was concentrated under reduced pressure. The resulting residue was redissolved in dichloromethane (10 mL) and the solution was dried over anhydrous Na_2SO_4. The decanted dichloromethane solution was again concentrated and the product was purified by silica gel column chromatography with 4:1 CH_2Cl_2:EtOAc to obtain **1** (0.328 g, 35%) as a white solid: mp 108–110 °C; IR (ν, cm^{-1}) 3236 (broad, m), 2944 (w), 2816 (w), 2797 (w), 2762 (w), 2738 (w), 1699 (w), 1683 (w), 1413 (m), 1314 (m), 1201 (w), 1128 (w), 1033 (s), 982 (s), 930 (w), 869 (m), 825 (w), 781 (s), 693 (s); ^{1}H NMR (400 MHz, CD_3OD, 23 °C, δ) OO*H* resonance not observed due to exchange with CD_3OD, 7.45 (s, 4H, C*H*), 6.10 (s, 2H, C*H*); ^{13}C{^{1}H} NMR (101 MHz, CD_3OD, 23 °C, ppm) 136.78 (aryl *C*), 128.02 (aryl *C*H), 110.73 (peroxy *C*H); Anal. Calcd for $C_8H_{10}O_8$: C, 41.04; H, 4.30. Found: C, 41.02; H, 4.50. Colorless,

diamond-shaped single crystals of **4** (0.218 g, 23%) were obtained by layering a solution of **4** in 1:1 THF:diethyl ether with hexane.

1,1,4,4-tetrahydroperoxycyclohexane (5)

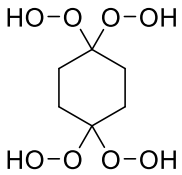

1,4-Cyclohexadione (0.210 g, 2.62 mmol) was treated with a 30 wt.% aqueous solution of H_2O_2 (2.50 mL, 0.83 g, 24.4 mmol). After 1,4-cyclohexadione was dissolved completely, 3 drops of concentrated HCl were added and the reaction vessel was shaken cautiously. After four days a white solid precipitate was obtained. It was filtered off and washed with diethyl ether to obtain **5** (0.261 g, 47%) as a white solid: IR (ν, cm^{-1}) 3510 (m), 3264 (s), 3180 (s), 2958 (m), 2844 (m), 2340 (w), 1715 (w), 1584 (m), 1459 (m), 1437 (m), 1393 (m), 1371 (m), 1333 (m), 1287 (m), 1265 (s), 1159 (m), 1071 (s), 1002 (m), 973 (w), 955 (s), 913 (s), 876 (m), 858 (s), 772 (w), 630 (s); ^{1}H NMR (400 MHz, CD_3OD, 23 °C, δ) OO*H* resonances not observed due to exchange with CD_3OD, 1.86 (s, 8H, C*H*$_2$); ^{13}C{^{1}H} NMR (101 MHz, CD_3OD, 23 °C, ppm) 109.83 (peroxy *C*), 26.73 (*C*H_2); Anal. Calcd. For $C_6H_{12}O_8$: C, 33.97; H, 5.70. Found: C, 33.61; H, 6.03. An X-ray quality single crystal of was isolated upon slow evaporation of the solvent from the reaction mixture.

2. Energetic Materials Testing Procedures

Impact Tests



Impact sensitivity tests were carried out according to STANAG 4489[3] modified instructions[4] using a BAM (Bundesanstalt für Materialforschung) drop hammer.[5] Approximately 0.4 mL volume of a compound was placed in the sample holder (between two steel cylindrical blocks that are contained in a hollow steel cylinder) and a series of increasing weights was dropped from a fixed height or a fixed weight was dropped from varying heights. A test was considered positive when a sound (160 dB) was heard. Sensitivity was obtained when one out of six tests was positive.

Friction Tests

Friction sensitivity tests were carried out according to STANAG 4487[6] modified instruction[7] using the BAM friction tester. A line of approximately 5 mg of a compound was laid on a ceramic plate and a ceramic peg was kept on it. The ceramic plate was then moved from side-to-side so that the ceramic peg was exerting force on the sample. The force exerted on the sample was regulated by the weight and distance of the weight. A test was considered positive when a detonation was observed. Sensitivity was obtained when one out of six tests was positive.

Electrostatic Discharge Tests

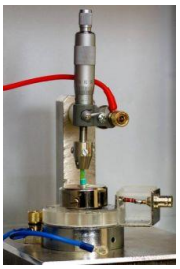

Compounds were tested for the sensitivity towards electrical discharge using an OZM Electric Spark Tester ESD 2010 EN according to STANAG 4515 instructions.[8] Approximately 0.1 mL volume of a compound was incorporated in a plastic tube and a charge is exerted through a steel electrode. The test is positive when a small hole was observed after the electricity interacted with the compound.

1. (a) K. Žmitek, M. Zupan, S. Stavber and J. Iskra, Org. Lett., 2006, **8**, 2491-2494. (b) K. Žmitek, M. Zupan, S. Stavber and J. Iskara, J. Org. Chem., 2007, **72**, 6534-6540.
2. C. W. Still, M. Kahn, A. Mitra, *J. Org. Chem.* 1978, **43**, 2923–2925.
3. NATO standardization agreement (STANAG) on explosives, *Impact Sensitivity Tests*, no. 4489, 1st ed., Sept. 17, **1999**.
4. WIWEB-Standardarbeitsanweisung 4-5.1.02, Ermittlung der Explosionsgefährlichkeit, hier der Schlagempfindlichkeit mit dem Fallhammer, Nov. 8, **2002**.
5. http://www.bam.de.
6. NATO Standardization Agreement (STANAG) on Explosives, *Friction Sensitivity Tests*, no. 4487, 1st ed., Aug. 22, **2002**.
7. WIWEB-Standardarbeitsanweisung 4-5.1.03, Ermittlung der Explosionsgefährlichkeit oder der Reibeempfindlichkeit mit dem Reibeapparat, Nov. 8, **2002**.

8. a) http://www.ozm.cz (accessed January 29, **2013**). b) NATO Standardization Agreement 4515, August 23, **2002**.

3. NMR Spectra of 1-5 are shown in the following pages.

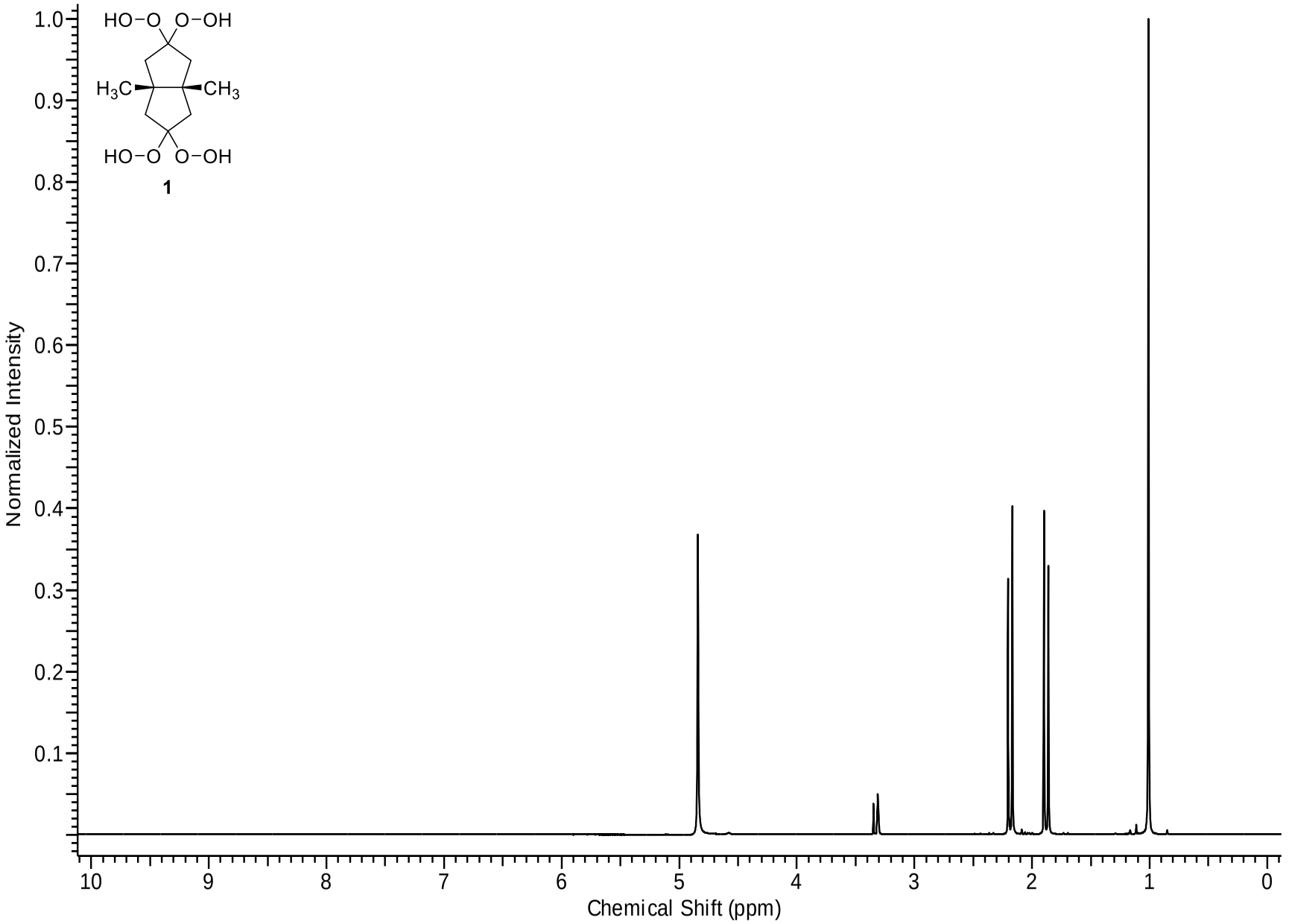
HO–O O–OH
H3C
CH3
HO–O O–OH
1
Normalized Intensity
1.0
0.9
0.8
0.7
0.6
0.5
0.4
0.3
0.2
0.1
10
9
8
7
6
5
4
3
2
1
0
Chemical Shift (ppm)

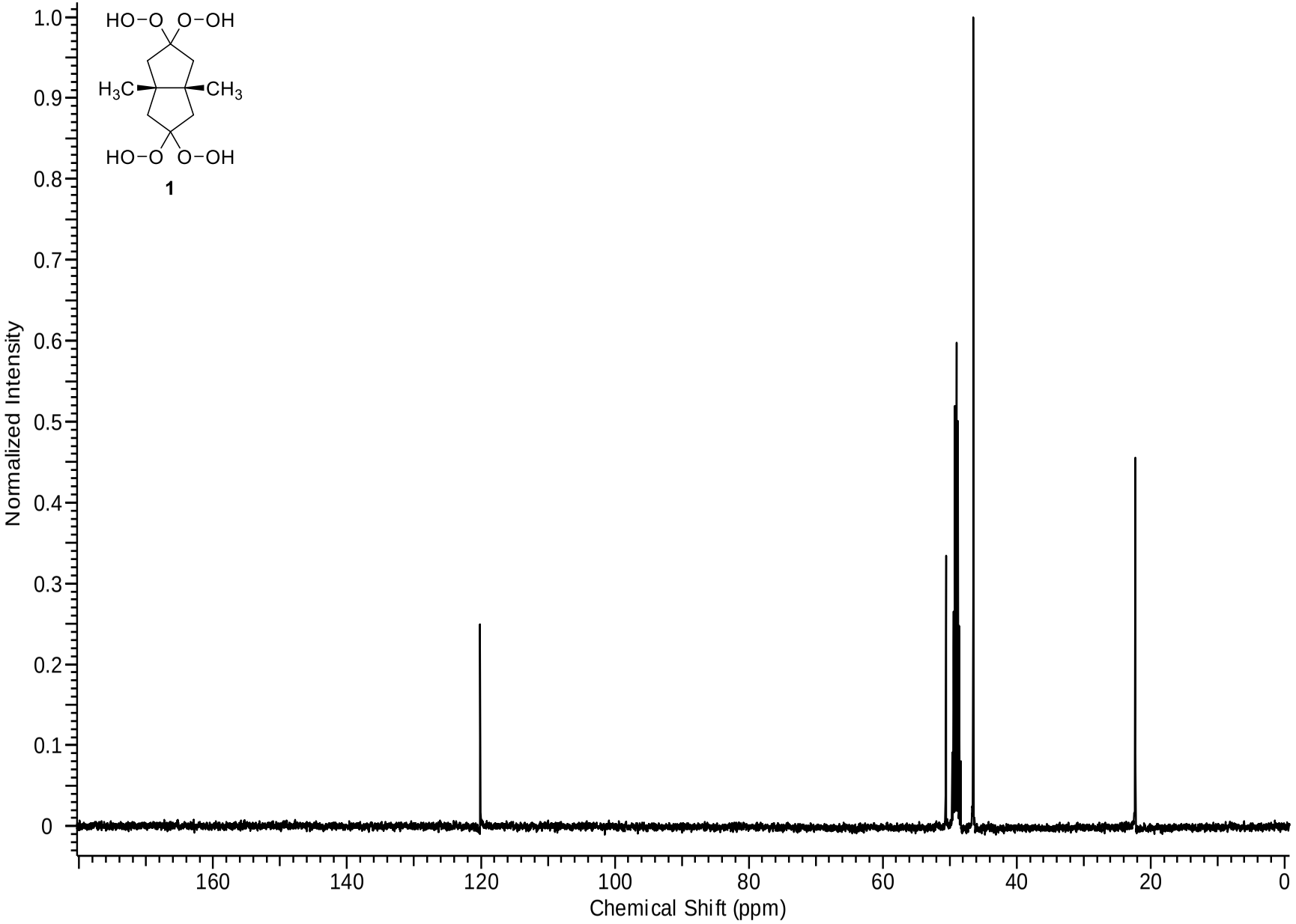
HO–O O–OH
H3C
CH3
HO–O O–OH
1
Normalized Intensity
1.0
0.9
0.8
0.7
0.6
0.5
0.4
0.3
0.2
0.1
0
160
140
120
100
80
60
40
20
0
Chemical Shift (ppm)

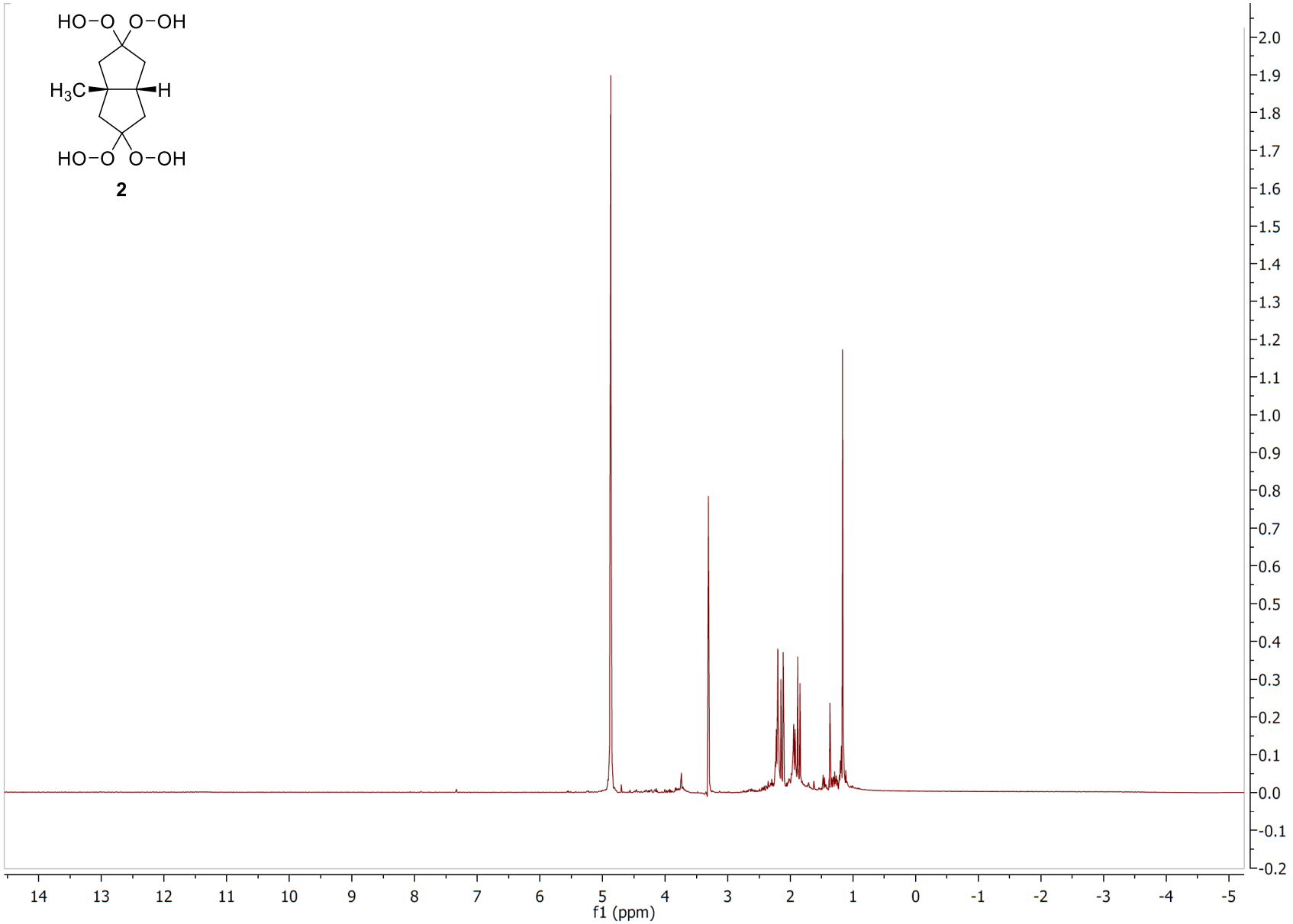
HO–O O–OH
H3C
H
HO–O O–OH
2
2.0
1.9
1.8
1.7
1.6
1.5
1.4
1.3
1.2
1.1
1.0
0.9
0.8
0.7
0.6
0.5
0.4
0.3
0.2
0.1
0.0
-0.1
-0.2
14 13 12 11 10 9 8 7 6 5 4 3 2 1 0 -1 -2 -3 -4 -5
f1 (ppm)

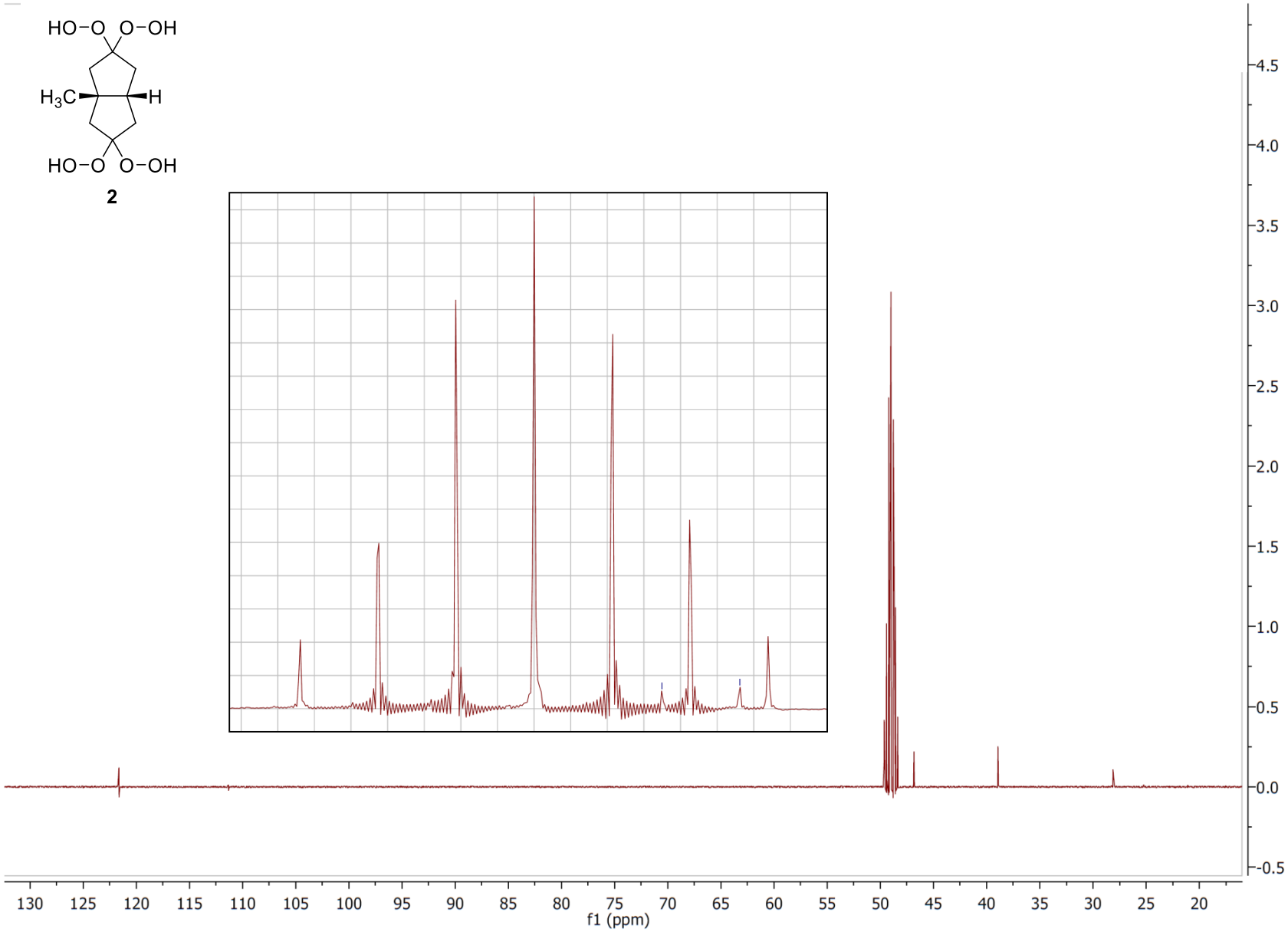
HO–O O–OH
H3C
H
HO–O O–OH
2
4.5
4.0
3.5
3.0
2.5
2.0
1.5
1.0
0.5
0.0
-0.5
130 125 120 115 110 105 100 95 90 85 80 75 70 65 60 55 50 45 40 35 30 25 20
f1 (ppm)

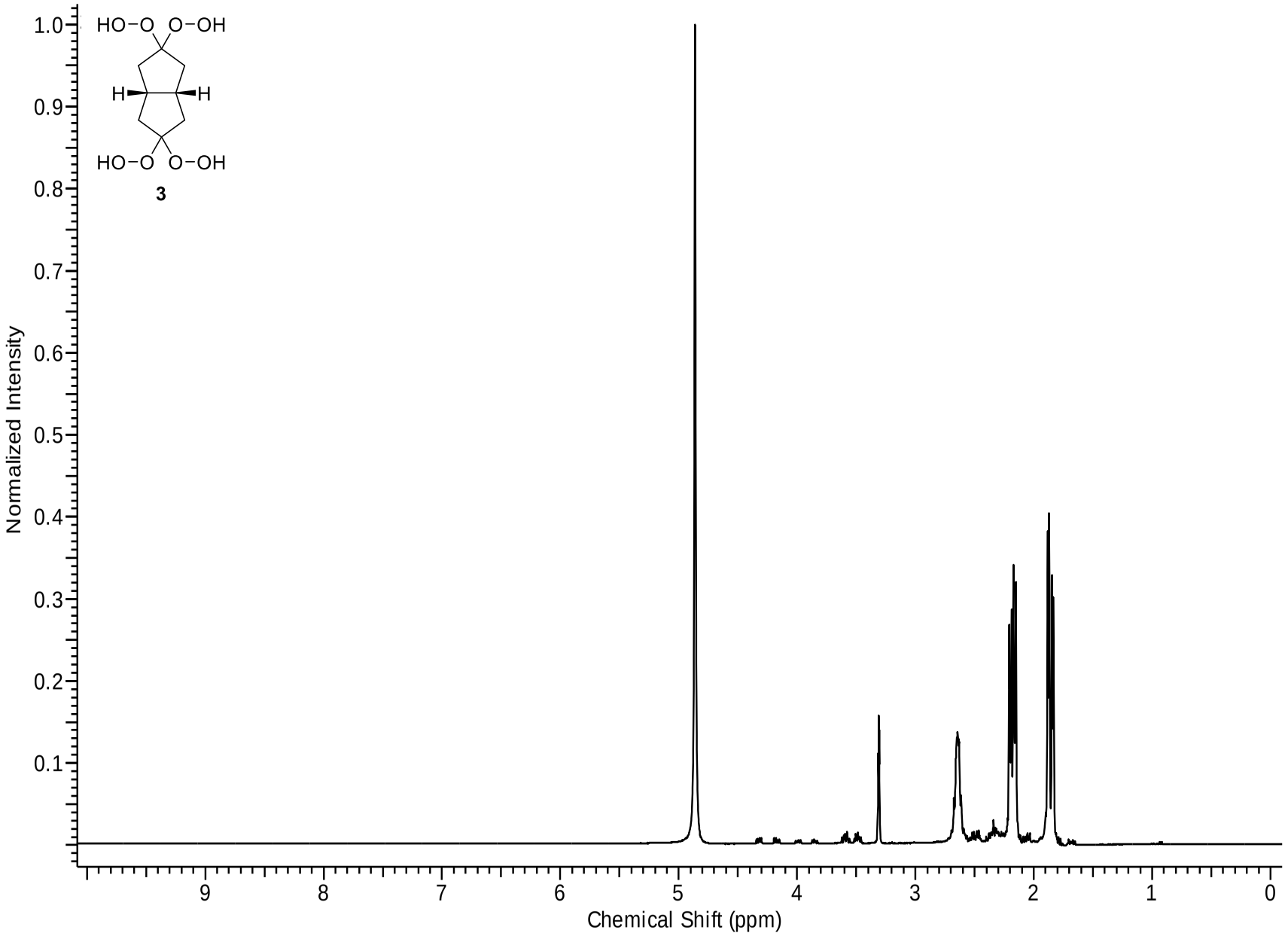
HO–O O–OH
H
H
HO–O O–OH
3
Normalized Intensity
1.0
0.9
0.8
0.7
0.6
0.5
0.4
0.3
0.2
0.1
9
8
7
6
5
4
3
2
1
0
Chemical Shift (ppm)

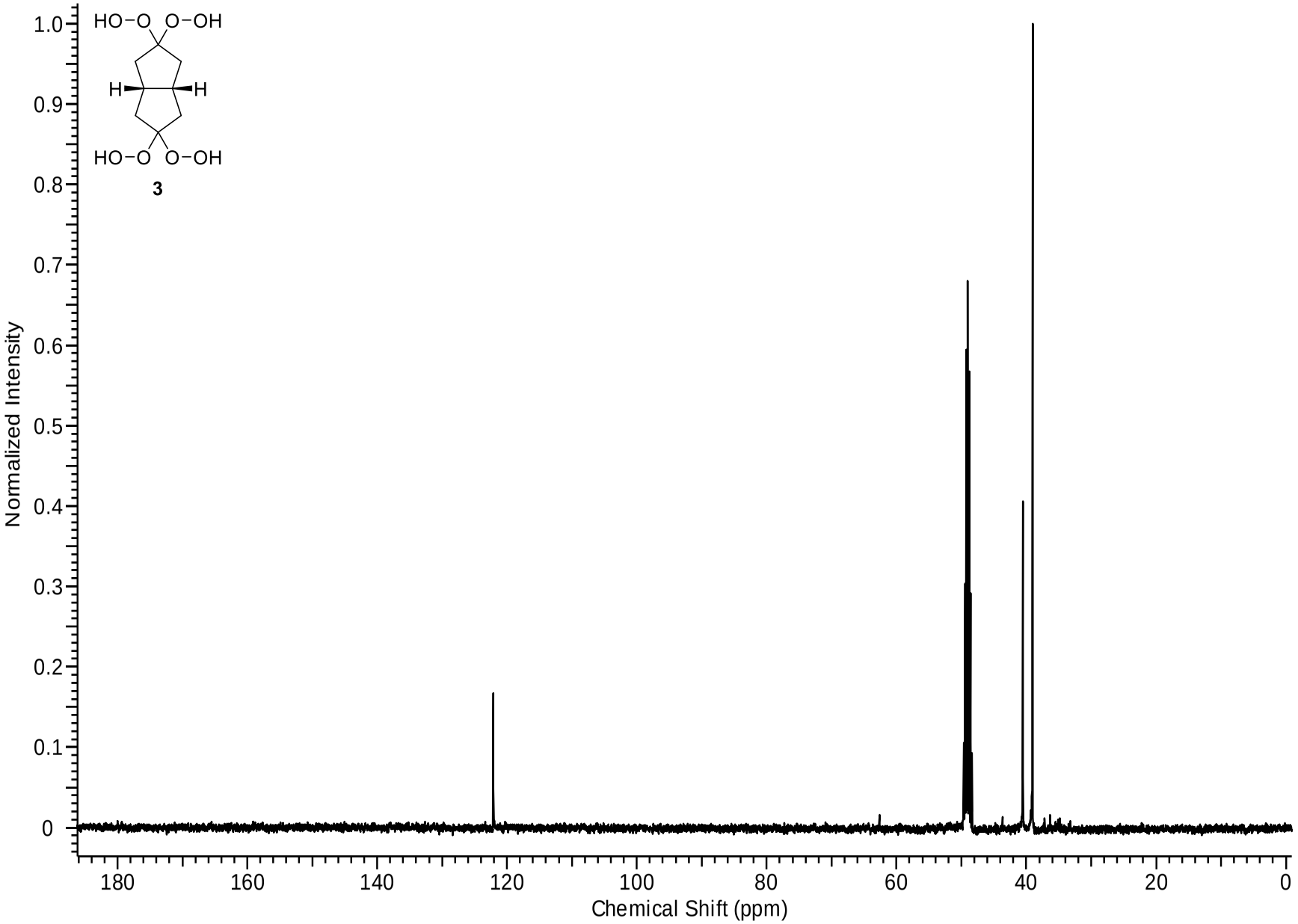
HO–O O–OH
H
H
HO–O O–OH
3
Normalized Intensity
1.0
0.9
0.8
0.7
0.6
0.5
0.4
0.3
0.2
0.1
0
180
160
140
120
100
80
60
40
20
0
Chemical Shift (ppm)

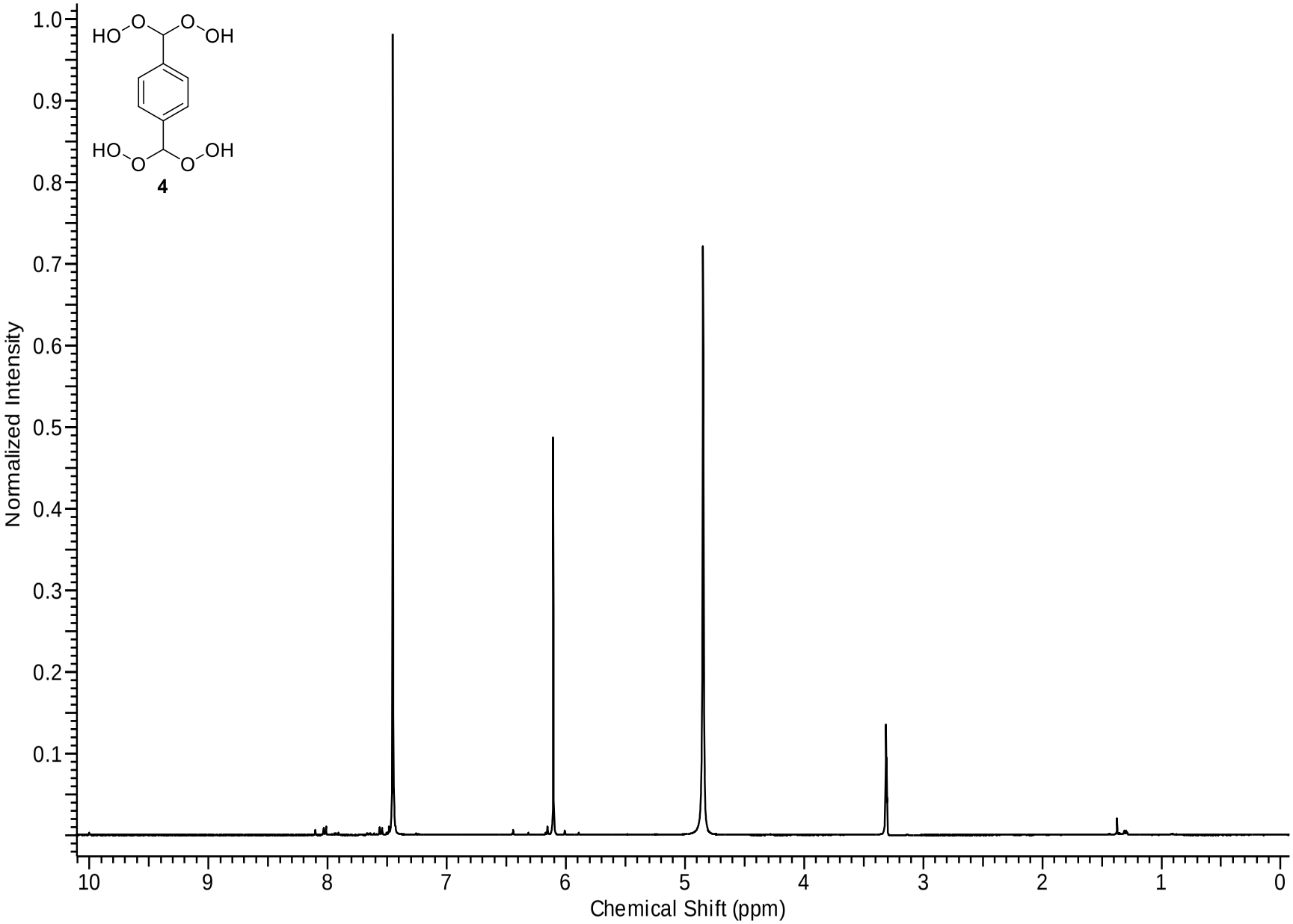
HO
O
O
OH
HO
O
O
OH
4
Normalized Intensity
1.0
0.9
0.8
0.7
0.6
0.5
0.4
0.3
0.2
0.1
10
9
8
7
6
5
4
3
2
1
0
Chemical Shift (ppm)

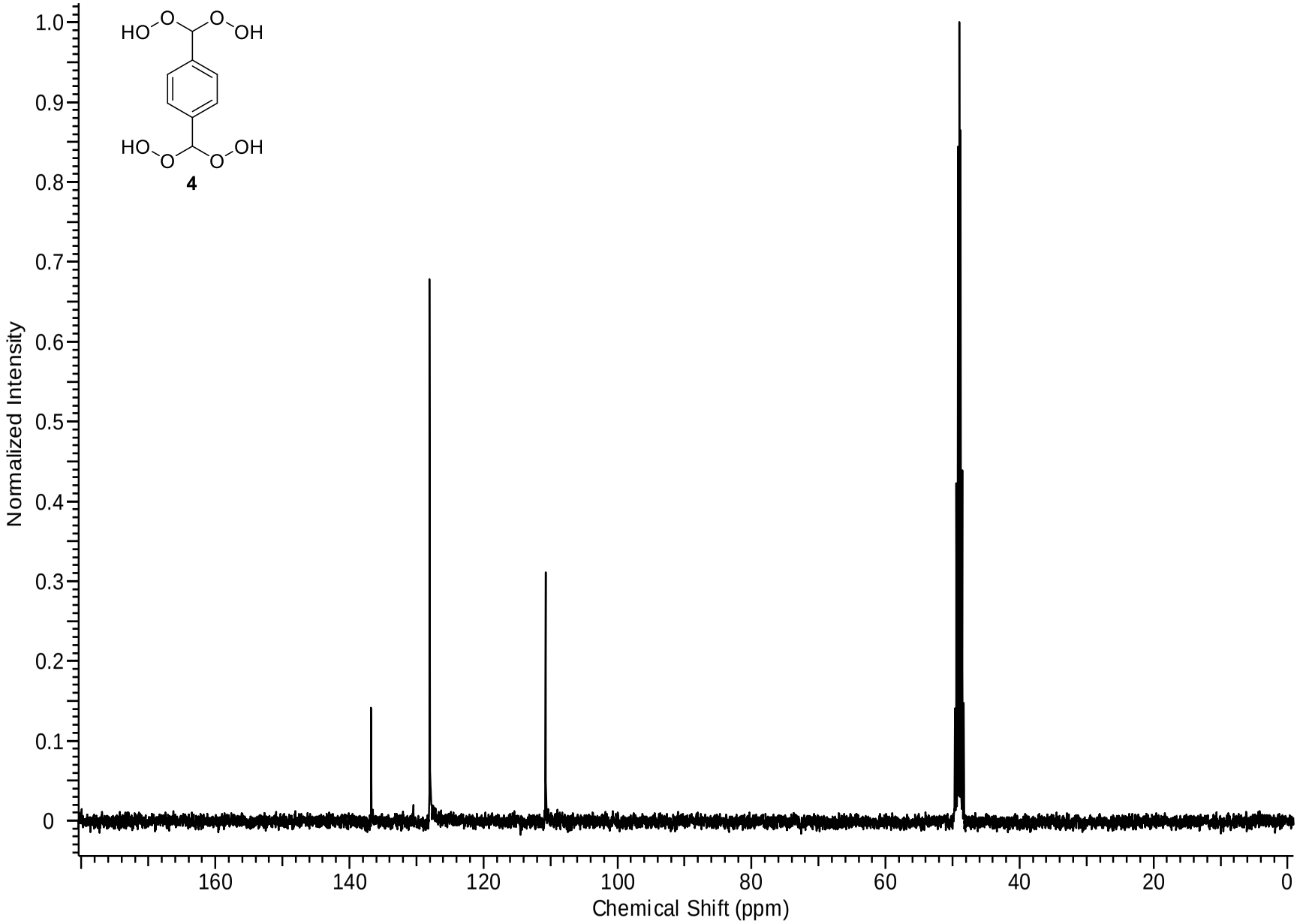
HO
O
O
OH
HO
O
O
OH
4
Normalized Intensity
1.0
0.9
0.8
0.7
0.6
0.5
0.4
0.3
0.2
0.1
0
160
140
120
100
80
60
40
20
0
Chemical Shift (ppm)

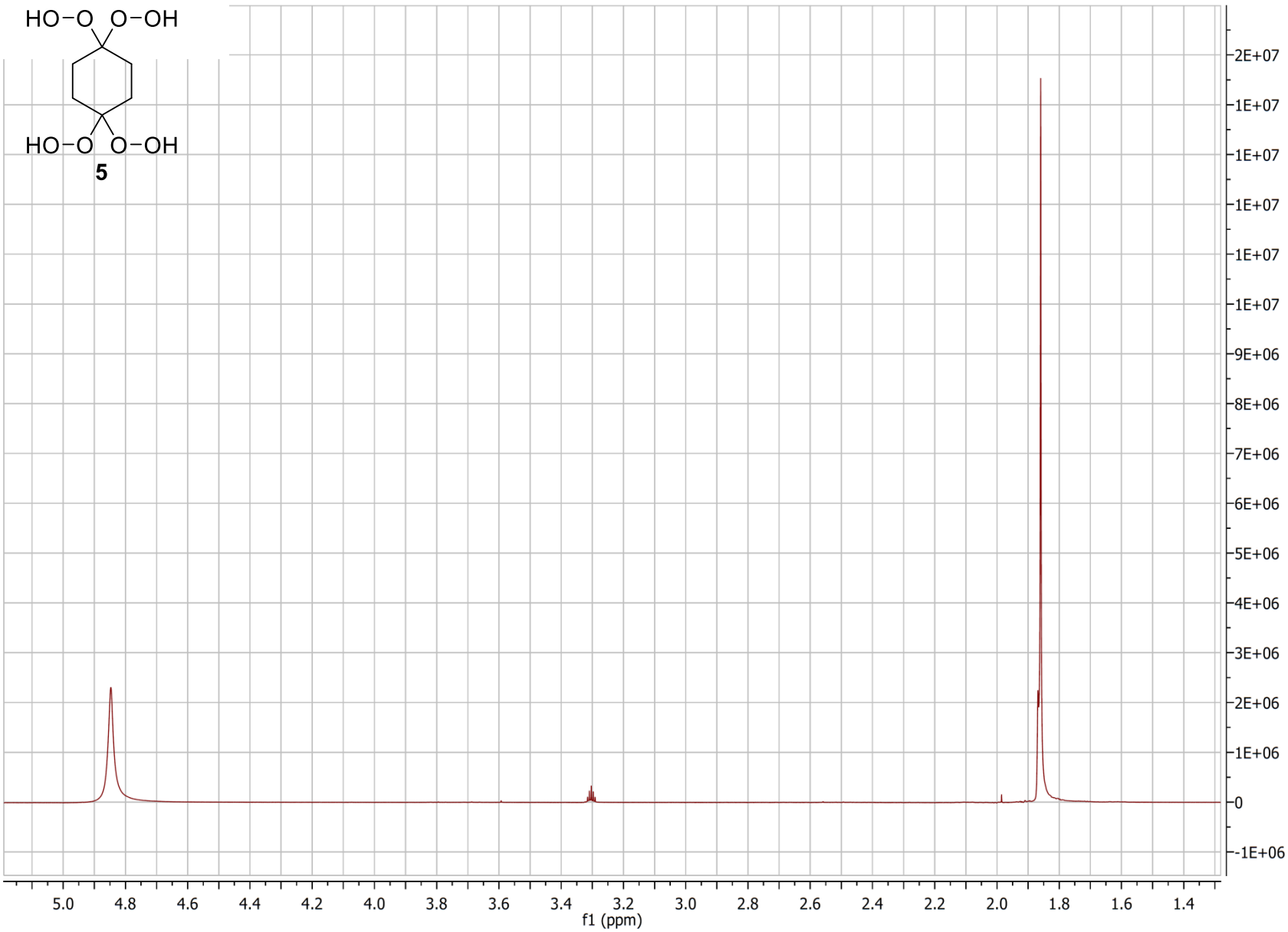
HO–O O–OH
HO–O O–OH
5
2E+07
1E+07
1E+07
1E+07
1E+07
1E+07
9E+06
8E+06
7E+06
6E+06
5E+06
4E+06
3E+06
2E+06
1E+06
0
-1E+06
5.0
4.8
4.6
4.4
4.2
4.0
3.8
3.6
3.4
3.2
3.0
2.8
2.6
2.4
2.2
2.0
1.8
1.6
1.4
f1 (ppm)

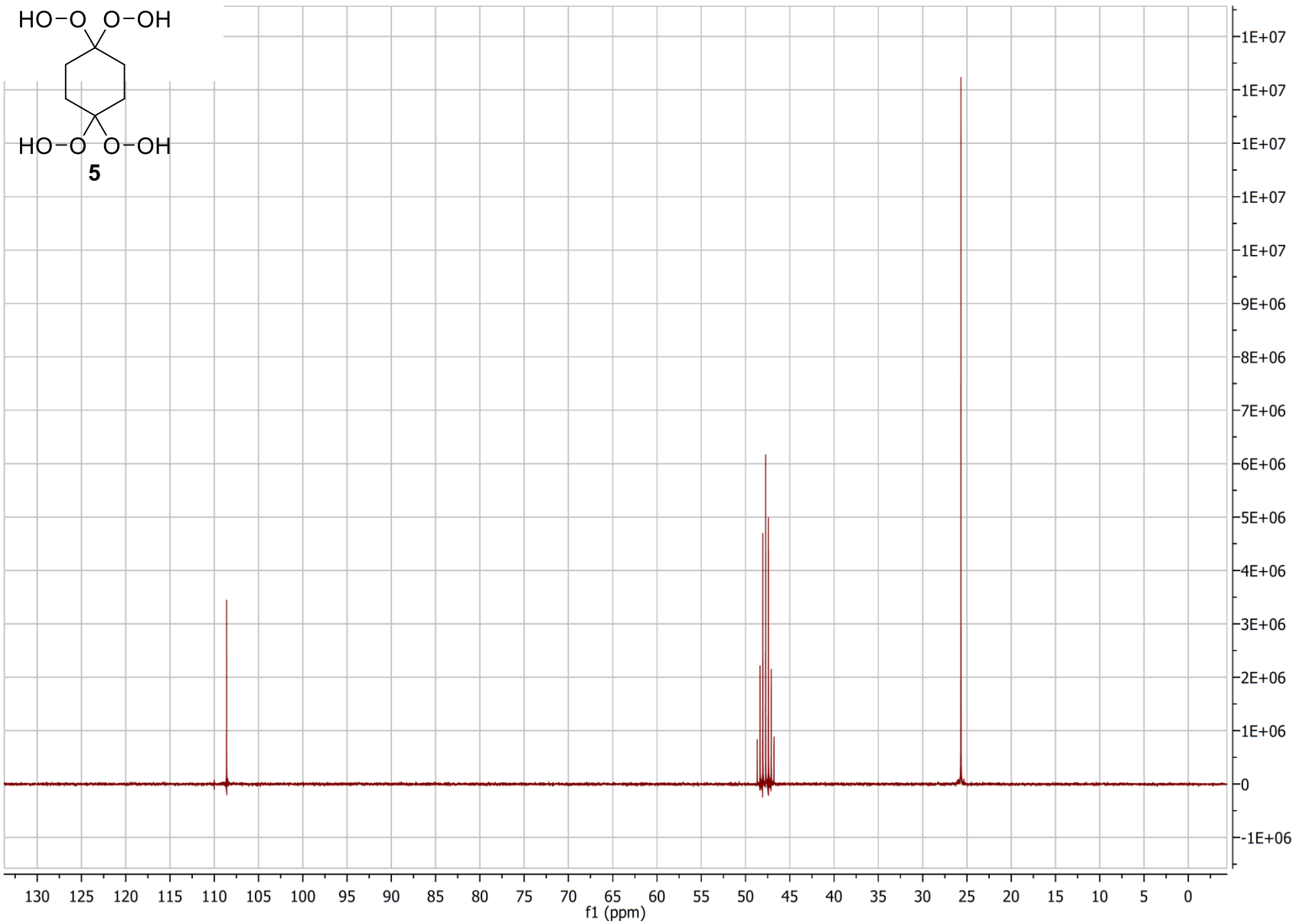
HO–O O–OH
HO–O O–OH
5
1E+07
1E+07
1E+07
1E+07
1E+07
9E+06
8E+06
7E+06
6E+06
5E+06
4E+06
3E+06
2E+06
1E+06
0
-1E+06
130 125 120 115 110 105 100 95 90 85 80 75 70 65 60 55 50 45 40 35 30 25 20 15 10 5 0
f1 (ppm)

EurJOC European Journal of Organic Chemistry

FULL PAPER

DOI: 10.1002/ejoc.201500919

Energetic Organic Peroxides – Synthesis and Characterization of 1,4-Dimethyl-2,3,5,6-tetraoxabicyclo[2.2.1]heptanes

Thomas M. Klapötke,*[a] Benedikt Stiasny,[a] Jörg Stierstorfer,[a] and Charles H. Winter[b]

Keywords: Energetic materials / Peroxides / Structure elucidation

1,4-Dimethyl-2,3,5,6-tetraoxabicyclo[2.2.1]heptane and several similar alkyl-derivatives were synthesized applying two different strategies. Crystal structures of the compounds were determined and their energetic properties including sensitivities towards impact, friction and electrostatic discharge as well as their thermal behaviour were determined and compared to tricacetone triperoxide (TATP). The enthalpies of formation and the resulting explosive properties were calculated using the EXPLO5 program.

Introduction

Organic peroxides are of great interest today as they show activity in various antimalaria[1] and antitumor agents.[2] Another field of application that has been discussed is the use as additives to diesel fuel to increase the cetane number and thus providing good initiation of the fuel under cold weather conditions.[3] On the other hand peroxides are known as potent explosives since the discovery of TATP (triacetone triperoxide) by Wolffenstein at the end of the 19th century.[4] The reaction of ketones with hydrogen peroxide can be applied not only to acetone but also to different substrates like acetylacetone[5] and its 3-alkyl analogue which is part of an ongoing research cooperation.[6–8] In this paper we focus on 1,4-dimethyl-2,3,5,6-tetraoxabicyclo[2.2.1]heptanes. 1,4-Dimethyl-2,3,5,6-tetraoxabicyclo[2.2.1]heptane was discovered by Milas in 1963.[5] Other molecules which have this functionality were prepared by Terentev in the 21st century.[9] He also showed that the moiety is stable to some standard chemical procedures such as epoxidations and brominations of double bonds.[10] The substance class of bridged tetroxanes is a very potent building block in drugs against schistosomiasis.[11] The performance of an energetic material directly corresponds with the number of energetic groups and the percentage these groups are in the whole molecule. For the molecules studied in this paper this means, that the lower the carbon content the higher the energetic performance of the molecule. Most of the currently known molecules carrying this bicyclic core structure, however, carry large substituents on the bridging carbon, which weakens their energetic properties. The molecules with simple alkyl derivatives such as ethyl and methyl are still unknown today. Further on these molecules can be potential, environmentally friendly replacements for heavy-metal containing primary explosives such as the widely used lead azide.

Results and Discussion

Synthesis

Six different peroxides were prepared using two different strategies. (1*R*,4*S*)-1,4,7-Trimethyl-2,3,5,6-tetraoxabicyclo-[2.2.1]heptane (**1**), (1*R*,4*S*)-7-ethyl-1,4-dimethyl-2,3,5,6-tetraoxabicyclo[2.2.1]heptane (**2**), (1*R*,4*S*)-7-ethyl-1,4,7-trimethyl-2,3,5,6-tetraoxabicyclo[2.2.1]heptane (**3**) and (1*R*,4*R*)-7,7-diethyl-1,4-dimethyl-2,3,5,6-tetraoxabicyclo-[2.2.1]heptane (**4**) were prepared by reacting their corresponding 3-alkyl-acetylacetone derivatives with an excess of aqueous 30% H_2O_2 and catalytic amounts of concentrated aqueous HCl at room temperature overnight following the procedure shown in Scheme 1.

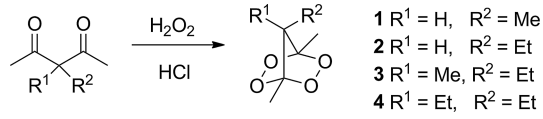

Scheme 1. Reaction equation for the synthesis of **1**, **2**, **3** and **4**.

For all this reactions, the reaction mixture consisted of a suspension of the ketone in aqueous hydrogen peroxide. No solvent was applied because this would result in the formation of the corresponding dioxolanes. In the case of peroxide **1**, precipitation of a white solid could be observed, which is the pure product. For compounds **2**, **3**, and **4** no precipitate is formed. After the reaction, the mixtures were

[a] Department of Chemistry, Ludwig-Maximilian University of Munich,
81377 Munich, Germany
E-mail: tmk@cup.uni-muenchen.de
www.hedm.cup.uni-muenchen.de
[b] Department of Chemistry, Wayne State University,
Detroit, Michigan 48202, USA
Supporting information for this article is available on the WWW under http://dx.doi.org/10.1002/ejoc.201500919.

extracted with diethyl ether which was removed in vacuo to yield the raw products. These were purified by silica column chromatography. In case of compound **3** problems occurred during purification. All attempts failed to get a pure product. The time of drying has to be kept as low as possible to avoid loss of the volatile products. At ambient temperature and pressure no excessive loss of the compounds can be observed, but if high vacuum is applied about 5 mg of substance evaporate per hour, also depending on the molecular weight of the compound. The yields obtained lie between 10 and 35%. The clean compounds are colorless oils which crystallize at –30 °C. For compounds (1*R*,4*R*)-1,4-dimethyl-2,3,5,6-tetraoxabicyclo[2.2.1]heptane (**5**) and (1*R*,4*R*)-1,4,7,7-tetramethyl-2,3,5,6-tetraoxabicyclo[2.2.1]heptane (**6**) the procedure given in Scheme 1 resulted in the formation of the corresponding dioxolanes. To overcome this problem, the corresponding hydroxy-hydroperoxy-dioxolanes were treated with P_4O_{10} in diluted etheric solutions at 0 °C following Scheme 2.[5]

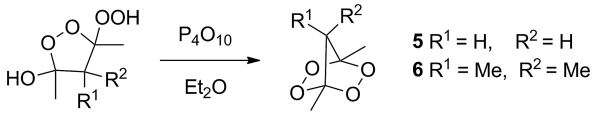

Scheme 2. Reaction equation for the synthesis of **5** and **6**.

After washing the reaction mixture with saturated $NaHCO_3$ solution and removal of the ether, peroxides **5** and **6** could be isolated as white solids in 14 and 73% yield respectively.

^{13}C NMR spectroscopy is a valuable method for identification of **1**–**6**. The characteristic signal is the one of the bridging-head carbons. It lies between 111.2 and 113.4 ppm and is therefore characteristic of O–O–C–O–O for bridged tetraoxanes. The shift to higher ppm values of the methyl resonances is also characteristic for bridged tetraoxanes.

Crystal Structures

Single crystals for all of the synthesized compounds were obtained by recrystallization from diethyl ether at –30 °C. Details of the X-ray diffraction measurements are given in the SI. The compounds crystallize in common space groups (**1**: *Pnma*, **2**: $P2_1/c$, **3** and **4**: *Pbca*, **5**: *Pbcn*, **6**: *Cmcm*) and the molecular moieties are shown in Figures 1, 2, and 3. Further information regarding the measurement and refinement of the structures are gathered in Table 1.

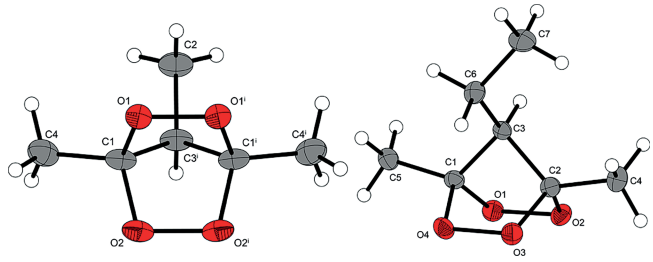

Figure 1. Molecular structures of **1** and **2** with the atom labelling scheme. Thermal ellipsoids in all structures represent the 50% probability level and hydrogen atoms are shown as small spheres of arbitrary radius.

The densities lie between 1.267 and 1.465 g cm^{-3} which is in the range or slightly higher than the densities of commonly known cyclic peroxides like TATP (1.22 g cm^{-3})[14] but lower than that of HMTD with 1.58 g cm^{-3}.[15] In all of the structures the bicyclic structure of the molecular core can clearly be observed. In the case of the ethyl-substituted molecules, it can be observed that the substituents are bent to the inside and not the outside of the molecule. Table 1 lists the corresponding angles and bond lengths for each compound.

The bond lengths of the O–O single bond lie between δ = 150 and 152 ppm. This values also correspond nicely with

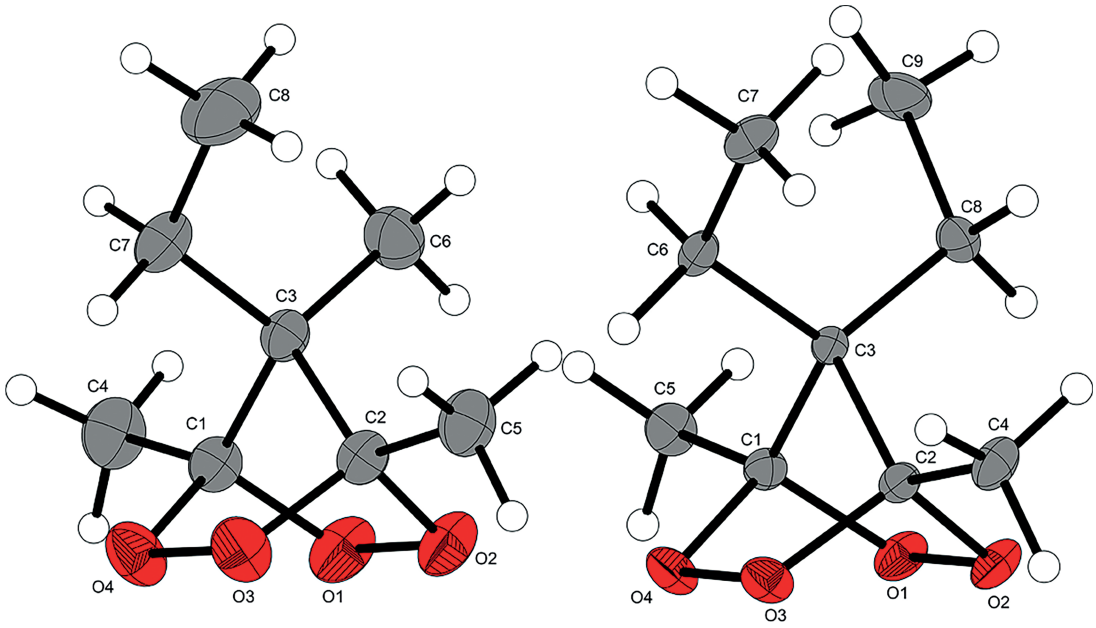

Figure 2. Molecular structures of **3** and **4** with the atom labelling scheme.

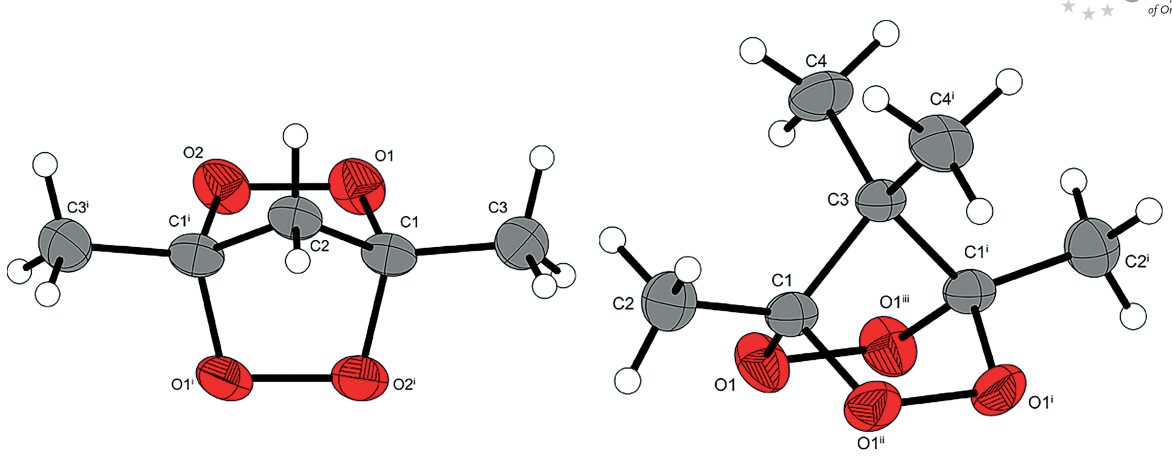

Figure 3. Molecular structures of **5** and **6** with the atom labelling scheme.

Table 1. Bond angles and bond lengths of the bicyclic core structures for compounds **1**–**6**.

	1	**2**	**3**	**4**	**5**	**6**
Bond lengths [pm]						
O1–O2 / O2–O1 / O1–O1^{iii}	151.77(14)	150.76(14)	150.70(12)	150.68(17)	150.56(15)	150.80(11)
O3–O4 / O2^{i}–O2^{i} / O1^{i}–O2^{i} / O1^{i}–O1^{ii}	150.25(13)	151.01(14)	151.08(13)	151.00(18)	150.56(15)	150.80(11)
C1–O1 / C1^{i}–O2	142.71(16)	142.65(15)	142.21(15)	142.7(2)	142.75(18)	142.37(12)
C1–O4 / C1–O2 / C1^{i}–O1^{i} / C1–O1^{ii}	142.72(16)	143.02(14)	142.07(15)	142.9(2)	142.75(18)	142.37(12)
C2–O2 / C1^{i}–O1^{i} / C1–O1 / C1^{i}–O1^{iii}	142.71(16)	143.11(16)	142.60(15)	142.6(2)	142.75(18)	142.37(12)
C2–O3 / C1^{i}–O2^{i} / C1–O2^{i} / C1^{i}–O1^{i}	142.72(16)	142.83(15)	142.23(15)	142.7(2)	142.75(18)	142.37(12)
C1–C3 / C1^{i}–C2	151.57(19)	151.92(17)	153.48(17)	153.8(2)	149.7(2)	152.4(2)
C2–C3 / C1–C2	151.57(19)	151.75(18)	153.47(16)	154.1(2)	149.7(2)	152.4(2)
Bond angle [°]						
O2–O1–C1 / O1^{i}–C1–C3 / O1–O2–C1^{i} / O1^{iii}–O1–C1	102.64(9)	102.61(8)	102.57(8)	102.18(11)	102.96(9)	102.61(8)
O1–O2–C2 / O1–O1^{i}–C1^{i} / O2–O1–C1 / O1^{i}–O1^{iii}–C1^{i}	102.64(9)	102.81(8)	102.78(8)	103.41(11)	102.80(9)	102.61(8)
O4–O3–C2 / O2–O2^{i}–C1^{i} / O1^{i}–O2^{i}–C1 / O1^{iii}–O1–C1	102.96(9)	102.80(8)	102.79(8)	102.64(11)	102.96(9)	102.61(8)
O3–O4–C1 / O2^{i}–O2–C1 / / O2^{i}–O1^{i}–C1^{i} / O1^{ii}–O1^{i}–C1	102.96(9)	102.51 (8)	102.44(8)	102.79(11)	102.80(9)	102.61(8)
O1–C1–O4 / O1–C1–O2 / O2–C1^{i}–O1^{i} / O1–C1–O1^{ii}	107.72(10)	107.51(10)	107.74(10)	107.55(13)	107.66(11)	107.79(11)
O2–C2–O3 / O1^{i}–C1^{i}–O2^{i} / O1–C1–O2^{i} / O1^{iii}–C1^{i}–O1^{i}	107.72(10)	107.93(10)	107.85(9)	107.87(13)	107.66(11)	107.79(11)
O4–C1–C3 / O2–C1–C3 / O1^{i}–C1^{i}–C2 / O1^{ii}–C1–C3	103.37(11)	103.51(10)	104.12(9)	103.86(13)	109.12(12)	103.83(8)
O1–C1–C3 / O2–C1^{i}–C2	103.23(11)	103.94(10)	104.21(9)	104.38(13)	109.42(12)	103.83(8)
O2–C2–C3 / O1^{i}–C1^{i}–C3 / O1–C1–C2 / O1^{iii}–C1^{i}–C3	103.23(11)	103.02(10)	103.66(9)	103.39(13)	109.12(12)	103.83(8)
O3–C2–C3 / O2^{i}–C1^{i}–C3 / O2^{i}–C1–C2 / O1^{i}–C1^{i}–C3	103.37(11)	103.76(10)	103.92(9)	103.93(13)	109.42(12)	103.83(8)

values given in the literature determined for (3-methyl)-benzyl- and cyanoethyl-substituted molecules which have O–O-bond length of 150.2 and 150.1 ppm respectively.[10] Compound **1** has the shortest and the longest bond in the same molecule but all in all the bonds have more or less the same length.

Energetic Properties

The performance data of the compounds were calculated using the EXPLO5 program in its latest version 6.02. Heats of formation were calculated with the atomization method based on CBS-4M electronic enthalpies. Table 2 gathers the energetic properties. Compound **3** has not been included since it was not obtained in a pure solid form.

Impact sensitivities were observed with values below 1 J for compounds **1**, **2**, **5** and **6** (which is the lowest value with our drophammer) and 1.5 J for compound **4**. Friction sensitivities are below 5 N for the solid compounds, which is also the lowest value of the BAM friction tester. Thus, all compounds have sensitivities in the range of typical primary explosives and should be handled with great care! The sensitivities toward electrostatic discharge lie between 0.1 J and 0.2 J. Compound **2** is a solid at room temperature but becomes liquid during ESD sensitivity determination as a consequence of the heat created by the spark at 0.1 J. Thermal decomposition points lie between 103 °C and 136 °C, which is in a normal range for organic peroxides although being quite low for potential utilization. The calculated detonation velocities lie between 6048 and 6343 m s^{-1}. The calculated detonation velocity (based on a density of

Table 2. Energetic properties of compound **1**, **2**, **4**, **5** and **6** compared with TATP.

	1	**2**	**4**	**5**	**6**	**TATP**
Formula	$C_6H_{10}O_4$	$C_7H_{12}O_4$	$C_9H_{16}O_4$	$C_5H_8O_4$	$C_7H_{12}O_4$	$C_9H_{18}O_6$
F_w [g/mol]	146.16	160.19	188.25	132.13	160.19	222.27
IS [J] [a]	<1	<1	1.5	<1	<1	0.3
FS [N][b]	<5	<5	<5	<5	<5	0.1
ESD [J][c]	0.15	0.1	0.2	0.2	0.1	0.16
Ω_{CO2} [%][d]	–142.3	–159.8	–187.0	–121.1	–159.8	–151.2
T_m/T_{dec} [°C][e]	56/136	–/108	48/116	–/121	85/110	150–160[15]
ρ [g/cm³][f]	1.339	1.314	1.244	1.438	1.321	1.25[16]
$\Delta_f H_m°$ [kJ/mol][g]	–347.7	–381.4	–402.0	–429.0	–318.7	–631.4
$\Delta_f U°$ [kJ/kg][h]	–2261	–2258	–2148	–2300	–2351	–2707
EXPLO5 6.02 values						
$-\Delta_{ex}U$ [kJ/kg][i]	4372	4000	3555	4781	3915	3986
T_{det} [K] [j]	2499	2264	1997	2775	2231	2245
P_{CJ} [kbar][k]	109	105	97	133	106	108
V_{det}[m/s][l]	6048	6135	6127	6343	6141	6315
$V°$ [L/kg][m]	809	828	838	772	826	916

[a] Impact sensitivity according to the BAM drophammer (method 1 of 6). [b] Friction sensitivity according to the BAM friction tester (method 1 of 6). [c] Electrostatic discharge sensitivity (OZM ESD tester). [d] Oxygen balance. [e] Temperature of decomposition according to DTA (onset temperatures at a heating rate of 5 °C/min). [f] Low temperature X-ray densities. These were calculated by the low-temperature X-ray values using the equation: $\{\rho_{298\,K} = \rho_T/[1 + \alpha_V(298 - T_0)]$; $\alpha_V = 1.5\ 10^{-4}\ K^{-1}\}$. [g] Calculated heat of formation using the atomization method and CBS-4M electronic enthalpies. [h] Calculated energy of formation. [i] Heat of detonation. [j] Temperature of detonation. [k] Detonation pressure. [l] Detonation velocity. [m] Volume of gases after detonation.

1.25 g cm^{-3} and a calcd. heat of formation of –631.4 kJ mol^{-1}) for TATP is 6315 m s^{-1} and therefore slightly higher than those of **1**, **2**, **4** and **6**. The higher detonation velocities of the bicyclic compounds can mostly be explained with the additional ring-strain. The detonation pressure of **5** is 133 kbar which is the highest value calculated for the compounds in this study and also significantly higher than that of TATP. The other values are all between 97 and 109 kbar and therefore in the same range.

Conclusions

We succeeded in the synthesis of various bridged tetraoxanes, namely (1*R*,4*S*)-1,4,7-trimethyl-2,3,5,6-tetraoxabicyclo[2.2.1]heptane (**1**), (1*R*,4*S*)-7-ethyl-1,4-dimethyl-2,3,5,6-tetraoxabicyclo[2.2.1]-heptane (**2**), (1*R*,4*R*)-7,7-diethyl-1,4-dimethyl-2,3,5,6-tetraoxabicyclo[2.2.1]heptane (**4**), (1*R*,4*R*)-1,4-dimethyl-2,3,5,6-tetraoxabicyclo[2.2.1]heptane (**5**), and (1*R*,4*R*)-1,4,7,7-tetramethyl-2,3,5,6-tetraoxabicyclo[2.2.1]-heptane (**6**) by two simple synthetic protocols. The yields we obtained were low to moderate (10–73 %). All compounds could be crystallized and their molecular structures were determined by X-ray diffraction. In addition the crystal structure of (1*R*,4*S*)-7-ethyl-1,4,7-trimethyl-2,3,5,6-tetraoxabicyclo[2.2.1]heptane (**3**) could be determined although it was not possible for us to get the clean compound. Most of them crystallize in orthorhombic space groups (**1**: *Pnma*, **2**: $P2_1/c$, **3** and **4**: *Pbca*, **5**: *Pbcn*, **6**: *Cmcm*) with densities between 1.244 and 1.438 g cm^{-3}. The compounds are very sensitive toward impact (≤ 1.5 J) and friction (<5 N) and must therefore be handled as primary explosives. However, due to their volatility and high sensitivities a utilization is disputable.

Experimental Section

CAUTION! All investigated compounds are potentially explosive energetic materials, although no hazards were observed during preparation and handling these compounds. Nevertheless, this necessitates additional meticulous safety precautions (earthed equipment, Kevlar gloves, Kevlar sleeves, face shield, leather coat, and earplugs).

General: All chemicals were received from Sigma–Aldrich and used without further purification. Sensitivity measurements were performed on a BAM-drophammer, a BAM friction tester and OZM-ESD-tester. Infrared spectra were recorded on a Perkin–Elmer One FT-IR Spectrum BX II with a Smith ATR Dura Sample IRII. NMR spectra were recorded on a Bruker 400 MHz-spectrometer operating at 400 MHz for proton spectra. Melting points and decomposition points were recorded on an OZM Research DTA 552-Ex instrument.

3-Methylpentane-2,4-dione and 3-ethylpentane-2,4-dione were synthesized according to procedures given in ref.[12] 3,3-Dimethylpentane-2,4-dione and 3,3-diethylpentane-2,4-dione were synthesized following literature procedures given in ref.[13] 3-Ethyl-3-methylpentane-2,4-dione was synthesized by a slightly modified literature procedure in a stepwise manner. Acetylacetone was first ethylated and the resulting product was methylated.[12].

(1*R*,4*S*)-1,4,7-Trimethyl-2,3,5,6-tetraoxabicyclo[2.2.1]heptane (1): 0.980 g of 3-methylpentane-2,4-dione (8.58 mmol, 1.00 mL) was suspended in 5.00 mL of 30% aqueous H_2O_2 solution, and two drops of concentrated aqueous HCl were added. This mixture was stirred at room temperature overnight. During that time a white precipitate had formed, which was collected by filtration, washed with water and ethanol and dried briefly in high vacuum. Single crystals of the compound were grown in diethyl ether at –30 °C, yield 0.123 g (10%). DTA (5 °C min^{-1}) T_m/°C(onset) = 56; T_{dec}/°C(onset) = 136. ^{1}H NMR (CD_3OD, 400 MHz, 300 K): δ = 2.78 (q, J = 6.8 Hz, 1 H), 1.47 (s, 6 H), 1.16 (d, J = 6.8 Hz, 3 H) ppm. ^{13}C NMR (CD_3OD, 100 MHz, 300 K): δ = 112.1 (MeCOO), 55.6 (MeCH), 9.3

($OCOCH_3$), 8.4 ($HCCH_3$) ppm. IR (ATR): $\tilde{\nu}$ = 3011 (w), 2981 (w), 2949 (w), 1462 (w), 1443 (w), 1382 (m), 1365 (w), 1312 (m), 1217 (w), 1197 (m), 1163 (s), 1110 (m), 1034 (m), 902 (m), 840 (s), 791 (m), 670 (m) cm^{-1}. Raman (1064 nm): $\tilde{\nu}$ = 3011 (61), 3003 (61), 2981 (50), 2951 (100), 2753 (13), 1457 (31), 1296 (19), 1197 (13), 1034 (13), 902 (13), 852 (13), 802 (38), 793 (50), 668 (10), 611 (91), 561 (99), 515 (25). EA found (calcd.): C 49.00 (49.30), H 6.83 (6.91). IS: <1 J. FS: <5 N. ESD: 0.15 J.

(1*R*,4*S*)-7-Ethyl-1,4-dimethyl-2,3,5,6-tetraoxabicyclo[2.2.1]heptane (2): 0.960 g of 3-ethylpentane-2,4-dione (7.48 mmol, 1.00 mL) was suspended in 6.00 mL of 30% H_2O_2 solution, and 2 drops of concentrated aqueous HCl were added. The mixture was stirred overnight. The next day, the reaction mixture was extracted three times with 10 mL of diethyl ether and the diethyl ether phase was dried with anhydrous sodium sulfate. The diethyl ether was removed in vacuo, and the crude product was purified by column chromatography on silica gel using ethyl acetate/pentane (2:9) as eluent. Single crystals of the compound were grown in diethyl ether at –30 °C, yield 0.14 g (12%). DTA (5 °C min^{-1}) T_{dec}/°C(onset) = 108. ^{1}H NMR (CD_3OD, 400 MHz, 300 K): δ = 2.60 (t, J = 6.0 Hz, 1 H), 1.68–1.58 (m, 2 H), 1.51 (s, 6 H), 1.12 (t, J = 7.6 Hz, 3 H) ppm. ^{13}C NMR (CD_3OD, 100 MHz, 300 K): δ = 112.1 (MeCOO), 61.9 (EtCH), 18.2 ($OCOCH_3$), 12.4 ($MeCH_2$), 9.8 (CH_2CH_3) ppm. IR (ATR): $\tilde{\nu}$ = 2977 (w), 2949 (w), 2885 (w), 1466 (w), 1380 (m), 1338 (w), 1316 (w), 1286 (w), 1264 (w), 1195 (s), 1164 (s), 1124 (s), 1092 (m), 1050 (w), 962 (w), 929 (w), 903 (m), 875 (s), 833 (s), 673 (s) cm^{-1}. Raman (1064 nm): $\tilde{\nu}$ = 3010 (33), 2952 (100), 2884 (25), 1456 (21), 1039 (8), 910 (25), 847 (33), 751 (17), 575 (17), 500 (13), 356 (21). IS: <1 J. FS: <5 N. ESD: becomes liquid during measurement.

(1*R*,4*S*)-7-Ethyl-1,4,7-trimethyl-2,3,5,6-tetraoxabicyclo[2.2.1]heptane (3): 2.00 mL of 3-ethyl-3-methylpentane-2,4-dione (1.84 g, 12.9 mmol) was suspended in 6.00 mL of 30% aqueous H_2O_2 solution. To this mixture 5 drops of concentrated aqueous hydrochloric acid were added. The mixture was stirred at room temperature overnight. After this time, the solvent was removed in vacuo to obtain a colorless oil as the raw product. This oil was purified by column chromatography on silica using pentane/ethyl acetate (10:1) as solvent. Single crystals of the compound were grown in diethyl ether at –30 °C, yield 0.279 g (12%). DTA (5 °C min^{-1}) T_{dec}/°C(onset) = 103. ^{1}H NMR (CD_3OD, 400 MHz, 300 K): δ = 1.69 (q, J = 8.0 Hz, 2 H), 1.39 (s, 6 H), 1.19 (s, 3 H), 1.04 (t, J = 8.0 Hz, 3 H) ppm. ^{13}C NMR (CD_3OD, 100 MHz, 300 K): δ = 113.3 (MeCOO), 61.9 (EtCMe), 23.9 ($OCOCH_3$), 12.9 (CH_3CH_2), 9.0 ($EtCCH_3$), 8.8 (CH_2CH_3) ppm. IR (ATR): $\tilde{\nu}$ = 2976 (w), 2947 (w), 2887 (w), 2745 (w), 1590 (w), 1463 (m), 1385 (m), 1332 (w), 1301 (w), 1281 (w), 1222 (w), 1197 (w), 1137 (s), 1097 (w), 1042 (w), 1009 (w), 954 (w), 891 (m), 850 (s), 802 (w), 766 (w), 687 (m), 665 (m), 611 (w), 585 (m), 563 (w) cm^{-1}. IR (Raman) (1064 nm): $\tilde{\nu}$ = 3005 (33), 2948 (100), 2743 (6), 1446 (28), 1282 (6), 1223 (6), 1042 (6), 803 (27), 688 (22), 667 (72), 636 (22), 587 (17), 564 (56), 542 (17). IS: <1 J. FS: <5 N; ESD: oil at room-temperature and therefore not measureable.

(1*R*,4*R*)-7,7-Diethyl-1,4-dimethyl-2,3,5,6-tetraoxabicyclo[2.2.1]heptane (4): 0.459 g of 3,3-diethylpentane-2,4-dione (2.94 mmol, 0.500 mL) was suspended in 5.00 mL of 30% aqueous H_2O_2 solution, and three drops of concentrated aqueous HCl were added. The mixture was stirred at room temperature overnight. The next day, the reaction mixture was extracted three times with 10 mL of diethyl ether and the ethereal phase dried with anhydrous sodium sulfate. The diethyl ether was removed in vacuo, and the crude product was purified by column chromatography on silica gel using ethyl acetate/pentane (1:9) as eluent. Single crystals of the compound were grown in diethyl ether at –30 °C, yield 0.19 g (35%). DTA (5 °C min^{-1}) T_m/°C(onset) = 48, DTA (5 °C/min) T_{dec}/°C(onset) = 116. ^{1}H NMR (CD_3OD, 400 MHz, 300 K): δ = 1.79 (q, J = 7.6 Hz, 4 H), 1.41 (s, 6 H), 1.05 (t, J = 7.6 Hz, 6 H) ppm. ^{13}C NMR (CD_3OD, 100 MHz, 300 K): δ = 113.4 (MeCOO), 61.8 (EtCEt), 20.0 ($OCOCH_3$), 9.6 (CH_3CH_2), 8.7 (CH_2CH_3) ppm. IR (ATR): $\tilde{\nu}$ = 3429 (w), 2984 (m), 2951 (m), 2890 (m), 2360 (m), 2342 (m), 1734 (w), 1717 (w), 1700 (w), 1684 (w), 1559 (w), 1540 (w), 1522 (w), 1507 (w), 1497 (w), 1489 (w), 1456 (m), 1419 (w), 1382 (m), 1342 (w), 1322 (w), 1298 (w), 1258 (w), 1226 (m), 1209 (m), 1133 (s), 1092 (m), 1056 (w), 956 (m), 926 (w), 890 (m), 845 (s), 805 (w), 791 (w), 740 (w), 684 (s), 668 (w) cm^{-1}. IR (Raman) (1064 nm): $\tilde{\nu}$ = 3022 (30), 3009 (28), 2987 (42), 2973 (42), 2948 (100), 2894 (35), 2739 (7), 1473 (22), 1446 (23), 1285 (15), 1211 (10), 1058 (10), 1040 (10), 956 (5), 892 (5), 807 (15), 670 (46), 633 (30), 571 (40), 550 (20), 526 (15), 423 (15); EA found (calcd.): C 57.68 (57.42), H 8.63 (8.58). IS: 1.5 J. FS: <5 N. ESD: 0.5 J.

(1*R*,4*R*)-1,4-Dimethyl-2,3,5,6-tetraoxabicyclo[2.2.1]heptane (5): The synthesis was performed following directly the one given in ref.[5] 0.300 g of 5-hydroperoxy-3,5-dimethyl-1,2-dioxolan-3-ol (2.00 mmol) was dissolved in 300 mL of diethyl ether and cooled to 0 °C. To this solution 6.00 g of P_4O_{10} (42.3 mmol) was added in eight equal portions over the course of 8 h. Then the reaction mixture was stirred overnight during which time it reached room temperature. The reaction mixture was filtered into a separatory funnel, washed with 150 mL of a saturated $NaHCO_3$ solution and water. The diethyl ether phase was dried with $MgSO_4$ and concentrated in vacuo. Single crystals of the compound were grown in diethyl ether at –30 °C, yield 0.037 g (14%). DTA (5 °C min^{-1}) T_{dec}/°C(onset) = 121. ^{1}H NMR (CD_3OD, 400 MHz, 300 K): δ = 2.75 (s, 2 H), 1.60 (s, 6 H) ppm. ^{13}C NMR (CD_3OD, 100 MHz, 300 K): δ = 111.2 (MeCOO), 51.4 (CH_2), 10.5 (-CH_3) ppm. IR (ATR): $\tilde{\nu}$ = 2952 (w), 1725 (w), 1445 (m), 1380 (m), 1323 (m), 1218 (w), 1164 (s), 1081 (m), 1042 (w), 992 (w), 950 (w), 926 (w), 855 (m), 824 (s) cm^{-1}. IR (Raman) (1064 nm): $\tilde{\nu}$ = 3050 (10), 3011 (25), 2999 (25), 2955 (53), 1460 (13), 1322 (5), 1195 (8), 1163 (8), 928 (15), 859 (30), 827 (20), 802 (38), 579 (100), 562 (10), 542 (30); EA found (calcd.): C 45.13 (45.45), H 6.12 (6.16). IS: <1 J. FS: <5 N. ESD: 0.2 J.

(1*R*,4*R*)-1,4,7,7-Tetramethyl-2,3,5,6-tetraoxabicyclo[2.2.1]heptane (6): 0.148 g of 5-hydroperoxy-3,4,4,5-tetramethyl-1,2-dioxolan-3-ol (0.830 mmol) was dissolved in 150 mL of diethyl ether and cooled to 0 °C. To this mixture, 3.00 g of P_4O_{10} (21.2 mmol) was added in 8 equal portions over the course of 8 h. Then the reaction mixture was stirred overnight during which time it reached room temperature. The next day the mixture was filtered in a separatory funnel and washed with 100 mL of saturated $NaHCO_3$ solution and water. The diethyl ether phase was dried with Na_2SO_4 and concentrated in vacuo. Single crystals of the compound were grown in diethyl ether at –30 °C, yield 0.097 g (73%). DTA (5 °C min^{-1}) T_m/°C(onset) = 85, T_{dec}/°C(onset) = 110. ^{1}H NMR (CD_3OD, 400 MHz, 300 K): δ = 1.38 (s, 6 H), 1.18 (s, 6 H) ppm. ^{13}C NMR(CD_3OD, 100 MHz, 300 K): δ = 113.0 (MeCOO), 57.5 (MeCMe), 16.6 ($OCOCH_3$), 8.0 ($MeCCH_3$) ppm. IR (ATR): $\tilde{\nu}$ = 3020 (w), 2970 (w), 2943 (w), 1727 (w), 1464 (w), 1439 (m), 1388 (w), 1378 (m), 1296 (w), 1247 (w), 1228 (w), 1140 (s), 957 (w), 899 (m), 849 (s), 678 (m) cm^{-1}. IR (Raman) (1064 nm): $\tilde{\nu}$ = 3021 (20), 3000 (56), 2972 (20), 2945(72), 1452 (32), 1325 (8), 1251 (16), 958 (8), 901 (8), 858 (8), 797 (20), 682 (100), 636 (16), 567 (72), 530 (16). EA found (calcd.): C 52.33 (52.48), H 7.58 (7.56). IS: <1 J. FS: <5 N. ESD: 0.1 J.

Acknowledgments

Financial support of this work by the Ludwig Maximilian University (LMU), Munich and the Office of Naval Research (ONR), USA (grant N00014-12-1-0526 to C. H. W., grant N00014-12-1-0538 to T. M. K.) is gratefully acknowledged. The authors acknowledge collaborations with Dr. Mila Krupka (OZM Research, Czech Republic) in the development of new testing and evaluation methods for energetic materials and with Dr. Muhamed Suceska (Brodarski Institute, Croatia) in the development of new computational codes to predict the detonation and propulsion parameters of novel explosives. The authors thank Mr. Stefan Huber for sensitivity measurements. The authors also would like to thank Ms. Nipuni-Dhanesha H. Gamage at Wayne State University for many inspiring discussions.

[1] C. W. Jefford, *Drug Discovery Today* **2007**, *12*, 487–495.
[2] V. M. Dembitsky, T. A. Gloriozova, V. V. Poroikov, *Mini-Rev. Med. Chem.* **2007**, *7*, 571–589.
[3] A. B. Rode, K. Chung, Y.-W. Kim, I. S. Hong, *Energy Fuels* **2010**, *24*, 1636–1639.
[4] R. Wollfenstein, *Ber. Dtsch. Chem. Ges.* **1895**, *28*, 2265.
[5] N. A. Milas, O. L. Magelli, A. Golubovic, R. W. Arndt, J. C. J. Ho, *J. Am. Chem. Soc.* **1963**, *24*, 222–226.
[6] N.-D. Gamage, C. H. Winter, private communication.
[7] N.-D. H. Gamage, B. Stiasny, J. Stierstorfer, P. D. Martin, T. M. Klapötke, C. H. Winter, *Chem. Eur. J.*, submitted.
[8] N.-D. H. Gamage, B. Stiasny, J. Stierstorfer, P. D. Martin, T. M. Klapötke, C. H. Winter, *Chem. Commun.* **2015**, 51, 13298–13300.
[9] A. O. Terent'ev, I. A. Yaremenko, V. A. Vil, I. K. Moiseev, S. A. Kon'kov, V. M. Dembitsky, D. O. Levitska, G. I. Nikishin, *Org. Biomol. Chem.* **2013**, *11*, 2613–2623.
[10] A. O. Terent'ev, D. A. Borisov, V. V. Chernyshev, G. I. Nikishin, *J. Org. Chem.* **2009**, *74*, 3335–3340.
[11] K. Ingarm, I. A. Yaremenko, I. B. Krylov, L. Hofer, A. O. Terent'ev, J. Keiser, *J. Med. Chem.* **2012**, *55*, 8700–8711.
[12] D. Kalaitzakis, J. D. Rozzell, I. Smonou, S. Kambourakis, *Adv. Synth. Catal.* **2006**, *348*, 1958–1969.
[13] K. Beck, S. Hünig, *Chem. Ber.* **1987**, *120*, 477–483.
[14] *Römpp Online*, Thieme, Stuttgart, Germany, version 2.3.2015.
[15] W. P. Schaefer, J. T. Fourkas, B. G. Tiemann, *J. Am. Chem. Soc.* **1985**, *107*, 2461–2463.
[16] F. Dubnikova, R. Kosloff, J. Almog, Y. Zeiri, R. Boese, H. Itzhaky, A. Alt, E. Keinan, *J. Am. Chem. Soc.* **2005**, *127*, 1146–1159.

Received: July 10, 2015
Published Online: August 21, 2015

Eur. J. Org. Chem. **2015** · ISSN 1099–0682

SUPPORTING INFORMATION

DOI: 10.1002/ejoc.201500919
Title: Energetic Organic Peroxides – Synthesis and Characterization of 1,4-Dimethyl-2,3,5,6-tetraoxabicyclo[2.2.1]heptanes
Author(s): Thomas M. Klapötke,* Benedikt Stiasny, Jörg Stierstorfer, Charles H. Winter

Table of contents

1. NMR Spectroscopy

(1R,4S)-1,4,7-Trimethyl-2,3,5,6-tetraoxabicyclo[2.2.1]heptane (1):

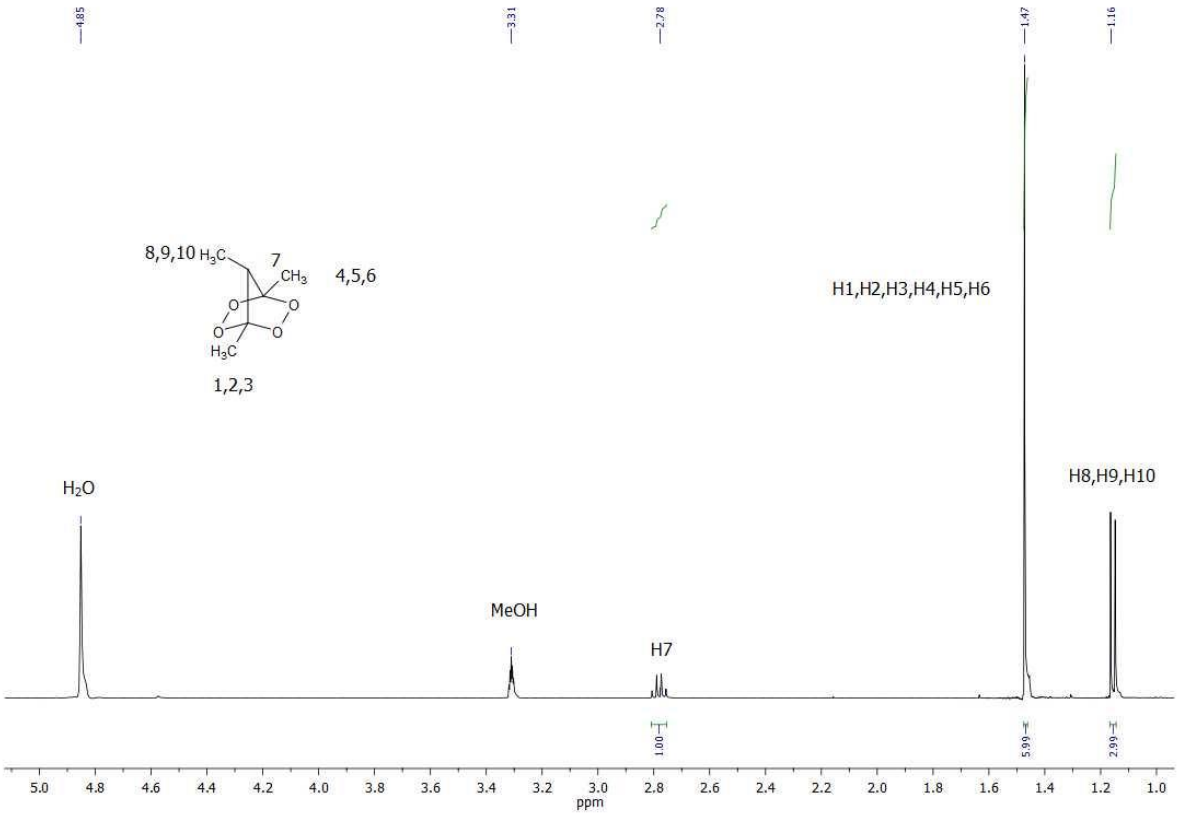

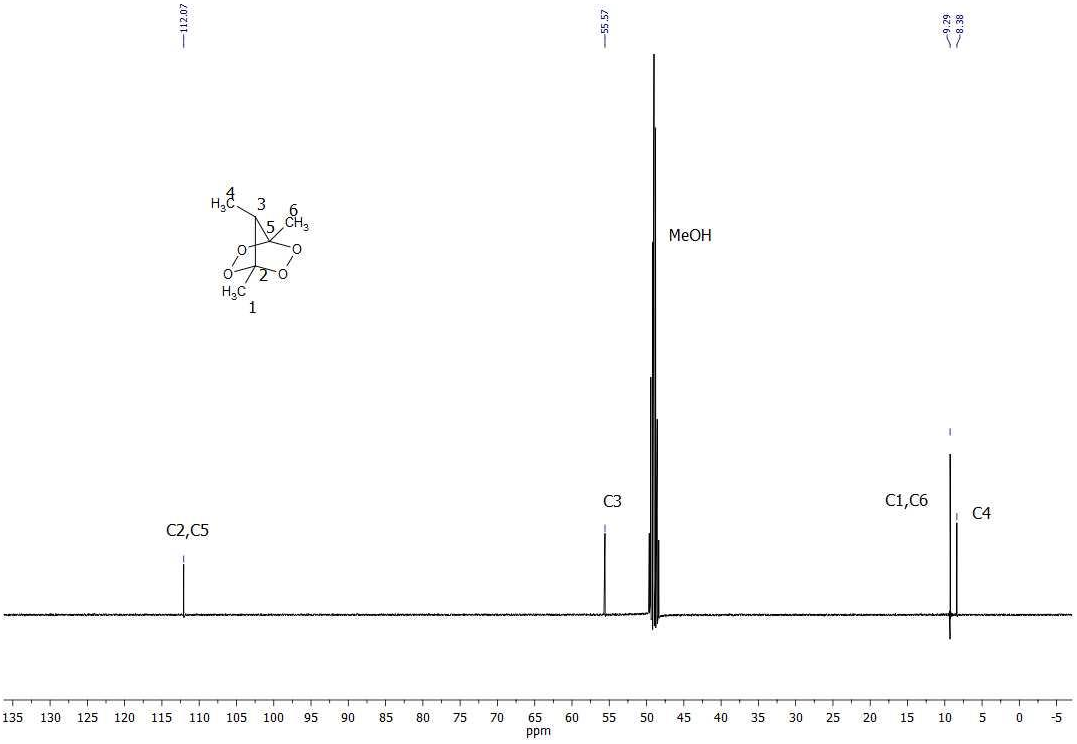

(1R,4S)-7-Ethyl-1,4-dimethyl-2,3,5,6-tetraoxabicyclo[2.2.1]heptane (2):

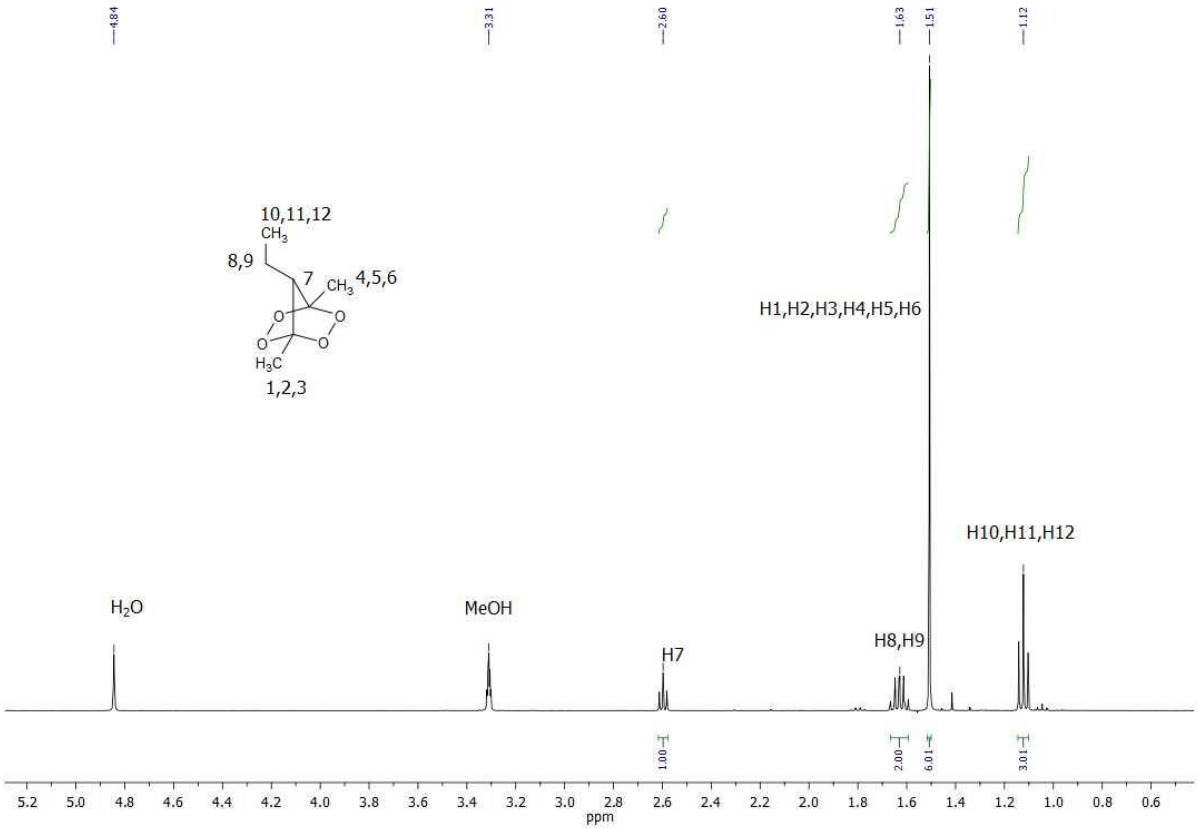

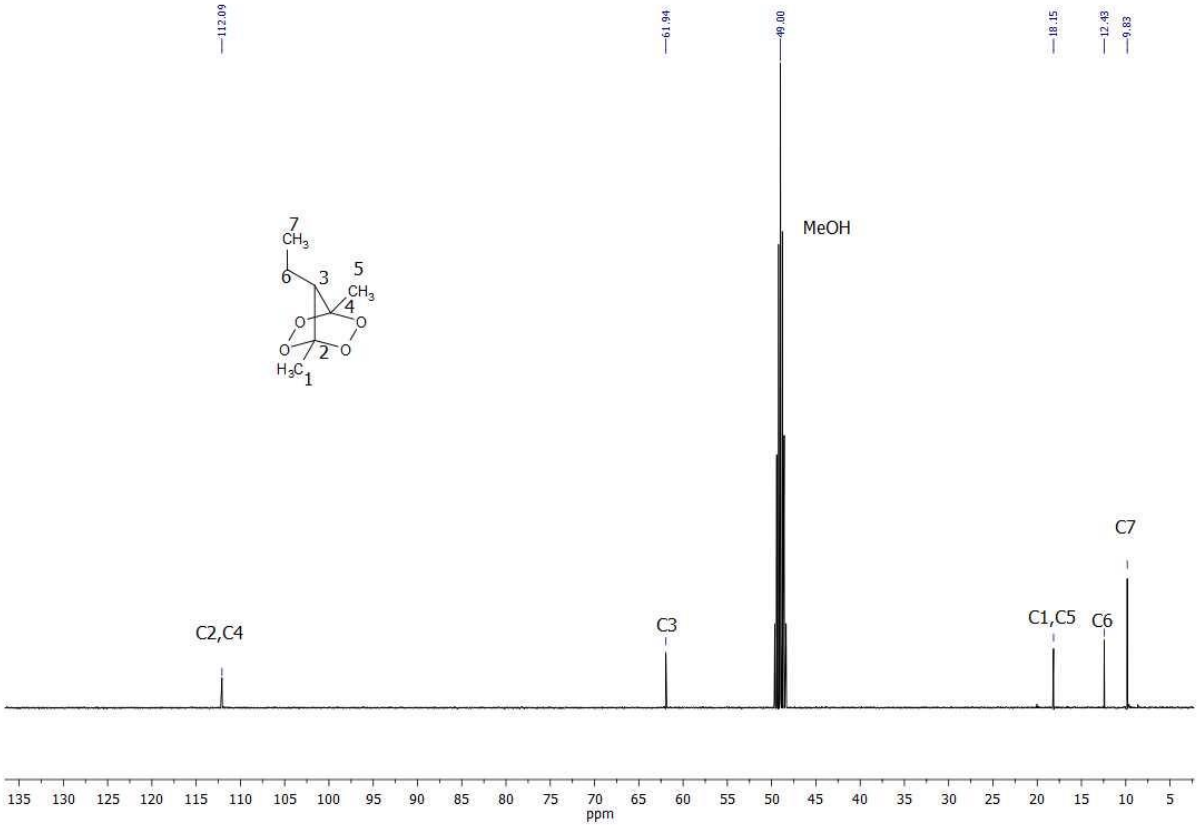

(1R,4S)-7-Ethyl-1,4,7-trimethyl-2,3,5,6-tetraoxabicyclo[2.2.1]heptanes (3):

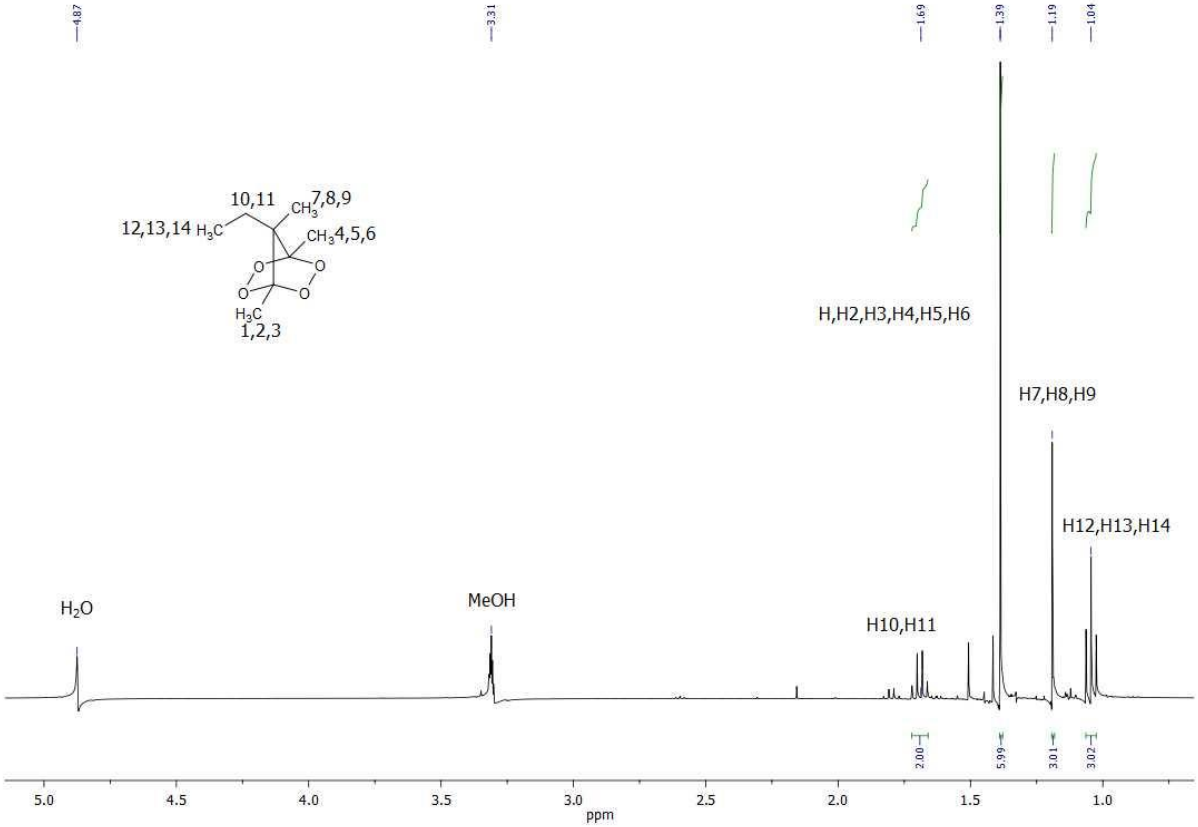

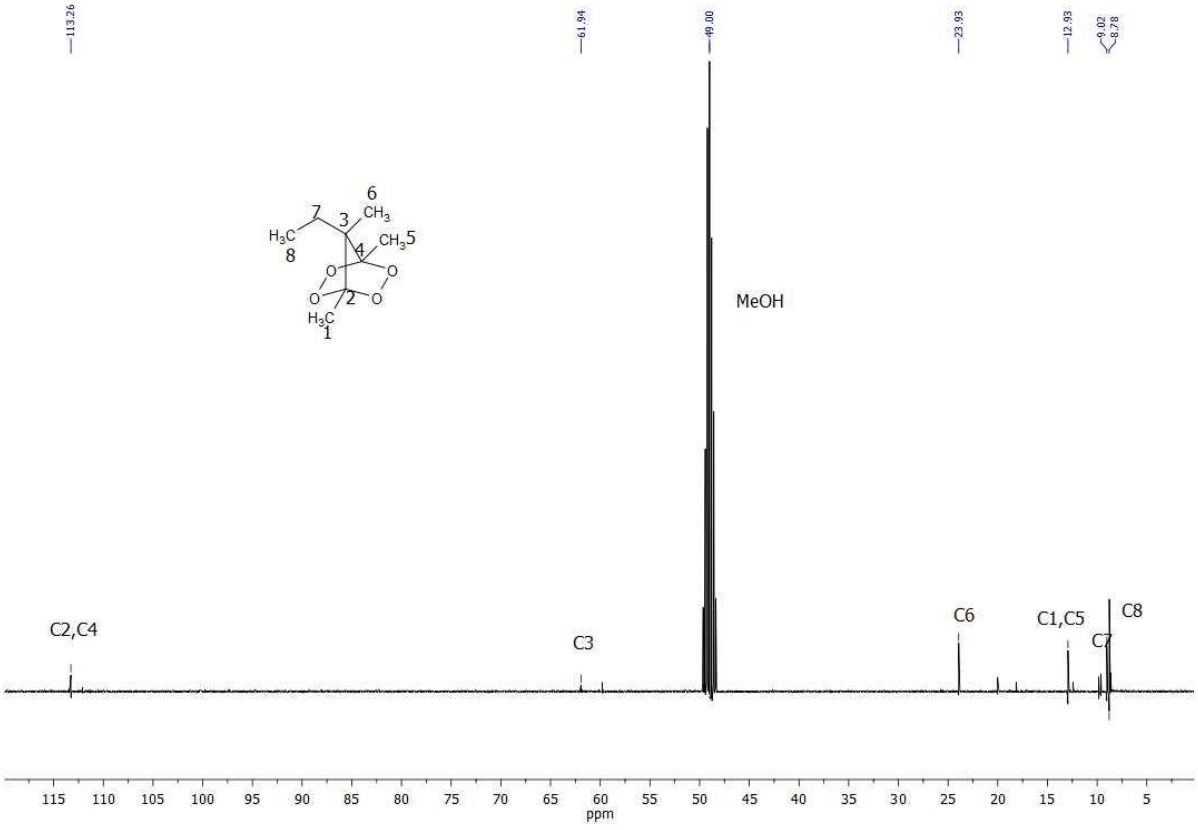

(1R,4R)-7,7-Diethyl-1,4-dimethyl-2,3,5,6-tetraoxabicyclo[2.2.1]heptane (4):

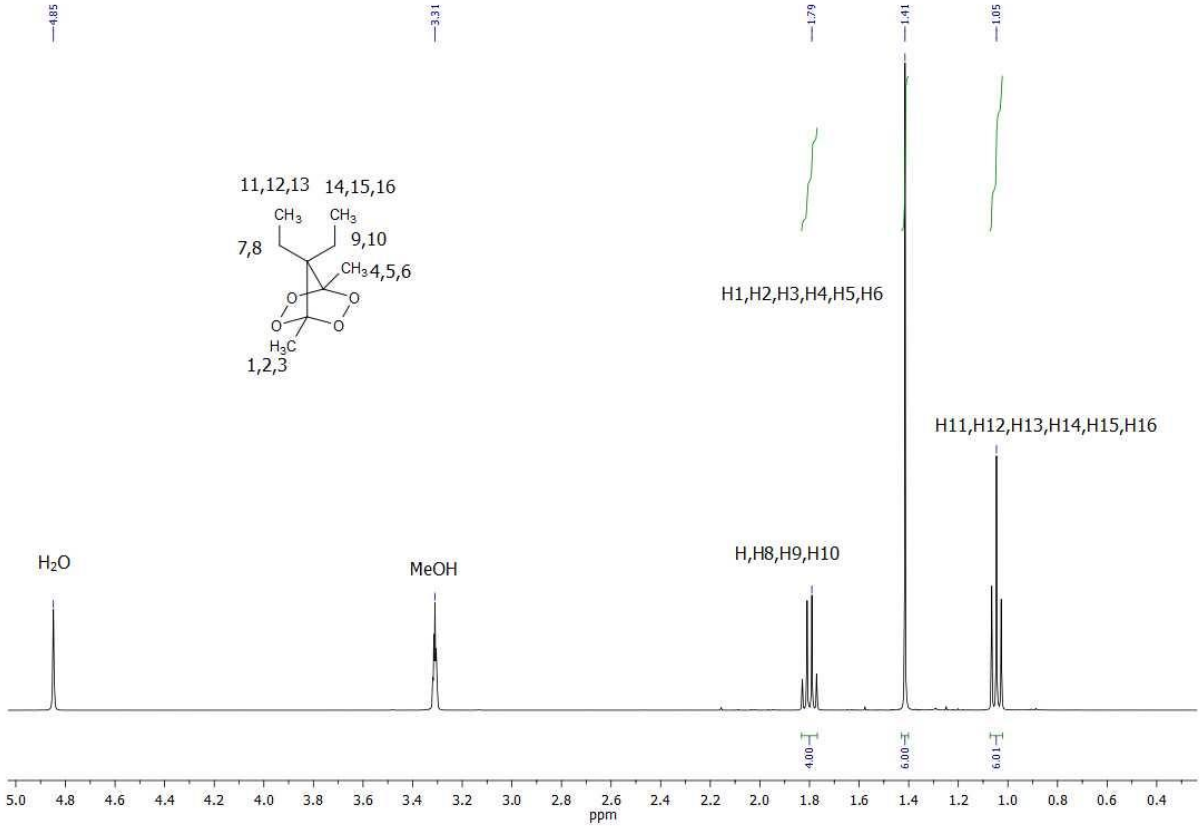

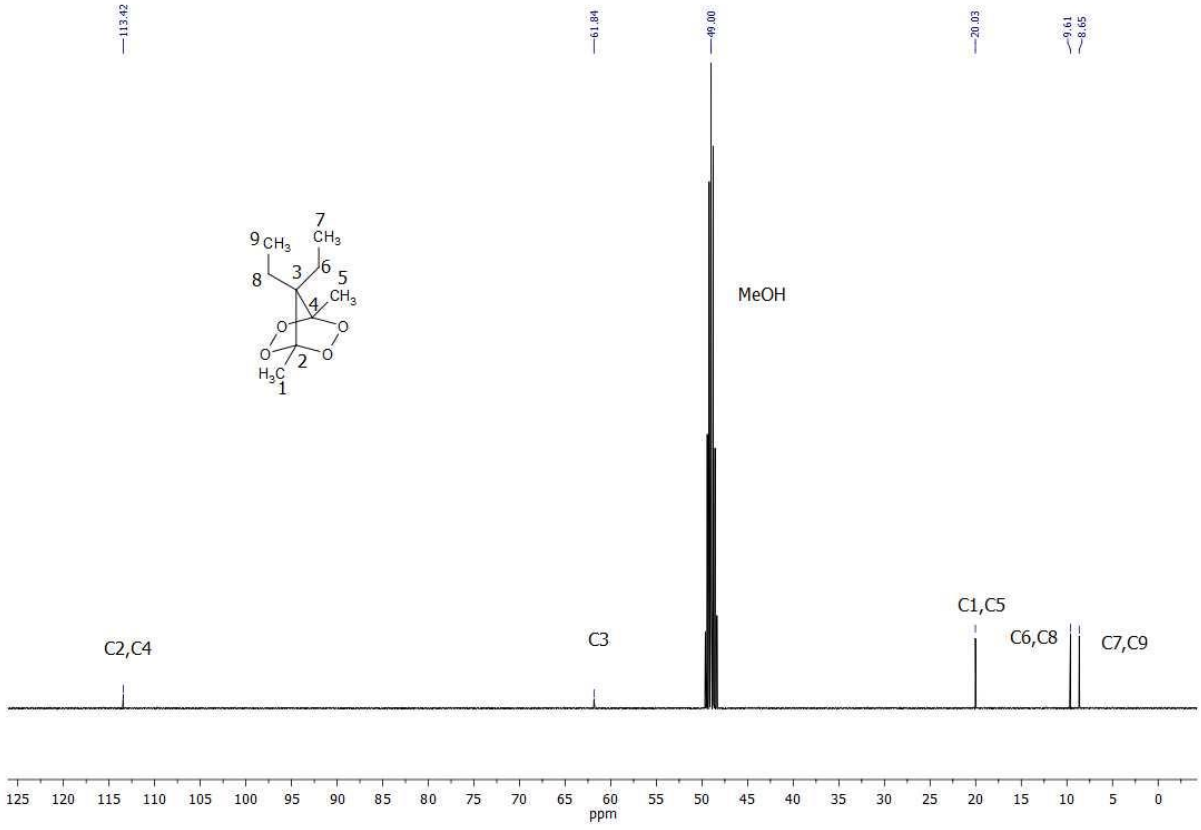

(1R,4R)-1,4-Dimethyl-2,3,5,6-tetraoxabicyclo[2.2.1]heptane (5):

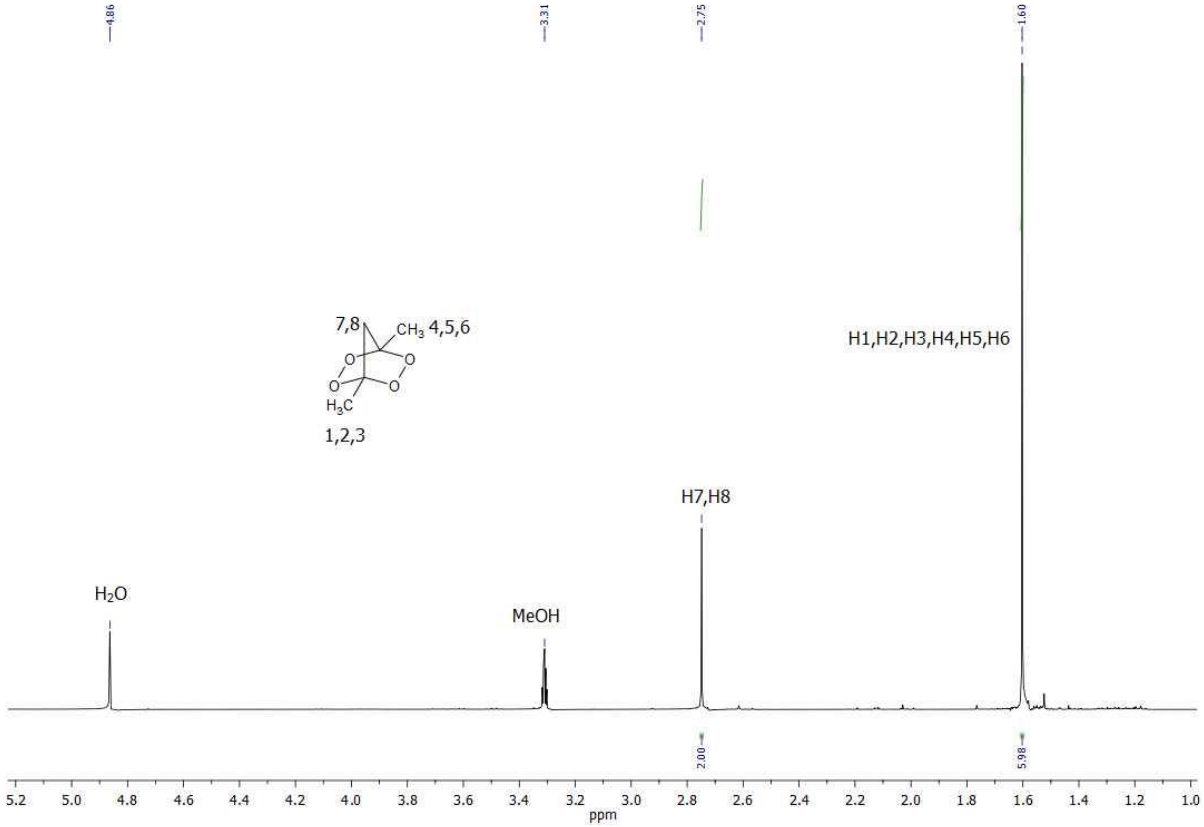

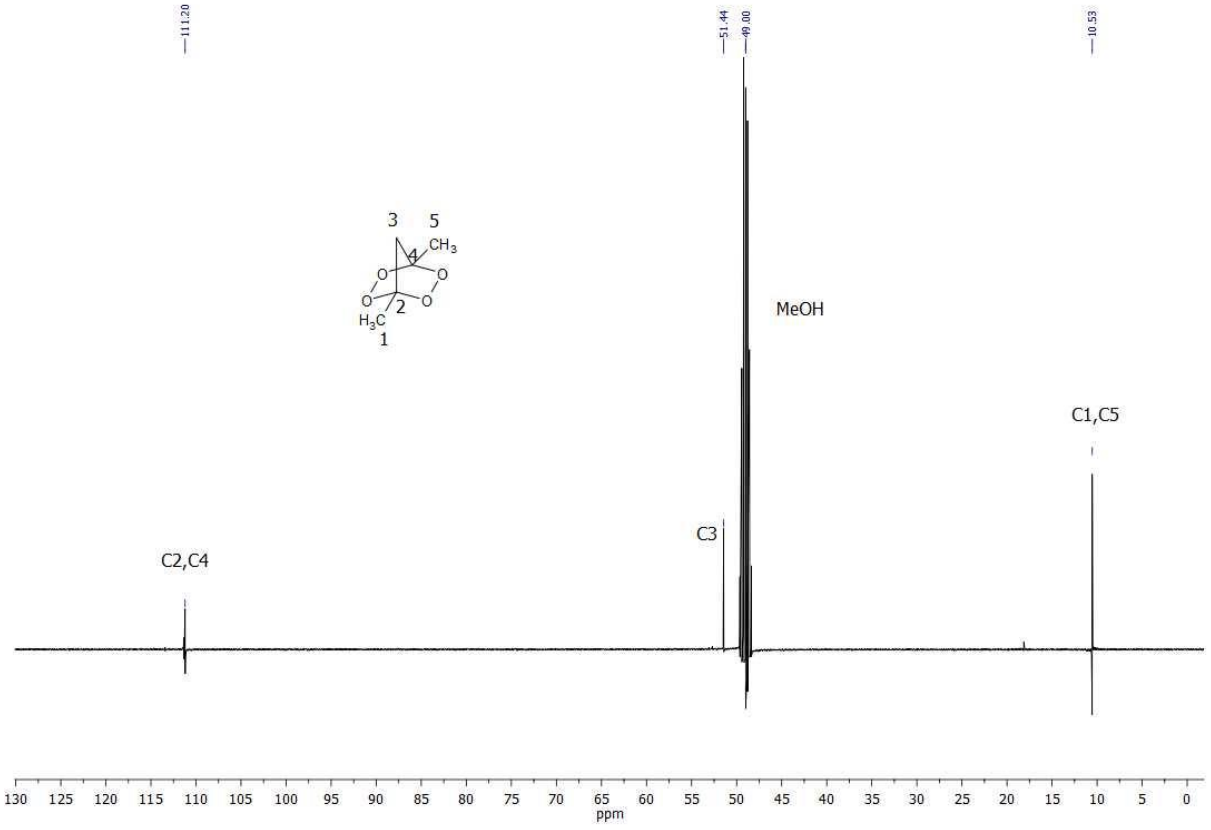

(1R,4R)-1,4,7,7-Tetramethyl-2,3,5,6-tetraoxabicyclo[2.2.1]heptane (6):

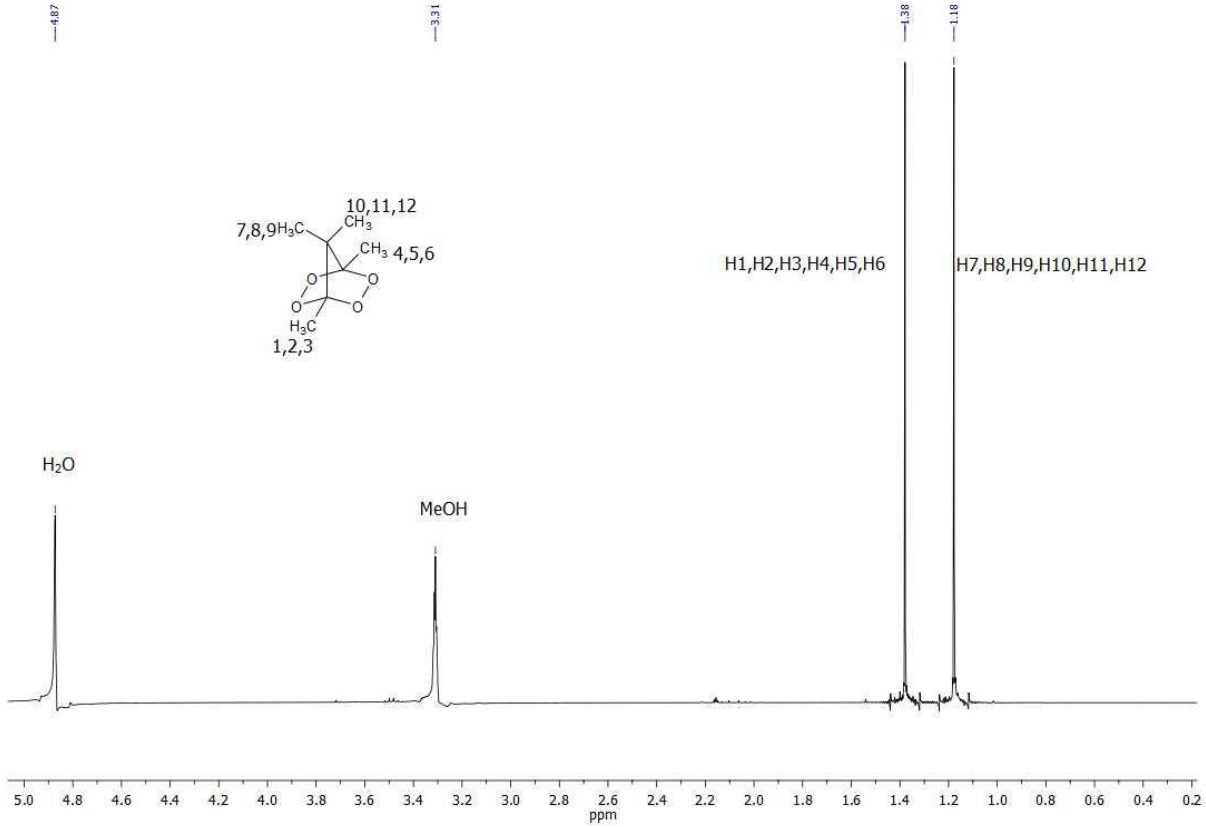

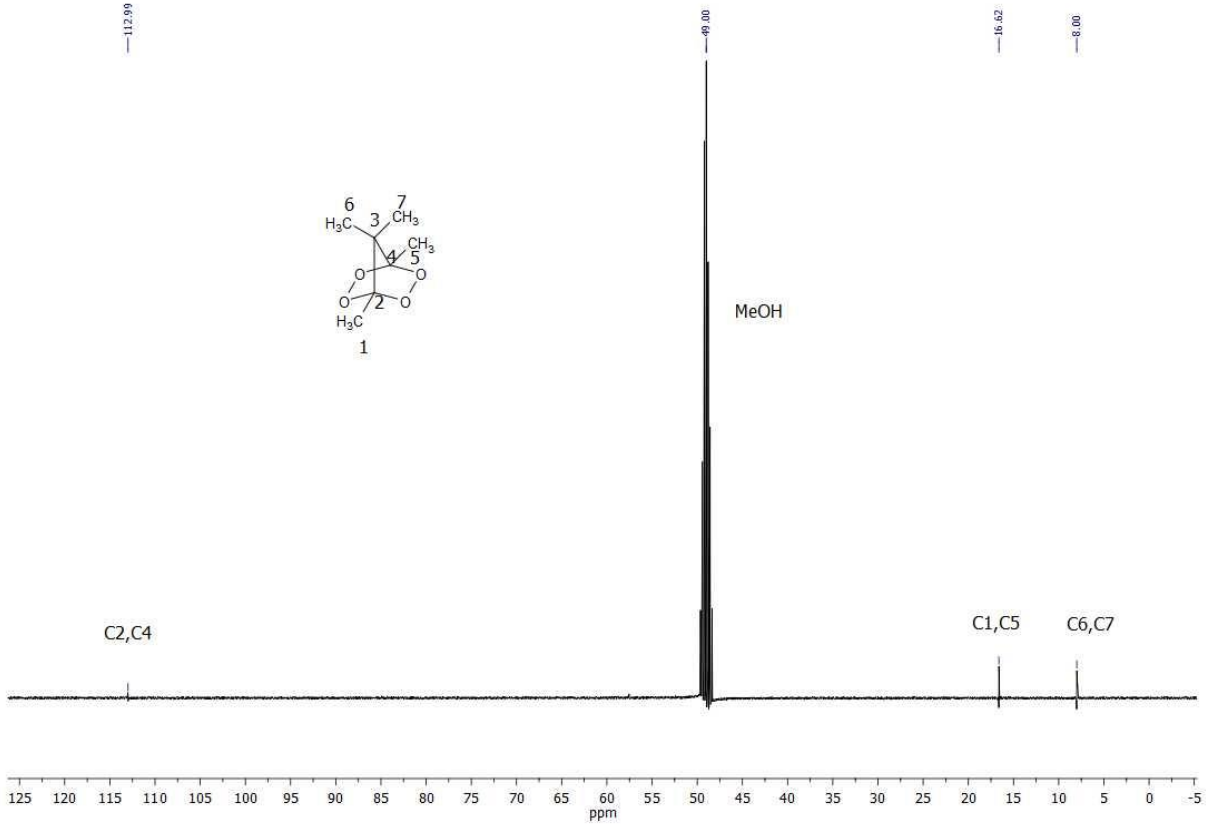

NMR-Data for the starting hydroxy-hydroperoxy compounds for the synthesis of **5** and **6** are not added to this supporting information since they will be part of a paper whose manuscript is under preparation at the moment.

2. X-ray diffraction

For all compounds, an Oxford Xcalibur3 diffractometer with a CCD area detector was employed for data collection using Mo-*K*α radiation (*λ* = 0.71073 Å). By using the CRYSALISPRO software[S1] the data collection and reduction were performed. The structures were solved by direct methods (SIR-92, [S3] SIR-97[S3] or SHELXS-97[S4]) and refined by full-matrix least-squares on *F*2 (SHELXL [S4]) and finally checked using the PLATON software [S5] integrated in the WinGX software suite. The non-hydrogen atoms were refined anisotropically and the hydrogen atoms were located and freely refined. The absorptions were corrected by a SCALE3 ABSPACK multiscan method.[S6]. All DIAMOND2 plots are shown with thermal ellipsoids at the 50% probability level and hydrogen atoms are shown as small spheres of arbitrary radius.

Table S1. Crystallographic data and refinement parameters of compounds **1**–**6**.

	1	**2**	**3**	**4**	**5**	**6**
Formula	$C_6H_{10}O_4$	$C_7H_{12}O_4$	$C_8H_{14}O_4$	$C_9H_{16}O_4$	$C_5H_8O_4$	$C_7H_{12}O_4$
FW [g/mol]	146.16	160.19	174.22	188.25	132.13	160.19
Crystal system	orthorhombic	monoclinic	orthorhombic	orthorhombic	orthorhombic	orthorhombic
Space Group	*Pnma* (No.62)	$P2_1/c$ (No.14)	*Pbca* (No.61)	*Pbca* (No.61)	*Pbcn* (No.60)	*Cmcm* (No.63)
Color / Habit	colorless block	colorless plate	colorless plate	colorless plate	colorless block	colorless plate
Size [mm]	0.20 x 0.10 x 0.20	0.38 x 0.32 x 0.02	0.086 x 0.407 x 0.426	0.38 x 0.32 x 0.08	0.38 x 0.36 x 0.30	0.029 x 0.169 x 0.337
a [Å]	9.6258(8)	8.1509(4)	11.9758(4)	11.4791(9)	7.1270(5)	9.2328(6)
b [Å]	8.8342(12)	8.7188(5)	10.8565(4)	11.1114(9)	8.6011(6)	9.9072(5)
c [Å]	8.3613(11)	11.4142(7)	13.4341(5)	15.4767(13)	9.7734(8)	8.6411(6)
α [°]	90	90	90	90	90	90
β [°]	90	101.573(5)	90	90	90	90
γ [°]	90	90	90	90	90	90
V [Å^3]	711.01(15)	794.67(8)	1746.64(11)	1974.04(30)	599.11(8)	790.41(9)
Z	4	4	8	8	4	4
$\rho_{calc.}$ [g cm^{-3}]	1.365	1.339	1.325	1.267	1.465	1.346
μ [mm^{-1}]	0.115	0.110	0.106	0.099	0.129	0.110
F(000)	312	344	752	816	280	344
$\lambda_{MoK\alpha}$[Å]	0.71073	0.71073	0.71073	0.71073	0.71073	0.71073
T [K]	173	173	173	173	173	173
ϑ min-max [°]	4.2, 26.0	4.1, 26.5	4.4, 26.0	4.3, 26.0	4.3, 26.5	4.4, 26.4
Dataset h; k; l	−11:11;−10:10;−9:10	−10:8;−10:6;−10:14	−14:7;−12:13;−16:14	−8:14;−13:11;−9:16	−8:8;−10:10;−11:12	−11:11;−12:12;−8:10
Reflect. coll.	4905	3266	4570	4691	3767	2706
Independ. refl.	739	1632	1701	1932	620	469
R_{int}	0.036	0.016	0.019	0.029	0.040	0.028
Reflection obs.	739	1632	1701	1932	620	469
No. parameters	71	148	165	182	58	46
R_1 (obs)	0.0324	0.0325	0.0346	0.0422	0.0449	0.0322
wR_2 (all data)	0.0810	0.0785	0.0914	0.1019	0.1306	0.0850
S	1.06	1.03	1.04	1.02	1.10	1.06
Resd. Dens. [e Å^{-3}]	−0.13, 0.18	−0.14, 0.23	−0.16, 0.34	−0.18,0.28	−0.26,0.24	−0.18,0.32
Device type	Oxford Xcalibur3 CCD	Oxford Xcalibur 3 CCD	Oxford Xcalibur 3 CCD	Oxford Xcalibur 3 CCD	Oxford Xcalibur 3 CCD	Oxford Xcalibur 3 CCD
Solution	SIR-92	SHELXS-97	SIR-92	SIR-92	SHELXL-97	SIR-92
Refinement	SHELXL-97	SHELXL-97	SHELXL-97	SHELXL-97	SHELXL-97	SHELXL-97
Absorpt. corr.	multi-scan	multi-scan	multi-scan	multi-scan	multi-scan	multi-scan
CCDC	1052987	1052988	1052992	1052989	1052990	1052991

3. Heat of formation calculations

All calculations were carried out using the Gaussian G09W (revision A.02) program package.[S7] The enthalpies (H), listed in Table S3, were calculated using the complete basis set (CBS) method of Petersson and coworkers in order to obtain very accurate energies. The CBS models use the known asymptotic convergence of pair natural orbital expressions to extrapolate from calculations using a finite basis set to the estimated complete basis set limit. CBS-4 begins with a HF/3-21G(d) geometry optimization; the zero point energy is computed at the same level. It then uses a large basis set SCF calculation as a base energy, and a MP2/6-31+G calculation with a CBS extrapolation to correct the energy through second order. A MP4(SDQ)/6-31+(d,p) calculation is used to approximate higher order contributions. In this study we applied the modified CBS-4M method (M referring to the use of Minimal Population localization) which is a re-parametrized version of the original CBS-4 method and also includes some additional empirical corrections.[S8] The enthalpies of the gas-phase species M were computed according to the atomization energy method (eq.1).

$$\Delta_f H^\circ_{(g,\,M,\,298)} = H_{(Molecule,\,298)} - \sum H^\circ_{(Atoms,\,298)} + \sum \Delta_f H^\circ_{(Atoms,\,298)} \quad \textbf{(1)}$$

Table S2. CBS-4M results and calculated gas-phase enthalpies

	M	$-H^{298}$ / a.u.	$\Delta_f H^\circ$(g,M) / kcal mol^{-1}	ΔH_{sub} / kcal mol^{-1}
1	$C_6H_{10}O_4$	534.646296	−68.3	14.8
2	$C_7H_{12}O_4$	573.882269	−74.0	17.1
3	$C_8H_{14}O_4$	613.124019	−83.3	12.7
4	$C_9H_{16}O_4$	652.358439	−88.0	14.4
5	$C_5H_8O_4$	495.403725	−58.4	17.7
6	$C_7H_{12}O_4$	573.889612	−78.6	16.1

Table S3 CBS-4M values and literature values for atomic $\Delta H^\circ_f{}^{298}$ / kcal mol^{-1}

	$-H^{298}$ / a.u.	NIST [S9] / $\Delta H^\circ_f{}^{298}$
H	0.500991	52.1
C	37.786156	171.3
O	74.991202	59.6

The gas phase heats of formation of **1**–**6** are converted to the solid state value by subtracting the sublimation enthalpies calculated with Trouton's rule ($\Delta H_{sub} = 188 \cdot T_m$). These molar standard enthalpies of formation (ΔH_m) were used to calculate the molar solid state energies of formation (ΔU_m) according to equation 2.

$$\Delta U_m = \Delta H_m - \Delta n\, RT \quad \textbf{(2)}$$

(Δn being the change of moles of gaseous components)

Table S4. Solid state energies of formation ($\Delta_f U°$)

	$\Delta_f H°$(s) / kcal mol^{-1}	$\Delta_f H°$(s) / kJ mol^{-1}	Δn	$\Delta_f U°$(s) / kJ mol^{-1}	M / g mol^{-1}	$\Delta_f U°$(s) / kJ kg^{-1}
1	−83.0	−347.7	7	−330.3	146.1	−2260.4
2	−91.1	−381.4	8	−361.5	160.2	−2257.2
3	−96.0	−402.0	9	−379.8	174.2	−2179.8
4	−102.5	−429.0	10	−404.2	188.2	−2147.4
5	−76.1	−318.7	6	−303.8	132.1	−2412.1
6	−94.7	−396.3	8	−396.3	160.2	−2350.7

4. References

[S1] *CrysAlisPro*, Oxford Diffraction Ltd., version 171.33.41, **2009**.

[S2] *SIR-92*, *A program for crystal structure solution*: A. Altomare, G. Cascarano, C. Giacovazzo, A. Guagliardi, *J. Appl. Crystallogr.* **1993**, *26*, 343.

[S3] a) A. Altomare, G. Cascarano, C. Giacovazzo, A. Guagliardi, A. G. G. Moliterni, M. C. Burla, G. Polidori, M. Camalli, R. Spagna, *SIR97*, **1997**; b) A. Altomare, M. C. Burla, M. Camalli, G. L. Cascarano, C. Giacovazzo, A. Guagliardi, A. G. G. Moliterni, G. Polidori, R. Spagna, *J. Appl. Crystallogr.* **1999**, *32*, 115–119.

[S4] a) G. M. Sheldrick, *SHELX-97*, University of Göttingen, Göttingen, Germany, **1997**; b) G. M. Sheldrick, *Acta Crystallogr., Sect. A* **2008**, *64*, 112–122.

[S5] A. L. Spek, *PLATON*, *A Multipurpose Crystallographic Tool*, Utrecht University, The Netherlands, **1999**.

[S6] *SCALE3 ABSPACK – An Oxford Diffraction program* (1.0.4, gui: 1.0.3), Oxford Diffraction Ltd., **2005**.

[S7] Gaussian 09, M. J. Frisch, G. W. Trucks, H. B. Schlegel, G. E. Scuseria, M. A. Robb, J. R. Cheeseman, G. Scalmani, V. Barone, B. Mennucci, G. A. Petersson, H. Nakatsuji, M. Caricato, X. Li, H. P. Hratchian, A. F. Izmaylov, J. Bloino, G. Zheng, J.

L. Sonnenberg, M. Hada, M. Ehara, K. Toyota, R. Fukuda, J. Hasegawa, M. Ishida, T. Nakajima, Y. Honda, O. Kitao, H. Nakai, T. Vreven, J. A. Montgomery, Jr., J. E. Peralta, F. Ogliaro, M. Bearpark, J. J. Heyd, E. Brothers, K. N. Kudin, V. N. Staroverov, R. Kobayashi, J. Normand, K. Raghavachari, A. Rendell, J. C. Burant, S. S. Iyengar, J. Tomasi, M. Cossi, N. Rega, J. M. Millam, M. Klene, J. E. Knox, J. B. Cross, V. Bakken, C. Adamo, J. Jaramillo, R. Gomperts, R. E. Stratmann, O. Yazyev, A. J. Austin, R. Cammi, C. Pomelli, J. W. Ochterski, R. L. Martin, K. Morokuma, V. G. Zakrzewski, G. A. Voth, P. Salvador, J. J. Dannenberg, S. Dapprich, A. D. Daniels, Ö. Farkas, J. B. Foresman, J. V. Ortiz, J. Cioslowski, and D. J. Fox, Gaussian, Inc., Wallingford CT, 2009.

[S8] a) J. W. Ochterski, G. A. Petersson, J. A. Montgomery, *J. Chem. Phys*. **1996**, *104*, 2598–2619; b) J. A. Montgomery, M. J. Frisch, J. W. Ochterski, G. A. Petersson, *J. Chem. Phys.* 2**000**, *12*, 6532–6542.

[S9] P. J. Lindstrom, W. G. Mallard (Editors), NIST Standard Reference Database Number 69, http://webbook.nist.gov/chemistry/ (Juni **2011**).

Energetic Materials – *tert*-Butyl-Peroxy Esters as Peroxides with Relatively Low Sensitivity

Nipuni-Dhanesha H. Gamage[a], Benedikt Stiasny[b], Jörg Stierstorfer[b], Philip D. Martin[a], Thomas M. Klapötke[b] and Charles H. Winter[a]

Abstract: Eight different *tert*-butyl-peroxyesters with varying molecular structures, peroxo content, and additional functional groups were prepared by treatment of the corresponding acyl chlorides with *tert*-butyl hydroperoxide. The compounds were characterized by standard analytical methods (NMR, IR, EA) and the molecular structures were determined by X-ray diffraction. The sensitivities toward impact, friction, and electrostatic discharge were determined, compared with each other, and correlated to the molecular structure. Moreover the thermal behavior was investigated by DTA. Heats of formation and the resulting explosive properties were calculated by using the EXPLO5 program.

Introduction

Peroxides are are characterized by the O–O single bond. They have applications in numerous different fields ranging from initiation reagents for radical polymerizations to the addition to diesel fuel and are important building block in pharmaceutically active compounds.[1-3] Peroxides are also an interesting class of explosives. The best known explosive peroxide is probably acetone peroxide, which was discovered accidentally by Wolffenstein at the end of the 19th century.[4] However a significant drawback for possible application is the extremely high sensitivity and low thermal stability of most peroxides. For a long time, the quantitative sensitivities were only reported for the well known peroxides TATP and HMTD, [5,6] Recently, other peroxide classes were investigated in more detail with respect to their energetic potential.[7-10] Comparing the sensitivities of the compounds studied in these papers, a clear trend can be recognized. Compounds with an O–O bond whose oxygen atoms do not participate in a π-conjugation are highly sensitive, whereas aromatic peroxy acids and peroxy anhydrides have surprisingly low sensitivities. The low sensitivities of aromatic peroxides led to the question whether an alternative peroxide class with conjugated peroxy O-atoms would show similar results and thus yield an alternative class of low sensitivity peroxide-based explosives. As representative examples, *tert*-butyl-peroxy esters were envisioned. These molecules can be prepared by a number of different approaches. The two most important ones are the reaction of acid anhydrides with *tert*-butyl hydroperoxide[11] or the reaction of an acyl chloride with *tert*-butyl hydroperoxide.[12],[13] Also the application of non-activated carbonic acids is possible.[14] In this context, trifluoromethyl acetic anhydride proved to be an effective activating agent.[15] *Tert*-butyl-peroxy esters are valuable starting materials for radical polymerization.[1],[16] The compounds oxalylic bis-*tert*-butylperoxy ester and acetic acid *tert*-butyl-peroxy ester are used on industrial scales.[1,16] The latter compound is also used for stereoselective allylic oxidations.[17] Herein, we describe the syntheses of a number of energetic *tert*-butyl-peroxy esters with a varying peroxo content. Also, aromatic isomers are compared to assess if the substitution pattern of the benzene ring has an influence on the performance of a compound. Moreover, nitrated benzene derivatives are studied to determine if more energetic and higher density materials could be obtained.

[a] Dr. Nipuni-Dhanesha H. Gamage, Dr. Philip D. Martin, Prof. Dr. Charles H. Winter
Department of Chemistry, Wayne State University, Detroit, Michigan 48202, United States
E-mail: chw@chem.wayne.edu
[b] Mr. Benedikt Stiasny, Dr. Jörg Stierstorfer, Prof. Dr. Thomas M. Klapötke
Department of Chemistry, Ludwig-Maximilians University, Butenandtstr. 5-13 (D), 81377 München, Germany
E-mail: tmk@cup.uni-muenchen.de

Supporting information for this article is given via a link at the end of the document.

Results and Discussion

Synthesis

Bis-*tert*-butyl benzene-1,4-bis(carboperoxoate) (**1**), bis-*tert*-butyl benzene-1,2-bis(carboperoxoate) (**2**), tris-*tert*-butyl benzene-1,3,5-tris(carboxylperoxoate) (**3**), tetrakis-*tert*-butyl benzene-1,2,4,5-tetrakis(carboxylperoxoate) (**4**), *tert*-butyl 3,5-dinitrobenzoperoxoate (**5**), di-*tert*-butyl 4,6-dinitrobenzene-1,3-bis(carboperoxoate) (**6**) and di-*tert*-butyl ethanebis(peroxoate) (**7**) were prepared using the same synthesis strategy. A solution of the corresponding acyl chloride in an appropriate solvent (**1**, **3**, **7**: pentane; **2**, **4**, **6**: CH_2Cl_2; **5:** Et_2O) was added dropwise to a mixture consisting of a stoichiometric amount of dry pyridine and a molar excessof a 5.5M solution of ^{t}BuOOH in decane at −4 °C under an argon atmosphere. Scheme 1 displays the synthetic pathway. To separate the pyridinium chloride precipitate formed during the condensation, the reaction mixtures were filtered over Celite. Afterwards, the solvents were removed under reduced pressure to yield the crude products. Compound **1** was purified by recrystallization from 1:1 hexane: dichloromethane, whereas **3** was >98% pure by NMR. Compounds **2** and **4**–**6** were purified by column chromatography over silica with mixtures of ethyl acetate/hexane or ethyl acetate/dichloromethane as eluents. Eluents are given in the experimental section. Compound **7** was purified by repeated recrystallization from pentane at −29 °C. The yields obtained after workup are between **6** (compound **2**) and 77% (compound **3**). All compounds studied herein are colorless solids. An additional compound that was obtained under similar reaction conditions was hexakis-*tert*-butyl benzene-1,2,3,4,5,6-hexakis(carboxylperoxoate) (**8**, Scheme 2). Compound 8 was isolated in a yield of 29% after column chromatography over silica using pure dichloromethane as eluent. Compound **8** could not be prepared on a scale large enough to permit full sensitivity testing, because of its extreme sensitivity.

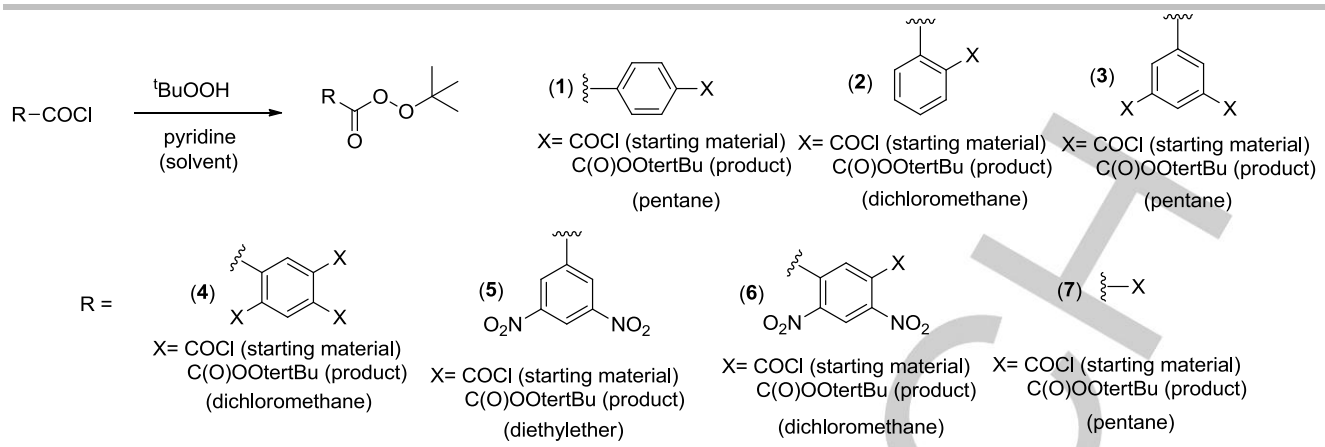

Scheme 1: Synthetic pathway for compounds **1**, **2**, **3,** **4**, **5**, **6**, and **7**.

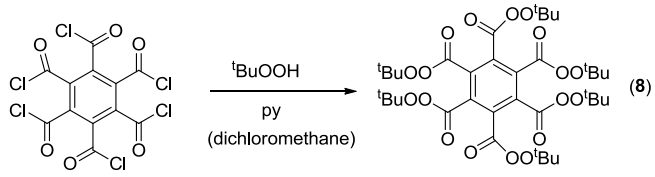

Scheme 2. Reaction equation for the preparation of **8**.

Crystal structures

Single crystals of **1**-**8** suitable for X-ray diffraction measurements were obtained by recrystallization. Details regarding the solvents and temperatures used are given in the experimental section for each compound. Figure 1 displays the X-ray crystal structures of **1**, **2**, **3** and **4**. The X-ray crystal structures of **5**, **6**, **7** and **8** are depicted in figure 2. Further details concerning the measurement and refinement are given in the supporting information. The compounds crystallize in common space groups ($P2_1/c$ (**1**, **6**), $Pna2_1$ (**2**), $P\bar{1}$ (**3**, **5**, **7**), $C2/c$ (**4**), and Cc (**8**)) with room temperature densities between 1.131 g cm^{-3} (**8**) and 1.460 g cm^{-3} (**5**). These values are in the normal range for organic peroxides (density of TATP: 1.25 g cm^{-3} [18]). The nitrated compounds **5** and **6** have the highest densities. Bond distances of the O–O single bonds range between 145.7 pm and 147.8 pm and are therefore typical for O−O single bonds (O-O-distance in TATP: 147 pm [19]) and also for *tert*-butyl-peroxy esters.[18,20] Compound **1** has the longest and the shortest bond in one molecule. The average O-O bond distances are 146.5 pm, but all of the bond distances are very similar. The COO bond angles range between 105.10° and 111.02°. The ^{quart}C-O-O angle for all compounds is around 110° and is therefore a slightly larger than the O–C–O angle of the carboxyl groups (always around 105°). These values are in good accordance with literature reports.[20] Also, the torsion angles of the OO^{t}Bu-group have values around 126°, which fits values given in the literature very well .[20]

Energetic properties

The performance data of the compounds were calculated using the EXPLO5 program in version 6.02. Heats of formation were calculated with the atomization method based on CBS-4M electronic enthalpies. Table 1 gathers the energetic properties of **1**–**7**. Impact sensitivities are between 40 J for **1** and **2** and less than 1 J for **7**. The impact sensitivity classification therefore ranges from insensitive (**1** and **2**), to sensitive (**3**, **5**, and **6**), to very sensitive (**4** and **7**). The values for friction sensitivity are 360 N (insensitive, **1**, **2**, and **5**), 240 N (sensitive, **3**), 96 N (sensitive, **6**), 60 N (very sensitive, **4**), and less than 5 N (extremely sensitive, **7**). The sensitivities increase with increasing number of peroxo groups. The sensitivities toward electrostatic discharge for **1** to **6** are between 0.4 and 0.7 J and are therefore significantly higher than the maximum charge of the human body (0.020 J).[21] By contrast, **7** has an ESD value of only 0.015 J, which means it can be initiated accidentally upon routine handling. Moreover **7** detonated violently during ESD measurement and does not only decompose without explosion like most secondary explosives e.g. hexogen and trinitrotoluene. Accordingly, the sensitivities of the aromatic compounds **1**-**6** are lower than that of acyclic **7**. This trend can be rationalized by the higher oxygen content in **7**, as well as the stabilization afforded by conjugation of the carbonyl groups with the aromatic cores in **1**-**6**. Calculated detonation velocities are between 4906 and 6003 m s^{-1} and are therefore slightly lower or in the range of structurally similar low sensitivity peroxy acids (5262 to 7885 m s^{-1})[7] and peroxy anhydrides (5315 to 7087 m s^{-1})[10]. The calculated detonation pressure of 60 to 118 kbar is in general lower than for the aromatic peracids (88 to 269 kbar)[7] and peroxy anhydrides (90 to 200 kbar)[10]. Compounds **1** and **2** are isomeric, but **1** gives higher energetic performance than **2**. This effect may be related to steric interactions that are present in **2**, but not in **1**. According to the calculations, nitrated compound **5** has the best performance values (detonation velocity 6003 ms^{-1}, detonation pressure 118 kbar), followed by the other nitrated compound **6**. Compound **6** has one peroxy group more than **5**, but the lower solid state density of **6** might explain the weaker performance in comparison to **5**. Generally, the nitrated compounds **5** and **6** have slightly better energetic performance than the non nitrated compounds **1**-**4**. The presence of nitro groups is known to increase the performance of organic peroxide explosives.[10] Concerning the other non nitrated, aromatic compounds **3**-**5**, the energetic performance seems again to be governed more by the solid state density than by the varying peroxo content. The decomposition points of most compounds are in the range between 95 and 132 °C and are therefore normal for organic peroxides.[7-9] The decomposition point of **7** is very low (53 °C onset). A high vapor pressure is reported in the literature for TATP.[22] However we experienced no significant tendency of sublimation.

Conclusions

We succeeded in the synthesis of the eight *tert*-butyl peroxy esters **1**-**8** in low to moderate yields (6 to 77%). All were

Table 1 : Energetic properties of compounds **1** to **7**.

characterized by standard spectral and analytical methods and by X-ray diffraction. The densities of the compounds are between 1.161 and 1.460 g cm^{-3} and they crystallize in common space groups. Additionally the sensitivities toward impact, friction, electrostatic discharge and heat were determined. Values range from totally insensitive compounds to those with the sensitivity of primary explosives. Some of the compounds have surprisingly low sensitivities toward outer stimuli with more than 40 J impact and more than 360 N friction sensitivity. The low sensitivity might be explained with a conjugative interaction. However their low decomposition temperature (maximum 132 °C for **2**) and only relatively weak calculated performance values most likely will preclude any possible application as advanced energetic materials.

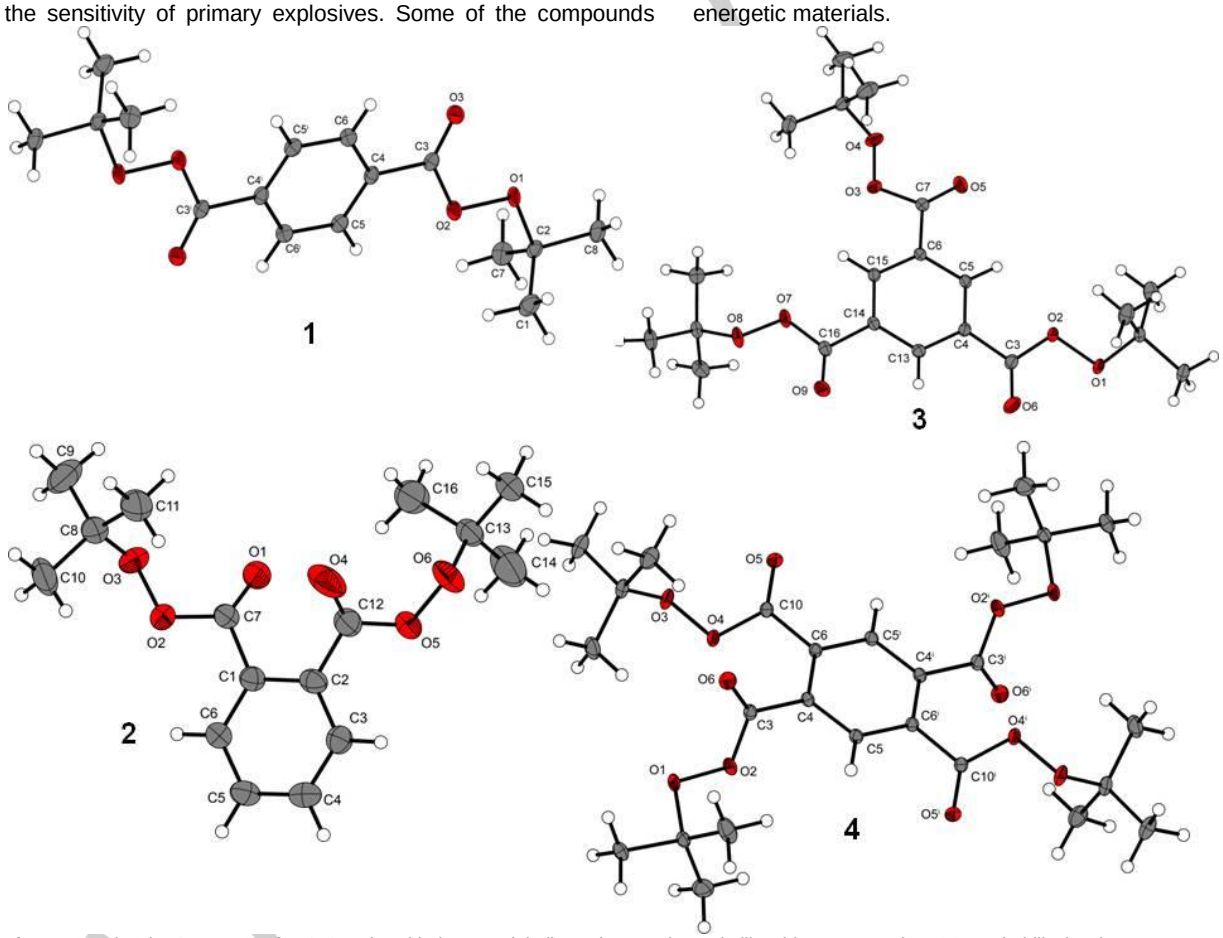

Figure 1: Molecular Structures of **1**, **2**, **3** and **4** with the atom labeling scheme. Thermal ellipsoids represent the 50 % probability level

	1	2	3	4	5	6	7
Formula	$C_{16}H_{22}O_6$	$C_{16}H_{22}O_6$	$C_{21}H_{30}O_9$	$C_{26}H_{38}O_{12}$	$C_{11}H_{12}N_2O_7$	$C_{16}H_{20}N_2O_{10}$	$C_{10}H_{18}O_6$
F_W [g/mol]	310.28	310.28	426.51	542.57	284.06	400.34	234.28
IS [J][a]	40	40	20	2	10	5	<1
FS [N][b]	>360	>360	240	60	>360	96	<5
ESD [J][c]	0.7	0.5	0.5	0.7	0.5	0.4	0.015
Ω_{CO2} [%][d]	−190.75	−190.75	−180.08	−173.98	−118.21	−127.89	−157.10
T_m/T_{dec} [°C][e]	-/122	37/132	-/123	-/123	85/121	-/95	48/53
ρ [g/cm^3][f]	1.232	1.178	1.200	1.192	1.460	1.405	1.210
$\Delta_f H_m^0$[kJ/mol][g]	−820.7	−802.0	−1211.3	−1584.7	−436.9	−790.0	−811.4
EXPLO5-values							
$-\Delta_{ex}U^0$[kJ/kg][h]	2589	2637	2726	2836	4099	3950	3124
P_{CJ} [kbar][i]	63	56	60	61	118	104	75
V_{det}[m/s][j]	5038	4749	4906	4896	6003	5764	5361
V^0 [L/kg][k]	707	711	731	745	670	699	836

[a] Impact sensitivity according to BAM drophammer (method 1 of 6). [b] Friction sensitivity according to BAM friction tester (method 1 of 6). [c] Electrostatic discharge sensitivity (OZM ESD tester). [d] Oxygen balance. [e] Melting point resp. Temperature of decomposition according to DTA (onset temperatures at a heating rate of 5°C/min). [f] Room temperature X-ray densities. Those were calculated by the low temperature X-ray values using the equation {$\rho 298\ K = \rho T/[1 + \alpha V(298 - T0)]$; $\alpha V = 1.5\ 10^{-4}\ K^{-1}$} . [g] calculated heat of formation using the atomization method and CBS-4M electronic enthalpies. [h] Heat of detonation. [i] Detonation pressure. [j] Detonation velocity. [k] Volume of gas after detonation.

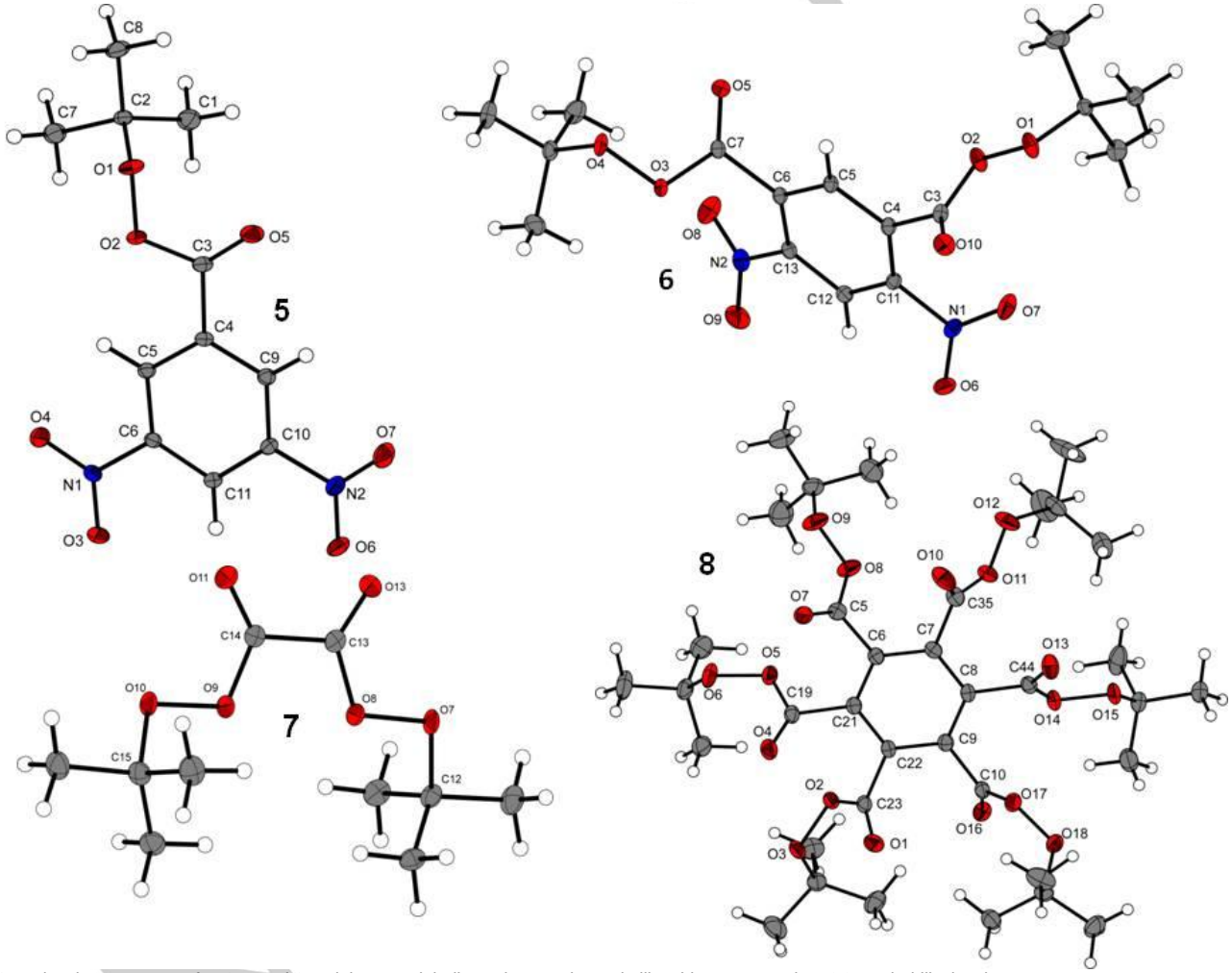

Figure 2: Molecular structures of **5**, **6**, **7** and **8** and the atom labeling scheme. Thermal ellipsoids represent the 50 % probability level.

Experimental Section

CAUTION! All investigated compounds are potentially explosive energetic materials, although no hazards were observed during preparation and handling these compounds. Nevertheless, this necessitates additional meticulous safety precautions (earthed

equipment, Kevlar gloves, Kevlar sleeves, face shield, leather coat, and ear plugs).

General: All chemicals were received from Sigma-Aldrich, Acros Organics or Alfa Aesar and used without further purification. Sensitivity measurements were performed on a BAM-drophammer, a BAM friction tester and an OZM ESD- tester. Infrared spectra were recorded with a Perkin–Elmer One FT-IR Spectrum BX II with a Smith ATR Dura Sample IRII and with a Shimadzu MIRacle 10 IRAffinity-1 equipped with a single reflection ATR accessory. NMR spectra were recorded on an NMR-spectrometer operating at 400 MHz for proton spectra. Melting points and decomposition points were recorded on an OZM Research DTA 552-Ex instrument.

Phthalic acid was prepared by reacting phthalic acid anhydride in excessive water with catalytic amounts of conc. HCl under reflux conditions. Phthalic acid dichloride and benzene-1,2,4,5-tetracarbonylchloride were prepared by reacting the corresponding acids with excessive $SOCl_2$ and catalytic amounts of DMF.[23] Mellitic acid hexachloride was produced by reacting mellitic acid with PCl_5 at 150 °C.[24] 4,6- Dinitroisophthaloyl chloride was prepared following a literature procedure.[25] The reactions to the peroxy esters were performed under Schlenk conditions using Ar as inert gas. Bis-tert-butyl ethanebis(peroxoate) (**7**) was synthesized by a procedure adapted from published procedures.[26, 27]

Bis-tert-butyl benzene-1,4-bis(carboperoxoate) (1) To a solution of anhydrous pyridine (0.13 mL, 3.0 mmol) and 5.5M ^{t}BuOOH in decane (0.60 mL, 3.0 mmol) in a 100 mL Schlenk flask, which was kept at –4 °C (ice-water-salt bath), a solution of terephthaloyl chloride (0.305 g, 1.50 mmol) in anhydrous pentane (25 mL) was added drop wisely with a needle over a period of 15 min. Then, the reaction was stirred for about 15 min at –4 °C. Afterwards, the reaction was allowed to warm up to room temperature and was filtered through a 1.5 cm pad of Celite on a coarse glass frit. Then, the filtrate was dried to obtain 0.35 g (75%) of crude **1** as a white solid. Recrystallization in 1:1 hexane:dichloromethane by slow evaporation resulted in 0.280 g (60%) of colorless, square-shaped crystals of **1**. (X-ray quality colorless, square-shaped single crystals were obtained by slow evaporation in diethyl ether.) DTA (5 °C min^{-1}) T_{dec}/°C (onset) = 122; ^{1}H NMR (400 MHz, $CDCl_3$, 23 °C, TMS): δ=8.04 (s, 4H, C*H*), 1.42 (s, 18H, CH_3) ppm; ^{13}C NMR (100 MHz, $CDCl_3$, 23 °C, TMS): δ=163.5 (*C*), 131.6 (*C*), 129.5 (*C*H), 84.6 (*C*), 26.4 (CH_3) ppm; IR (ν cm^{-1}): 2982 (m), 2935 (w), 2902 (w), 2873 (w), 1753 (s), 1692 (m), 1527 (w), 1501 (w), 1455 (w), 1404 (m), 1387 (w), 1366 (m), 1295 (w), 1263 (m), 1233 (s), 1186 (s), 1117 (w), 1069 (s), 1011(s), 901 (w), 872 (m), 851 (m), 820 (m), 799 (m), 744 (w), 721 (s); elemental analysis calcd (%) for $C_{16}H_{22}O_6$: C 61.93, H 7.16; found: C 61.75, H 7.09; IS: 40 J, FS: >360 N, ESD: 0.7 J.

Bis-tert-butyl benzene-1,2-bis(carboperoxoate) (2) To a solution a of 1.20 mL ^{t}BuOOH (5.5M in decane) (6.60 mmol) and 0.26 ml anhydrous pyridine (3.2 mmol) a solution of phthaloylchloride (0.61 g, 3.0 mmol) in 10 mL anhydrous dichloromethane was added drop-wisely at −4 °C over a period of 5 min. The reaction-mixture was stirred at this temperature for 2 h. After this time it was allowed to reach room-temperature. Then the solution was filtered over a 1.5 cm pad of celite and the solvent was removed in vacuum to obtain a colorless oil as raw product. The substance was purified by column-chromatography over silica, using ethylacetate / hexane 1:3 as the eluent. After evaporation of the solvent 0.056 g (6%) of **2** were obtained as a white solid. Needle like single crystals of the compound were grown from acetone at room temperature. R_f=0.15 (EtOAc/hexane 1:3); DTA (5 °C min^{-1}) T_m/°C (onset) = 37; T_{dec}/°C (onset) = 132; ^{1}H NMR (400 MHz, $CDCl_3$, 23 °C, TMS): δ=7.74-7.71 (m, 2H, C*H*), 7.62-7.58 (m, 2H, C*H*), 1.39 (s, 18 H, CH_3) ppm; ^{13}C NMR (100 MHz, $CDCl_3$, 23 °C, TMS): δ=164.8 (*C*), 132.0 (*C*) , 129.6(*C*), 129.4 (*C*), 84.6 (*C*), 26.4 (CH_3) ppm; IR (ν cm^{-1}) = 2984 (m), 2943 (w), 1759 (s), 1593 (w), 1579 (w), 1475 (w), 1444 (w), 1391 (w), 1367 (m), 1244 (s), 1226 (s), 1185 (s), 1125 (m), 1079 (m), 1041 (m), 1023 (s), 980 (w), 898 (w), 849 (w), 839 (w), 822 (w), 796 (m), 780 (w), 736 (m), 701 (w), 681 (m); elemental analysis calcd (%) for $C_{16}H_{22}O_6$: C 61.93, H 7.16; found: C 61.98, H 7.18; IS: 40 J, FS: >360 N, ESD: 0.5 J.

Tris-tert-butyl benzene-1,3,5-tris(carboxylperoxoate) (3) To a solution of anhydrous pyridine (0.13 mL, 3.0 mmol) and 5.5M ^{t}BuOOH in decane (1.0 mL, 5.0 mmol) in a 100 mL Schlenk flask, which was kept at –4 °C (ice-water-salt bath), a solution of benzene-1,3,5-tricarbonyl trichloride (0.270 g, 1.00 mmol) in anhydrous pentane (10 mL) was added slowly using a needle over a period of 5 min. Then, the reaction was stirred for about 1 h while allowing it to warm up to 10 °C. Afterwards, the reaction was allowed to warm up to room temperature and it was filtered through a 1.5 cm pad of Celite on a coarse glass frit. Then, the filtrate was dried to obtain 0.328 g (77%) of **3** as a white solid. Recrystallization in 1:1 petroleum ether (boiling point range = 35–60 °C): diethyl ether by slow evaporation resulted in 0.272 g (64%) of **3** as colorless, thin, long, plate-like single crystals. DTA (5 °C min^{-1}) T_{dec}/°C (onset) = 123; ^{1}H NMR (400 MHz, CD_3OD, 23 °C, TMS): δ=8.68 (s, 3H, C*H*), 1.43 (s, 27H, CH_3) ppm; ^{13}C NMR (100 MHz, CD_3OD, 23 °C, TMS): δ=162.4 (*C*), 133.9 (*C*H), 129.6 (*C*), 85.0 (*C*), 26.4 (CH_3) ppm; IR (ν cm^{-1}): 2980 (m), 2936 (w), 2872 (w), 1753 (s), 1701 (m), 1631 (w), 1526 (m), 1495 (w), 1458 (w), 1391 (m), 1366 (m), 1315 (m), 1260 (m), 1173 (s), 1103 (s), 1022 (w), 922 (m), 881 (m), 845 (s), 802 (m), 764 (m), 719 (s); elemental analysis calcd (%) for $C_{21}H_{30}O_9$: C 59.13, H 7.10; found: C 58.90, H 7.16; IS: 20 J, FS: 240 N, ESD: 0.5 J.

Tetrakis-tert-butyl benzene-1,2,4,5-tetrakis(carboxylperoxoate) (4) To a solution of anhydrous pyridine (0.20 mL, 4.7 mmol) and 5.5M ^{t}BuOOH in decane (1.6 mL, 7.9 mmol) in a 100 mL Schlenk flask, which was kept at –4 °C (ice-water-salt bath), a solution of benzene-1,2,4,5-tetracarbonyl tetrachloride (0.387 g, 1.18 mmol) in distilled dichloromethane (10 mL) was added slowly with a needle over a period of 5 min. Then the reaction was stirred for about 1 h while allowing it to warm up to 10 °C. Afterwards, the reaction was allowed to warm up to room temperature and it was filtered through a 1.5 cm pad of Celite on a coarse glass frit. Then, the filtrate was concentrated and the product was purified by silica gel column chromatography with 10:1 CH_2Cl_2:EtOAc to obtain 0.27 g (42%) of **4** as a white solid. Recrystallization in 10:1 diethyl ether:THF by slow evaporation resulted in 0.163 g (25%) of colorless, thick, hexagonal single crystals of **4**. R_f=0.03 (EtOAc/CH_2Cl_2 1:10); DTA (5 °C min^{-1}) T_{dec}/°C (onset) = 123; ^{1}H NMR (400 MHz, $CDCl_3$, 23 °C, TMS): δ=7.98 (s, 2H, C*H*), 1.39 (s, 36H, CH_3) ppm; ^{13}C NMR (100 MHz, $CDCl_3$, 23 °C, TMS): δ=162.3 (*C*), 132.2 (*C*), 120.9 (*C*H), 86.2 (*C*), 26.3 (CH_3) ppm; IR (ν cm^{-1}): 2984 (m), 2934 (w), 2870 (w), 1771 (s), 1759 (s), 1651 (w), 1541 (w), 1366 (m), 1294 (m), 1240 (m), 1209 (m), 1184 (s), 1096 (s), 1061 (s), 1028 (m), 926 (m), 890 (w), 835 (m), 814 (m), 773 (w), 748 (m), 719 (m); elemental analysis calcd (%) for $C_{26}H_{38}O_{12}$: C 57.55, H 7.07; found: C 57.26, H 7.14; IS: 2 J, FS: 60 N, ESD: 0.7 J.

Tert-butyl 3,5-dinitrobenzoperoxoate (5) To a solution of anhydrous pyridine (0.13 mL, 3.0 mmol) and 5.5M ^{t}BuOOH in decane (0.60 mL, 3.0 mmol) in a 100 mL Schlenk flask, which was kept at –4 °C (ice-water-salt bath), a solution of 3,5-dinitrobenzoyl chloride (0.346 g, 1.50 mmol) in distilled diethyl ether (25 mL) was added slowly with a syringe over a period of 5 min. Then, the reaction was stirred for about 1 h while allowing it to warm up to 10 °C. Afterwards, the reaction was allowed to warm up to room temperature and it was filtered through a 1.5 cm pad of Celite on a coarse glass frit. Then, the filtrate was dried to obtain 0.333 g (78%) of crude **5** as a beige solid. The product was purified by silica gel column chromatography with 20:1 hexane:EtOAc to obtain 0.26 g (61%) of **5** as a white solid. Recrystallization in toluene by slow evaporation resulted in colorless, thick, long single crystals of **5**. R_f=0.09 (EtOAc/hexane 1:20); DTA (5 °C min^{-1}) T_m/°C (onset) = 85; T_{dec}/°C (onset) = 121; ^{1}H NMR (400 MHz, $CDCl_3$, 23 °C, TMS): δ=9.26 (s, 1H, C*H*), 9.06 (s, 2H, C*H*), 1.46 (s, 9H, CH_3) ppm; ^{13}C NMR (100 MHz, $CDCl_3$, 23 °C, TMS): δ=160.6 (*C*), 149.0 (*C*), 131.5 (*C*), 129.1 (*C*H), 122.9 (*C*H), 85.7 (*C*), 26.4 (CH_3) ppm; IR (ν cm^{-1}): 3422 (w), 3110 (w), 2982 (m), 2943 (w), 2880 (w), 1761 (m), 1749 (m), 1694 (w), 1630 (m), 1539 (s), 1491 (m), 1458 (m), 1389 (m), 1366 (m), 1342 (s), 1288 (m), 1252 (m), 1182 (m), 1132 (s), 1072 (m), 1018 (m), 945 (m), 916 (m), 845 (m), 820 (m), 800 (m), 762 (w), 729 (m), 716 (s); elemental analysis calcd (%) for $C_{11}H_{12}N_2O_7$: C 46.50, H 4.45, N 10.28; found: C 46.89, H 4.57, N 9.91; IS: 10 J, FS: >360 N, ESD: 0.5 J.

Bis-tert-butyl 4,6-dinitrobenzene-1,3-bis(carboperoxoate) (6) To a solution of anhydrous pyridine (0.0650 mL, 1.50 mmol) and 5.5M ^{t}BuOOH in decane (0.30 mL, 1.5 mmol) in a 100 mL Schlenk flask, which was kept at –4 °C (ice-water-salt bath), a solution of 4,6-dinitroisophthaloyl dichloride (0.22 g, 0.75 mmol) in distilled dichloromethane (10 mL) was slowly added with a syringe. Then, the reaction was stirred for about 1 h while allowing it to warm up to 10 °C. The reaction was concentrated and the product was purified by silica gel column chromatography with 9:1 hexane:EtOAc to obtain 0.22 g (74%) of **6** as a white solid. Recrystallization in toluene by slow evaporation resulted in 0.195 g (65%) of colorless, thick, needle-like single crystals of **6**. R_f=0.06 (EtOAc/hexane 1:9); DTA (5 °C min^{-1}) T_{dec}/°C (onset) = 95; ^{1}H NMR (400 MHz, $CDCl_3$, 23 °C, TMS): δ=8.72 (s, 1H, C*H*), 7.98 (s, 1H, C*H*), 1.39 (s, 18H, CH_3) ppm; ^{13}C NMR (100 MHz, $CDCl_3$, 23 °C, TMS): δ=161.0 (C), 148.2 (C), 132.2 (*CH*), 130.2 (*C*), 120.9 (*C*H), 86.2 (*C*), 26.3 (CH_3) ppm; IR (ν cm^{-1}): 3117 (w), 3042 (w), 2984 (m), 2936 (w), 2874 (w), 1775 (s), 1697 (w), 1605 (m), 1531 (s), 1474 (w), 1456 (w), 1389 (w), 1368 (m), 1348 (s), 1295 (w), 1312 (w), 1261 (m), 1248 (w), 1200 (m), 1182 (s), 1136 (w), 1011(s), 1078 (m), 1032 (w), 968 (m), 926 (m), 899 (w), 876 (m), 835 (m), 818 (m), 773 (w), 758 (m), 746 (w), 719 (m);

elemental analysis calcd (%) for $C_{16}H_{20}N_2O_{10}$: C 48.00, H 5.36, N 6.99; found: C 47.71, H 5.65, N 6.97; IS: 5 J, FS: 96 N, ESD: 0.4 J.

Bis-tert-butyl ethanebis(peroxoate) (7) To a solution of anhydrous pyridine (0.5 mL, 6 mmol) and 5.5M ^{t}BuOOH in decane (1.10 mL, 6.0 mmol), which was kept at –4 °C (ice-water-salt bath), a solution of oxalyl chloride (0.25 mL, 3.0 mmol) in anhydrous pentane (5 mL) was added drop wisely with a syringe over a period of 15 min. Since stirring ceased, more anhydrous pentane (5 mL) was added to the reaction. Then, the reaction was allowed to warm up in a water bath for about 10 minutes. Afterwards, it was filtered through a 1.5 cm pad of Celite on a coarse glass frit. The solvent was evaporated in vacuum afterwards. Repeated recrystallization in pentane –29 °C was carried out to obtain 0.3 g (43%) of **7** as colorless, thick, long, needle-like single crystals. DTA (5 °C min^{-1}) T_m/°C (onset) = 48; T_{dec}/°C (onset) = 53; ^{1}H NMR (400 MHz, $CDCl_3$, 23 °C, TMS): δ=1.37 (s, 18H, CH_3) ppm; ^{13}C NMR (100 MHz, $CDCl_3$, 23 °C, TMS): δ=157.2, 86.0 (*C*), 26.2 (*C*H$_3$) ppm; IR (ν cm^{-1}): 2984 (m), 2938 (w), 2876 (s), 1805 (s), 1744 (m), 1653 (w), 1466 (w), 1369 (m), 1252 (m), 1204 (s), 1182 (s), 1121 (s), 1034(m), 930 (w), 889 (m), 831 (m), 789 (w), 743 (w); elemental analysis calcd (%) for $C_{10}H_{18}O_6$: C 51,26, H 7.76; found: C 51.22, 7.70; IS: 1 J, FS: <5 N, ESD: 0.015 J.

Hexakis-tert-butyl benzene-1,2,3,4,5,6-hexakis(carboxylperoxoate) (8) To a solution of anhydrous pyridine (0.0750 mL, 1.75 mmol) and 5.5M ^{t}BuOOH in decane (0.60 mL, 3.30 mmol) in a 100 mL Schlenk flask, which was kept at –4 °C (ice-water-salt bath), a solution of benzene-1,2,3,4,5,6-hexacarbonyl hexachloride (**B**) (0.113 g, 0.250 mmol) in distilled dichloromethane (10 mL) was slowly added with a syringe. Then, the reaction was stirred for about 2 h while allowing it to warm up to room temperature. The reaction was concentrated and the product was purified by silica gel column chromatography with CH_2Cl_2 to obtain 0.070 g (36%) of **8** as a white solid. Recrystallization in 1:1 dichloromethane:hexane at –29 °C resulted in 0.057 g (29%) of colorless, thick, polygonal single crystals of **8**. Compound **8** decomposed around 81 °C before melting. ^{1}H NMR (400 MHz, $CDCl_3$, 23 °C, TMS): δ=1.37 (s, 54H, CH_3) ppm; ^{13}C NMR (100 MHz, $CDCl_3$, 23 °C, TMS): δ=161.1 (*C*), 133.1 (*C*), 85.7 (*C*), 26.5 (*C*H$_3$) ppm; IR (ν cm^{-1}): 2982 (m), 2932 (w), 2870 (w), 1775 (s), 1462 (w), 1412 (w), 1393 (w), 1368 (m), 1327 (w), 1298 (w), 1263 (w), 1248 (w), 1140 (s), 1109 (m), 1076 (m), 1032(m), 970 (m), 922 (w), 868 (w), 835 (m), 804 (w), 739 (w), 727 (w).

Acknowledgements

Financial support of this work by the Ludwig-Maximilian University of Munich (LMU), the Office of Naval Research (ONR) under grant no. ONR.N00014-16-1-2062, and the Bundeswehr - Wehrtechnische Dienststelle für Waffen und Munition (WTD 91) under grant no. E/E91S/FC015/CF049 is gratefully acknowledged. The authors thank Mr. St. Huber for the sensitivity measurements.

Keywords: energetic materials • peroxides • peroxy-esters • sensitivities • structure elucidation

[1] L. Wenzel, S. Lee, *Polymer Engineering and Science* **2016**, *4*, 435-440.
[2] A. B. Rode, K. Chung, Y.-W. Kim, I. S. Hong, *Energy Fuels* **2010**, *24*, 1636-1639.
[3] C. W. Jefford, *Drug Discovery Today* **2007**, *12*, 487-495.
[4] R. Wolffenstein, *Ber. Dtsch. Chem. Ges.* **1895**, *28*, 2265.
[5] *Beilsteins Handbuch der org. Chem.* **1918-31**, 4.Auflage
[6] J. Köhler, R. Meyer, A. Homburg, *Explosivstoffe*, 10. Auflage, Wiley VCH, **2008**.
[7] N.-D. H. Gamage, B. Stiasny, J. Stierstorfer, P. D. Martin, T. M. Klapötke, C. H. Winter, *Cem. Eur. J.* **2016**, *22*, 2582-2585.
[8] T. M. Klapötke, B. Stiasny, J. Stierstorfer, C. H. Winter, *Eur. J. Org. Chem.* **2015**, *28*, 6237-6242.
[9] N.-D. H. Gamage, B. Stiasny, J. Stierstorfer, P. D. Martin, T. M. Klapötke, C. H. Winter, *Chem. Commun.* **2015**, *51*, 13298-13300.
[10] T. M. Klapötke, B. Stiasny, J. Stierstorfer, *ChemistrySelect* **2016**, *1*, 4057-4061.
[11] Y. Li, L. Ma, F. Jia, Z. Li., *J. Org. Chem.* **2013**, *11*, 5638-5646.
[12] P. D. Bartlett, R. R. Hiatt, *J. Am. Chem. Soc.* **1958**, *80*, 1398-1405.
[13] H. Hock, *Chem. Ber.* **1955**, *88*, 1544-1550.
[14] Ch. Ruchardt, H. Hecht, *Chem. Ber.* **1964**, *97*, 2716.
[15] V. A. Donchak, A. A: Voronov, R. S. Yur´ev, *Russ. J. Org. Chem.* **2006**, *42*, 505-508.
[16] Md. Abdul Mannan, A. Ichikawa, Y. Miura, *Polymer* **2007**, *3*, 743-749.
[17] A. L. J. Beckwith, A. A. Zavitsas, *J. Am. Chem. Soc.* **1986**, *26*, 8230-8234.
[18] F. Dubnikova, R. Kosloff, J. Almog, Y. Zeiri, R. Boese, H. Itzhaky, A. Alt,E. Keinan, *J. Am. Chem. Soc.* **2005**, *127*, 1146-1159.
[19] P. Groth, *Acta Chem. Scand.* **1996**, *23*, 1311-1329.
[20] L. Golic, I. Liban, *Acta Cryst.* **1984**, C*40*, 447-450.
[21] T. M. Klapötke, *Chemsitry of High-Energy Materials*, de Gruyter, Berlin/ Boston, 2nd edition, **2012**.
[22] J. C. Oxley, J. L. Smith, K Shinde, J. Moran, *Propellants Explos. Pyrotech.* **2005**, *30*, 127-130.
[23] S. Dalapati, R. Saha, S. Jana, A. K. Patra, A. Bhaumik, S. Kumar, N. Guchhait, *Angew. Chem. Int. Ed.* **2012,** *51,* 12534–12537.
[24] Ranganathan, S.; Muraleedharan, K. M.; Rao, C. H. C.; Vairamani, M.; Karle, I. L.; Gilardi, R. D. *Chem. Commun.* **2001,** *51,* 2544–2545.
[25] A. Zhang, Y. Han, K. Yamato, X. C. Zeng, B. Gong, *Org. Lett.* **2006,** *8,* 803–806.
[26] A. Dalia, G. M. Asri Abd, M. F. Cunningham, *Can. J. Chem.* **2004,** *82,* 1393–1402.
[27] P. D. Bartlett, E. P. Benzing, R. E. Pincock, *J. Am. Chem. Soc.* **1960,** *82,* 1762–1768.

FULL PAPER

Surprisingly low sensitive tert-butyl peroxy esters of selected carbonic acid chlorides were prepared and tested with respect to their sensitivity towards outer stimuli. In addition their performance as an energetic material were calculated using the EXPLO-5 thermochemical code and their molecular structures were determined by x-ray diffraction measurements.

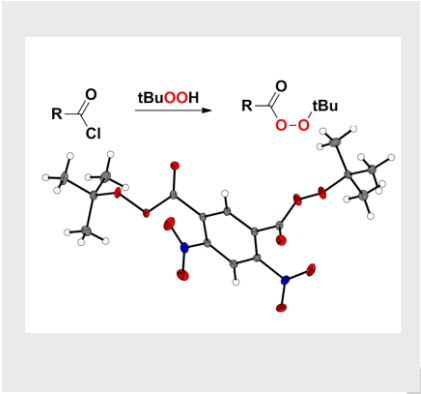

Nipuni-Dhanesha H. Gamage, Benedikt Stiasny, Jörg Stierstorfer, Philipp D. Martin, Thomas M. Klapötke and Charles H. Winter

Page No. – Page No.

Energetic materials – tert-Bu-Peroxy Esters as Peroxides with a Relatively Low Sensitivity

1.X-ray diffraction

For compound 2, an Oxford Xcalibur3 diffractometer with a CCD area detector was employed for data collection using Mo-Kα radiation (λ = 0.71073 Å). By using the Crystalispro software[S1] the data collection and reduction were performed. The structures were solved by direct methods (SIR-92[S2], SIR-97[S3] and SHELXS-97[S4]) and refined by fullmatrix least-squares on *F*2 (SHELXL [S4]) and finally checked by using the PLATON software [S5] integrated in the WinGX software suite. The non-hydrogen atoms were refined anisotropically and the hydrogen atoms were located and freely refined. The absorptions were corrected by a SCALE3 ABSPACK multiscan method [S6]. All DIAMOND2 plots are shown with thermal ellipsoids at 50% probability level and hydrogen atoms are shown as small spheres of arbitrary radius.

Table S1. X-ray diffraction parameters

	1	**2**	**3**	**4**	**5**	**6**	**7**	**8**
Formula	$C_{16}H_{22}O_6$	$C_{16}H_{22}O_6$	$C_{21}H_{30}O_9$	$C_{26}H_{38}O_{12}$	$C_{11}H_{12}N_2O_7$	$C_{16}H_{20}N_2O_{10}$	$C_{10}H_{18}O_6$	$C_{42}H_{68}O_{18}$
FW [g/mol]	310.33	310.34	426.45	542.56	284.23	400.34	234.28	860.96
Crystal system	monoclinic	orthorhombic	triclinic	monoclinic	triclinic	monoclinic	triclinic	monoclinic
Space Group	P1 21/c1	Pna21	P−1	C12/c1	P−1	P1 21/c1	P−1	C1c1
a [Å]	17.5862(13)	16.1127(7)	5.9235(4)	27.942(2)	5.8362(4)	15.0401(9)	10.4787(4)	22.1254(16)
b [Å]	9.3966(7)	14.3472(6)	12.4414(7)	7.9924(5)	10.2950(7)	5.7008(3)	14.5660(6)	19.4588(16)
c [Å]	9.9604(7)	22.2819(11)	16.3240(10)	29.958(2)	10.8250(7)	21.6710(13)	16.5368(7)	11.4416(9)
α [°]	90	90	81.703(3)	90	101.907(3)	90	89.976(2)	90
β [°]	93.884(4)	90	85.497(3)	117.419(3)	92.880(3)	91.330(3)	90.014(2)	90.089(4)
γ [°]	90	90	76.950(3)	90	92.203(4)	90	90.027(2)	90
V [$Å^3$]	1642.2(2)	5151.0(4)	1158.37(13)	5938.8(7)	634.81(7)	1857.58(19)	2524.06(18)	4926.0(7)
Z	4	12	2	8	2	4	2	4
$\rho_{cacl.}$ [g cm^{-3}]	1.255	1.201	1.223	1.214	1.487	1.431	1.233	1.161
μ [mm^{-1}]	0.096	0.091	0.095	0.096	0.126	0.121	0.102	0.090
F (000)	664	1992	456	2320	296	840	1008	1856
$\lambda_{MoK\alpha}$ [Å]	0.71073	0.71073	0.71073	0.71073	0.71073	0.71073	0.71073	0.71073
T [K]	100(2)	173	100(2)	100(2)	100(2)	100(2)	100(2)	100(2)
ϑ min max [°]	2.32, 26.41	4.1, 27.0	1.26, 32.46	1.64, 34.13	1.93, 35.99	1.35, 34.85	1.23, 24.76	1.39,30.64
Dataset h; k; l	−18:21; −11:11; −12:12	−16:20; −18:18; −27:28	−8:8; −18:18; −24:24	−44:44; −8:12; −47:47	−9:9; −16:16; −16:17	−24:24; −9:8; −34:34	−10:12; −17:17; −19:18	−30:31; −27:27; −16:15
Reflect. coll.	19073	40377	61214	48176	36834	113244	35654	103422
Independ. refl.	3254	5748	8299	12202	5822	8063	8144	14329
R_{Int}	0.0390	0.095	0.0274	0.0377	0.0299	0.0303	0.0314	0.0317
Reflection obs.	3254	3638	8299	12202	5822	8063	8144	14329
No. parameters	205	613	280	355	184	259	602	563
R_1 obs.	0.0612	0.0688	0.0400	0.0446	0.0383	0.0362	0.0354	0.0467
wR_2 (all data)	0.1823	0.1852	0.1158	0.1462	0.1145	0.1272	0.0791	0.1324
S	1.15	1.02	1.03	0.96	1.04	0.85	1.02	0.97
Resd. Dens. [e $Å^{-3}$]	−0.285;0.321	−0.38;0.54	−0.236;0.448	−0.288;0.581	−0.256;0.534	−0.259;0.495	−0.191;0.167	−0.231;0.597
Device type		SIR-92						
Solution	SHELXL-2013	SHELXL-97	SHELXL-2013	SHELXL-2013	SHELXL2013	SHELXL-2013	SHELXL-2013	SHELXL-2013
Refinement	multi-scan	multi-scan	multi-scan	multi-scan	multi-scan	multi-scan	multi-scan	multi-scan

2. Computations

All calculations were carried out using the Gaussian G09W (revision A.02) program package. The enthalpies (H), listed in Table S2, were calculated using the complete basis set (CBS) method of Petersson and coworkers in order to obtain very accurate energies. The CBS models use the known asymptotic convergence of pair natural orbital expressions to extrapolate from calculations using a finite basis set to the estimated complete basis set limit. CBS-4 begins with a HF/3-21G(d) geometry optimization; the zero point energy is computed at the same level. It then uses a large basis set SCF calculation as a base energy, and a MP2/6-31+G calculation with a CBS extrapolation to correct the energy through second order. A MP4(SDQ)/6-31+(d,p) calculation is used to approximate higher order contributions. In this study we applied the modified CBS-4M method (M referring to the use of Minimal Population localization) which is a re-parametrized version of the original CBS-4 method and also includes some additional empirical corrections.[S8,S9] The enthalpies of the gas-phase species M were computed according to the atomization energy method (eq.1).[S10,S11]

$$\Delta_f H°_{(g,\,M,\,298)} = H_{(Molecule,\,298)} - \sum H°_{(Atoms,\,298)} + \sum \Delta_f H°_{(Atoms,\,298)} \quad (1)$$

Table S2. CBS-4M results and calculated gas-phase enthalpies

	M	$-H^{298}$ / a.u.	$\Delta_f H°$(g,M) / kcal mol^{-1}
1	$C_{16}H_{22}O_6$	1072.590470	−178.3
2	$C_{16}H_{22}O_6$	1072.589915	−177.8
3	$C_{21}H_{30}O_9$	1492.963912	−271.5
4	$C_{26}H_{38}O_{12}$	1913.330641	−360.7
5	$C_{11}H_{12}N_2O_7$	1060.803719	−88.3
6	$C_{16}H_{20}N_2O_{10}$	1481.162002	−172.2
7	$C_{10}H_{18}O_6$	841.902973	−179.4

Table S3. CBS-4M values and literature values for atomic $\Delta H°_f{}^{298}$ / kcal mol^{-1}

	$-H^{298}$ / a.u.	NIST [S12] / $\Delta H°_f{}^{298}$
H	0.500991	52.1
C	37.786156	171.3
O	74.991202	59.6

The gas phase heat of formation of **X** and **X** is converted into the solid state (standard conditions) enthalpy of formation (Table S6) by subtracting its sublimation enthalpy calculated with Trouton's rule ($\Delta H_{sub} = 188 \cdot T_m$ = 72.0 kJ mol^{-1}). These molar standard enthalpies of formation (ΔH_m) were used to calculate the molar solid state energies of formation (ΔU_m) according to equation 2.

$$\Delta U_m = \Delta H_m - \Delta n\, RT \quad \textbf{(2)}$$

(Δn being the change of moles of gaseous components)

Table S4. Calculated gas phase heat of formation, molecular volumes, lattice energies and lattice enthalpies of **1** to **7**.

	$\Delta_f H°$(g,M) / kJ mol^{-1}	T_m / T_{dec}	ΔH_{sub} / kJ mol^{-1}
1	−746.5	-/122	74.3
2	−744.3	37/132	58.3
3	−1136.9	-/123	74.5
4	−1510.3	-/123	74.5
5	−369.6	85/121	67.3
6	−720.9	-/95	69.2
7	−751.1	48/53	60.4

Table S5. Solid state energies of formation ($\Delta_f U°$)

	$\Delta_f H°$(s) / kJ mol^{-1}	Δn	$\Delta_f U°$(s) / kJ mol^{-1}	M / g mol^{-1}	$\Delta_f U°$(s) / kJ kg^{-1}
1	−820.7	14	−786.0	310.28	−2532.7
2	−802.0	14	−767.9	310.28	−2474.3
3	−1211.3	19.5	−1162.9	426.51	−2727.0
4	−1584.7	25	−1522.7	542.57	−2806.5
5	−436.9	10.5	−410.9	284.06	−1445.7
6	−790.0	16	−750.4	400.34	−1874.4
7	−811.4	12	−781.7	234.28	−3337.0

Notes: Δn being the change of moles of gaseous components when formed.

3. References

[S1] *CrysAlisPro*, Oxford Diffraction Ltd., version 171.33.41, **2009**.

[S2] *SIR-92, A program for crystal structure solution*: A. Altomare, G. Cascarano, C. Giacovazzo, A. Guagliardi, *J. Appl. Crystallogr*. **1993**, *26*, 343.

[S3] a) A. Altomare, G. Cascarano, C. Giacovazzo, A. Guagliardi, A. G. G. Moliterni, M. C. Burla, G. Polidori, M. Camalli, R. Spagna, *SIR97*, **1997**; b) A. Altomare, M. C. Burla, M. Camalli, G. L. Cascarano, C. Giacovazzo, A. Guagliardi, A. G. G. Moliterni, G. Polidori, R. Spagna, *J. Appl. Crystallogr*. **1999**, *32*, 115–119.

[S4] a) G. M. Sheldrick, *SHELX-97*, University of Göttingen, Göttingen, Germany, **1997**; b) G. M. Sheldrick, *Acta Crystallogr., Sect. A* **2008**, *64*, 112–122.

[S5] A. L. Spek, *PLATON, A Multipurpose Crystallographic Tool*, Utrecht University, The Netherlands, **1999**.

[S6] *SCALE3 ABSPACK – An Oxford Diffraction program* (1.0.4, gui: 1.0.3), Oxford Diffraction Ltd., **2005**.

[S7] Gaussian 09, M. J. Frisch, G. W. Trucks, H. B. Schlegel, G. E. Scuseria, M. A. Robb, J. R. Cheeseman, G. Scalmani, V. Barone, B. Mennucci, G. A. Petersson, H. Nakatsuji, M. Caricato, X. Li, H. P. Hratchian, A. F. Izmaylov, J. Bloino, G. Zheng, J. L. Sonnenberg, M. Hada, M. Ehara, K. Toyota, R. Fukuda, J. Hasegawa, M. Ishida, T. Nakajima, Y. Honda, O. Kitao, H. Nakai, T. Vreven, J. A. Montgomery, Jr., J. E. Peralta, F. Ogliaro, M. Bearpark, J. J. Heyd, E. Brothers, K. N. Kudin, V. N. Staroverov, R. Kobayashi, J. Normand, K. Raghavachari, A. Rendell, J. C. Burant, S. S. Iyengar, J. Tomasi, M. Cossi, N. Rega, J. M. Millam, M. Klene, J. E. Knox, J. B. Cross, V. Bakken, C. Adamo, J. Jaramillo, R. Gomperts, R. E. Stratmann, O. Yazyev, A. J. Austin, R. Cammi, C. Pomelli, J. W. Ochterski, R. L. Martin, K. Morokuma, V. G. Zakrzewski, G. A. Voth, P. Salvador, J. J. Dannenberg, S. Dapprich, A. D. Daniels, Ö. Farkas, J. B. Foresman, J. V. Ortiz, J. Cioslowski, and D. J. Fox, Gaussian, Inc., Wallingford CT, 2009.

[S8] J. W. Ochterski, G. A. Petersson, J. A. Montgomery, *J. Chem. Phys*. **1996**, *104*, 2598–2619;

[S9] J. A. Montgomery Jr., M. J. Frisch, J. W. Ochterski, and G. A. Petersson, *J. Chem. Phys*. **112**, 6532 (2000).

[S10] Byrd, Edward F. C.; Rice, Betsy M. Improved Prediction of Heats of Formation of Energetic Materials Using Quantum Mechanical Calculations. Journal of Physical Chemistry A (2006), 110(3), 1005-1013.

[S11] Rice, Betsy M.; Pai, Sharmila V.; Hare, Jennifer. Predicting heats of formation of energetic materials using quantum mechanical calculations. Combustion and Flame (1999), 118(3),

445-458.

[S12] P. J. Lindstrom, W. G. Mallard (Editors), NIST Standard Reference Database Number 69, http://webbook.nist.gov/chemistry/ (Juni **2011**).

ChemPubSoc Europe

DOI: 10.1002/ejic.201600767

EurJIC European Journal of Inorganic Chemistry

Full Paper

Energetic Materials

Energetic Materials Trends in 5- and 6-Membered Cyclic Peroxides Containing Hydroperoxy and Hydroxy Substituents

Nipuni-Dhanesha H. Gamage,[a] Benedikt Stiasny,[b] Eric G. Kratz,[a] Jörg Stierstorfer,[b] Philip D. Martin,[a] G. Andrés Cisneros,[a] Thomas M. Klapötke*[b] and Charles H. Winter*[a]

Abstract: Ten peroxide compounds based upon the 3,6-di(hydroperoxy)-1,2-dioxane, 2-hydroxy-6-hydroperoxy-1,2-dioxane, 3,5-di(hydroperoxy)-1,2-dioxolane, and 3-hydroxy-5-hydroperoxy-1,2-dioxolane skeletons have been synthesized, structurally characterized, and fully evaluated for their energetic materials properties. The solid-state structures of these compounds are dominated by hydrogen bonding interactions involving the hydroperoxy and hydroxy groups. Energetic materials testing shows that most of the compounds are highly sensitive toward impact and friction, with similar properties to highly sensitive peroxides such as triacetone triperoxide. 3,5-Diethyl-5-hydroperoxy-1,2-dioxolan-3-ol (**3b**) and 3,5-dimethyl-5-hydroperoxy-1,2-dioxolan-3-ol (**5b**) have lower impact and friction sensitivities than the other compounds, with values that are appropriate for use as primary explosives.

Introduction

Peroxo compounds contain one or more O–O bonds and are widely used as polymerization initiators, curing and vulcanizing agents, cross-linking agents, bleaching and disinfecting agents, and homemade explosives.[1–3] Until recently, detailed information about the energetic materials properties of peroxides was only available for triacetone triperoxide (TATP), diacetone diperoxide (DADP), hexamethylene triperoxide diamine (HMTD), and methyl ethyl ketone peroxide (MEKP).[1–3] TATP, DADP, HMTD, and MEKP are very sensitive and can explode violently upon routine handling. As such, there are no military and civilian applications of peroxide explosives. However, TATP is easily synthesized and is frequently used as a homemade explosive in terrorist attacks.[1,2] Based upon the well-documented high sensitivities of TATP, DADP, HMTD, and MEKP, organic peroxides remain largely unexplored as energetic materials.

We are interested in exploring the limits of oxygen atom incorporation into organic compounds, with the aim of synthesizing low sensitivity, oxygen-rich compounds that might be used as explosives and high energy dense oxidizers.[4] We recently reported new classes of organic peroxides that are much less sensitive toward stimuli than TATP, DADP, HMTD, and MEKP.[5–7] In particular, cyclic and bicyclic compounds containing two geminal hydroperoxy groups have appropriate sensitivity values for use as primary explosives,[5] and nitroaromatic peroxy acids have low enough sensitivities to be classified as secondary energetic materials.[6] There have been several reports of organic peroxides with O/C ratios of > 1, but most of these compounds are reported to decompose readily or explode violently.[8] Herein, we report the synthesis, structure, and energetic properties of a series of oxygen-rich compounds based upon the 6-hydroperoxy-1,2-dioxane (**A**) and 5-hydroperoxy-1,2-dioxolane (**B**) skeletons, where X is OOH or OH (Scheme 1). Compounds where X is OOH are very sensitive, with impact, friction, and electrostatic discharge sensitivities that are similar to TATP, DADP, HMTD, and MEKP. Several compounds where X is OH exhibit lower sensitivities, without a significant loss in the energetic materials performance. We have also carried out calculations to understand the solid state interactions that contribute to sensitivity differences.

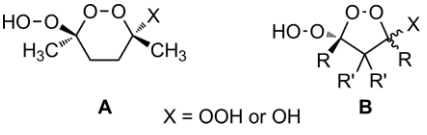

Scheme 1. Six-membered (**A**) and five-membered (**B**) peroxides studied herein.

Results and Discussion

Compounds **1**–**5** were prepared upon treatment of γ- or β-diketones with 50 wt.-% aqueous H_2O_2 in the presence of the catalysts I_2, H_2SO_4, or $SnCl_2{\cdot}2H_2O$ at or below room temperature [Equation (1)].[9–11] Compounds **1a**,[10] **5a**,[9b,11] and **5b**[11] were reported previously, and **2b** was briefly mentioned in one of our recent papers.[7] The other compounds have not been pre-

[a] Department of Chemistry, Wayne State University, Detroit, Michigan 48202, United States, USA
E-mail: chw@chem.wayne.edu
http://clas.wayne.edu/wintergroup/
[b] Department of Chemistry, Ludwig-Maximilians-Universität, Butenandtstr. 5–13 (D), 81377 München, Germany
E-mail: tmk@cup.uni-muenchen.de
www.hedm.cup.uni-muenchen.de

Supporting information and ORCID(s) from the author(s) for this article are available on the WWW under http://dx.doi.org/10.1002/ejic.201600767.

viously reported. The indicated yields are for the optimum syntheses. Compounds **3a** and **5a** were obtained upon treatment of the diketones with a catalytic amount of concentrated H_2SO_4 and were recrystallized to afford pure materials. Reactions using catalytic I_2 or $SnCl_2{\cdot}2H_2O$ gave variable mixtures of **1a**–**5a** and **1b**–**5b**, with the former generally predominating. These mixtures were easily separated by silica gel column chromatography to afford the pure compounds. In this way, **1a**, **2a**, **2b**, **3b**, **4a**, and **4b** were obtained using catalytic I_2 and **1b** and **5b** were synthesized with $SnCl_2{\cdot}2H_2O$. Further efforts to optimize the syntheses of **1**–**5** were not made, because of their energetic nature and the facile separations by column chromatography. The structures and compositions of **1**–**5** were established by a combination of spectral and analytical data and by X-ray crystal structure determinations of all compounds except **1b**, which exists as an oil. The relative stereochemistries of **1**–**5** were obtained from the X-ray crystal structures. Compounds **1**–**5** showed the expected resonances in the ^1H and ^{13}C NMR spectra, and the infrared spectra were consistent with the structures. The ^{13}C NMR resonances of the oxygen-substituted carbon atoms were the most diagnostic spectroscopic feature. In **1a**, this resonance appeared at δ = 109.3 ppm. In **1b**, the C(OO)(OOH) carbon atom resonated at δ = 107.2 ppm, while the C(OO)(OH) carbon atom appeared at δ = 100.0 ppm. For the five-membered ring compounds **2a**–**5a**, the C(OO)(OOH) carbon atom resonated between 113.4 and 115.6 ppm. For **2b**–**5b**, the C(OO)(OOH) and C(OO)(OH) carbon atom resonances were observed between 113.7 and 115.9 ppm and 106.5 and 108.6 ppm, respectively.

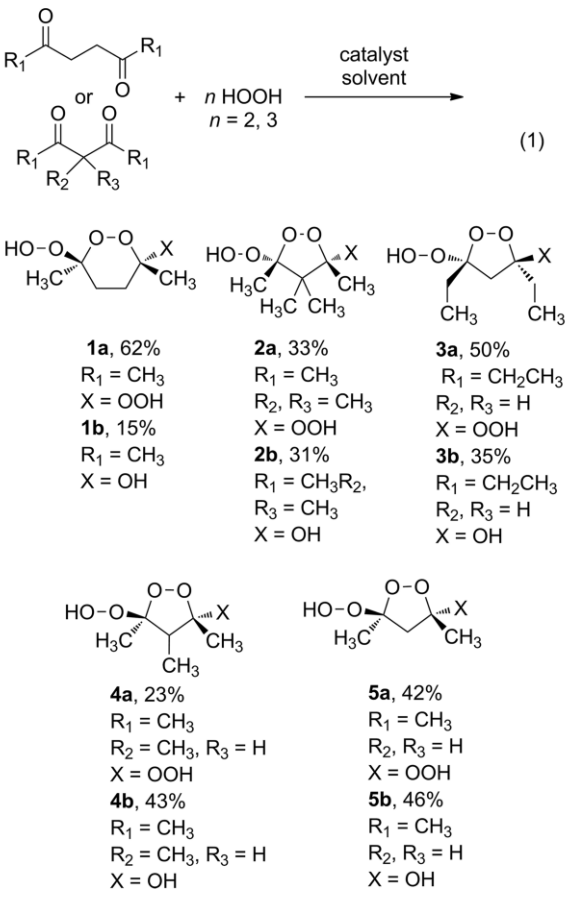

Table 1. Crystal data and structure refinement for **1a** and **2**–**5**.

	1a	**2a,2b**	**3a,3b**	**4a,4b**	**5a,5b**
Formula	$C_5H_{10}O_7$	$C_{14}H_{28}O_{12}$, $C_7H_{14}O_5$	$C_7H_{14}O_6$, $C_7H_{14}O_5$	$C_6H_{12}O_6$, $C_6H_{12}O_5$	$C_5H_{10}O_6$, $C_5H_{10}O_5$
M_r	182.13	388.36, 178.18	194.18, 178.18	180.16, 164.16	166.13, 150.13
Crystal system	tetragonal	orthorhombic, monoclinic	monoclinic, orthorhombic	orthorhombic, monoclinic	monoclinic, monoclinic
Space group	I4bar	*Pbca*, $P2_1/n$	$P2_1/n$, *Pbca*	*Pbca*, $P2_1/n$	$P2_1/n$, $P2_1/n$
a [Å]	14.0266(7)	12.6452(16), 8.811(2)	5.6429(3), 9.9659(7)	8.1894(6), 7.6155(5)	5.5729(5), 8.6193(6)
b [Å]	14.0266(7)	12.5922(15), 8.8031(18)	17.6201(9), 10.7296(7)	6.6753(4), 11.9510(8)	15.4498(12), 8.7945(6)
c [Å]	8.7135(5)	23.364(3), 11.281(3)	9.1491(5), 16.6680(12)	30.7184(19), 9.3339(6)	8.7244(7), 9.2016(6)
β [°]	–	–, 95.900(14)	90.610(3), –	–, 113.494(3)	90.055(4), 104.0770(10)
V [Å^3]	1714.3(2)	3720.3(8), 870.4(3)	909.63(8), 1782.3(2)	1679.27(19), 779.08(9)	751.17(11), 676.56(8)
Z	8	8, 4	4, 8	8, 4	4, 4
D_c [g cm^{-3}]	1.411	1.387, 1.360	1.418,1.328	1.425,1.400	1.469,1.474
μ(Mo-K_α) [mm^{-1}]	0.136	0.122, 0.166	0.125,0.113	0.129,0.123	0.138,0.134
T [K]	100(2)	100(2), 100(2)	100(2), 100(2)	100(2), 100(2)	100(2), 100(2)
Observed reflections	5455	5148,2047	4490,4760	1437, 2728	3631, 3774
Parameters	117	255,119	126,117	118,109	108,99
GOF	0.620	1.040,1.199	1.111,1.033	1.201, 1.094	1.959,0.948
R_1[a][b]	0.0321 (0.0293)	0.0400 (0.0305), 0.0593 (0.0485)	0.0521 (0.0380), 0.0357 (0.0301)	0.0487 (0.0450), 0.0466 (0.0357)	0.0803 (0.0618), 0.0448 (0.0362)
wR_2[c]	0.0883 (0.0838)	0.0822 (0.0761), 0.1371 (0.1319)	0.1093 (0.1032), 0.0915 (0.0866)	0.1254 (0.1236), 0.0941 (0.0890)	0.2333 (0.2203), 0.1261 (0.1169)
Largest difference in peak and hole [e Å^3]	0.356 and –0.271	0.364 and –0.195, 0.374 and –0.324	0.473 and –0.286, 0.449 and –0.283	0.395 and –0.221, 0.426 and –0.293	0.513 and –0.548, 0.548 and –0.223

[a] $R_1 = \Sigma||F_o| - |F_c||/\Sigma|F_o|$. [b] Values in parentheses for reflections with $I > 2\sigma(I)$. [c] $wR_2 = [\Sigma w(F_o^2 - F_c^2)^2/\Sigma w(F_o^2)^2]^{1/2}$.

The X-ray crystal structures of **1a** and **2**–**5** were determined to obtain molecular structures and to understand intermolecular interactions. Table 1 gives crystal data for **1a** and **2**–**5** and Figure 1 shows representative perspective views of **5a** and **5b**, along with selected bond lengths and angles. The X-ray crystal structures of **1a** and **2**–**5** are contained in the supporting information. Compounds **1a** and **3**–**5** exhibit *anti* arrangement of the oxygen substituents within the rings, most likely to minimize steric interactions between the alkyl groups. By contrast, the oxygen groups in **2a** and **2b** are *syn*. The cyclic peroxide O–O bond lengths in **1a** and **2**–**5** range from 1.4613(8) Å in **1a** to 1.4956(9) and 1.493(2) Å in **2a** and **2b**, respectively. The *syn*-oxygen substituents and four methyl groups on the rings in **2a** and **2b** may introduce strain into the five-membered rings that cause the slightly longer O–O bond lengths, compared to **3**–**5**. The O–O bond lengths in the OOH substituents fall within the narrow range of 1.4575(2) to 1.465(2) Å. These values are very similar to the O–O bond lengths in recent compounds reported by our group that contain OOH substituents.[5,6] Solid state densities range from 1.328 to 1.474 g/cm^3 (Table 1). The dihydroperoxy compounds **2a**–**5a** have slightly higher densities than the corresponding hydroperoxy compounds **2b**–**5b**, consistent with their higher molecular weights.

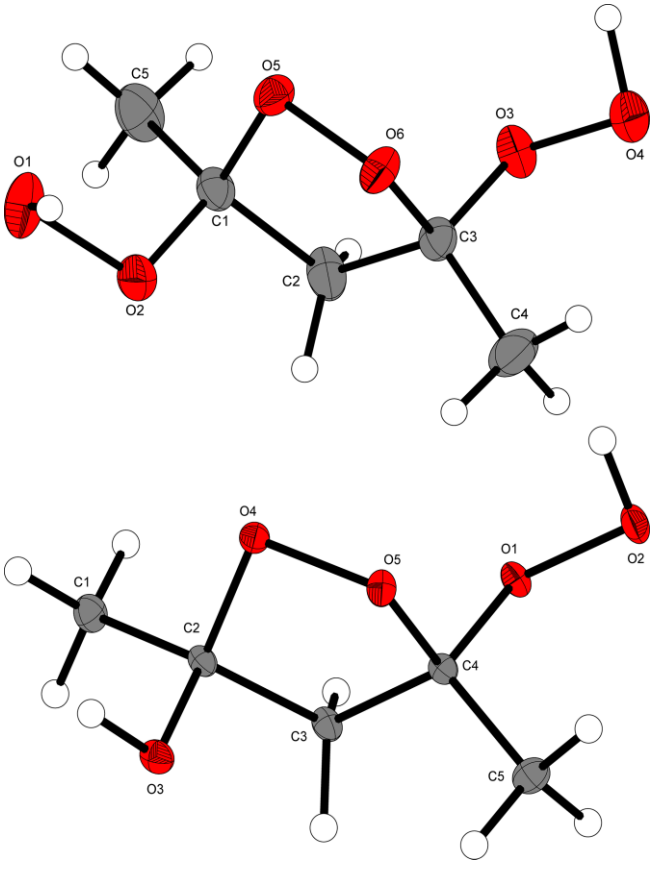

Figure 1. Perspective views of **5a** (top) and **5b** (bottom). Selected bond lengths [Å]: **5a**, O1–O2 1.458(1), O3–O4 1.460(1), O5–O6 1.475(1); **5b**, O1–O2 1.4638(6), O5–O6 1.4783(6).

Tables S1–S9 and Figures S1–S9 in the supporting information document the intermolecular interactions in **1a** and **2**–**5**. The intermolecular interactions in these compounds are dominated by O···H and O···O contacts that are within the van der Waals radii of these atoms (2.62 Å for O···H, 3.04 Å for O···O).[12] As expected, these O···H and O···O close contacts occur through hydrogen bond formation involving the OOH and OH groups. The lattices in **1a** and **2**–**5** are composed of various O–H···O hydrogen bonded motifs, including 1-dimensional chains (**1a**), dimers (**2a**, **2b**, **3b**), two-dimensional sheets (**3a**, **4a**, **4b**, **5a**), and tetramers (**5b**). Compounds **1a**, **2a**, **2b**, **4b**, and **5b** contain one or more H···H close contacts, **2b**, **4a**, **4b**, and **5b** each exhibit one or more C···H close contacts, and **3a** and **4a** each have one close C···O close contact. The H···H, C···H, and C···O close contacts appear to arise through maximization of the hydrogen bond networks associated with the OOH and OH groups.

Electronic structure calculations can be used to determine the strength of stabilizing intermolecular interactions within the crystal lattice. Representative compounds **5a** and **5b** were chosen for these studies. Stabilization energies for **5a** and **5b** were calculated to be –89.0 and –89.4 kJ/mol, respectively. Because the lattice energies of these two crystals are nearly identical, a non-covalent interaction (NCI) analysis[13] was performed on **5a** and **5b** to gain further insights into the interactions within the crystal lattices. Attractive interactions (and the neighboring atoms responsible) around each functional group in **5a** and **5b** are shown in Figure 2 and Figure 3, respectively. Key interactions within the lattice are circled and the surfaces are color coded based on the strength of the interactions. The color scale used for the NCI surfaces varies between weakly attractive (green) and strongly attractive (dark blue). The OOH groups in **5a** form a zigzag two-dimensional $[OOH\cdots]_n$ hydrogen-bond donor–acceptor chain across the crystal. The OOH and OH groups in **5b** form a tetrameric $[OH\cdots OOH]_2$ hydrogen-bond donor–ac-

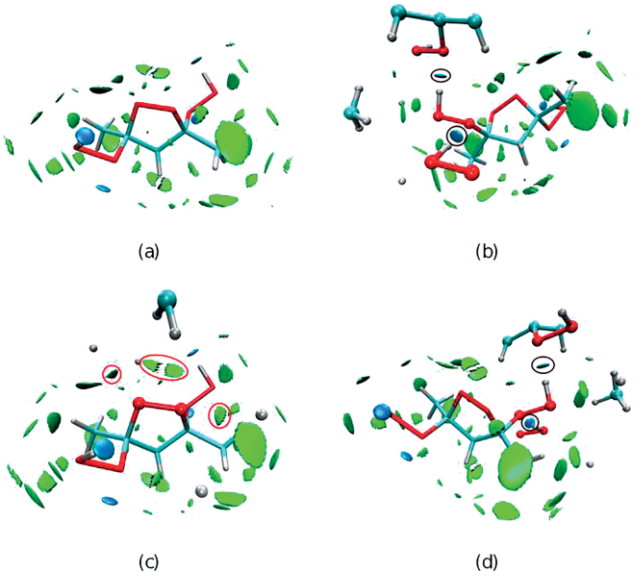

Figure 2. Attractive intermolecular interactions between **5a** and nearest neighbors within 4 Å. Strongly attractive interactions are shown in blue and weaker interactions are green. Surfaces are shown for (a) the whole molecule, (b) the first OOH group, (c) the central COOC group (CH···O distance: 2.8–3.0 Å), and (d) the second OOH group. Key interactions (black: hydrogen bond, red: CH···O contacts) are circled for each functional group. Neighboring atoms within 3.5 Å of each functional group are shown to highlight the atoms responsible for the intermolecular interactions.

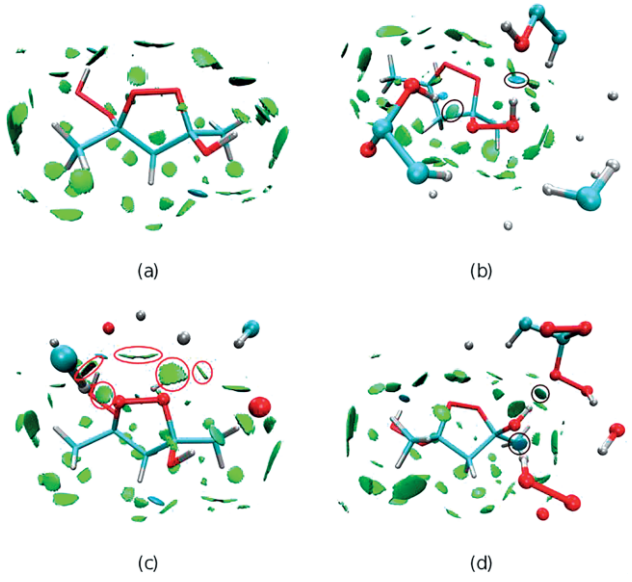

Figure 3. Attractive intermolecular interactions between structure **5b** and nearest neighbors within 4 Å. Strongly attractive interactions are shown in blue and weaker interactions are green. Surfaces are shown for (a) the whole molecule, (b) the OOH group, (c) the central COOC group (CH···O distance: 2.6–2.9 Å), and (d) the OH group. Key interactions (black: hydrogen bond, red: CH···O contacts) are circled for each functional group. Neighboring atoms within 3.5 Å of each functional group are shown to highlight the atoms responsible for the intermolecular interactions.

ceptor ring (see supporting information). The peroxide bonds in the C_3O_2 rings of **5a** and **5b** show only weak CH···O interactions in the X-ray crystal structures. Our calculations confirm the presence of four weak CH···O close contacts in **5a** between the core ring oxygen atoms and a ring C–H bond and a methyl group from another molecule. In **5b**, calculations show six CH···O close contacts between the core ring oxygen atoms and methyl groups from adjacent molecules. The C···H and C···O close contacts that are observed in the crystal structure of **5b** are not observed as attractive in the calculations, suggesting very weak interactions at best. The nearly identical calculated lattice energies for **5a** and **5b** suggest that intermolecular interactions alone cannot explain the observed sensitivity differences (vide infra).

The thermal behavior of **1**–**5** was studied using thermogravimetric analysis (TGA) and differential thermal analysis (DTA). As shown in Table 2, decomposition onset temperatures by DTA range from 82 to 133 °C, except for **2a** and **2b**, which show decomposition onsets at 64 and 67 °C, respectively. The *syn* arrangements of the oxygen ring substituents in **2a** and **2b** and their long ring O–O bond lengths may correlate with their lower decomposition temperatures. Compound **5b** is the most thermally stable, with a decomposition temperature of 133 °C. CBS-4M electronic enthalpies were calculated with the Gaussian09 software package.[14] The heats of formation range from –542.7 to –509.1 kJ/kg for **1a**–**5a** and –646.5 to –590.7 kJ/kg for **1b**–**5b** (Table 2). Dihydroperoxy compounds **1a**–**5a** have more positive heats of formation values than the corresponding hydroperoxy compounds **1b**–**5b**, consistent with the larger number of weak O–O bonds in **1a**–**5a**.

Impact, friction, and electrostatic discharge sensitivities were determined with a BAM drop hammer, a BAM friction tester, and an electrostatic discharge tester using standard test methods.[15] Sensitivity classifications are based on the "UN Recommendations on the Transport of Dangerous Goods".[16] Energetic performance data were calculated using the EXPLO5 V6.02 software.[17] As shown in Table 2, impact and friction sensitivities for **1a**–**5a** are ≤ 2 J and < 5 N, respectively. Accordingly, these compounds are "very sensitive" toward impact and "extremely sensitive" toward friction.[16] These values are similar to those of TATP and DADP,[1–3] and thus **1a**–**5a** must be handled with great care. Compounds **1b**–**5b** each contain one fewer oxygen atom and one fewer peroxide linkage than the corresponding compounds **1a**–**5a**. Compounds **1b**, **2b**, and **4b** have impact sensitivities of < 2 J, whereas **3b** and **5b** each has an impact sensitivity of 3 J. The central ring carbon atoms in **2b** and **4b** are substituted with one or two methyl groups, while these carbon atoms are unsubstituted in **3b** and **5b**. The ring substitution thus might influence impact sensitivity. Compounds **3b** and **5b** are less sensitive toward impact than **1a**, **1b**,

Table 2. Sensitivities and energetic performance of peroxo-based oxygen-rich compounds **1**–**5**.

	1a,**1b**	**2a**,**2b**	**3a**,**3b**	**4a**,**4b**	**5a**,**5b**
IS[a] [J]	< 1, 1	< 1, 2	2, 3	< 1, 1	< 1, 3
FS[b] [N]	< 5, 5	< 5, 6	< 5, 14	< 5, 40	< 5, 40
ESD[c] [J]	0.15, oil n.d.	0.065, 0.10	0.15, 0.20	0.10, 0.20	0.5, 0.15
Ω[d] [%]	–106.57, –126.70	–123.59, –143.67	–123.59, –143.67	–106.57, –126.70	–86.68, –106.57
T_{Dec}[e] [°C]	124,131	64,67	129,95	96,82	118,133
ϱ[f] [g/cm³]	1.411, oil n.d.	1.387,1.360	1.418,1.328	1.425,1.400	1.469,1.474
$\Delta_f H°$[g] [kJ/kg]	–541.2, –627.2	–542.7, –646.5	–538.7, –641.6	–529.6, –615.4	–509.1, –590.7
$\Delta_f U°$[h] [kJ/kg]	–2945.3, –3692.2	–2667.1, –3496.1	–2646.7, –3468.9	–2816.0, –3620.5	–2945.3, –3810.5
Explo v.6.02					
$\Delta_{Ex}U°$[i] [kJ/kg]	–4885, –	–4748, –3498	–4783, –3517	–4952, –3780	–5133, –4572
P_{CJ}[j] (kbar)	130, –	124, 104	132, 98	134, 109	154, 136
V_{Det}[k] [m/s]	6350, –	6357, 6100	6501, 5954	6511, 6103	6694, 6461
V_o[l] [L/kg]	853, –	871, 876	869, 878	853, 864	840, 842

[a] BAM drophammer. [b] BAM friction. [c] Electrostatic discharge sensitivity. [d] Oxygen balance. [e] Decomposition onset temperature from DTA (5 °C min^{-1}). [f] Low temperature X-ray densities. Values at 298 K were calculated from the low-temperature X-ray values using the equation: $\varrho_{298K} = \varrho_T/[1 + \alpha_V(298 - T_0)]$; $\alpha_V = 1.5 \times 10^{-4}$ K^{-1}]. [g] Calculated molar enthalpy of formation. [h] Energy of formation. [i] Total energy of detonation. [j] Detonation pressure. [k] Detonation velocity. [l] Volume of detonation products.

2a, **2b**, **3a**, **4a**, **4b**, and **5a**, although they are still classified as "very sensitive" according to the UN classification. The friction senstivities decrease in the order **1b** (5 N) > **2b** (6 N) > **3b** (14 N) > **4b**, **5b** (40 N). Compounds **1b** and **2b** are classified as "extremely sensitive" toward friction, while **3b**–**5b** are "very sensitive". The electrostatic discharge sensitivity values of **1**–**5** are greater than what can be generated by the human body (0.025 J).[1b]

Compounds **1a**–**5a** have calculated detonation velocity values (V_{Det}) that increase from 6350 m/s in **1a** to 6694 m/s in **5a**. The V_{Det} value trend in **1a**–**5a** correlates approximately with the increasing solid state densities. For comparison, **2b**–**5b** have calculated V_{Det} values of **3b** (5954 m/s) < **2b** (6100 m/s) < **4b** (6103 m/s) < **5b** (6461 m/s). This trend exactly mirrors the order of increasing solid state density values in Table 2. Compounds **5a** and **5b** have the highest V_{Det} values (6694, 6461 m/s), the highest solid state densities (1.469, 1.474 g/cm^3), and the highest oxygen/carbon ratios (1.20, 1.00) among the series **1**–**5**.

Table 3 lists selected energetic materials properties for TNT, TATP, and $Pb(N_3)_2$, to provide comparisons for **1**–**5**. TNT is classified as a relatively insensitive secondary explosive, TATP is a very sensitive primary explosive, and $Pb(N_3)_2$ is a widely used primary explosive.[1b] Typical sensitivity values for primary explosives are ≤ 4 J (impact), ≤ 10 N (friction), and 0.002–0.20 J (ESD), whereas the related values for secondary explosives are ≥ 4 J (impact), ≥ 50 N (friction), and ≥ 0.1 J (ESD).[1b] The impact sensitivities of **1a**, **1b**, **2a**, **2b**, **3a**, **4a**, **4b**, and **5a** are ≤ 2 J, which are in the range of the value for highly sensitive TATP (the lowest value of our drophammer is 1 J). The impact sensitivities of **3b** and **5b** are both 3 J, which makes them slightly less sensitive than the others and similar to the value for the widely used primary explosive $Pb(N_3)_2$. Compounds **1a**, **1b**, **2a**, **2b**, **3a**, **4a**, **4b**, and **5a** have friction sensitivities that are ≤ 6 N, which are within the typical range for primary explosives and are similar to the value for $Pb(N_3)_2$ (5 N is the lower limit for our friction sensitivity apparatus). By contrast, the friction sensitivity values for **3b** (14 N), **4b** (40 N), and **5b** (40 N) are in between those for typical primary and secondary explosives, but are still "very sensitive" according to the UN classifications. Among **1**–**5**, **3b** and **5b** stand out as having reduced impact and friction sensitivities. For comparison, our recently reported organic peroxides containing geminal hydroperoxy groups have impact and friction sensitivities of 1–3 J and ≤ 5 N, respectively, and were the first peroxides that exhibit safe primary explosive properties.[5] The related sensitivity values for **3b** and **5b** are similar to or better than the geminal hydroperoxy compounds. Thus, **3b** and **5b** have useful sensitivities for application as primary energetic materials. The thermal decomposition temperatures would need to be improved to > 150 °C for widescale practical use.

There are no clear structural features that account for the lower impact and friction sensitivities of **3b** and **5b**, compared to the others. The calculated lattice energies of **5a** and **5b** are nearly identical, and are dominated by O–H···O hydrogen bonds. Less sensitive **3b** and **5b** each contain an unsubstituted central ring carbon atom, compared to alkyl substitution in more sensitive **2** and **4**. The lower alkyl content in **3b** and **5b** may afford more efficient packing by reducing steric bulk around the oxygen atoms, thereby decreasing the sensitivities slightly by leaving less room for motion of the weak O–O bonds in the crystal. Alkyl substitution on the central ring carbon atom may lead to increased ring strain, which may weaken the ring O–O bond slightly and thus increase sensitivity. Moreover, **1a**–**5a** each contain three peroxide groups per molecule, while **1b**–**5b** contain only two peroxide groups per molecule. Hence, the probability of breaking a weak O–O bond is higher in **1a**–**5a**, compared to the corresponding **1b**–**5b** analogs, thereby making **1a**–**5a** more sensitive toward stimuli. Desite the lower oxygen contents in **2b**–**5b**, the calculated detonation velocities are only 3.6–9.2 % lower than the **2a**–**5a** analogs and **5b** is only 3.6 % lower than **5a**. Thus, the decreased sensitivity in **5b**, relative to **5a**, is only associated with a small decrease in the detonation velocity.

Table 3. Selected sensitivities and energetic performance for TNT, TATP, and $Pb(N_3)_2$.

	TNT[a]	TATP[b]	$Pb(N_3)_2$[c]
IS [J]	15	0.3	2.5–4
FS [N]	353	0.1	< 1
ESD [J]	0.57	0.16	0.005
Ω_{CO2} [%]	–73.96	–151.2	
T_{Dec} [°C]	240	150–160	
ϱ [g/cm^3]	1.704, 1.713	1.25	
$\Delta_f H°$ [kJ/mol]	–70.6	–631.4	
P_{CJ} [kbar]	190	108	343
V_{Det} [m/s]	6900	6315	4600–5100
V_o [L/kg]	825	916	

[a] Data are taken from ref.[5] [b] Data taken from ref.[7] [c] Data taken from ref.[1b]

Conclusions

The cyclic peroxide compounds **1**–**5** were synthesized in 15–62 % yields by simple synthetic methods entailing treatment of γ- or β-diketones with concentrated aqueous H_2O_2 using the catalysts I_2, H_2SO_4, or $SnCl_2{\cdot}2H_2O$. Compounds **3a** and **5a** were obtained as pure compounds upon crystallization, whereas the others were obtained as mixtures (**1a**/**1b**, **2a**/**2b**, **3a**/**3b**, **4a**/**4b**, **5a**/**5b**) that were easily separated by column chromatography. All compounds except for **1b** were characterized by X-ray crystallography. The solid-state structures are dominated by hydrogen bonding involving the OOH and OH groups. The solid state densities range from 1.328 to 1.474 g cm^{-3}, which are high for organic peroxides. Compounds **1a**, **1b**, **2a**, **2b**, **3a**, **4a**, **4b**, and **5a** are very sensitive toward impact (≤ 2 J) and friction (≤ 6 N) and should thus be treated as primary explosives. By contrast, **3b** and **5b** are less sensitive than the others, with impact sensitivities of 3 J and friction sensitivities of 14 and 40 N, respectively. Compounds **5a** and **5b** were studied by NCI to probe solid state interactions that could explain their differing sensitivities. Surprisingly, calculated stabilization energies for **5a** and **5b** are identical, suggesting that solid state interactions alone cannot explain the sensitivity differences. The lower sensitivities of **3b** and **5b** are proposed to arise from their lower ring alkyl substitution and concomitant tighter packing of the peroxy groups, as well as the presence of three peroxy groups in

1a–**5a**, compared to two peroxy groups in **1b**–**5b**. Compounds **3b** and **5b** have useful sensitivity values for application as primary explosives, although their decomposition temperatures (95, 133 °C) are likely too low for widespread practical applications. The present study greatly increases the number of organic peroxides whose detailed energetic properties are described.[1–3,5–7]

Experimental Section

Experimental Details: The syntheses of **1**–**5** were carried at room temperature under ambient atmosphere in appropriately sized round-bottomed flasks. Chemicals were purchased from Sigma–Aldrich, Acros Organics, EMD, or Alfa Aesar and were used without further purification. ACS grade solvents were obtained from EMD and Fisher Scientific. The synthesis of **5a**[10] was carried out using a modified published procedure. Silica gel 60, 230–400 mesh (EMD Chemicals) was used to perform silica gel column chromatography. ASTM TLC plates precoated with silica gel 60 F_{254} (250 μm layer thickness) were used for thin-layer chromatography (TLC). TLC spots were observed using a UV lamp and/or a potassium permanganate solution as a stain (3 g of $KMnO_4$, 20 g of K_2CO_3, 5 mL of 5 % w/v aqueous NaOH, 300 mL of H_2O). The spots on the stained TLC plates were visualized after heating with a heat gun. ^1H and $^{13}C\{^1H\}$ NMR spectra were obtained at 400 MHz and 101 MHz, respectively, in CD_3OD as indicated and were referenced to the residual proton and carbon resonances of the solvent (^1H δ = 3.31 ppm, ^{13}C δ = 49.00 ppm). Mass spectra were obtained on an electrospray time-of-flight high-resolution Waters Micromass LCT Premier XE mass spectrometer. Infrared spectra were obtained from a Shimadzu MIRacle 10 IRAffinity-1 equipped with a single reflection ATR accessory. Melting points were determined on an Electrothermal IA 9300 melting point apparatus and are uncorrected. The decomposition characteristics were studied by TGA and DTA, which were carried out with a SDT-2960 TGA/DTA instrument. Decomposition points were determined on an OZM Research DTA 552 Ex instrument.

CAUTION! The organic peroxides **1**–**5** are sensitive and highly explosive and require handling with extreme care. The H_2O_2 solutions are strong oxidizers that may cause explosions. Reactions and manipulations should be run in fume hoods behind blast shields. Personal safety gear should include a face shield, leather gloves, a leather apron, hearing protection, and plastic spatulas. Peroxide compounds should not come into contact with strong acids, metal salts, or easily oxidized species. All reactions should be run at or below room temperature and performed on small scales.

Computational Methods: Intermolecular interactions between compounds **5a** and **5b** and all neighbors within 4 Å of the central molecule were calculated. Symmetry adapted perturbation theory (SAPT)[18,19] was employed to calculate intermolecular interactions of the compound-neighbor pairs at the SAPT2+3/6-31++G(d,p) level of theory. The total lattice stabilization energy was estimated by the sum of the pairwise energies,

$$E_{x,lat} = {}^1/_2\Sigma E_{x,j},$$

where $E_{x,lat}$ is the total lattice stabilization energy of compound *x*, and $E_{x,j}$ is the intermolecular interaction energy of structure *x* with neighbor *j*. In addition to the lattice energies, NCI surfaces were generated using the crystal structures for compounds **5a** and **5b** and all nearest neighbors within 4 Å. Each surface was created using the NCIPLOT software package,[13] with an isovalue of 0.3 and a reduced density cutoff of 0.07 a.u. Due to the large size of the system, precalculated atomic densities were used to represent the total molecular electron density. The NCI surfaces were then post-processed (see supporting information) to display only surfaces that are due to the attractive intermolecular interactions.

3,6-Dihydroperoxy-3,6-dimethyl-1,2-dioxane (1a): To a solution of I_2 (0.102 g, 0.400 mmol) in CH_3CN (5 mL) was added a 50 wt.-% aqueous solution of H_2O_2 (1.4 mL, 24 mmol) and 2,5-hexanedione (0.24 mL, 2.0 mmol). The resultant mixture was stirred for 24 h at ambient temperature. The solvent and volatile components were removed under reduced pressure, and the resultant residue was dissolved in methanol (10 mL). Storage of this solution at –29 °C for 24 h led to crystallization, and afforded **1a** (0.225 g, 62 %) as thick, colorless plates after decanting of the methanol solvent and brief vacuum drying, m.p. 128–130 °C (lit[10] 131 °C). ^1H NMR (CD_3OD, 23 °C): δ = OO*H* resonance not observed due to exchange with CD_3OD, 1.89–1.77 (m, 2 H), 1.60–1.47 (m, 2 H), 1.38 (s, 6 H, *CH*$_3$) ppm. $^{13}C\{^1H\}$ NMR (CD_3OD, 23 °C): δ = 109.29 (*C*), 27.97 (*CH*$_2$), 19.05 (*CH*$_3$) ppm. IR: $\tilde{\nu}$ = 3332 (broad, m), 3300 (broad, m), 3277 (broad, m), 3246 (broad, m), 2999 (w), 2947 (w), 1439 (m), 1377 (s), 1344 (m), 1272 (m), 1250 (w), 1157 (m), 1120 (s), 1062 (s), 1022 (w), 960 (w), 924 (w), 893 (w), 862 (s), 761 (w) cm^{-1}. $C_6H_{12}O_6$ (180.16): calcd. C 40.00, H 6.71; found C 40.35, H 6.76. TGA/DTA decomposition onset/max: 124/126 °C.

6-Hydroperoxy-3,6-dimethyl-1,2-dioxan-3-ol (1b): To a stirred solution of 2,5-hexanedione (0.24 mL, 2.0 mmol) in CH_3CN (10 mL) was added $SnCl_2{\cdot}2H_2O$ (0.090 g, 0.400 mmol) at ambient temperature. Then, a 50 wt.-% aqueous solution of H_2O_2 (0.6 mL, 10 mmol) was added and the mixture was stirred at ambient temperature for 18 h. At this point, distilled water (30 mL) was added and the aqueous phase was extracted with three 20 mL portions of ethyl acetate. The combined organic layers were dried with anhydrous magnesium sulfate, filtered through a fluted filter paper, and then the resulting solution was concentrated under reduced pressure. The residue was subjected to silica gel column chromatography with 4:1 dichloromethane/ethyl acetate to afford **1b** (R_f = 0.25, 0.048 g, 15 %) as a colorless oil. ^1H NMR (CD_3OD, 23 °C): δ = OO*H* and O*H* resonances not observed due to exchange with CD_3OD, 1.80–1.96 (m, 2 H), 1.61–1.78 (m, 1 H), 1.44–1.60 (m, 1 H), 1.40 (s, 3 H, *CH*$_3$), 1.30 (s, 3 H, *CH*$_3$) ppm. $^{13}C\{^1H\}$ NMR (CD_3OD, 23 °C): δ = 107.21 [*C*(OOH)], 100.04 [*C*(OH)], 30.02 (*CH*$_2$), 26.99 (*CH*$_2$), 22.52 (*CH*$_3$), 18.08 (*CH*$_3$) ppm. IR: $\tilde{\nu}$ = 3399 (broad, m), 2992 (w), 2972 (w), 2943 (w), 2870 (w), 1703 (w), 1634 (w), 1449 (m), 1400 (m), 1377 (m), 1337 (m), 1256 (m), 1231 (m), 1167 (m), 1148 (m), 1115 (s), 1070 (s), 1024 (w), 964 (m), 943 (m), 881 (w), 849 (s), 766 (w), 743 (w) cm^{-1}. $C_6H_{12}O_5$ (164.16): calcd. C 43.90, H 7.37; found C 43.60, H 7.35. TGA/DTA decomposition onset/max: 131/134 °C.

3,5-Dihydroperoxy-3,4,4,5-tetramethyl-1,2-dioxolane (2a): A solution of I_2 (0.103 g, 0.400 mmol) in CH_3CN (10 mL) was treated with a 50 wt.-% aqueous solution of H_2O_2 (0.7 mL, 12 mmol), followed by 3,3-dimethylpentane-2,4-dione (0.26 mL, 2 mmol). The mixture was then stirred at ambient temperature for 5 h. At this point, the solution was concentrated under reduced pressure, and the residue was dissolved in dichloromethane (10 mL). The resulting solution was filtered through a pad of anhydrous Na_2SO_4 to remove water. The dichloromethane solution was again concentrated and the product was purified by silica gel column chromatography with 9:1 dichloromethane/ethyl acetate, followed by 4:1 dichloromethane/ethyl acetate, to afford **2a** (R_f = 0.20 in 9:1 dichloromethane/ethyl acetate, R_f = 0.30 in 4:1 dichloromethane/ethyl acetate, 0.129 g, 33 %) as a white solid. Colorless polygons of **2a** were grown by slow evaporation of a diethyl ether solution. Crystals of **2a** exploded at 84 °C in the capillary tube upon attempting to measure the mp. ^1H NMR (CD_3OD, 23 °C): δ = OO*H* resonance not observed due to

exchange with CD_3OD, 1.45 (s, 6 H, CH_3), 1.16 (s, 3 H, CH_3), 1.01 (s, 3 H, CH_3) ppm. $^{13}C\{^1H\}$ NMR (CD_3OD, 23 °C): δ = 113.62 [*C*(OOH)], 60.69 (*C*), 24.06 (CH_3), 15.99 (CH_3), 15.33 (CH_3) ppm. IR: $\tilde{\nu}$ = 3414 (broad, m), 3011 (w), 2956 (w), 2523 (m), 1456 (m), 1396 (m), 1377 (m), 1267 (w), 1221 (w), 1142 (m), 1098 (s), 1043 (w), 951 (w), 925 (w), 887 (s), 849 (m), 798 (w), 732 (w) cm^{-1}. $C_7H_{14}O_6$ (194.18): calcd. C 43.30, H 7.27; found C 42.99, H 7.10. TGA/DTA decomposition onset/max: 64/65 °C.

5-Hydroperoxy-3,4,4,5-tetramethyl-1,2-dioxolan-3-ol (2b): To a solution of I_2 (0.102 g, 0.400 mmol) in CH_3CN (10 mL) was added a 50 wt.-% aqueous solution of H_2O_2 (0.7 mL, 12 mmol), followed by 3,3-dimethylpentane-2,4-dione (0.26 mL, 2.0 mmol). The mixture was then stirred at ambient temperature for 5 h. At this point, the solution was concentrated under reduced pressure, and the residue was dissolved in dichloromethane (10 mL). The resulting solution was filtered through a pad of anhydrous Na_2SO_4 to remove water. The decanted dichloromethane solution was again concentrated and the product was purified by silica gel column chromatography with 9:1 dichloromethane/ethyl acetate to afford **2b** (R_f = 0.50), (0.111 g, 31 %) as a white solid. Colorless polygons of **2b** were obtained from 2:1 dichloromethane/methanol at –29 °C: m.p. 79–81 °C. ^1H NMR (CD_3OD, 23 °C): δ = OO*H* and O*H* resonances not observed due to exchange with CD_3OD, 1.48 (s, 3 H, CH_3), 1.31 (s, 3 H, CH_3), 1.11 (s, 3 H, CH_3), 1.09 (s, 3 H, CH_3) ppm. ^{13}C NMR (CD_3OD, 23 °C): δ = 114.86 [*C*(OOH)], 108.05 [*C*(OH)], 59.73 (*C*), 23.41 (CH_3), 18.72 (CH_3), 16.94 (CH_3), 14.41 (CH_3) ppm. IR: $\tilde{\nu}$ = 3455 (m), 3260 (broad, m), 3005 (w), 2943 (w), 2874 (w), 2555 (w), 2419 (w), 1454 (m), 1396 (m), 1375 (m), 1279 (w), 1253 (w), 1213 (m), 1140 (s), 1115 (s), 1098 (s), 1063 (m), 943 (m), 916 (m), 880 (s), 851 (m), 810 (w), 791 (w), 734 (w) cm^{-1}. $C_7H_{14}O_5$ (178.18): calcd. C 47.19, H 7.92; found C 47.20, H 7.93. TGA/DTA decomposition onset/max: 67/68 °C.

3,5-Diethyl-3,5-dihydroperoxy-1,2-dioxolane (3a): To a 50 wt.-% aqueous solution of H_2O_2 (1.20 mL, 19.2 mmol) was added concentrated H_2SO_4 (0.038 g, 0.400 mmol), followed by heptane-3,5-dione (0.41 mL, 3.0 mmol) in a dropwise fashion at 0 °C. The mixture was then stirred for 1 h at 0 °C. The reaction solution was then concentrated under reduced pressure to afford a crude white solid. This solid was crystallized by slow evaporation of a diethyl ether solution to afford **3a** (0.290 g, 50 %) as colorless, thick needle-like crystals: m.p. 118–120 °C. ^1H NMR (CD_3OD, 23 °C): δ = OO*H* resonance not observed due to exchange with CD_3OD, 2.49 (s, 2 H), 1.96–2.10 (m, 2 H), 1.62–1.75 (m, 2 H), 0.99 (t, 6 H, J = 7.6 Hz, CH_3) ppm. ^{13}C NMR (CD_3OD, 23 °C): δ = 115.61 (*C*), 48.43 (ring CH_2), 24.92 (CH_2), 9.26 (CH_3) ppm. IR: $\tilde{\nu}$ = 3377 (m, broad), 2982 (w), 2947 (w), 2885 (w), 2511 (w), 1462 (m), 1443 (w), 1425 (w), 1383 (w), 1341 (m), 1321 (m), 1275 (w), 1219 (m), 1159 (s), 1121 (m), 1084 (m), 1020 (m), 1003 (m), 984 (w), 953 (s), 895 (w), 876 (w), 847 (w), 826 (w), 787 (s), 736 (w) cm^{-1}. $C_7H_{14}O_6$ (194.18): calcd. C 43.30, H 7.27; found C 43.40, H 7.37. TGA/DTA decomposition onset/max: 129/132 °C.

3,5-Diethyl-5-hydroperoxy-1,2-dioxolan-3-ol (3b): To a stirred solution of I_2 (0.103 g, 0.400 mmol) in CH_3CN (10 mL) was added a 50 wt.-% aqueous solution of H_2O_2 (0.7 mL, 12 mmol) at ambient temperature. To this solution was added heptane-3,5-dione (0.26 mL, 1.9 mmol) and the mixture was stirred at ambient temperature for 5 h. At this point, the solution was concentrated under reduced pressure, and the residue was dissolved in dichloromethane (10 mL). The resulting solution was filtered through a pad of anhydrous Na_2SO_4 to remove water. The decanted dichloromethane solution was again concentrated and the product was purified by silica gel column chromatography with dichloromethane followed by 4:1 dichloromethane/ethyl acetate to afford **3b** (R_f = 0.45, 0.126 g, 35 %) as a white solid. Colorless plate-like crystals were obtained by slow evaporation from a 10:1 mixture of toluene/diethyl ether, m.p. 79–81 °C. ^1H NMR (CD_3OD, 23 °C): δ = OO*H* and O*H* resonances not observed due to exchange with CD_3OD, 2.47 (q, 2 H, J = 10.0 Hz, CH_2), 2.05–2.17 (s, 1 H), 1.66–1.81 (m, 3 H), 1.00 (t, 6 H, J = 7.6 Hz, CH_3) ppm. ^{13}C NMR (CD_3OD, 23 °C): δ = 115.93 [*C*(OOH)], 108.57 [*C*(OH)], 51.79 (CH_2), 30.07 (CH_2), 25.17 (CH_2), 9.40 (CH_3), 9.35 (CH_3) ppm. IR: $\tilde{\nu}$ = 3410 (broad, m), 3333 (broad, m), 2982 (m), 2947 (w), 2887 (w), 2797 (w), 2359 (s), 2160 (w), 2023 (w), 1973 (w), 1742 (w), 1690 (m), 1647 (w), 1551 (m), 1526 (m), 1458 (m), 1406 (m), 1306 (m), 1260 (m), 1213 (w), 1163 (m), 1113 (m), 1072 (m), 1018 (m), 934 (m), 899 (m), 851 (m), 800 (m), 718 (m) cm^{-1}. $C_7H_{14}O_5$ (178.18): calcd. C 47.19, H 7.92; found C 46.98, H 7.89. TGA/DTA decomposition onset/max: 95/98 °C.

3,5-Dihydroperoxy-3,4,5-trimethyl-1,2-dioxolane (4a): To a stirred solution of I_2 (0.103 g, 0.400 mmol) in CH_3CN (10 mL) was added a 50 wt.-% aqueous solution of H_2O_2 (0.7 mL, 12 mmol) at ambient temperature. To this solution was added 3-methyl-2,4-pentanedione (0.23 mL, 2.0 mmol) and the mixture was stirred at ambient temperature for 5 h. At this point, the reaction mixture was concentrated under reduced pressure and was dissolved in dichloromethane (10 mL). The resulting solution was filtered through a pad of anhydrous Na_2SO_4 to remove water. The dichloromethane solution was again concentrated under reduced pressure and the crude product mixture was purified by silica gel column chromatography with 9:1 dichloromethane/ethyl acetate to obtain **4a** (R_f = 0.20, 0.083 g, 23 %) as a white solid. Colorless polygons of **4a** were obtained at –29 °C from a 2:1 mixture of toluene/dichloromethane, m.p. 59–61 °C. ^1H NMR (CD_3OD, 23 °C): δ = OO*H* resonance not observed due to exchange with CD_3OD, 2.70 (q, 1 H, J = 8.0 Hz, *CH*), 1.50 (s, 3 H, CH_3), 1.39 (s, 3 H, CH_3), 1.06 (d, 6 H, J = 8.0 Hz, CH_3) ppm. ^{13}C NMR (CD_3OD, 23 °C): δ = 114.86 (*C*), 113.00 (*C*), 57.08 (*CH*), 16.69 (CH_3), 16.14 (CH_3), 9.18 (CH_3) ppm. IR: $\tilde{\nu}$ = 3410 (broad, m), 3364 (broad, m), 2999 (w), 2945 (w), 1713 (w), 1628 (w), 1464 (m), 1439 (m), 1377 (s), 1337 (m), 1263 (w), 1229 (w), 1165 (s), 1124 (m), 1086 (s), 1047 (m), 1009 (m), 947 (w), 874 (s), 802 (m), 754 (w) cm^{-1}. $C_6H_{12}O_6$ (180.16): calcd. C 40.00, H 6.71; found C 39.68, H 6.63. TGA/DTA decomposition onset/max: 96/98 °C.

5-Hydroperoxy-3,4,5-trimethyl-1,2-dioxolan-3-ol (4b): The crude product from the synthesis of **4a** was further eluted with 4:1 dichloromethane/ethyl acetate to afford **4b** (R_f = 0.2, 0.140 g, 43 %) as a white solid. Colorless hexagons of **4b** were obtained at –29 °C from a 5:1 mixture of toluene/diethyl ether: m.p. 71–73 °C. ^1H NMR (CD_3OD, 23 °C): δ = OO*H* and O*H* resonances not observed due to exchange with CD_3OD, 2.48 (q, 1 H, J = 7.6 Hz, *CH*), 1.42 (s, 3 H, CH_3), 1.41 (s, 3 H, CH_3), 1.06 (d, 6 H, J = 7.2 Hz, CH_3) ppm. ^{13}C NMR (CD_3OD, 23 °C): δ = 115.18 [*C*(OOH)], 107.01 [*C*(OH)], 57.02 (*CH*), 21.63 (CH_3), 16.09 (CH_3), 10.24 (CH_3) ppm. IR: $\tilde{\nu}$ = 3445 (broad, m), 3296 (broad, m), 2995 (w), 2947 (w), 2888 (w), 1649 (w), 1622 (w), 1558 (m), 1510 (w), 1467 (m), 1383 (s), 1342 (w), 1290 (w), 1263 (w), 1209 (m), 1171 (s), 1124 (s), 1084 (s), 1011 (m), 949 (s), 854 (s), 797 (m), 758 (m) cm^{-1}. $C_6H_{12}O_5$ (164.16): calcd. C 43.90, H 7.37; found C 43.71, H 7.45. TGA/DTA decomposition onset/max: 82/87 °C.

3,5-Dihydroperoxy-3,5-dimethyl-1,2-dioxolane (5a): A 50 mL round bottomed flask was cooled to 0 °C and was charged with a magnetic stir bar, a 50 wt.-% aqueous solution of H_2O_2 (0.6 mL, 9.6 mmol), and concentrated H_2SO_4 (0.019 g, 0.194 mmol). To this solution was added 2,4-pentanedione (0.32 mL, 3.1 mmol) in a dropwise fashion. The mixture was then stirred for 1 h at 0 °C and was kept in a refrigerator (2–8 °C) for 18 h. Then, the reaction mixture was added to a separatory funnel, and was extracted with three 5 mL portions of diethyl ether. The separated diethyl ether mixture was dried with anhydrous magnesium sulfate, filtered

through a Whatman No. 1 filter paper, and the diethyl ether was removed under reduced pressure to afford 0.295 g of a white solid. Crystallization of this crude solid from a 20:1 dichloromethane/ethyl acetate mixture afforded **5a** as colorless polygons (0.209 g, 42 %), m.p. 98–100 °C (lit[9b] 98–100 °C). ^{1}H NMR (CD_3OD, 23 °C): δ = OO*H* resonance not observed due to exchange with CD_3OD, 2.61 (s, 2 H, CH_2), 1.52 (s, 6 H, CH_3) ppm. $^{13}C\{^1H\}$ NMR (CD_3OD, 23 °C): δ = 113.42 (*C*), 52.69 (CH_2), 18.14 (CH_3) ppm. IR: $\tilde{\nu}$ = 3362 (m, broad), 3003 (w), 2953 (w), 1431 (m), 1379 (m), 1329 (m), 1225 (m), 1167 (s), 1088 (m), 1028 (w), 953 (w), 920 (w), 889 (w), 849 (m), 820 (w), 789 (m), 750 (w) cm^{-1}. $C_5H_{10}O_6$ (166.13): calcd. C 36.15, H 6.07; found C 36.07, H 5.98. TGA/DTA decomposition onset/max: 118/121 °C.

5-Hydroperoxy-3,5-dimethyl-1,2-dioxolan-3-ol (5b): To a stirred solution of 2,4-pentanedione (0.21 mL, 2.0 mmol) in CH_3CN (10 mL) was added $SnCl_2{\cdot}2H_2O$ (0.090 g, 0.400 mmol) at room temperature. Then, a 50 wt.-% aqueous solution of H_2O_2 (0.6 mL, 10 mmol) was added and the mixture was stirred at ambient temperature for 24 h. At this point, distilled water (30 mL) was added to the reaction mixture and the products were extracted with two 20 mL portions of ethyl acetate. The separated organic layer was dried with anhydrous $MgSO_4$, filtered through a fluted filter paper, and was concentrated under reduced pressure. The product was purified by silica gel column chromatography with 4:1 dichloromethane/ethyl acetate to afford **5b** (R_f = 0.30, 0.137 g, 46 %) as a white solid. Colorless polygons of **5b** were grown by slow evaporation of a diethyl ether solution, m.p. 112–114 °C (lit[11b] 110–112 °C). ^{1}H NMR (CD_3OD, 23 °C): δ = OO*H* and O*H* resonances not observed due to exchange with CD_3OD, 2.58 (s, 2 H, CH_2), 1.58 (s, 3 H, CH_3), 1.47 (s, 3 H, CH_3) ppm. ^{13}C NMR (CD_3OD, 23 °C): δ = 113.69 [*C*(OOH)], 106.53 [*C*(OH)], 56.11 (CH_2), 22.80 (CH_3), 18.54 (CH_3) ppm. IR: $\tilde{\nu}$ = 3439 (broad, m), 3260 (broad, m), 3005 (w), 2956 (w), 2835 (s), 1439 (m), 1381 (m), 1331 (m), 1308 (m), 1217 (m), 1173 (s), 1078 (m), 1057 (m), 959 (m), 918 (w), 883 (w), 845 (s), 808 (s), 799 (s) cm^{-1}. $C_5H_{10}O_5$ (150.13): calcd. C 40.00, H 6.71; found C 40.35, H 6.66. TGA/DTA decomposition onset/max: 133/147 °C.

X-ray Crystal Structure Determinations of 1a and 2–5: Single crystals were grown as described in the experimental procedures. CCDC 1487198–1487206. CCDC 1487198 (for **1a**), 1487199 (for **2a**), 1487200 (for **2b**), 1487201 (for **3a**), 1487202 (for **3b**), 1487203 (for **4a**), 1487204 (for **4b**), 1487205 (for **5a**), and 1487206 (for **5b**) contain the supplementary crystallographic data for this paper. These data can be obtained free of charge from The Cambridge Crystallographic Data Centre.

Acknowledgments

The authors acknowledge generous support from the US Office of Naval Research (grant N00014-12-1-0526 to C. H. W., grant N00014-16-1-2062 to T. M. K.). Financial support of this work by the Ludwig Maximilians University of Munich (grants to T. M. K.) is also gratefully acknowledged. E. G. K. and G. A. C. thank the Wayne State University for computing time and partial financial support.

Keywords: Energetic materials · Peroxides · Structure elucidation · Sensitivities

[1] a) T. M. Klapötke, T. Wloka, *Peroxide Explosives*, in: *Patai's Chemistry of Functional Groups*, **2014**, 1–28; b) T. M. Klapötke, *Chemistry of High-Energy Materials*, de Gruyter, Berlin/Boston, 3rd ed., **2015**; c) J. J. Sabatini, K. D. Oyler, *Crystals* **2016**, *6*, 5; DOI: 10.3390/cryst6010005.
[2] a) J. C. Oxley, J. L. Smith, H. Chen, *Propellants Explos. Pyrotech.* **2002**, *27*, 209–216; b) F. Dubnikova, R. Kosloff, J. Almog, Y. Zeiri, R. Boese, H. Itzhaky, A. Alt, E. Keinan, *J. Am. Chem. Soc.* **2005**, *127*, 1146–1159; c) C. Denekamp, L. Gottlieb, T. Tamiri, A. Tsoglin, R. Shilav, M. Kapon, *Org. Lett.* **2005**, *7*, 2461–2464; d) O. Reany, M. Kapon, M. Botoshansky, E. Keinan, *Cryst. Growth Des.* **2009**, *9*, 3661–3670; e) R. Matyáš, J. Šelešovský, *J. Hazard. Mater.* **2009**, *165*, 95–99; f) A. E. Contini, A. J. Bellamy, L. N. Ahad, *Propellants Explos. Pyrotech.* **2012**, *37*, 320–328; g) G. R. Peterson, W. P. Bassett, B. L. Weeks, L. J. Hope-Weeks, *Cryst. Growth Des.* **2013**, *13*, 2307–2311; h) V. P. Sinditskii, V. I. Kolesov, V. Y. Egorshev, D. I. Patrikeev, O. V. Dorofeeva, *Thermochim. Acta* **2014**, *585*, 10–15.
[3] J. C. Oxley, J. L. Smith, H. Chen, E. Cioffi, *Thermochim. Acta* **2002**, *388*, 215–225.
[4] a) A. Baumann, A. Erbacher, C. Evangelisti, T. M. Klapötke, B. Krumm, S. F. Rest, M. Reynders, V. Sproll, *Chem. Eur. J.* **2013**, *19*, 15627–15638; b) T. M. Klapötke, B. Krumm, S. F. Rest, M. Reynders, R. Scharf, *Eur. J. Inorg. Chem.* **2013**, 5871–5878.
[5] N.-D. H. Gamage, B. Stiasny, J. Stierstorfer, P. D. Martin, T. M. Klapötke, C. H. Winter, *Chem. Commun.* **2015**, *51*, 13298–13300.
[6] N.-D. H. Gamage, B. Stiasny, J. Stierstorfer, P. D. Martin, T. M. Klapötke, C. H. Winter, *Chem. Eur. J.* **2016**, *22*, 2582–2585.
[7] T. M. Klapötke, B. Stiasny, J. Stierstorfer, C. H. Winter, *Eur. J. Org. Chem.* **2015**, 6237–6242.
[8] a) N. L. Jorge, J. M. Romero, A. Grand, A. Hernandez-Laguna, *Chem. Phys.* **2012**, *393*, 37–45; b) F. Wang, H. Sun, J. Sun, X. Jia, Y. Zhang, Y. Tang, X. Pan, Z. Su, L. Hao, R. Wang, *J. Phys. Chem. A* **2010**, *114*, 3516–3522; c) H.-J. Hamann, A. Bunge, J. Liebscher, *Chem. Eur. J.* **2008**, *14*, 6849–6851.
[9] a) K. Žmitek, M. Zupan, S. Stavber, J. Iskra, *J. Org. Chem.* **2007**, *72*, 6534–6540; b) D. Azarifar, K. Khosravi, *Eur. J. Chem.* **2010**, *1*, 15–19.
[10] N. A. Milas, A. Golubovic, *J. Org. Chem.* **1962**, *27*, 4319–4323.
[11] a) N. A. Milas, O. L. Mageli, A. Golubović, R. W. Arndt, J. C. J. Ho, *J. Am. Chem. Soc.* **1963**, *85*, 222–226; b) A. Rieche, C. Bischoff, *Chem. Ber.* **1962**, *95*, 77–82.
[12] M. Mantina, A. C. Chamberlain, R. Valero, C. J. Cramer, D. G. Truhlar, *J. Phys. Chem. A* **2009**, *113*, 5806–5812.
[13] J. Contreras-García, E. R. Johnson, S. Keinan, R. Chaudret, J. P. Piquemal, D. N. Beratan, W. Yang, *J. Chem. Theory Comput.* **2011**, *7*, 625–632.
[14] M. J. Frisch, G. W. Trucks, H. B. Schlegel, G. E. Scuseria, M. A. Robb, J. R. Cheeseman, G. Scalmani, V. Barone, B. Mennucci, G. A. Petersson, H. Nakatsuji, M. Caricato, X. Li, H. P. Hratchian, A. F. Izmaylov, J. Bloino, G. Zheng, J. L. Sonnenberg, M. Hada, M. Ehara, K. Toyota, R. Fukuda, J. Hasegawa, M. Ishida, T. Nakajima, Y. Honda, O. Kitao, H. Nakai, T. Vreven, J. A. Montgomery Jr., J. E. Peralta, F. Ogliaro, M. Bearpark, J. J. Heyd, E. Brothers, K. N. Kudin, V. N. Staroverov, R. Kobayashi, J. Normand, K. Raghavachari, A. Rendell, J. C. Burant, S. S. Iyengar, J. Tomasi, M. Cossi, N. Rega, J. M. Millam, M. Klene, J. E. Knox, J. B. Cross, V. Bakken, C. Adamo, J. Jaramillo, R. Gomperts, R. E. Stratmann, O. Yazyev, A. J. Austin, R. Cammi, C. Pomelli, J. W. Ochterski, R. L. Martin, K. Morokuma, V. G. Zakrzewski, G. A. Voth, P. Salvador, J. J. Dannenberg, S. Dapprich, A. D. Daniels, Ö. Farkas, J. B. Foresman, J. V. Ortiz, J. Cioslowski, D. J. Fox, *Gaussian 09*, revision A.1, Gaussian, Inc., Wallingford CT, **2009**.
[15] a) NATO Standardization Agreement (STANAG) on Explosives, *Impact Sensitivity Tests*, No. 4489, 1st ed., Sept. 17, **1999**; b) WIWEB-Standardarbeitsanweisung 4–5.1.02, *Ermittlung der Explosionsgefährlichkeit*, Nov. 8, **2002**; c) http://www.bam.de; d) NATO Standardization Agreement (STANAG) on Explosives, *Friction Sensitivity Tests*, No. 4487, 1st ed., Aug. 22, **2002**.
[16] a) *Test Methods According to the UN Manual of Tests and Criteria, Recommendations on the Transport of Dangerous Goods*, United Nations Publications, New York, Geneva, 4th revised ed., **2003**; b) www.reichel-partner.de.
[17] M. Sućeska, *EXPLO5*, v.6.02, Brodarski Institute, Zagreb, Croatia, **2014**.
[18] E. G. Hohenstein, C. D. Sherrill, *WIREs Comput. Mol. Sci.* **2012**, *2*, 304–326.
[19] T. M. Parker, L. A. Burns, R. M. Parrish, A. G. Ryno, C. D. Sherrill, *J. Chem. Phys.* **2014**, *140*, 094106.

Received: June 27, 2016
Published Online: ■

Energetic Materials

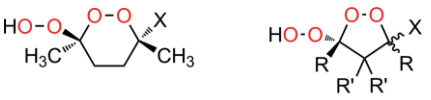

X = OOH or OH

Oxygen-rich 5- and six-membered cyclic peroxides have been prepared and fully characterized, including by X-ray crystallography, electronic structure calculations, and detailed energetic materials testing. Most compounds are highly sensitive toward impact and friction, but two compounds where X = OH have reduced sensitivities.

DOI: 10.1002/ejic.201600767

Eur. J. Inorg. Chem. **2016** · ISSN 1099–0682

SUPPORTING INFORMATION

DOI: 10.1002/ejic.201600767
Title: Energetic Materials Trends in 5- and 6-Membered Cyclic Peroxides Containing Hydroperoxy and Hydroxy Substituents
Author(s): Nipuni-Dhanesha H. Gamage, Benedikt Stiasny, Eric G. Kratz, Jörg Stierstorfer, Philip D. Martin, G. Andrés Cisneros, Thomas M. Klapötke,* Charles H. Winter*

Table S1. Intermolecular close contacts for **1a**.

Number	Atom1	Atom2	Symm. op. 1	Symm. op. 2	Length	Length-VdW
1	O1	O6	x,y,z	x,y,-1+z	2.726	-0.314
2	O1	H2	x,y,z	x,y,-1+z	1.954	-0.766
3	H1	H2	x,y,z	x,y,-1+z	2.340	-0.060
4	O4	H6A	x,y,z	1+y,1-x,-z	2.679	-0.041
5	H5	H5	x,y,z	1+y,1-x,1-z	2.387	-0.013
6	H6A	O6	x,y,z	1/2+y,1/2-x,1/2-z	2.570	-0.150
7	O1	O4	x,y,z	1.5-x,1/2-y,-1/2+z	2.877	-0.163
8	H1	O4	x,y,z	1.5-x,1/2-y,-1/2+z	2.535	-0.185
9	H1	O6	x,y,z	1.5-x,1/2-y,-1/2+z	2.076	-0.644
10	O3	O6	x,y,z	1.5-x,1/2-y,-1/2+z	3.022	-0.018
11	O4	O6	x,y,z	1.5-x,1/2-y,-1/2+z	2.940	-0.100
12	O4	H2	x,y,z	1.5-x,1/2-y,-1/2+z	2.706	-0.014

Table S2. Intermolecular close contacts for **2a**.

Number	Atom1	Atom2	Symm. op. 1	Symm. op. 2	Length	Length-VdW
1	O2	H3	x,y,z	2-x,-1/2+y,1/2-z	2.646	-0.074
2	H10	O4	x,y,z	-1/2+x,y,1/2-z	2.523	-0.197
3	O1	O12	x,y,z	1+x,y,z	2.856	-0.184
4	H1	O12	x,y,z	1+x,y,z	1.991	-0.729
5	O2	O10	x,y,z	1+x,y,z	2.873	-0.167
6	O2	H16	x,y,z	1+x,y,z	2.172	-0.548
7	O3	O10	x,y,z	1+x,y,z	2.867	-0.173
8	O3	H16	x,y,z	1+x,y,z	2.133	-0.587
9	O4	O8	x,y,z	1+x,y,z	2.875	-0.165
10	O4	O9	x,y,z	1+x,y,z	2.844	-0.196

11	H2	O8	x,y,z	1+x,y,z	2.213	-0.507
12	H2	O9	x,y,z	1+x,y,z	2.117	-0.603
13	H2	H16	x,y,z	1+x,y,z	2.388	-0.012
14	O6	O7	x,y,z	1+x,y,z	2.855	-0.185
15	O6	H15	x,y,z	1+x,y,z	2.017	-0.703
16	O5	H18	x,y,z	1/2+x,1.5-y,-z	2.628	-0.092
17	H11	O10	x,y,z	1-x,1/2+y,1/2-z	2.454	-0.266
18	O4	C13	x,y,z	1.5-x,1/2+y,z	3.169	-0.051
19	O4	H23	x,y,z	1.5-x,1/2+y,z	2.461	-0.259
20	O11	H18	x,y,z	-1/2+x,1.5-y,-z	2.659	-0.061
21	O12	H22	x,y,z	-x,1-y,-z	2.549	-0.171
22	H23	O8	x,y,z	1/2-x,-1/2+y,z	2.585	-0.135

Table S3. Intermolecular close contacts for **2b**.

Number	Atom1	Atom2	Symm. op. 1	Symm. op. 2	Length	Length-VdW
1	O3	H9	x,y,z	1/2-x,-1/2+y,1.5-z	2.606	-0.114
2	O1	H10	x,y,z	1.5-x,-1/2+y,1.5-z	2.615	-0.105
3	O1	O3	x,y,z	1-x,-y,2-z	2.746	-0.294
4	O1	H5	x,y,z	1-x,-y,2-z	2.710	-0.010
5	H1	O3	x,y,z	1-x,-y,2-z	1.885	-0.835
6	H1	H2	x,y,z	1-x,-y,2-z	2.398	-0.002
7	H1	C3	x,y,z	1-x,-y,2-z	2.733	-0.167
8	H1	H5	x,y,z	1-x,-y,2-z	2.356	-0.044
9	O4	H11	x,y,z	1-x,1-y,2-z	2.720	-0.000
10	O5	H11	x,y,z	1-x,1-y,2-z	2.599	-0.121
11	H6	O4	x,y,z	-1/2+x,1/2-y,-1/2+z	2.631	-0.089

Table S4. Intermolecular close contacts for **3a**.

Number	Atom1	Atom2	Symm. op. 1	Symm. op. 2	Length	Length-VdW

1	O4	H8	x,y,z	-1+x,y,z	2.711	-0.009
2	O6	C1	x,y,z	1-x,-y,-z	3.199	-0.021
3	O6	O2	x,y,z	-1/2+x,1/2-y,-1/2+z	2.788	-0.252
4	H4	O1	x,y,z	-1/2+x,1/2-y,-1/2+z	2.462	-0.258
5	H4	O2	x,y,z	-1/2+x,1/2-y,-1/2+z	1.919	-0.801
6	O1	O5	x,y,z	-1/2+x,1/2-y,1/2+z	2.783	-0.257
7	H3	O5	x,y,z	-1/2+x,1/2-y,1/2+z	1.932	-0.788
8	H3	O6	x,y,z	-1/2+x,1/2-y,1/2+z	2.413	-0.307

Table S5. Intermolecular close contacts for **3b**.

Number	Atom1	Atom2	Symm. op. 1	Symm. op. 2	Length	Length-VdW
1	O1	H9	x,y,z	1-x,-y,1-z	2.652	-0.068
2	O4	O5	x,y,z	2-x,-y,1-z	2.799	-0.241
3	O4	H3	x,y,z	2-x,-y,1-z	1.994	-0.726
4	O2	O5	x,y,z	1.5-x,-1/2+y,z	2.762	-0.278
5	H2	O5	x,y,z	1.5-x,-1/2+y,z	1.941	-0.779
6	O3	H8	x,y,z	1.5-x,-1/2+y,z	2.610	-0.110

Table S6. Intermolecular close contacts for **4a**.

Number	Atom1	Atom2	Symm. op. 1	Symm. op. 2	Length	Length-VdW
1	C4	O5	x,y,z	x,-1+y,z	3.188	-0.032
2	H3	O6	x,y,z	x,-1+y,z	2.656	-0.064
3	H5	O5	x,y,z	x,-1+y,z	2.683	-0.037
4	H11	O1	x,y,z	2-x,-1/2+y,1.5-z	2.610	-0.110
5	O4	H9	x,y,z	2-x,2-y,1-z	2.679	-0.041
6	O2	O1	x,y,z	1.5-x,-1/2+y,z	2.868	-0.172
7	O2	H1	x,y,z	1.5-x,-1/2+y,z	2.001	-0.719
8	C1	H1	x,y,z	1.5-x,-1/2+y,z	2.883	-0.017
9	H6	O6	x,y,z	1.5-x,-1/2+y,z	2.585	-0.135
10	H5	O2	x,y,z	1.5-x,-1/2+y,z	2.669	-0.051

11	O3	O4	x,y,z	2.5-x,-1/2+y,z	2.915	-0.125
12	O3	H2	x,y,z	2.5-x,-1/2+y,z	2.039	-0.681
13	O4	H2	x,y,z	2.5-x,-1/2+y,z	2.692	-0.028
14	H4	O3	x,y,z	2.5-x,-1/2+y,z	2.698	-0.022
15	H4	O5	x,y,z	2.5-x,-1/2+y,z	2.701	-0.019
16	O1	H10	x,y,z	-1/2+x,y,1.5-z	2.710	-0.010

Table S7. Intermolecular close contacts for **4b**.

Number	Atom1	Atom2	Symm. op. 1	Symm. op. 2	Length	Length-VdW
1	O2	O5	x,y,z	1.5-x,-1/2+y,1/2-z	2.722	-0.318
2	H2	O5	x,y,z	1.5-x,-1/2+y,1/2-z	1.875	-0.845
3	H2	H3	x,y,z	1.5-x,-1/2+y,1/2-z	2.394	-0.006
4	O3	H4	x,y,z	1.5-x,-1/2+y,1/2-z	2.696	-0.024
5	O2	H11	x,y,z	2-x,-y,-z	2.600	-0.120
6	C5	H8	x,y,z	2-x,1-y,-z	2.880	-0.020
7	H8	H8	x,y,z	2-x,1-y,-z	2.382	-0.018
8	O1	O5	x,y,z	-1/2+x,1/2-y,-1/2+z	2.837	-0.203
9	O1	H3	x,y,z	-1/2+x,1/2-y,-1/2+z	2.047	-0.673
10	O1	H7	x,y,z	-1/2+x,1/2-y,-1/2+z	2.708	-0.012
11	O1	H10	x,y,z	-1/2+x,1/2-y,-1/2+z	2.549	-0.171
12	O2	H7	x,y,z	-1/2+x,1/2-y,-1/2+z	2.661	-0.059
13	H9	O3	x,y,z	-1/2+x,1/2-y,-1/2+z	2.510	-0.210
14	H1	O2	x,y,z	-1/2+x,1/2-y,1/2+z	2.700	-0.020

Table S8. Intermolecular close contacts for **5a**.

Number	Atom1	Atom2	Symm. op. 1	Symm. op. 2	Length	Length-VdW
1	O1	O3	x,y,z	-1/2+x,1/2-y,-1/2+z	2.730	-0.310
2	H1	O3	x,y,z	-1/2+x,1/2-y,-1/2+z	1.752	-0.968
3	H1	O4	x,y,z	-1/2+x,1/2-y,-1/2+z	2.306	-0.414

4	H1	C3	x,y,z	-1/2+x,1/2-y,-1/2+z	2.900	-0.000
5	O4	O2	x,y,z	-1/2+x,1/2-y,1/2+z	2.727	-0.313
6	H2	O1	x,y,z	-1/2+x,1/2-y,1/2+z	2.285	-0.435
7	H2	O2	x,y,z	-1/2+x,1/2-y,1/2+z	1.707	-1.013
8	H2	C1	x,y,z	-1/2+x,1/2-y,1/2+z	2.825	-0.075

Table S9. Intermolecular close contacts for **5b**.

Number	Atom1	Atom2	Symm. op. 1	Symm. op. 2	Length	Length-VdW
1	O3	O1	x,y,z	1/2-x,-1/2+y,1/2-z	2.904	-0.136
2	H3	O1	x,y,z	1/2-x,-1/2+y,1/2-z	2.033	-0.687
3	O5	H10	x,y,z	1/2-x,-1/2+y,1/2-z	2.562	-0.158
4	H1	O1	x,y,z	1/2-x,-1/2+y,1/2-z	2.667	-0.053
5	H8	O2	x,y,z	1.5-x,-1/2+y,1/2-z	2.675	-0.045
6	O1	H7	x,y,z	1-x,2-y,-z	2.719	-0.001
7	O3	O2	x,y,z	-1/2+x,1.5-y,-1/2+z	2.733	-0.307
8	O3	H2	x,y,z	-1/2+x,1.5-y,-1/2+z	1.823	-0.897
9	H9	O4	x,y,z	-1/2+x,1.5-y,-1/2+z	2.636	-0.084
10	H9	O5	x,y,z	-1/2+x,1.5-y,-1/2+z	2.712	-0.008
11	C2	H2	x,y,z	-1/2+x,1.5-y,-1/2+z	2.875	-0.025
12	H5	H2	x,y,z	-1/2+x,1.5-y,-1/2+z	2.373	-0.027

Figure S1. Intermolecular close contacts in **1a**.

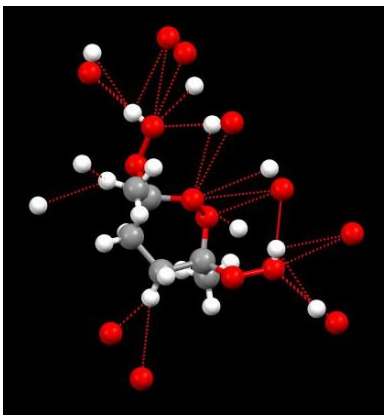

Figure S2. Intermolecular close contacts in **2a**.

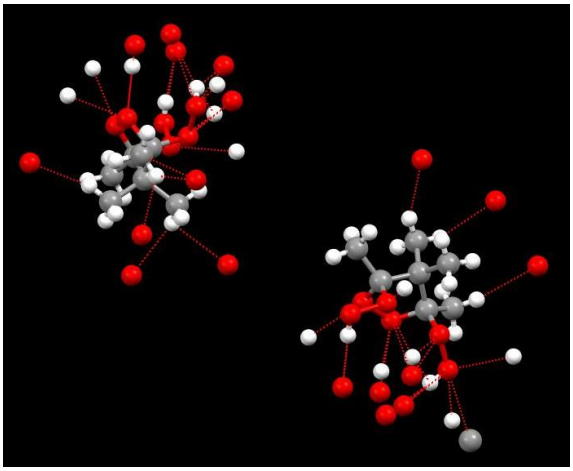

Figure S3. Intermolecular close contacts in **2b**.

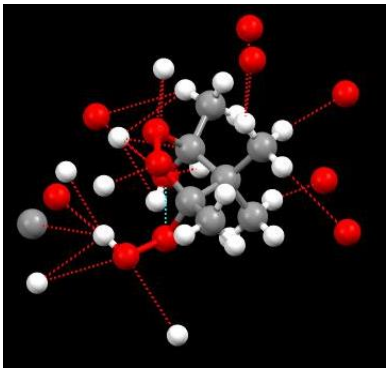

Figure S4. Intermolecular close contacts in **3a**.

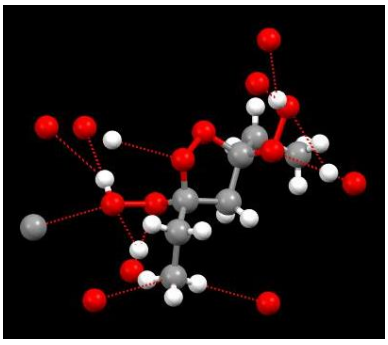

Figure S5. Intermolecular close contacts in **3b**.

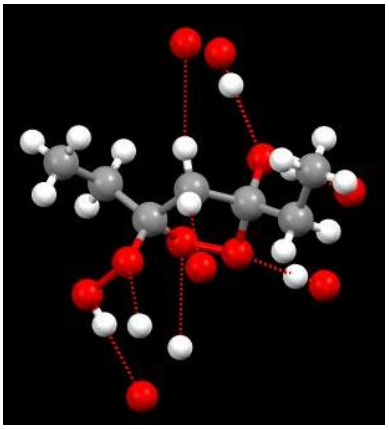

Figure S6. Intermolecular close contacts in **4a**.

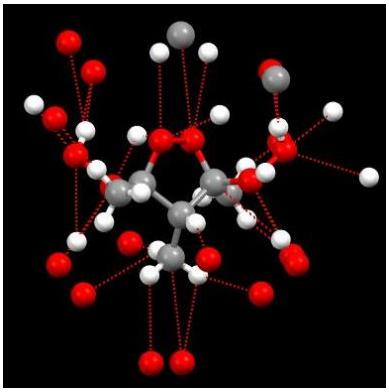

Figure S7. Intermolecular close contacts in **4b**.

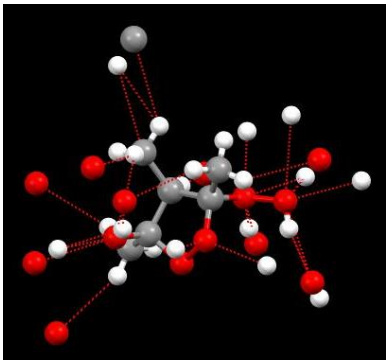

Figure S8. Intermolecular close contacts in **5a**.

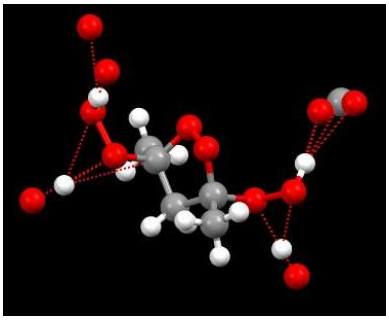

Figure S9. Intermolecular close contacts in **5b**.

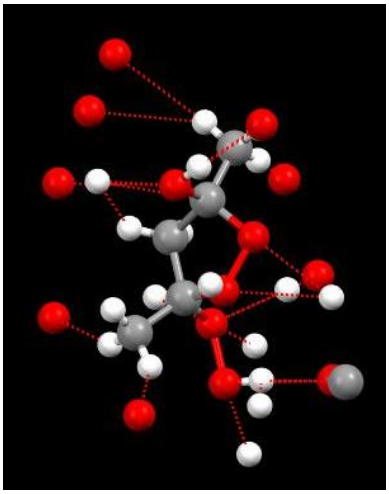

Details of the NCI Calculations

1. Non-covalent interaction analysis

An NCI analysis uses the curvature of the electron density to predict the strength and nature of the molecular interactions. The analysis produces a reduced density gradient, $\nabla\rho_r$,

$$\nabla\rho_r = \frac{|\nabla\rho|}{2(3\pi^2)^{1/3}\rho^{4/3}},$$

and a signed electron density, ρ',

$$\rho' = sign(\varepsilon_2)\rho,$$

where the sign used for an NCI analysis is determined from the second eigenvalue of the Hessian (ε_2) of the electron density,

$$\begin{bmatrix} x_1 & x_2 & x_3 \\ y_1 & y_2 & y_3 \\ z_1 & z_2 & z_3 \end{bmatrix}^{-1} \begin{bmatrix} \nabla_x\nabla_x\rho & \nabla_x\nabla_y\rho & \nabla_x\nabla_z\rho \\ \nabla_y\nabla_x\rho & \nabla_y\nabla_y\rho & \nabla_y\nabla_z\rho \\ \nabla_z\nabla_x\rho & \nabla_y\nabla_y\rho & \nabla_z\nabla_z\rho \end{bmatrix} \begin{bmatrix} x_1 & x_2 & x_3 \\ y_1 & y_2 & y_3 \\ z_1 & z_2 & z_3 \end{bmatrix} = \begin{bmatrix} \varepsilon_1 & 0 & 0 \\ 0 & \varepsilon_2 & 0 \\ 0 & 0 & \varepsilon_3 \end{bmatrix}.$$

All spacial points with a negative signed density are classified as attractive interactions, and points with a positive signed density are classified as repulsive interactions. The strength of the interactions can be estimated using the magnitude of the reduced density gradient, where $\nabla\rho_r = 0$ is a strong interaction and $\nabla\rho_r > \rho_{cut}$ is no interaction. The default cutoff in NCIPLOT is 0.07 a.u.

2. Attractive and repulsive NCI surfaces

The attractive and repulsive NCI surfaces for structure **5a**/**5b** are shown in Figures S10 and S11. For clarity, only the central molecules are shown. Small, strongly attractive interactions can clearly be seen near the functional groups. The repulsive interactions, on the other hand, form broad patches which are often between the functional groups. Since crystals composed of compounds **5a**/**5b** are at least metastable, the X-ray structures represent local minima in the potential. Thus, it would be surprising to find strongly repulsive interactions in the crystal and all repulsive interactions are in the weakly interacting range of the surface. For this reason, we have chosen to focus only on the attractive surfaces in our analysis.

3. 3D crystal structures for compounds 5a/5b

While the elemental composition and crystal symmetry are similar for compounds **5a**/**5b**, the alignment of the molecules can have a strong effect on the mechanical properties of the crystals. The 3D crystal structures of compounds **5a**/**5b** were oriented to highlight potential slip planes in the crystal (Figure S12). Slip planes represent regions where layers of the crystal can slide to relieve shear stress or allow the crystals to deform. Interestingly, the hydrogen bonding network in compound **5a** runs parallel to the slip plane in the lattice. Compound **5b**, on the other hand, has a hydrogen bonding network which crosses between potential slip planes in the lattice. The hydrogen bonding networks and slip plane orientations most likely make compound **5b** stiffer than compound **5a**.

4. Compound 5b donor-acceptor ring

While compound **5a** forms a nearly linear chain of hydrogen bonds along a crystal axis, the crystal structure of **5b** contains a tetrameric donor-acceptor ring. Due to the many-body nature of the hydrogen bonding networks, it is difficult to determine how the lattice stabilization energies are affected by the different hydrogen bonding arrangements in compounds **5a**/**5b**. However, NCI surfaces can easily be generated for molecular fragments using the precalculated electron densities for each atom. Attractive and repulsive NCI surfaces for the ring structure are shown in Figure S13.

Figure S10. NCI surfaces for the (a) attractive and (b) repulsive interactions in **5a**. While there are broad surfaces representing weak repulsive interactions, the strong attractive interactions stabilize the functional groups.

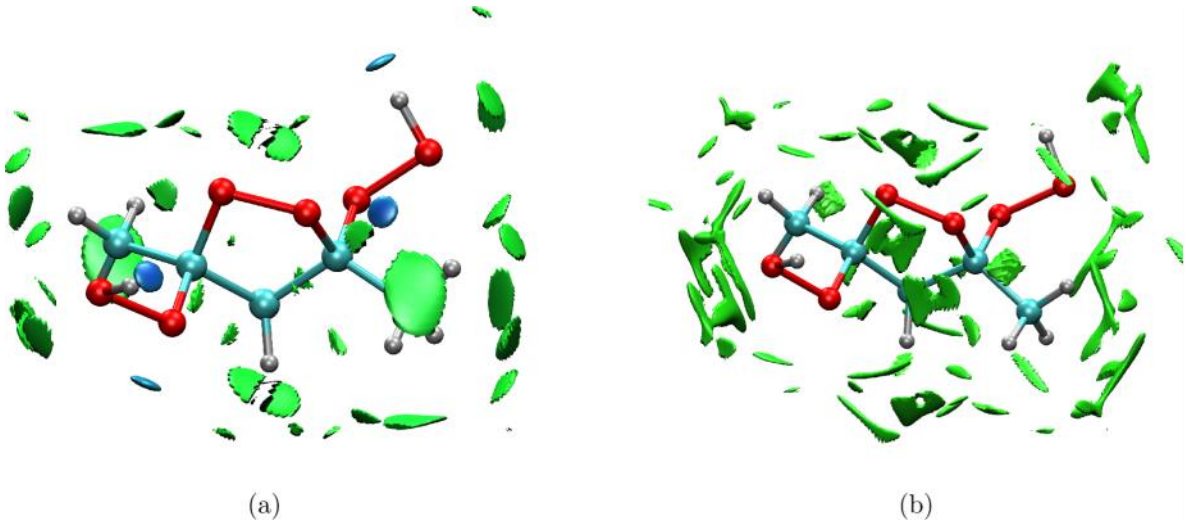

Figure S11. NCI surfaces for the (a) attractive and (b) repulsive interactions in **5b**. While there are broad surfaces representing weak repulsive interactions, the strong attractive interactions stabilize the functional groups.

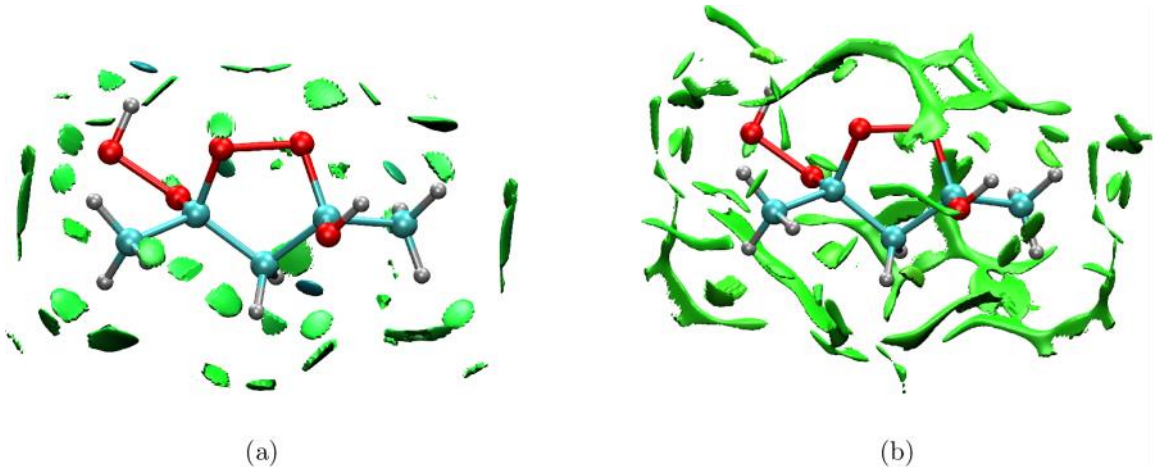

Figure S12. X-ray structures of (a) **5a** and (b) **5b** oriented to highlight potential slip planes within the lattice. The hydrogen bonding network in compound **5a** is aligned with the slip plane, while the network in **5b** includes inter-layer hydrogen bonds.

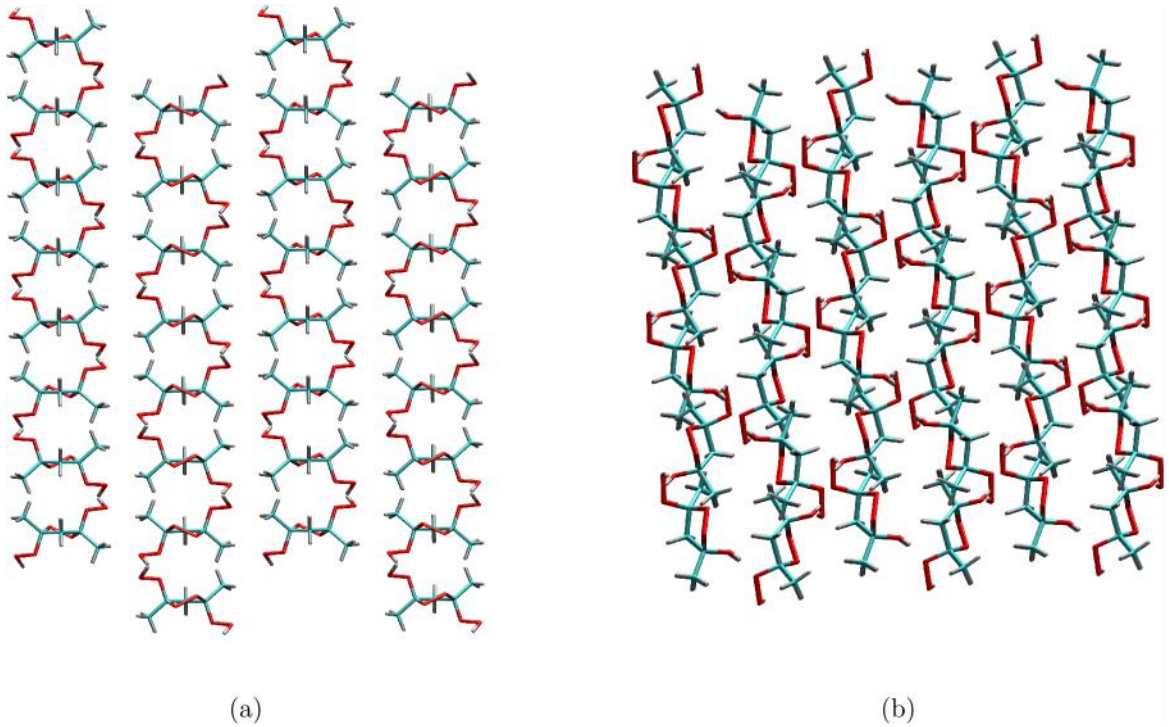

Figure S13. NCI surfaces for the (a) attractive and (b) repulsive interactions in the $[OH•••OOH]_2$ ring structure found in crystals composed of **5b**. The hydrogen bonding network involves many-body interactions between 4 molecules and multiple layers of the crystal. The only repulsive interaction forms at the center of the ring, which likely represents ring strain.

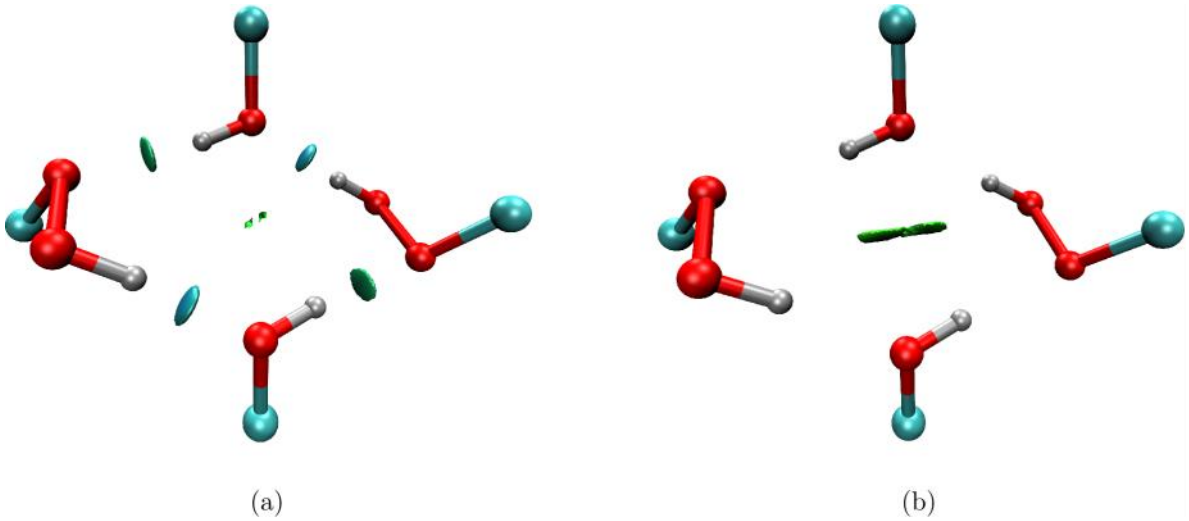

ChemPubSoc Europe

DOI: 10.1002/ejoc.201600717

EurJOC European Journal of Organic Chemistry

Full Paper

Organic Peroxides

Azido(*tert*-butylperoxy)methyl Compounds – An Exceptional Class of Energetic Materials

Thomas. M. Klapötke,*[a] Traian Rotariu,[b] Benedikt Stiasny,[a] Jörg Stierstorfer,[a] Sebastian Wiegmann,[a] and Teodora Zecheru[b]

Abstract: Azido(*tert*-butylperoxy)methyl group containing molecules derived from difunctional carbonyl compounds were prepared and fully characterized by using a range of analytical methods. The molecular structure of a representative compound was determined by X-ray diffraction, which is the first example of a molecular structure of this class of molecule. The sensitivities of the molecules were measured, and the performance values of the compounds were calculated by using the EXPLO5 program.

Introduction

Peroxides are an interesting class of chemical compounds that, in the form of their different subspecies, find application in many diverse fields, such as in the treatment of diseases,[1,2] as initiators for radical reactions,[3] on an industrial scale in polymerization reactions,[4] and in organic synthesis, for example in epoxidation reactions.[5] Another possible application that has been investigated with varying degrees of interest during the past century since the development of acetone peroxide in 1895 by Wolffenstein,[6] is their use as energetic materials.[7–10] However, until the 21st century there were almost no combinations of peroxides with different energetic groups. Pramanik and Ghorai developed an easy and efficient route to combine the energetic *tert*-butyl-peroxy group with an azido group.[11] They further investigated this class of compounds and were able to achieve the formation of *tert*-butyl esters by reacting molecules of the described structure with an organic base.[12] Surprisingly, this leads to the formation of the ester and not of the carbonyl azide.[12] However, Pramanik and Ghorai limited their research to compounds that only have one formyl or carbonyl group in the molecule. With respect to the performance, increment of the density of an energetic molecule is desired. So far, all compounds synthesized in this field have been colorless oils. In this study, additional compounds based on difunctional carbonyl compounds are reported. The crystal structure of 1,2-bis[azido(*tert*-butylperoxy)methyl]benzene is determined and represents the first example of a molecular structure of this class of molecule. The study also provides insight into the sensitivities and calculated performance values of the synthesized compounds.

[a] *Department of Chemistry, Ludwig-Maximilian University, 81377 Munich, Germany*
E-mail: tmk@cup.uni-muenchen.de
www.hedm.cup.uni-muenchen.de
[b] *Scientific Research Center for CBRN Defense and Ecology, 041309 Bucharest, Romania*

Supporting information for this article is available on the WWW under http://dx.doi.org/10.1002/ejoc.201600717.

Results and Discussion

The hitherto unknown molecules 1,4-diazido-1,4-bis(*tert*-butylperoxy)cyclohexane (**6**), 1,3-bis[azido(*tert*-butylperoxy)methyl]-benzene (**7**), 1,4-bis[azido(*tert*-butylperoxy)methyl]benzene (**8**), 1,2-bis[azido(*tert*-butylperoxy)methyl]benzene (**9**), and 4,4′-diazido-4,4′-bis(*tert*-butylperoxy)-1,1′-bi(cyclohexane) (**10**) were synthesized by applying the strategy developed by Pramanik and Ghorai.[11] First, the corresponding starting materials were dissolved in anhydrous dichloromethane and reacted with stoichiometric amounts of a 5.5 M solution of *tert*-butylOOH in decane and 1.15 to 2.5 equiv. (depending on the product, calculated on one carbonyl group) of trimethylsilyl azide under the catalysis of $FeCl_3$ (Scheme 1).

The reactions were performed under N_2 atmosphere at 0 °C and stirred overnight, then allowed to reach room temperature. After separation of the remaining $FeCl_3$ by vacuum filtration through silica and removal of the solvent under reduced pressure without heating, the desired products were obtained. In the case of compound **8**, the product was already pure, so that no further purification of the remaining colorless solid was necessary. The yield for this reaction was 60 %. To obtain **6** as a pure substance, it was purified by column chromatography over silica gel using a mixture of ethyl acetate and pentane as eluent. The compound was isolated as a colorless oil in a yield of 20 %. Purification of crude compounds **7** and **10** by chromatography was attempted, but these approaches were not successful because undefined impurities remained. To obtain pure compounds **7** and **10** it was necessary to wash the impure white solid with pentane cooled to –30 °C (care was taken to keep the time for one washing as short as possible and to perform four to five washing steps only, otherwise the loss of product was too excessive since it is also somewhat soluble in pentane), yields of these two compounds were 11 % (**7**) and 6 % (**10**).

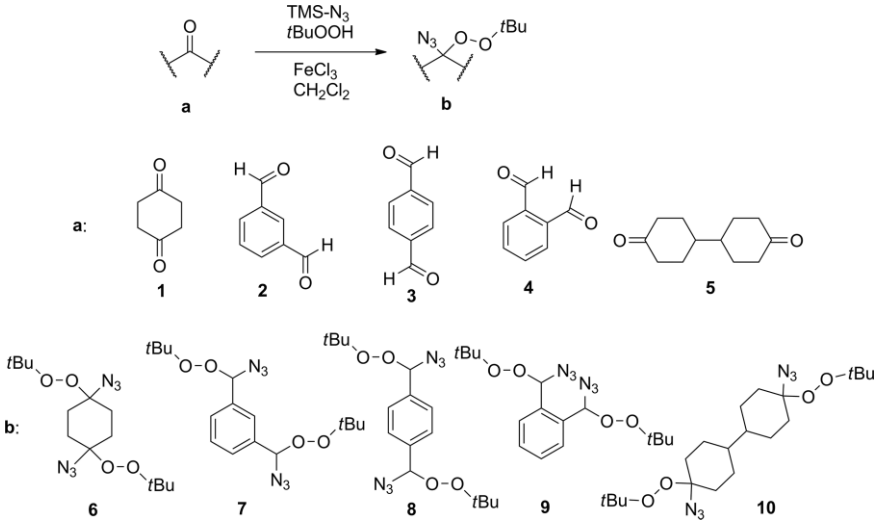

Scheme 1. Synthetic pathway for the synthesis of the difunctional molecules **6**–**10**.

Compound **9** was purified by column chromatography over silica gel using a mixture of ethyl acetate and isohexane as eluent. After removal of the solvent, a colorless oil was obtained that crystallized at –30 °C. However, ^{1}H NMR spectroscopic analysis showed that the solid was still not pure. A pure sample could be obtained by washing with –30 °C pentane. This means that, in the case of compound **9**, both purification methods described were required, which is the main reason for the poor yield of only 1 %. Product formation in general can easily be detected by ^{13}C NMR spectroscopy. Compared to that in the starting material, the ^{13}C NMR resonance in the product shifts to lower ppm values (below 100 ppm in $CDCl_3$ solution).

Crystal Structures

Single crystals of **9** were grown from acetone at 5 °C. Details of the X-ray diffraction measurement are given in the Supporting Information. The compound crystallizes in the monoclinic space group $P2_1/c$ with four molecular units per unit cell and a density of 1.248 g cm^{-3}. Figure 1 displays its molecular structure.

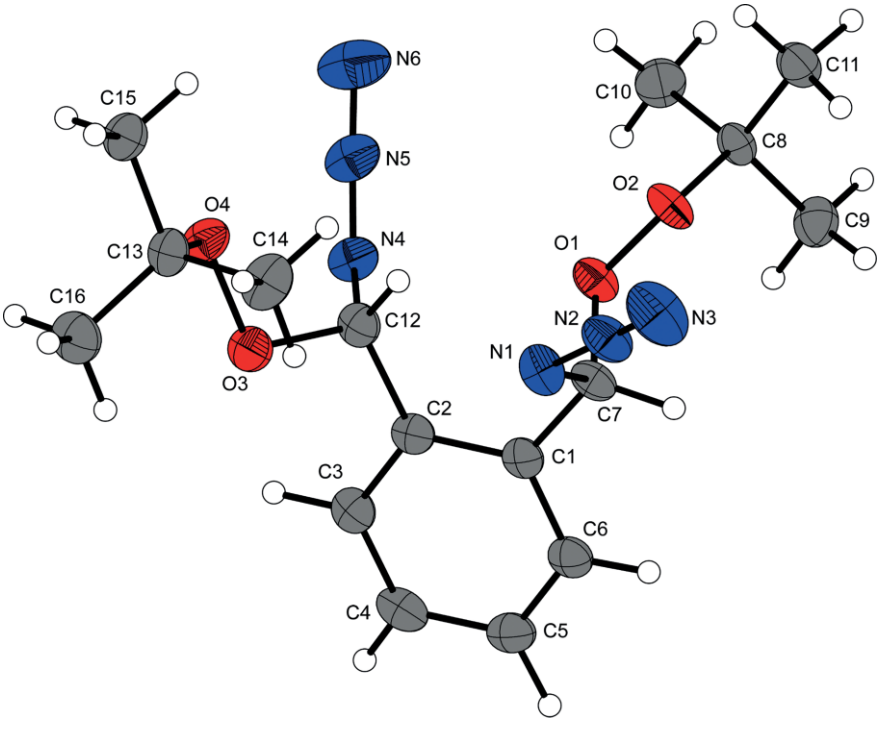

Figure 1. Molecular structure of **9** including its labeling scheme.

The O–O bond lengths show values between 147.8 and 148.2 pm and are therefore in the normal range for a typical O–O single bond (147.0 pm average bond length for O–O in TATP[13]). The (C)N–N bond length of the azide is between 123.0 and 125.1 pm and therefore comparable with reported values for azides.[14] The same is true for the (N)N–N bond, which has a length between 112.6 and 113.2 pm. The C–O–O bond angles are between 105.71 and 107.05°, which is slightly less than the corresponding bond angle in DADP (107.6°).[13] The N–N–N bond angle is between 172.6° and 173.1° and is therefore again in the usual range for a covalent azide.[14] The azide and the *t*Bu–O–O substituent are not on the same side of the molecule (on one substituted C-atom the azide sticks upwards and on the second C-atom the azide sticks downwards). The torsion angles for the corresponding groups also show differences. For C-7 the C–O–O angle is 140.1°, for C-12 the angle has a value of 125.9°. The C–N–N angle for C-7 is 158.3°, whereas for C-12 it is 153.3°. The larger torsion angles are therefore on C-7, the smaller on C-12.

Energetic Properties

The performance data of the compounds were calculated by using the EXPLO5 program (version 6.02). Heats of formation were calculated by using the atomization method based on CBS4-M electronic enthalpies. Table 1 gathers the energetic properties.

All investigated compounds must be classified as extremely sensitive toward impact, with sensitivities between <1 and 2 J. The friction sensitivities are between 14 and 360 N. Compound **6** features the highest value and is classified as insensitive towards friction. This abnormally high value can be explained by its liquid character. For the solid compounds **7**–**10**, the determined friction sensitivities lie between 14 and 32 N, which implies their classification as very sensitive. Compounds **7**– **10** have ESD sensitivities that lie in the range between 0.03 and 0.2 J. For ESD sensitivity, no internationally standardized classification exists. However, all determined values are significantly higher than the maximum electrostatic charge the human body can produce. For compound **6**, it was not possible to determine an ESD value with our apparatus because of its oily nature. Thermal decomposition points are mostly in the typical range for organic peroxides, between 100 and 120 °C.[10] Only compound **6** has a slightly higher decomposition point of 143 °C. The calculated detonation velocities are in a range between 5989 and 6435 ms^{-1} and are therefore comparable with other peroxide compounds.[8,10] However, they present higher velocities of detonation ($v_{det.}$) than *tert*-butylperoxy esters.[15] This difference can most likely be explained by the presence of the additional azide. For detonation pressure, values between 9 and 11 kbar were determined. These values also fit nicely with the values calculated for reported compounds.[10] The calculated v_{det} values are in a range of 7 %, which is in the margin of error of the used program. However, some tendencies can still be drawn from the values. Concerning isomers **7**– **9**, it is conspicuous that *ortho*-isomer **9** performs best ($v_{det.}$ = 6191 ms^{-1}) followed by *para*-isomer **8** ($v_{det.}$ = 6146 ms^{-1}) and *meta*-isomer **7** ($v_{det.}$ = 5989 ms^{-1}). The slightly superior performance of **9** can most likely be explained by the significant steric hindrance, which leads to a more positive enthalpy of formation of the molecule and therefore to a better performance. For compounds **7** and **8**, the explanation for the differences can probably be found in the slightly higher density of **8**, which is beneficial for increased performance values. All nonaromatic compounds studied here in general performed slightly better than the aromatic compounds [$v_{det.}$ (**6**) = 6338 ms^{-1}, $v_{det.}$ (**10**) = 6435 ms^{-1}]. Again, an increase in the steric hindrance can be the explanation, because in the aromatic reaction products the carbonyl C atom of the starting material has been converted into a tertiary C, whereas for the nonaromatic reaction products (derived from ketone starting materials), the corresponding C atom is quaternary and therefore sterically more crowded.

Table 1. Energetic properties of **6**–**10**.

	6	**7**	**8**	**9**	**10**
Formula	$C_{14}H_{26}N_6O_4$	$C_{16}H_{24}N_6O_4$	$C_{16}H_{24}N_6O_4$	$C_{16}H_{24}N_6O_4$	$C_{20}H_{36}N_6O_4$
F_W [g/mol]	342.40	364.40	364.40	364.40	424.56
IS [J][a]	<1	2	2	1.5	2
FS [N][b]	360	14	40	40	32
ESD [J][c]	oil	0.15	0.2	0.2	0.03
Ω_{CO2}[%][d]	–60.82	–52.77	–52.77	–52.77	–67.92
T_m/T_{decl}[°C][e]	143	104	87/129	119	115
ϱ [g cm^{-3}][f]	1.21 (pyc.)	1.21 (pyc.)	1.24 (pyc.)	1.248 (X-ray)	1.22 (pyc.)
$\Delta_f H_m^0$ [kJ mol^{-1}][g]	27	191	188	190	–138
$\Delta_f U_0$ [kJ kg^{-1}][h]	209	639	631	636	–191
EXPLO5 6.02 values					
$-\Delta_{ex}U^0$ [kJ kg^{-1}][i]	–3607	–3853	–3855	–3862	–3106
T_{det} [K][j]	2094	2249	2242	2243	1813
p_{CJ} [GPa][k]	11	9	10	10	10
$v_{det.}$ [m/s][l]	6338	5989	6146	6191	6435
V^0 [L kg^{-1}][m]	834	767	762	761	799

[a] Impact sensitivity according to BAM drop hammer (method 1 of 6). [b] Friction sensitivity according to BAM friction tester (method 1 of 6). [c] Electrostatic discharge sensitivity (OZM ESD tester). [d] Oxygen balance. [e] Temperature of decomposition according to DTA (onset temperatures at a heating rate of 5 °C/min). [f] Room temperature X-ray densities. Calculated based on the low-temperature X-ray values by using the equation $\{\varrho_{298}\ K = \varrho T/[1 + \alpha V(298 - T_0)]; \alpha V = 1.5 \times 10^{-4}\ K^{-1}\}$. [g] Calculated heat of formation using the atomization method and CBS-4M electronic enthalpies. [h] Calculated energy of formation. [i] Heat of detonation. [j] Temperature of detonation. [k] Detonation pressure. [l] Detonation velocity. [m] Volume of gas after detonation.

Conclusions

The synthesis and characterization by standard analytical methods of five new molecules containing an azido-*tert*-butyl methyl group, namely 1,4-diazido-1,4-bis(*tert*-butylperoxy)cyclohexane (**6**), 1,3-bis[azido(*tert*-butylperoxy)methyl]benzene (**7**), 1,4-bis-[azido(*tert*-butylperoxy)methyl]benzene (**8**), 1,2-bis[azido(*tert*-butylperoxy)methyl]benzene (**9**) and 4,4′-diazido-4,4′-bis(*tert*-butylperoxy)-1,1′-bi(cyclohexane) (**10**), is described. The yields obtained were very low to moderate (1–60 %). Compounds **7**–**10** are colorless solids and thereby are the first examples of solid compounds for the investigated class of substances. It was also possible to determine the crystal structure of **9**, which is the first example of a molecular structure containing the investigated energetic group. In addition, the sensitivities towards impact, friction, electrostatic discharge and heat were determined. The decomposition points of the compounds are mostly in a range between 100 and 120 °C. The compounds are all very sensitive towards impact (≤ 2 J). Friction sensitivity values are between 14 and 360 N. Therefore, the compounds must be handled as primary explosives.

Experimental Section

CAUTION! All investigated compounds are potentially explosive energetic materials, although no hazards were observed by us during the preparation and handling of these compounds. Nevertheless, this necessitates additional meticulous safety precautions (earthed equipment, Kevlar gloves, Kevlar sleeves, face shield, leather coat, and earplugs).

General: All chemicals were obtained from Sigma–Aldrich and used without further purification. Sensitivity measurements were performed with a BAM drop hammer, a BAM-friction tester, and OZM-ESD-tester. Infrared spectra were recorded with a Perkin–Elmer One FTIR Spectrum BX II with a Smith ATR Dura Sample IRII. For the recording of Raman spectra a Bruker MULTIRAM 1064 2000R NIR FT Raman Spectrometer, equipped with a Nd:YAG-Laser (1064 nm) was used. NMR spectra were recorded with a Bruker 400 MHz spectrometer operating at 400 MHz for proton spectra. Melting points and decomposition points were recorded with an OZM Research DTA 552-Ex instrument. The reactions were carried out under Schlenk conditions and anhydrous solvents were applied. For column chromatography the solvents were not previously dried.

1,4-Diazido-1,4-bis(*tert*-butylperoxy)cyclohexane (6): 1,4-Cyclohexanedione (0.200 g, 1.783 mmol) was dissolved in CH_2Cl_2 (10 mL) and cooled to 0 °C, and trimethylsilyl azide (1.18 mL, 1.027 g, 8.915 mmol) and *t*BuOOH (5.5 M in decane, 0.65 mL, 0.32 g, 3.57 mmol) were added. One spatula tip of water-free $FeCl_3$ was added and the solution was stirred overnight while it reached room temperature. $FeCl_3$ was then removed by vacuum filtration through silica. After removal of the solvent, the crude product was obtained as a colorless oil, which was purified by column chromatography over silica (ethyl acetate/pentane, 1:10) to give **6** (0.122 g, 20 %) as a colorless oil. DTA (5 °C min^{-1}) $T_{dec.}$ (onset) = 143 °C; IS: <1 J; FS: 360 N; ESD: oil/not measureable; IR (ATR): $\tilde{\nu}$ = 3332 (w), 2979 (m), 2936 (m), 2477 (w), 2103 (s), 1438 (m), 1388 (m), 1364 (m), 1243 (s), 1193 (s), 1141 (m), 1073 (m), 1050 (m), 951 (m), 915 (m), 878 (m), 753 (m), 714 (w), 674 (w) cm^{-1}. Raman (1064 nm): $\tilde{\nu}$ = 2984 (65), 2933 (100), 2753 (11), 2120 (23), 2462 (31), 1310 (28), 1072 (17), 952 (35), 834 (29), 590 (27), 510 (25), 486 (24), 88 (63) cm^{-1}. ^1H NMR (400 MHz, $CDCl_3$, 298 K): δ = 1.29 (s, 18 H), 1.81–2.07 (m, 8 H) ppm. ^{13}C NMR (100 MHz, $CDCl_3$, 298 K): δ = 26.5 (CH_3), 29.0 (CH_2), 80.6 [$C(CH_3)_3$], 95.2 (*C*NO) ppm. $C_{14}H_{26}N_6O_4$ (342.40): calcd. C 49.11, H 7.65, N 24.54; found C 49.03, H 7.33, N 24.91.

1,3-Bis[azido(*tert*-butylperoxy)methyl]benzene (7): Isoterephthalaldehyde (0.402 g, 3.065 mmol) was dissolved in CH_2Cl_2 (20 mL) and cooled to 0 °C, and trimethylsilyl azide (2.088 mL, 1.830 g, 15.00 mmol) and *t*BuOOH (5.5 M in decane, 1.11 mL; 0.54 g, 6.13 mmol) were added. After the addition of a spatula tip of anhydrous $FeCl_3$, the reaction mixture was stirred overnight and allowed to reach room temperature. The mixture was then filtered through silica to remove remaining $FeCl_3$ and the solvent was removed under reduced pressure to obtain the crude product as a colorless solid. After four washing steps with cold pentane (–30 °C), the product (0.125 g, 11 %) was isolated as a colorless solid. DTA (5 °C min^{-1}) $T_{dec.}$ (onset) = 104 °C; IS: 2 J; FS: 14 N; ESD: 0.150 J. IR (ATR): $\tilde{\nu}$ = 2981 (m), 2926 (w), 2108 (s), 1596 (w), 1469 (w), 1388 (m), 1364 (m), 1341 (m), 1330 (m), 1285 (s), 1246 (s), 1190 (s), 1157 (m), 1039 (m), 999 (s), 991 (s), 948 (m), 910 (s), 887 (m), 856 (m), 814 (s), 751 (m), 708 (m), 682 (m) cm^{-1}. Raman (1064 nm): $\tilde{\nu}$ = 3114 (19), 3021 (38), 2952 (45), 2123 (18), 1610 (22), 1482 (21), 1250 (19), 1000 (55), 818 (47), 720 (21), 93 (100) cm^{-1}. ^1H NMR (400 MHz, $CDCl_3$, 298 K): δ = 1.34 (s, 18 H), 6.21 (s, 2 H), 7.40–7.51 (m, 4 H) ppm. ^{13}C NMR (100 MHz, $CDCl_3$, 298 K): δ = 26.5 (CH_3), 82.1 [$OC(CH_3)_3$], 95.2 (ONCCH), 125.9 ($C_{arom}HCC$), 128.4 ($C_{arom}HCCC$), 129.0 [$C_{arom}H(CC)_2$], 134.6 ($C_{arom}CCC$) ppm. $C_{16}H_{24}N_6O_4$ (364.40): calcd. C 53.04, H 6.13, N 23.20; found C 52.86, H 6.32, N 23.15.

1,4-Bis[azido(*tert*-butylperoxy)methyl]benzene (8): Terephthalaldehyde (0.402 g, 3.065 mmol) was dissolved in CH_2Cl_2 (20 mL) and cooled to 0 °C, and trimethylsilyl azide (2.088 mL, 1.830 g, 15.00 mmol) and *t*BuOOH (5.5 M in decane, 1.11 mL, 0.540 g, 6.130 mmol) were added. After the addition of a spatula tip of anhydrous $FeCl_3$, the mixture was stirred overnight and allowed to reach room temperature. The mixture was then filtered through silica to remove remaining $FeCl_3$ and the solvent was removed under reduced pressure to obtain the pure product (0.666 g, 60 %) as a colorless solid. DTA (5 °C min^{-1}) T_m (onset) = 87 °C; $T_{dec.}$ (onset) = 129 °C; IS: 2 J; FS: 40 N; ESD: 0.2 J. IR (ATR): $\tilde{\nu}$ = 2981 (m), 2102 (s), 1712 (m), 1475 (w), 1408 (w), 1386 (w), 1366 (m), 1351 (m), 1287 (m), 1235 (s), 1183 (s), 1117 (m), 1040 (m), 1006 (m), 936 (m), 892 (m), 837 (s), 820 (m), 771 (m), 753 (m), 733 (m), 719 (m), 705 (m) cm^{-1}. Raman (1064 nm): $\tilde{\nu}$ = 3150 (21), 3129 (20), 2990 (43), 2936 (42), 2210 (32), 1618 (51), 1450 (23), 1240 (18), 1230 (37), 812 (21), 859 (43), 844 (44), 770 (19), 680 (22), 605 (10), 550 (21), 502 (20), 215 (22), 189 (40), 90 (100) cm^{-1}. ^1H NMR (400 MHz, $CDCl_3$, 298 K): δ = 1.33 (s, 18 H), 6.39 (s, 2 H), 7.45 (s, 4 H) ppm. ^{13}C NMR (100 MHz, $CDCl_3$, 298 K): δ = 26.5 (CH_3), 82.1 [$OC(CH_3)_3$], 95.4 (ONCCH), 127.4 ($C_{arom}CCH$), 135.5 ($C_{arom}CCC$) ppm. $C_{16}H_{24}N_6O_4$ (364.40): calcd. C 53.04, H 6.13, N 23.20; found C 52.70, H 6.52, N 23.17.

1,2-Bis[azido(*tert*-butylperoxy)methyl]benzene (9): Phthalaldehyde (1.206 g, 8.991 mmol) was dissolved in CH_2Cl_2 (30 mL) and cooled to 0 °C, and trimethylsilyazide (5.00 mL, 4.352 g, 37.78 mmol) and *t*BuOOH (5.5 M in decane, 3.24 mL, 1.603 g, 17.78 mmol) were added. One spatula tip of water-free $FeCl_3$ was added and the solution was stirred overnight and allowed to reach room temperature. $FeCl_3$ was then removed by vacuum filtration through silica gel. After removal of the solvent, the crude product was purified by column chromatography over silica gel (ethyl acetate/isohexane, 1:10). The obtained oil crystallized at –30 °C overnight. After washing this solid with –30 °C pentane, the pure product (0.036 g, 1 %) was obtained as a colorless solid. DTA (5 °C min^{-1}) $T_{dec.}$ (onset) = 119 °C; IS: 1.5 J; FS: 40 N; ESD: 0.2 J. IR (ATR): $\tilde{\nu}$ = 3330 (w), 2978

(m), 2929 (m), 2859 (w), 2360 (w), 2104 (s), 1728 (w), 1587 (w), 1455 (m), 1388 (m), 1364 (m), 1312 (m), 1278 (m), 1243 (m), 1193 (s), 1111 (m), 1041 (m), 1006 (m), 954 (m), 932 (m), 899 (m), 866 (m), 758 (s), 672 (m) cm^{-1}. Raman (1064 nm): $\tilde{\nu}$ = 3150 (21), 3129 (20), 2990 (43), 2936 (42), 2210 (32), 1618 (51), 1450 (23), 1240 (18), 1230 (37), 812 (21), 859 (43), 844 (44), 770 (19), 680 (22), 605 (10), 550 (21), 502 (20), 215 (22), 189 (40), 90 (100) cm^{-1}. ^1H NMR (400 MHz, $CDCl_3$, 298 K): δ = 1.35 (s,18 H), 6.55 (s, 2 H), 7.38–7.53 (m, 4 H) ppm. ^{13}C NMR (100 MHz, $CDCl_3$, 298 K): δ = 26.5 (CH_3), 82.0 [$C(CH_3)_3$], 93.3 [*C*NO], 128.0 [$C_{arom.}H(CH)_2$], 130.1 [$C_{arom.}H(CH)(CC)$], 132.1 [$C_{arom.}(C)_3$] ppm. $C_{16}H_{24}N_6O_4$ (364.40): calcd. C 53.04, H 6.13, N 23.20; found C 52.95, H 6.08, N 23.33.

4,4′-Diazido-4,4′-bis(*tert*-butylperoxy)-1,1′-bi(cyclohexane) (10): [1,1′-Bi(cyclohexane)]-4,4′-dione (1.00 g, 8.18 mmol) was dissolved in CH_2Cl_2 (20 mL) and cooled to 0 °C, and trimethylsilyl azide (3.358 mL, 18.75 mmol, 2.160 g) and *t*BuOOH (5.5 M in decane, 1.875 mL, 0.928 g, 10.30 mmol) were added. After the addition of one spatula tip of anhydrous $FeCl_3$, the mixture was stirred overnight and allowed to reach room temperature. On the next day the mixture was filtered through silica gel to remove $FeCl_3$ and the solvent was removed under vacuum to obtain a colorless solid. This product was purified by washing with pentane at –30 °C to obtain **10** (0.135 g, 6 %) as a colorless solid. DTA (5 °C min^{-1}) $T_{dec.}$ (onset) = 115 °C; IS: 2 J; FS: 32 N; ESD: 0.030 J. IR (ATR): $\tilde{\nu}$ = 3347 (w), 2968 (m), 2946 (m), 2933 (m), 2594 (w), 2362 (w), 2104 (s), 1721 (w), 1534 (w), 1473 (m), 1450 (m), 1386 (m), 1363 (s), 1350 (m), 1278 (m), 1250 (s), 1204 (m), 1193 (s), 1181 (m), 1126 (m), 1104 (w), 1080 (m), 1050 (s), 1032 (m), 969 (w), 944 (m), 928 (m), 908 (s), 871 (s), 821 (m), 788 (w), 769 (w), 753 (m), 699 (w), 668 (w) cm^{-1}. Raman (1064 nm): $\tilde{\nu}$ = 3110 (62), 3002 (70), 2992 (72), 2985 (74), 2920 (100), 2813 (52), 2793 (9), 2123 (25), 1483 (29), 1420 (15), 1482 (28), 1280 (11), 1132 (17), 923 (15), 885 (17), 810 (52), 720 (18), 710 (48), 612 (17), 482 (12), 302 (18), 103 (54), 92 (72) cm^{-1}. ^1H NMR (400 MHz, $CDCl_3$, 298 K): δ = 1.27 (s, 18 H), 1.47–2.14 (m, 18 H) ppm. ^{13}C NMR (100 MHz, $CDCl_3$, 298 K): δ = 26.3 (CH_3), 26.5 (CH_2C_2), 32.5 [$CH_2C(H)C(NO)$], 41.5 (CHC_3), 80.3 [$OC(CH_3)_3$], 97.3 [$ONC(CH)_2$] ppm. $C_{20}H_{36}N_6O_4$ (324.56): calcd. C 56.58, H 8.56, N 19.79; found C 56.28, H 8.45, N 20.57.

Acknowledgments

Financial support of this work by the Ludwig-Maximilian University of Munich (LMU), the Office of Naval Research (ONR) under grant number ONR.N00014-16-1-2062, the Bundeswehr – Wehrtechnische Dienststelle für Waffen und Munition (WTD 91) under grant number E/E91S/FC015/CF049 and the Romanian Ministry of Education and Scientific Research under grant POSDRU/159/1.5/S/140106 are gratefully acknowledged. The authors acknowledge collaborations with Dr. Mila Krupka (OZM Research, Czech Republic) in the development of new testing and evaluation methods for energetic materials and with Dr. Muhamed Suceska (Brodarski Institute, Croatia) in the development of new computational codes to predict the detonation and propulsion parameters of novel explosives. We are indebted to and thank Drs. Betsy M. Rice, Jesse Sabatini and Brad Forch (ARL, Aberdeen, Proving Ground, MD) for many inspired discussions. The authors thank Mr. St. Huber for the sensitivity measurements.

Keywords: Energetic materials · Peroxides · Azides · Structure elucidation · Sensitivity

[1] C. W. Jefford, *Drug Discov. Today* **2007**, *12*, 487–495.
[2] V. M. Dembitsky, T. A. Gloriozova, V. V. Poroiko, *Mini-Rev. Med. Chem.* **2007**, *7*, 571–589.
[3] R. Brückner, *Reaktionsmechanismen*, 3rd ed., Elsevier, München, Germany, **2004**.
[4] H. Klenk. P. H. Götz, R. Siegmeier, W. Mayr, *Ullmann's Encyclopedia of Industrial Chemistry*, Wiley-VCH, Weinheim, Germany, **2005**.
[5] K. W. Woods, P. Beak, *J. Am. Chem. Soc.* **1991**, *113*, 6281–6283.
[6] R. Wollfenstein, *Ber. Dtsch. Chem. Ges.* **1895**, *28*, 2265–2269.
[7] N. A. Milas, O. L. Magelli, A. Golubovic, R. W. Arndt, J. C. J. Ho, *J. Am. Chem. Soc.* **1963**, *24*, 222–226.
[8] N.-D. H. Gamage, B. Stiasny, J. Stierstorfer, P. D. Martin, T. M. Klapötke, C. H. Winter, *Chem. Eur. J.* **2015**, *21*, 1–5.
[9] N.-D. H. Gamage, B. Stiasny, J. Stierstorfer, P. D. Martin, T. M. Klapötke, C. H. Winter, *Chem. Commun.* **2015**, *51*, 13298–13300.
[10] T. M. Klapötke, B. Stiasny, J. Stierstorfer, C. H. Winter, *Eur. J. Org. Chem.* **2015**, 6237–6242.
[11] S. Pramanik, P. Ghorai, *Org. Lett.* **2013**, *15*, 3832–3835.
[12] S. Pramanik, R. R. Reddy, P. Ghorai, *Org. Lett.* **2015**, *17*, 1393–1396.
[13] F. Dubnikova, R. Kosloff, J. Almog, Y. Zeiri, R. Boese, H. Itzhaky, A. Alt, E. Keinan, *J. Am. Chem. Soc.* **2005**, *127*, 1146–1159.
[14] T. M. Klapötke, D. G. Piercey, J. Stierstorfer, *Chem. Eur. J.* **2011**, *17*, 13068–13077.
[15] N.-D. H. Gamage, B. Stiasny, J. Stierstorfer, P. D. Martin, T. N. Klapötke, C. H. Winter, *Chem. Eur. J.*, manuscript submitted.

Received: June 29, 2016
Published Online: August 5, 2016

Eur. J. Org. Chem. **2016** · ISSN 1099–0690

SUPPORTING INFORMATION

DOI: 10.1002/ejoc.201600717
Title: Azido(*tert*-butylperoxy)methyl Compounds – An Exceptional Class of Energetic Materials
Author(s): Thomas. M. Klapötke,* Traian Rotariu, Benedikt Stiasny, Jörg Stierstorfer, Sebastian Wiegmann, Teodora Zecheru

Table of contents

1.NMR-spectroscopy

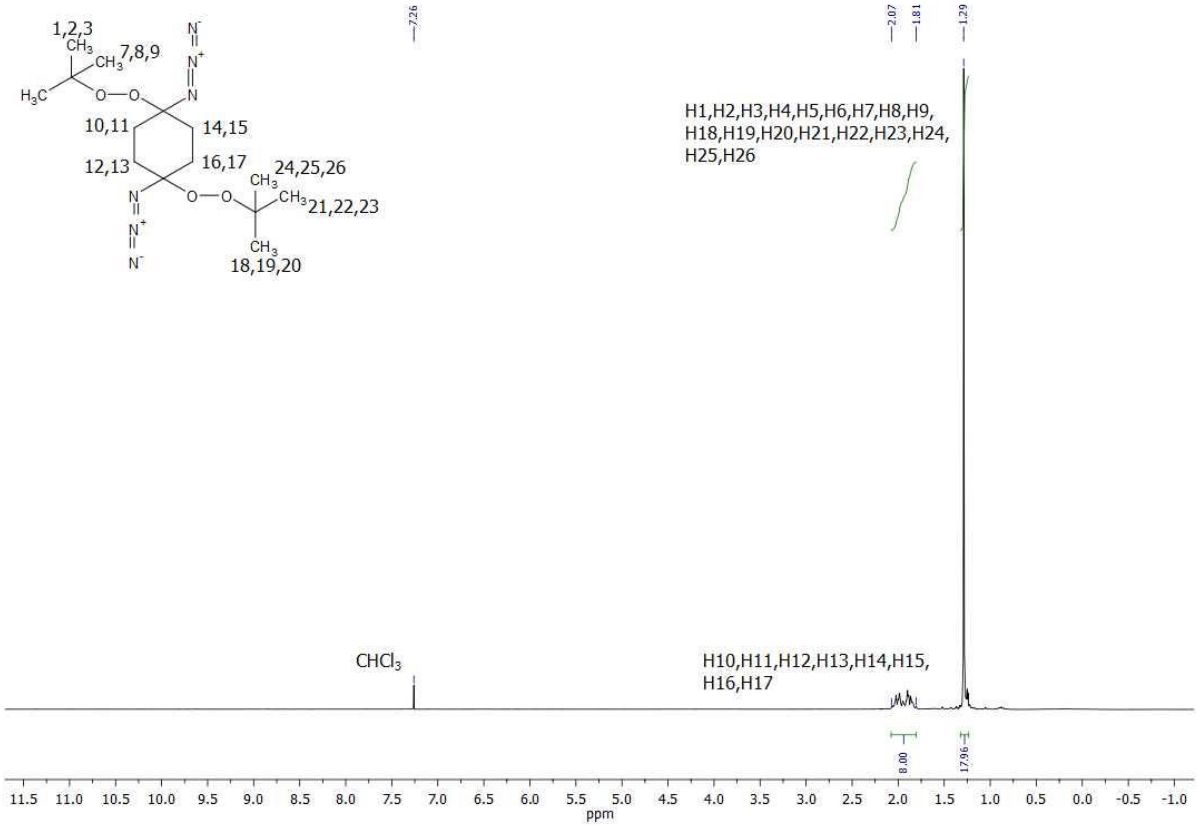

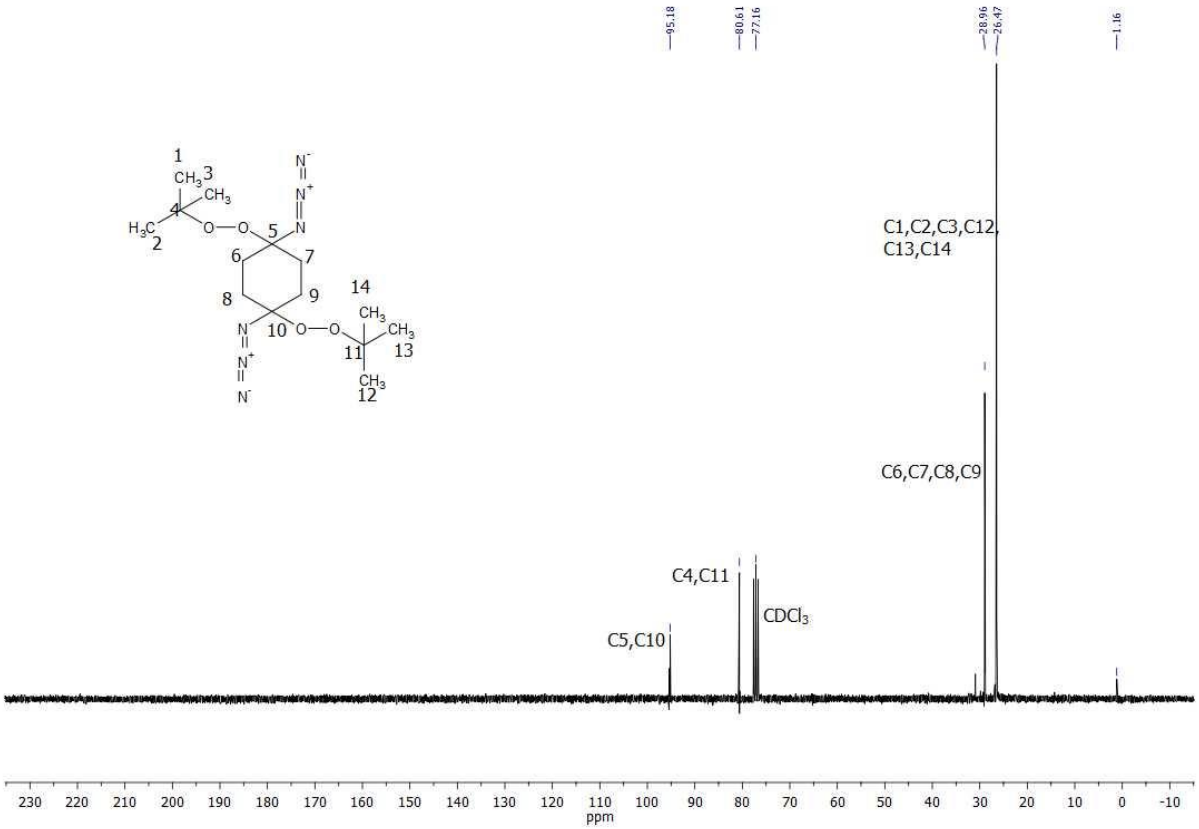

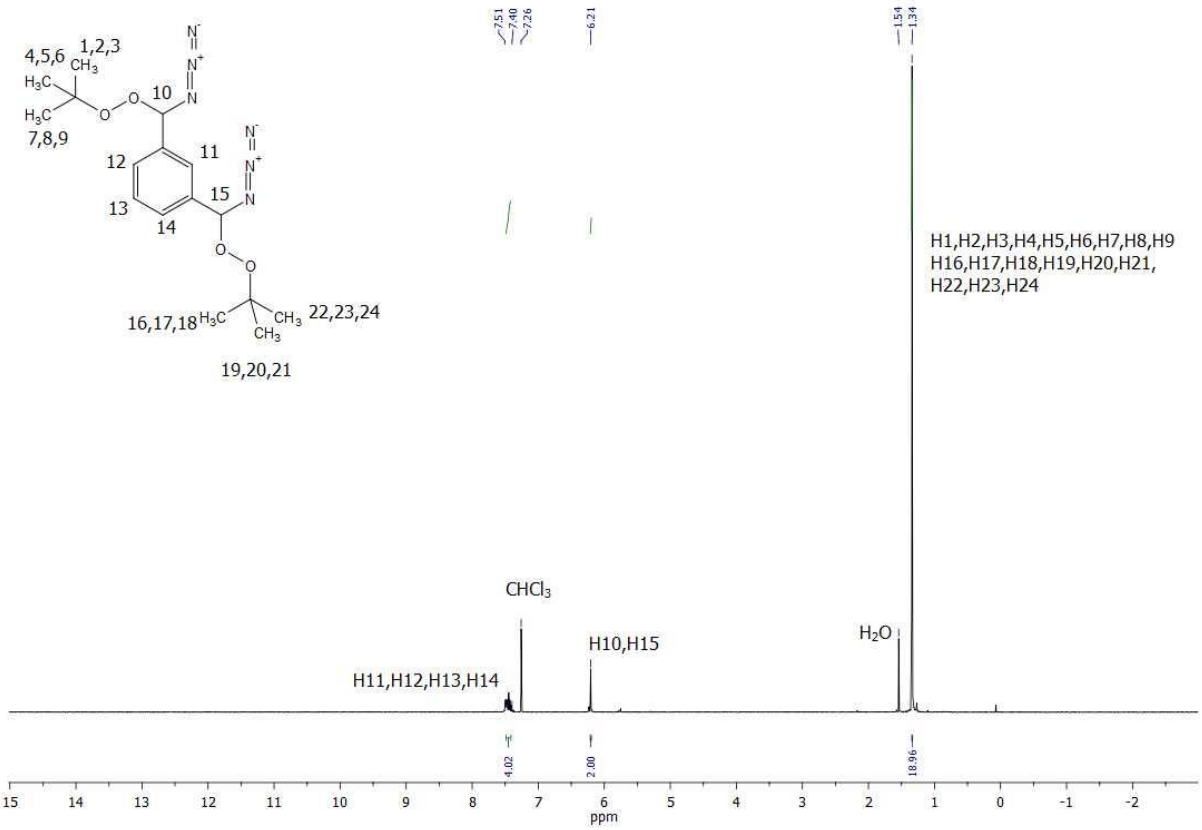
4,5,6
1,2,3
7,8,9
10
11
12
13
14
15
16,17,18
22,23,24
19,20,21
7.51
7.40
7.26
6.21
1.54
1.34
H1,H2,H3,H4,H5,H6,H7,H8,H9
H16,H17,H18,H19,H20,H21,
H22,H23,H24
CHCl3
H10,H15
H2O
H11,H12,H13,H14
4.02
2.00
18.96
ppm

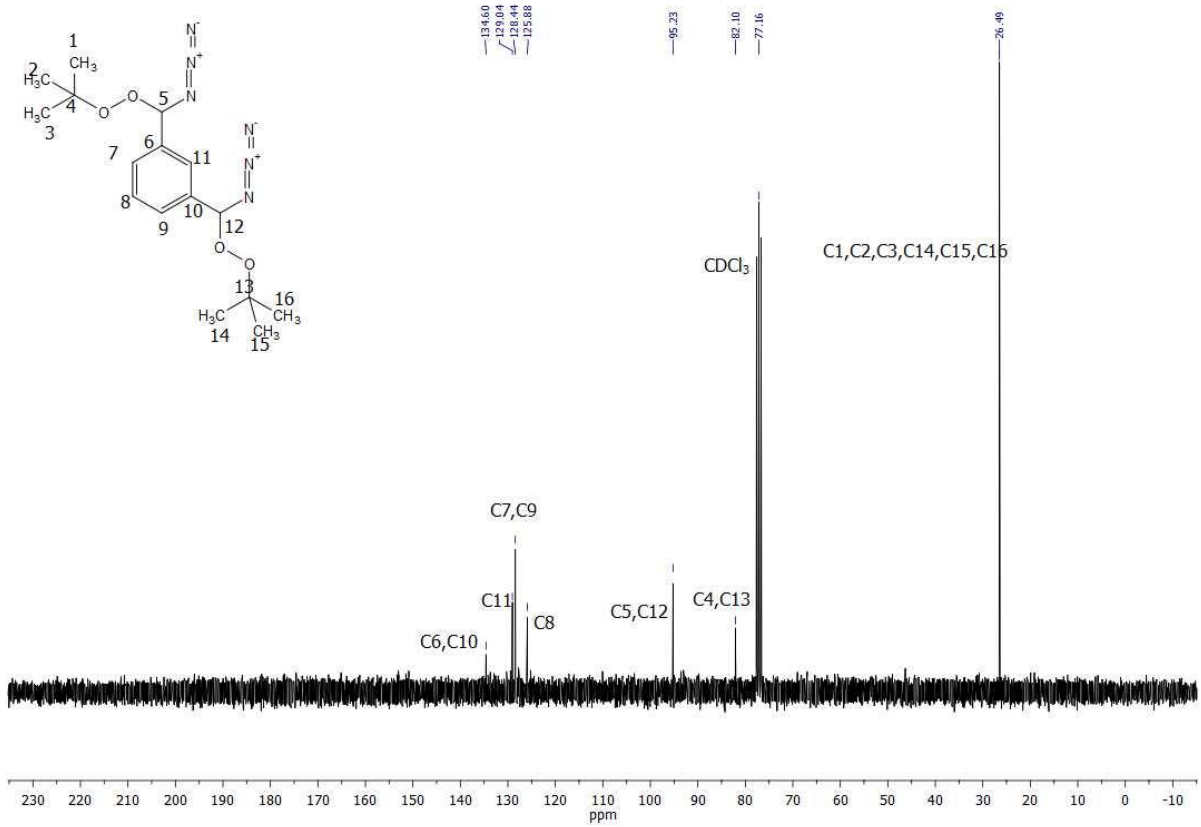
1
2
3
4
5
6
7
8
9
10
11
12
13
14
15
16
134.60
129.04
128.44
125.88
95.23
82.10
77.16
26.49
CDCl3
C1,C2,C3,C14,C15,C16
C7,C9
C11
C8
C6,C10
C5,C12
C4,C13
ppm

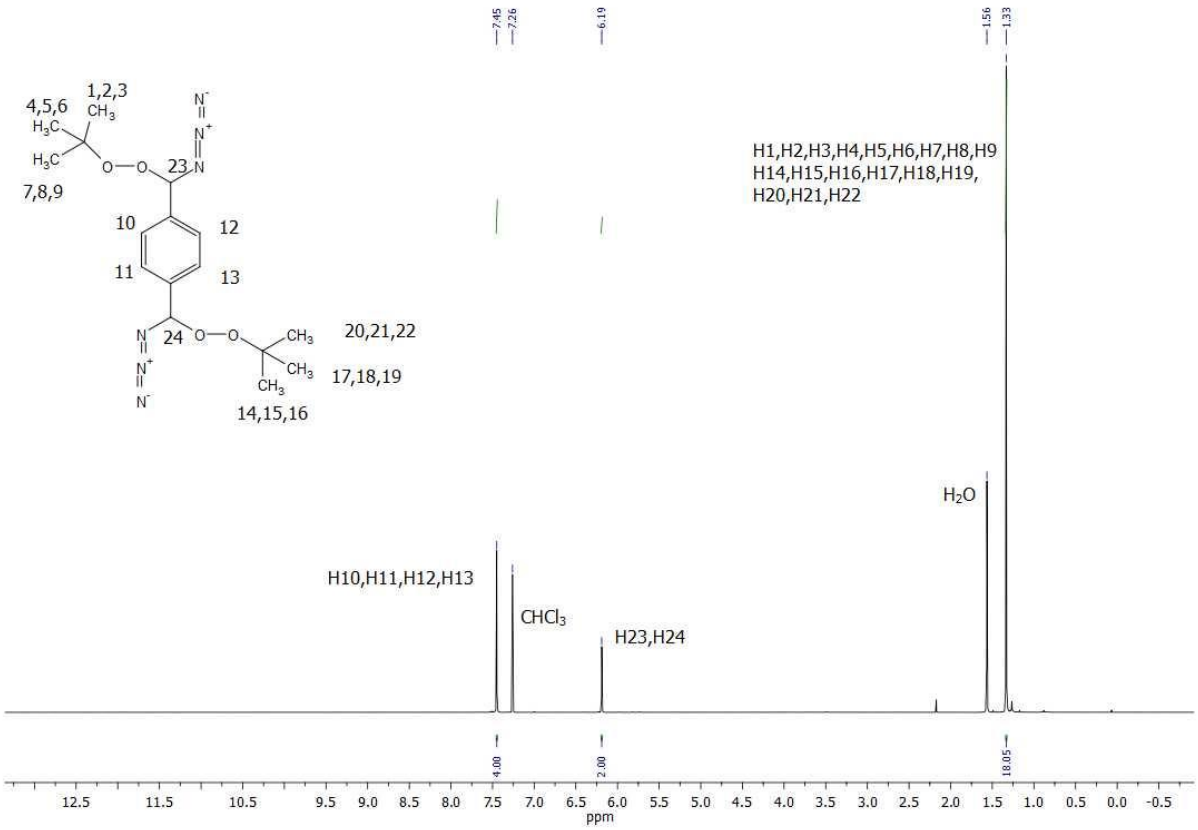
7.45
7.26
6.19
1.56
1.33
1,2,3
4,5,6
7,8,9
10
11
12
13
23
24
20,21,22
17,18,19
14,15,16
H1,H2,H3,H4,H5,H6,H7,H8,H9
H14,H15,H16,H17,H18,H19,
H20,H21,H22
H2O
H10,H11,H12,H13
CHCl3
H23,H24
4.00
2.00
18.05
ppm

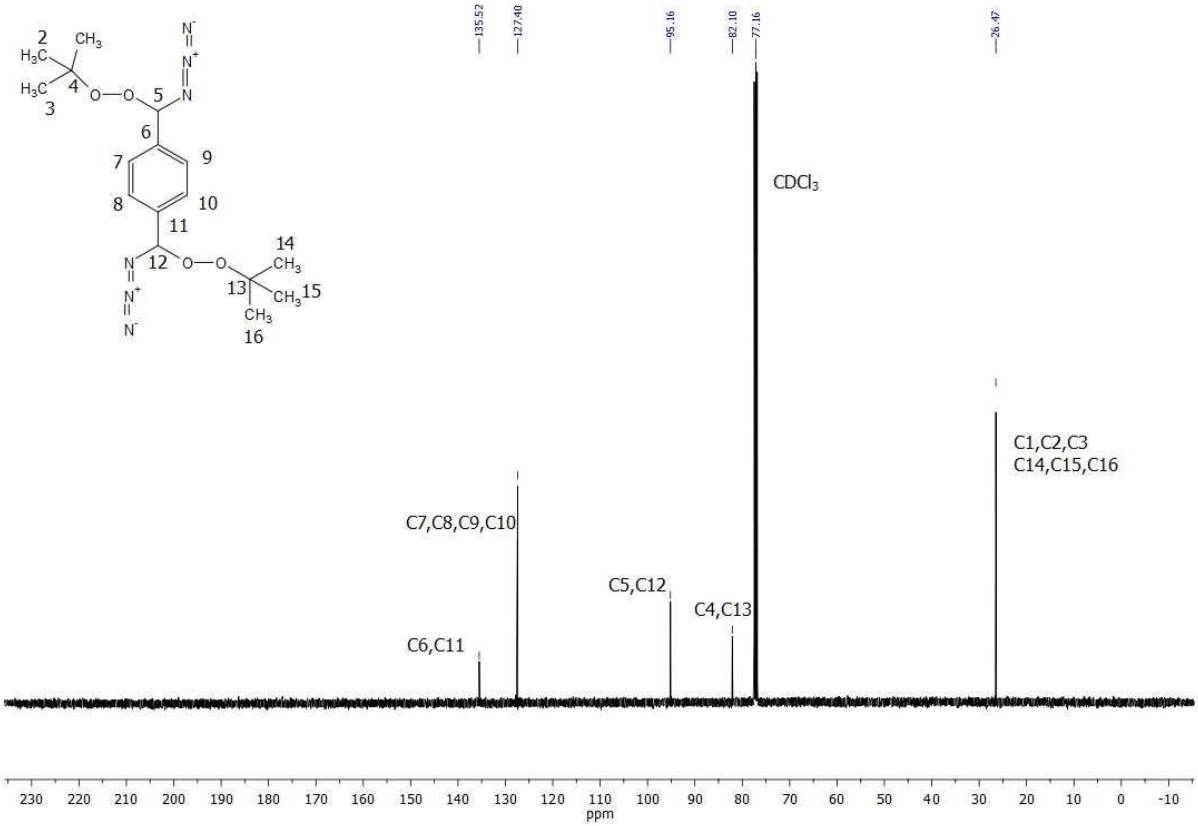
135.52
127.40
95.16
82.10
77.16
26.47
2
3
4
5
6
7
8
9
10
11
12
13
14
15
16
CDCl3
C1,C2,C3
C14,C15,C16
C7,C8,C9,C10
C5,C12
C4,C13
C6,C11
ppm

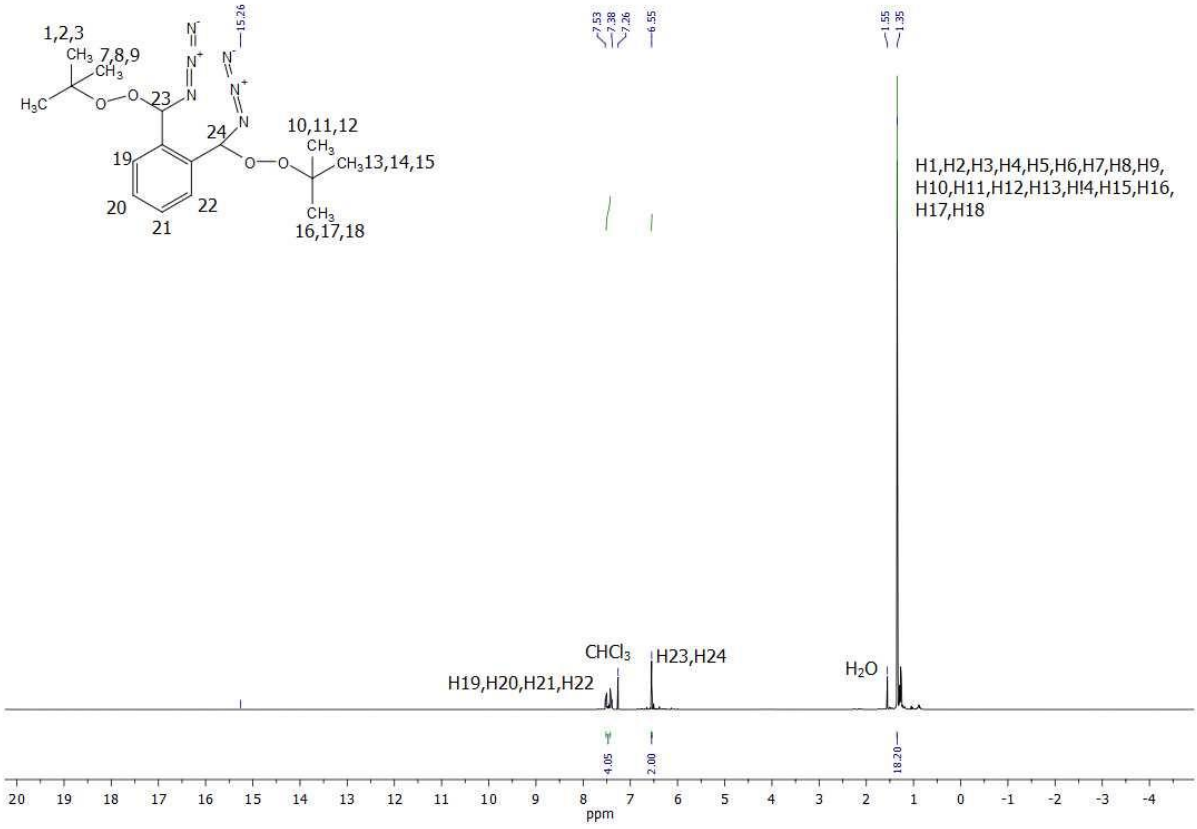
1,2,3
7,8,9
10,11,12
13,14,15
16,17,18
19
20
21
22
23
24
H1,H2,H3,H4,H5,H6,H7,H8,H9,
H10,H11,H12,H13,H!4,H15,H16,
H17,H18
CHCl3
H23,H24
H19,H20,H21,H22
H2O
ppm

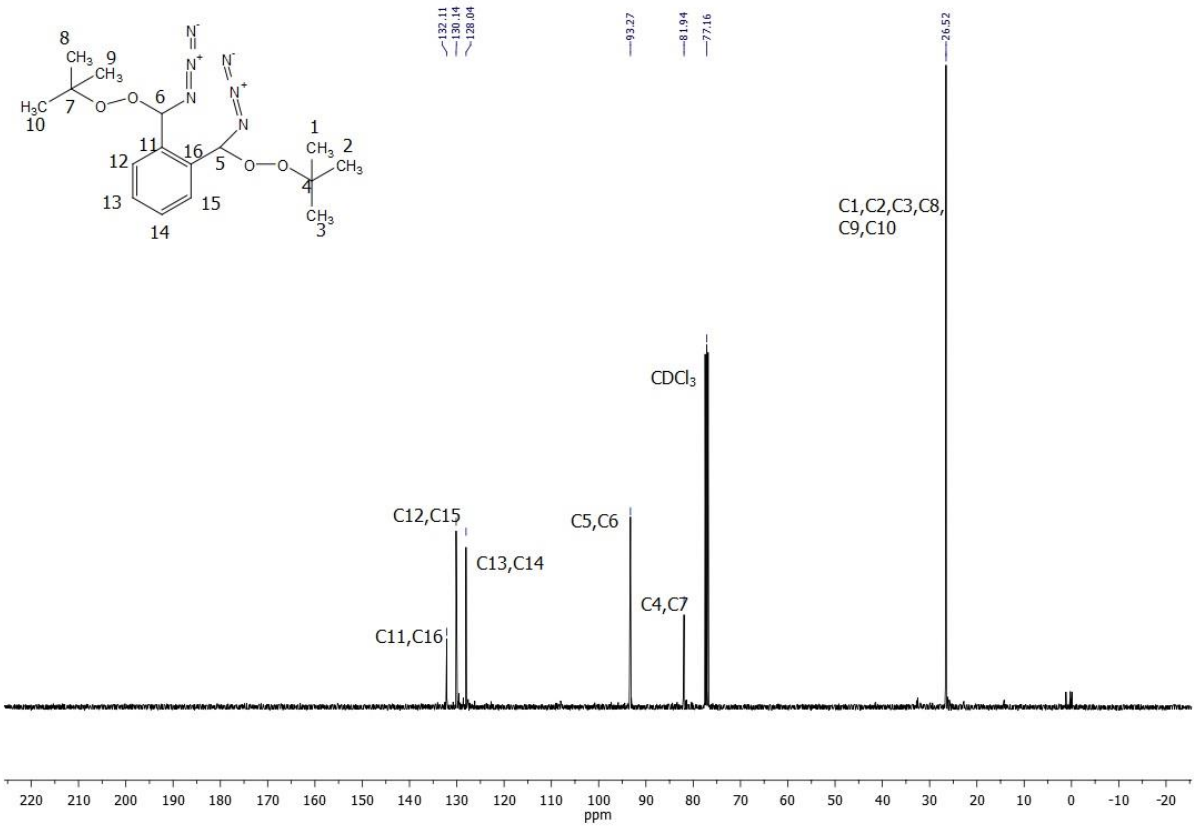
C1,C2,C3,C8,
C9,C10
CDCl3
C12,C15
C13,C14
C5,C6
C4,C7
C11,C16
ppm

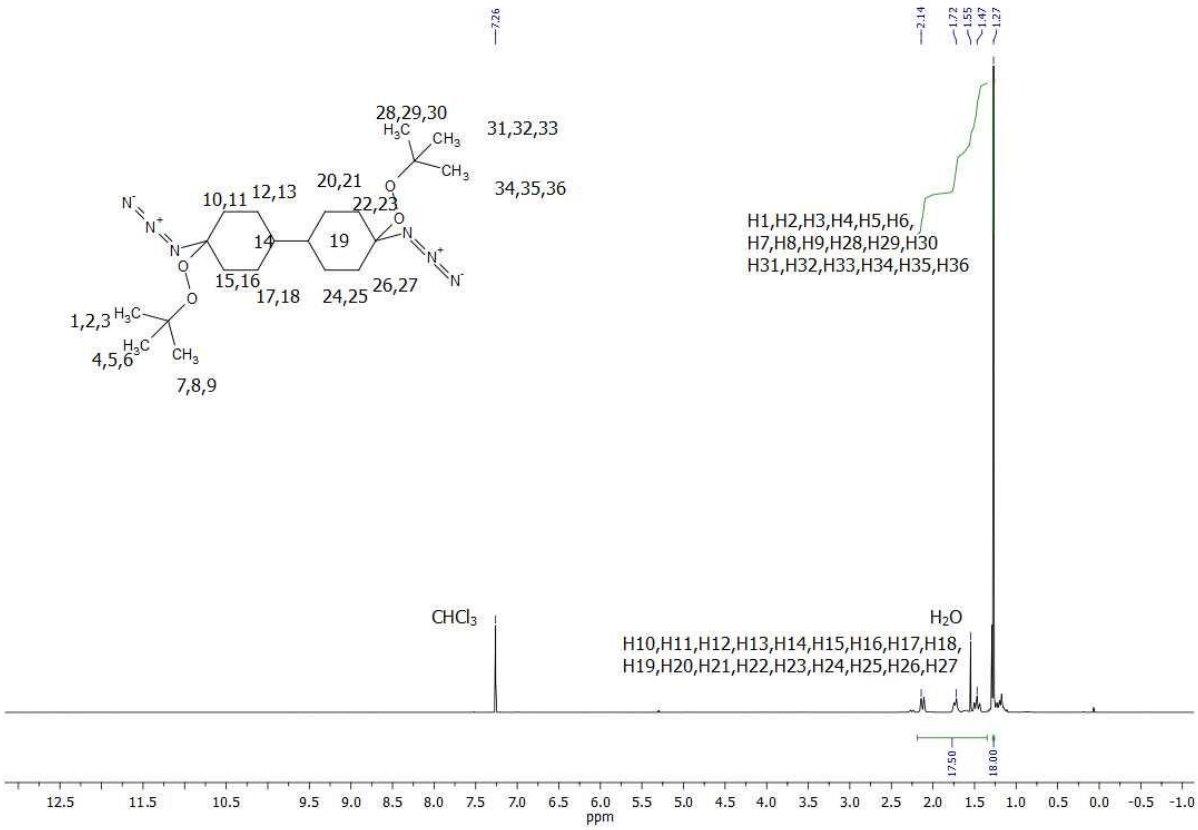
7.26
2.14
1.72
1.55
1.47
1.27
28,29,30
31,32,33
34,35,36
10,11
12,13
20,21
22,23
14
19
15,16
17,18
24,25
26,27
1,2,3
4,5,6
7,8,9
H1,H2,H3,H4,H5,H6,
H7,H8,H9,H28,H29,H30
H31,H32,H33,H34,H35,H36
CHCl3
H2O
H10,H11,H12,H13,H14,H15,H16,H17,H18,
H19,H20,H21,H22,H23,H24,H25,H26,H27
17.50
18.00
ppm

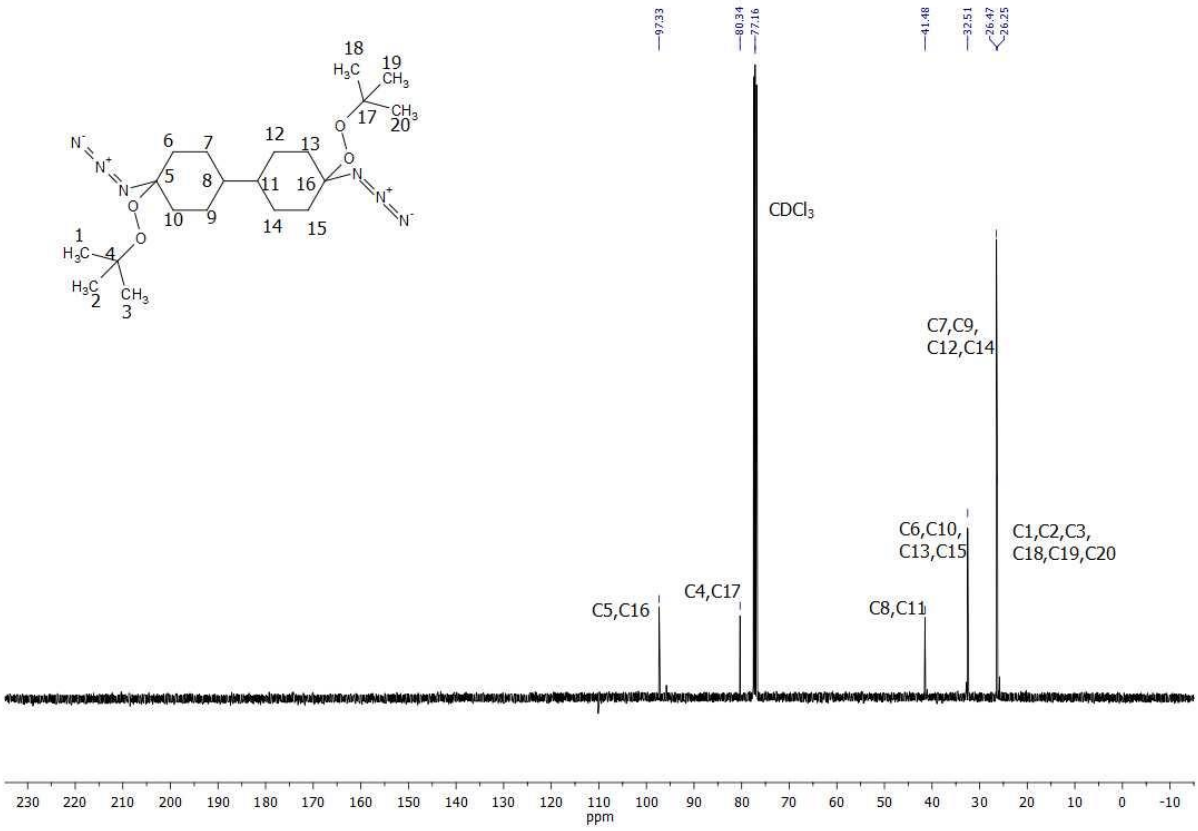
97.33
80.34
77.16
41.48
32.51
26.47
26.25
18
19
17
20
6
7
12
13
5
8
11
16
10
9
14
15
1
4
2
3
CDCl3
C7,C9,
C12,C14
C6,C10,
C13,C15
C1,C2,C3,
C18,C19,C20
C4,C17
C5,C16
C8,C11
ppm

2. X-ray Diffraction

For all compounds, an Oxford Xcalibur3 diffractometer with a CCD area detector was employed for data collection using Mo-Kα radiation (λ = 0.71073 Å). By using the Crystalispro software[S1] the data collection and reduction were performed. The structures were solved by direct methods (SIR-92[S2], SIR-97[S3] and SHELXS-97[S4]) and refined by fullmatrix least-squares on *F*2 (SHELXL [S4]) and finally checked by using the PLATON software [S5] integrated in the WinGX software suite. The non-hydrogen atoms were refined anisotropically and the hydrogen atoms were located and freely refined. The absorptions were corrected by a SCALE3 ABSPACK multiscan method [S6]. All DIAMOND2 plots are shown with thermal ellipsoids at 50% probability level and hydrogen atoms are shown as small spheres of arbitrary radius.

	9
Formula	$C_{14}H_8N_2O_8$
FW [g/mol]	332.22
Crystal system	monoclinic
Space Group	P21/c
Color / Habit	colorless plate
Size [mm]	0.20 x 0.50 x 0.50
a [Å]	15.058(2)
b [Å]	8.7366(10)
c [Å]	15.720(3)
α [°]	90
β [°]	110.299(18)
γ [°]	90
V [$Å^3$]	1939.6(6)
Z	4
$\rho_{cacl.}$ [g cm^{-3}]	1.248
μ [mm^{-1}]	0.092
F (000)	776
$\lambda_{MoK\alpha}$ [Å]	0.71073
T [K]	173
ϑ min max [°]	4.3, 26.0
Dataset h; k; l	−13:18; −10:9; −19:10
Reflect. coll.	8164
Independ. refl.	3787
R_{Int}	0.062
Reflection obs.	3787
No. parameters	265
R_1 obs.	0.0660
wR_2 (all data)	0.1696
S	0.99
Resd. Dens. [e $Å^{-3}$]	−0.20,0.34
Device type	Oxford Xcalibur3 CCD
Solution	SIR-92
Refinement	SHELXL-97
Absorption corr.	multi-scan
CCDC	1484073

3. Heat of Formation Calculations

All calculations were carried out using the Gaussian G09W (revision A.02) program package.[S7] The enthalpies (H), listed in Table S3, were calculated using the complete basis set (CBS) method of Petersson and coworkers in order to obtain accurate energies. The CBS models uses the known asymptotic convergence of pair natural orbital expressions to extrapolate from calculations using a finite basis set to the estimated complete basis set limit. CBS-4 begins with a HF/3-21G(d) structure optimization and the zero point energy is computed at the same level. Subsequently it uses a large basis set SCF calculation as a base energy, and a MP2/6-31+G calculation with a CBS extrapolation to correct the energy through second order. A MP4(SDQ)/6-31+(d,p) calculation is used to approximate higher order contributions. In this paper we applied the modified CBS-4M method (M referring to the use of Minimal Population localization) which is a re-parameterized version of the original CBS-4 method and also includes some additional empirical corrections. [S8] The the gas-phase enthalpies of species M were computed according to the atomization energy method (eq.1).

$$\Delta_f H^\circ_{(g,\,M,\,298)} = H_{(Molecule,\,298)} - \Sigma H^\circ_{(Atoms,\,298)} + \Sigma \Delta_f H^\circ_{(Atoms,\,298)} \quad \textbf{(1)}$$

$H^0_{Atoms,298}$ for the corresponding Atoms were determined experimentally and are reported in the literature. ${}_fH^0_{(Atoms,298)}$ are calculated theoretically [S10].

Atom	$\Delta_f H^0_{g,Atom}$ [kcal·mol^{-1}]	$H^0_{g,Atom}$ [Hartree·atom^{-1}]
H	52.103	−0.500991
C	171.29	−37.786156
N	112.97	−54.522462
O	59.56	−74.991202

Standard molar enthalpies of formation were calculated using $\Delta_f H^0_{g,Atom}$ and the standard molar enthalpies of sublimation (estimated by applying Trouton´s rule, Equation ggggg) [S11].

$$\Delta_f H^0_M = \Delta_f H^0_{(g,M,298)} - \Delta_{sub} H^0_M = \Delta_f H^0_{(g,M,298K)} - 188 \cdot T \left[\frac{J}{mol}\right]$$

Where T [K] is either the melting point or the decomposition temperature (if the compounds do not melt before they decompose)

Detonation parameters

The Chapman-Jougeut (C-J) characteristics, (i.e. heat of detonation, $\Delta_E U^0$, detonation temperature T_{C-J}, detonation pressure P_{C-J}, detonation velocity V_{C-J}) based on the calculated $\Delta_f H^0_M$ values and the theoretical maximum densities were computed using the EXPLO5 V6.02 thermochemical computer code [S12]. Calculations for explosives assume ideal behavior. The estimation of the detonation parameters is based on the chemical equilibrium steady-state model detonation. The Beckler-Kistiakowsky-Wilson equation of state (BKWEOS) with the following sets of constants: $\alpha = 0.5, \beta = 0.38, \kappa = 9.4, and\ \Theta = 4120$ for gaseous detonation products and the Murnaghan equation of state for condensed products (compressible solids and liquids) were applied. The calculation of the equilibrium composition of the detonation products uses modified White, Johnson and Dantzig´sfree energy minimization technique.

The specific energies of explosives(f) were calculated according to the equation for ideal gase equation of state where isochronic condition were assumed.

$$f = p_e \cdot V = n \cdot R \cdot T_0 \left[\frac{kJ}{kg}\right]$$

Where p_e is the maximum pressure through the explosion, V is the volume of detonation gases ($m^3 \cdot kg^{-1}$), n is the number of moles of gas formed by the explosion per kilogram of explosive (*Volume of Explosive Gases*), R is the ideal gas constant and T_C is the absolute temperature of the explosion [S12], [S13].

4. References

[S1] *CrysAlisPro*, Oxford Diffraction Ltd., version 171.33.41, **2009**.

[S2] *SIR-92*, *A program for crystal structure solution*: A. Altomare, G. Cascarano, C. Giacovazzo, A. Guagliardi, *J. Appl. Crystallogr.* **1993**, *26*, 343.

[S3] a) A. Altomare, G. Cascarano, C. Giacovazzo, A. Guagliardi, A. G. G. Moliterni, M. C. Burla, G. Polidori, M. Camalli, R. Spagna, *SIR97*, **1997**; b) A. Altomare, M. C. Burla, M. Camalli, G. L. Cascarano, C. Giacovazzo, A. Guagliardi, A. G. G. Moliterni, G. Polidori, R. Spagna, *J. Appl. Crystallogr.* **1999**, *32*, 115–119.

[S4] a) G. M. Sheldrick, *SHELX-97*, University of Göttingen, Göttingen, Germany, **1997**; b) G. M. Sheldrick, *Acta Crystallogr., Sect. A* **2008**, *64*, 112–122.

[S5] A. L. Spek, *PLATON*, *A Multipurpose Crystallographic Tool*, Utrecht University, The Netherlands, **1999**.

[S6] *SCALE3 ABSPACK – An Oxford Diffraction program* (1.0.4, gui: 1.0.3), Oxford Diffraction Ltd., **2005**.

[S7] Gaussian 09, M. J. Frisch, G. W. Trucks, H. B. Schlegel, G. E. Scuseria, M. A. Robb, J. R. Cheeseman, G. Scalmani, V. Barone, B. Mennucci, G. A. Petersson, H. Nakatsuji, M. Caricato, X. Li, H. P. Hratchian, A. F. Izmaylov, J. Bloino, G. Zheng, J. L. Sonnenberg, M. Hada, M. Ehara, K. Toyota, R. Fukuda, J. Hasegawa, M. Ishida, T. Nakajima, Y. Honda, O. Kitao, H. Nakai, T. Vreven, J. A. Montgomery, Jr., J. E. Peralta, F. Ogliaro, M. Bearpark, J. J. Heyd, E. Brothers, K. N. Kudin, V. N. Staroverov, R. Kobayashi, J. Normand, K. Raghavachari, A. Rendell, J. C. Burant, S. S. Iyengar, J. Tomasi, M. Cossi, N. Rega, J. M. Millam, M. Klene, J. E. Knox, J. B. Cross, V. Bakken, C. Adamo, J. Jaramillo, R. Gomperts, R. E. Stratmann, O. Yazyev, A. J. Austin, R. Cammi, C. Pomelli, J. W. Ochterski, R. L. Martin, K. Morokuma, V. G. Zakrzewski, G. A. Voth, P. Salvador, J. J. Dannenberg, S. Dapprich, A. D. Daniels, Ö. Farkas, J. B. Foresman, J. V. Ortiz, J. Cioslowski, and D. J. Fox, Gaussian, Inc., Wallingford CT, 2009.

[S8] a) J. W. Ochterski, G. A. Petersson, J. A. Montgomery, *J. Chem. Phys*. **1996**, *104*, 2598–2619; b) J. A. Montgomery, M. J. Frisch, J. W. Ochterski, G. A. Petersson, *J. Chem. Phys.* 2**000**, *12*, 6532–6542.

[S9] P. J. Lindstrom, W. G. Mallard (Editors), NIST Standard Reference Database Number 69, http://webbook.nist.gov/chemistry/ (Juni **2011**).

[S10] P. J. Linstorm, W. G. Mallard, *National Institute of Standards and Tehcnology*, Gaithersburg, MD, 20899.

[S11] a)F. Trouton, *Philos. Mag. (1876-1900)* **1884**, *18*, 54-57; b) M. S. Westwell, M. S. Searle, D. J. Wales, D. H. Willimas, *J. Am. Chem. Soc.* **1995**, *117*, 5013-5015.

[S12] M. Suceska, *Explo5 Version Users´s Guide*, January **2013**.

[S13] a)R. Meyer, J. Köhler, A. Homburg, *Explosives*, 6thedn. , Wiley, Weinheim, **2007**, p. 291-292; b)T. M. Klapötke, *Chemistry of High-Energy Materials*, de Gruyter, Berlin, **2015**

ChemPubSoc Europe

DOI: 10.1002/slct.201601114

Chemistry SELECT Full Papers

Inorganic Chemistry

Energetic Materials - Nitrated Phenyl Peroxy Anhydrides as Peroxide Based Explosives with Relatively High Densities and Thermal Stabilities

Thomas M. Klapötke,* Benedikt Stiasny, and Jörg Stierstorfer[a]

Nine different nitrated phenyl peroxy anhydrides were synthesized using two different strategies and crystal structures of two compounds were determined. Sensitivities of the compounds toward impact, friction and electrostatic discharge were measured and the thermal stability was determined. Some of the compounds are remarkable insensitive and they show relatively high thermal decomposition points for organic peroxides. Detonation parameters and performance data were calculated using the EXPLO5 program yielding performance values in the range of trinitrotoluene (TNT).

Introduction

Peroxy anhydrides are an interesting class of molecules which features the characteristic CO(OO)CO-moiety. The most prominent example is dibenzoyl peroxide which finds excessive application as initiator for radical polymerizations, since it is known to decompose in radicals.[1] However, detailed studies about the decomposition products of different, mostly polar substituted peroxy anhydrides revealed, that the compounds can decompose homolytically as well as heterolytically depending on the polarity of the environment.[2–3] Another application of dibenzoyl peroxide is the treatment of acne.[4] Peroxy anhydrides can also be used for the formation of C-C-bonds by exposing them to light, electric current or heat.[5] A very recent paper reports on the use of peroxyanhydrides as reagents for the synthesis of unsaturated esters starting from 1,3-dienes.[6] However there are a lot of other molecules which feature this moiety. Even cyclic derivaties are known, for example in the form of diphenoyl peroxide.[7] In this study, the compound was used for the production of electronically excited states. Another peroxy anhydride that is particularly interesting with respect to energetic materials is peroxy trifluoroacetic acid anhydride, which can be prepared by the reaction of trifluoroacetic acid and sodium peroxide at low temperatures.[8] This molecule has a positive oxygen balance which means it carries more oxygen in it as is needed for its complete combustion and could therefore be used as an oxidizer. However it is extremely sensitive toward outer stimuli and hydrolyses at ambient temperature into trifluoroacetic acid and peroxy trifluoroacetic acid.[8] The synthesis of organic peroxy anhydrides very often is performed by reacting the corresponding acyl chloride with aqueous hydrogen peroxide solution and an aqueous solution of sodium hydroxide[9–10] in situ (S_N2t-mechanism) forming sodium peroxide. This reacts via nucleophilic substitution with the acyl chlorides. The sodium peroxide can also be used directly, but this and the reaction conditions mentioned before only lead to symmetrically substituted molecules.[11] If dissymmetric substituted molecules are desired, the peroxy acids have to be reacted with the corresponding acyl chloride.[9] The organic residue in this reactions can be varied over a large scale of different aliphatic and aromatic backbones[6,10,12–13] but with respect to energetic materials, nitrated aromatic compounds are the most promising ones since they are relatively easy to prepare and stable at ambient conditions. An example for those compounds is synthesized by the reaction of a cyclic acid anhydride with p-nitro perbenzoic acid.[14] However this molecule cannot be considered as energetic since the alkyl content is too high. In addition to the before mentioned advantages the nitro group delivers a high density, which is beneficial for a potential application as an energetic material. Therefore, nitro aryl substituted molecules with as less as possible not energetic C, H content might form suitable energetic materials. One existing example for such nitrated molecules is the peroxy anhydride derived from 4-nitrobenzoic acid. This compound is also commercially available and was investigated for use as initiation reagent for radical polymerization processes.[15] In this paper we would like to give an insight in the synthesis and characterization of this and some other potentially energetic nitroaryl peroxy anhydrides and investigate them comparatively concerning their performances as energetic materials as well as their sensitivities toward outer stimuli namely impact, friction, electrostatic discharge and heat.

Results and Discussion

Since this study was started with the intention to investigate peroxy anhydrides as possible energetic materials, we choose to limit the synthesis and determination of the different properties to compounds, which have at least slightly energetic ar-

[a] T. M. Klapötke, B. Stiasny, J. Stierstorfer
Department of Chemistry
Ludwig-Maximilian University of Munich
Butenandtstr. 5–13, D-81377 München, Germany
E-mail: tmk@cup.uni-muenchen.de

Supporting information for this article is available on the WWW under http://dx.doi.org/10.1002/slct.201601114

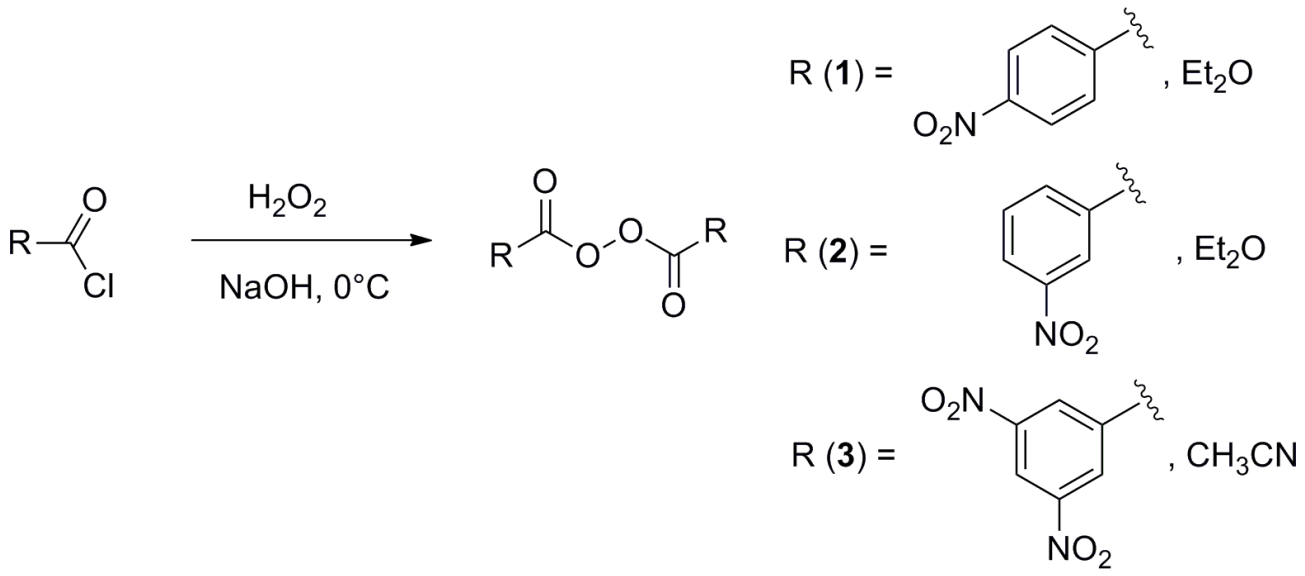

Scheme 1. Synthetic pathway for the preparation of **1**, **2** and **3**.

omatic residues and did not investigate compounds like dibenzoyl peroxide.

Synthesis

Eight new peroxy anhydrides and one literature known molecule for comparison were prepared using two different strategies. Bis-4-nitrobenzoyl peroxide (**1**),[15] bis-3-nitrobenzoyl peroxide (**2**) and bis-3,5-dinitrobenzoyl peroxide (**3**) were prepared by reacting the aqueous corresponding acyl chlorides with excessive amounts of 30% H_2O_2 solution in diethyl ether, respectively acetonitrile under the addition of a slightly excess of aqueous NaOH solution at 0 °C. The synthetic pathway is displayed in Scheme 1.

The reaction products precipitated instantly and were filtered off. After washing the solid residues with water and subsequently diethyl ether, the compounds were air dried and colorless solids were obtained in yields between 13% (**3**) and 37% (**1**). In the case of compound **3** a concurrent decomposition reaction takes place resulting in the formation of a red oil, what explains the poorer yield compared to compounds **1** and **2.**

The mixed binuclear peroxy anhydrides 3-nitrobenzoyl-4-nitrobenzoyl peroxide (**4**), 3,5-dinitrobenzoyl-3-nitrobenzoyl peroxide (**5**) and 3,5-dinitrobenzoyl-4-nitrobenzoyl peroxide (**6**) were prepared by reacting acyl chlorides with the corresponding peroxy acids in diethyl ether at 0 °C. The synthetic pathway is displayed in Scheme 2. The peroxy acids were prepared according to a literature procedure.[16] A base is still needed to catch the HCl formed during the condensation reaction. Since pyridine turned out to be too weak for this task, an aqueous NaOH solution in slight excess was applied. The reaction products again precipitated instantly. The yields obtained are between 53% (**5**) and 61% (**6**).

It is also possible to exchange the functionalities, but with the peroxy acid respectively acyl chloride combination displayed in Scheme 2 the higher yields were obtained.

The third topic examined in this paper is the preparation of peroxy anhydrides derived from terephthalic acid. For this reactions, terephthaloyl chloride was reacted with 4-nitroperbenzoic acid, 3,5-dinitroperbenzoic acid and 3-nitroperbenzoic acid in diethyl ether at 0 °C under the addition of slightly excessive aqueous NaOH solution resulting in the formation of bis-4-nitrobenzoyl-terephthaloyl peroxide (**7**), bis-3,5-dinitrobenzoyl-terephthaloyl peroxide (**8**) and bis-3-nitrobenzoyl terephthaloyl peroxide (**9**). Scheme 3 displays the synthetic pathway. The products again precipitated instantly from the reaction mixture as colorless solids, were filtered off and air dried after washing with water and diethyl ether. The obtained yields are between 14% (**8**) and 40% (**9**).

Since the starting materials and the products all behave very similar toward standard analytical methods, the best way to prove product formation is to light a small sample on the spatula tip. A test has to be considered as positive, when the compound intensively decomposes under the formation of smoke.

Crystal structures

Single crystals for compounds **2** and **3** were grown form acetone and acetonitrile, respectively, at room temperature. Details of the low temperature (123 K) X-ray measurements and refinements are given in the SI. Figure 1 shows the molecular structures of the respective compounds.

The compounds crystallize in the common space groups $P-1$ (**2**) and $C2/c$ (**3**). The observed densities are 1.65 g cm^{-3} (**2**) and 1.75 g cm^{-3}, respectively, (**3**) and therefore significantly higher than that of commonly known organic peroxides like TATP (1.22 g cm^{-3})[17] which is beneficial for their use as en-

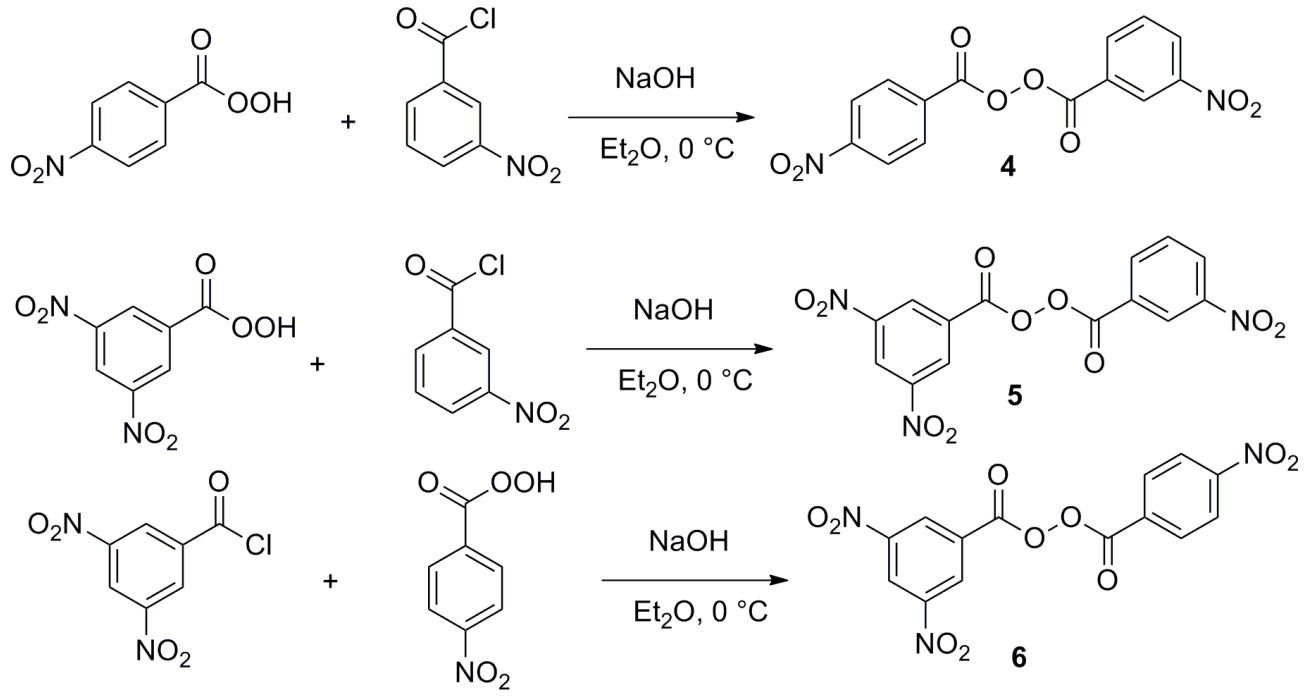

Scheme 2. Synthetic pathway for the preparation of **4**, **5** and **6**.

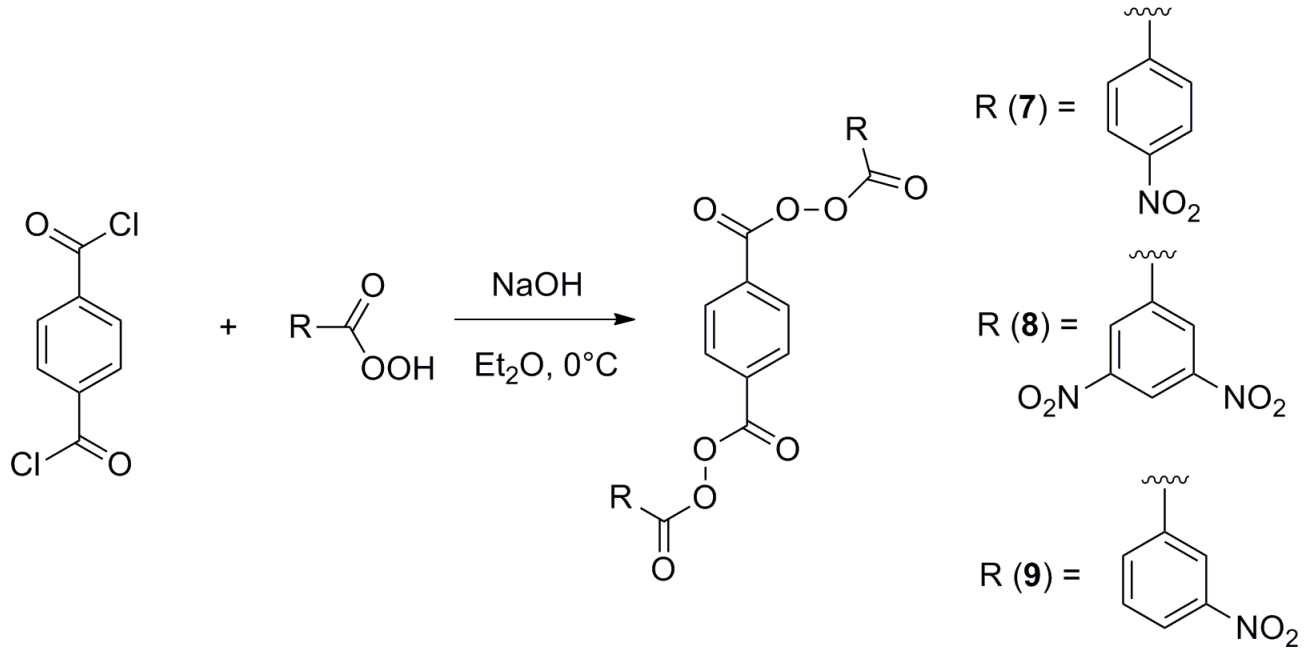

Scheme 3. Synthetic pathway for the preparation of **7**, **8** and **9**.

ergetic materials. They even are in the range or higher than the density of the commonly known and widely used secondary explosive trinitrotoluene (TNT) (1.654 g cm^{-3})[18] and close to the more potent RDX (1.82 g cm^{-3}).[12] The O–O bond distance is in the range between 144.1 and 145.3 pm. These values are in accurate accordance with values for other organic peroxy anhydrides published in the literature[19] and are also in the same range as the O–O bond distance of hydrogen peroxide (145.3 pm[20]). The O–O–C bond angles have values between 107.2° and 108.0° which is slightly lower than literature values (110.1° for the *m*-chloro substituted analogue).[19] The bond distances for the nitro group are in the range of 147 pm for C–N and 122 pm for N–O which are normal values for aromatic nitro compounds.[21–22] The same is true for the bond angles which

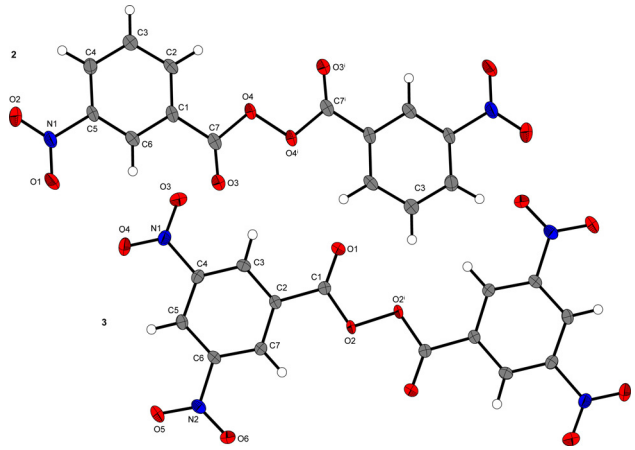

Figure 1. Molecular structures for compounds **2** and **3** and their labeling schemes. Thermal ellipsoids represent the 50% probability level. Both compounds do have a centre of inversion at the middle of the O–O bond. Symmetry codes: **2:** (i): -x, 1-y, -z; **3:** (i): -x, 2-y, -z.

properties of the compounds. Impact sensitivities are in the range between 1 and 5 J. Conspiciously, the biperoxides are more sensitive (1 J) in comparison to the monoperoxides (1.5 - 4 J), which is a direct result of the increased peroxide percentage. But according to BAM (Bundesamstalt für Materialforschung und Prüfung) these compounds all have to be classified as extremely sensitive toward impact. However in contrast to commonly used primary explosives and most peroxides they only show decomposition and do not explode/fulminate which makes them saver. Friction sensitivities for compounds **1–6** are in the range of 240 N to 360 N. According to the BAM regulations they have to be classified as slightly sensitive to insensitive. For compounds **7**, **8** and **9**, the friction sensitivities are between 8 and 18 N. This means the compounds must be classified as very sensitive (**8**) to extremely sensitive (**7**), (**9**). This obvious difference can again most likely be explained with the additional peroxy group of the latter compounds. The ESD value for all compounds is much higher than

Table 1. Energetic properties of compounds **1** to **9**

	1	**2**	**3**	**4**	**5**	**6**	**7**	**8**	**9**
Formula	$C_{14}H_8N_2O_8$	$C_{14}H_8N_2O_8$	$C_{14}H_6N_4O_{12}$	$C_{14}H_8N_2O_8$	$C_{14}H_7N_3O_{10}$	$C_{14}H_7N_3O_{10}$	$C_{22}H_{12}N_2O_{12}$	$C_{22}H_{10}N_4O_{16}$	$C_{22}H_{12}N_2O_{12}$
F_W[gmol^{-1}]	332.22	332.22	422.20	332.22	377.21	377.21	496.34	586.32	496.34
IS [J][a]	3	3	1.5	5	4	4	1	1	1
FS [N][b]	240	$\geq$360	240	$\geq$360	$\geq$360	$\geq$360	8	18	9
ESD [J][c]	0.300	0.108	0.300	0.15	0.150	0.100	0.056	0.064	0.050
Ω_{CO2} [%][d]	−115.6	−115.5	−72.0	−115.6	−91.2	−91.2	−122.5	−90.1	−122.5
T_{dec} [°C][e]	158	140	164	125	143	141	164	163	149
ρ [g cm^{-3}][f]	1.61/pyc.	1.608/X-ray	1.718/X-ray	1.67/pyc.	1.70/pyc.	1.69/pyc.	1.46/pyc.	1.51/pyc.	1.45/pyc.
$\Delta_f H_m$ [kJ mol^{-1}][g]	−415	−406	−410	−404	−405	−405	−761	−752	−752
$\Delta_f U$ [kJ kg^{-1}][h]	−1182	−1155	−906	−1149	−1008	−1009	−1468	−1219	−1449
EXPLO 5 6.02values									
$\Delta_{ex}U^0$[kJ kg^{-1}][i]	−3810	−3832	−4555	−3870	−4259	−4253	−3485	−4010	−3492
T_{det} [K][j]	2686	2697	3311	2693	3024	3025	2545	3015	2552
P_{CJ} [GPa][k]	13	13	20	9	18	17	9	13	9
V_{det}[ms^{-1}][l]	6129	6130	7087	6395	6796	6757	5315	6007	5284
V^0 [Lkg^{-1}][m]	536	536	566	528	547	549	531	572	533

[a] Impact sensitivity according to BAM drophammer (method 1 of 6). [b] Friction sensitivity according to BAM friction tester (method 1 of 6). [c] Electrostatic discharge sensitivity (OZM ESD tester). [d] Oxygen balance. [e] Melting point resp. Temperature of decomposition according to DTA (onset temperatures at a heating rate of 5 °C/min). [f] Room temperature X-ray densities. Those were calculated by the low temperature X-ray values using the equation $\{\rho 298\ K = \rho T/[1 + \alpha_V(298 - T^0)]$; $\alpha_V = 1.5\ 10^{-4}\ K^{-1}\}$. [g] Calculated heat of formation using the atomization method and CBS-4 M electronic enthalpies. [h] Energy of formation [i] Heat of detonation. [j] Detonation temperature. [k]Detonation pressure. [l] Detonation velocity. [m] Volume of gas after detonation

have values around 118° (C–N-O) and 125° (O–N-O).[21–22] The CO(OO)CO moiety is almost planar for both compounds **2** and **3** with torsion angles between 0 and 1°. In compound **2** the nitro groups are twisted with a torsion angle of −7.00°. For compound **3** again all nitro groups are twisted out of the molecular plane. One torsion angle is −9.9° the second one is 20.9°.

Energetic properties

The performance data of the compounds were calculated using the EXPLO5 program (version 6.02). The input heats of formation were calculated using the atomization method based on CBS-4 M electronic enthalpies. Table 1 gathers the energetic

the maximum electrostatic potential of the human body (20 mJ).[23] The detonation pressures and detonation velocities are compared to standard explosives TNT (6950 ms^{-1}, 21 GPa) and RDX (hexogen) (8750 ms^{-1}, 35 GPa).[24] Most of the synthesized compounds have calculated detonation velocities between 5300 and 6800 ms^{-1} which are lower than the ones of TNT and RDX. Compound **3** however has a calculated detonation velocity of 7087 ms^{-1} which is slightly better than that of TNT. Conspicuously the biperoxides have detonation velocities between 5300 and 6000 ms^{-1} and by this perform weaker than the monoperoxides. The total difference is quite small, however this general tendency can be recognized. The difference can be explained with the lower densities of the biperoxides. Compound **3** has the highest detonation pressure of all

the synthesized compounds with a calculated value of 20 GPa. This is close to the detonation pressure of TNT but only about 60% of the detention pressure of RDX. The synthesized compounds have decomposition points in a temperature range between 125 and 164 °C. While compound **4** features a decomposition point of 125 °C which is in the normal although higher range for an organic peroxide, the other decomposition points determined, especially for **3**, **7** and **8** with more than 160 °C are remarkable high for compounds containing a peroxide backbone.

Conclusions

Eight new and one literature known peroxy anhydrides namely bis-4-nitrobenzoyl peroxide (**1**), bis-3-nitrobenzoyl peroxide (**2**), bis-3,5-dintorbenzoyl peroxide (**3**), 3-nitrobezoyl-4-nitrobenzoyl peroxide (**4**), 3,5-dinitrobenzoyl-3-nitrobenzoyl peroxide (**5**), 3,5-dinitrobenzoyl-4-nitrobenzoyl peroxide (**6**), bis-4-nitrobenzoyl-terephthaloyl peroxide (**7**), bis-3,5-dinitrobenzoyl-terephthaloyl peroxide (**8**) and bis-3-nitrobenzoyl terephthaloyl peroxide (**9**) were prepared following an established synthetic procedure as well as a slight modification of it and tested regarding their sensitivities towards outer stimuli. Some of the prepared compounds can find possible application as radical initiators. Compounds **2** to **6** are as sensitive or slightly less sensitive as commercial available **1**. Compounds **7**, **8** and **9** however are too sensitive for a possible application. They are also the weaker performing energetic materials, although they feature two and not just one peroxy group, what can be explained by the lower density. Moreover the thermal stability of most synthesized compounds is remarkable high for organic peroxides and in contrast to most other peroxides they are long-term stable at room temperature. The monoperoxides also feature only low sensitivities toward friction. Another striking advantage is the remarkable density which is mainly based on the contained nitro groups and the accumulation of many heavy hetero atoms in the peroxy anhydride moiety. The CO(OO)CO moiety is also oxygen rich. These properties make alternative peroxy anhydrides potentially suitable for application as energetic materials especially in the oxidizer sector, where high oxygen contents are needed but the requirements to thermal stability and detonation performance are not extreme. However the high sensitivity towards impact is a significant drawback for possible application as an energetic material even though the compounds only decompose without any noticeable sound and do not detonate.

Supporting information

Full experimental details and characterization data are included in the SI. A table about crystallographic details with CCDC numbers is also part of the SI as well as NMR spectra and calculation details.

Acknowledgements

Financial support of this work by the Ludwig-Maximilian University of Munich (LMU), the Office of Naval Research (ONR) under grant no. ONR.N00014-16-1-2062, and the Bundeswehr – Wehrtechnische Dienststelle für Waffen und Munition (WTD 91) under grant no. E/E91S/FC015/CF049 is gratefully acknowledged. The authors acknowledge collaborations with Dr. Mila Krupka (OZM Research, Czech Republic) in the development of new testing and evaluation methods for energetic materials and with Dr. Muhamed Suceska (Brodarski Institute, Croatia) in the development of new computational codes to predict the detonation and propulsion parameters of novel explosives. We are indebted to and thank Drs. Betsy M. Rice, Jesse Sabatini and Brad Forch (ARL, Aberdeen, Proving Ground, MD) for many inspired discussions. The authors thank Stefan Huber for sensitivity measurements.

Keywords: crystal structure elucidation · energetic materials · performance values · peroxy anhydrides · sensitivities

[1] H. Klenk, P. H Götz, R. Siegmeier, W. Mayr, *Ullmanns Encyclopedia of Industrial Chemistry*, Weinheim **2007**, Wiley-VCH.
[2] J. E. Leffler, *J. Am. Chem. Soc.* **1950**, *72*, 67-72.
[3] J. E. Leffler, C. C. Petropoulos *J. Am Chem. Soc.* **1957**, *79*, 3068-3071.
[4] T. Simonart, *Am. J. Clin. Dermatol.* **2012**, 13, 6, 357–364.
[5] M. Feldhues, H. J. Schäfer, *Tetrahedron* **1985**, *41*, 4195-4212.
[6] Y. Li, Y. Han, H. Xiong, N. Zhu, B. Quian, Ch. Ye, E. A. B. Kantchev, H. Bao, *Org. Lett.* **2016**, *18*, 392–395.
[7] J.-Y. Koo, G. B. Schuster, *J. Am. Chem. Soc.* **1978**, *100*, 4496-4503.
[8] R. Kopitzky, H. Willner, A. Hermann, H. Oberhammer, *Inorg. Chem.* **2001**, *40*, 2693–2698.
[9] M. Feldhues, H. J. Schäfer, *Tetrahedron* **1985**, *41*, 4195–4212.
[10] Ch. Quiang, D. Lin, Y. Deng, X.Q. Zhang, H. Jiang, G. Miao, X. Tang, W. Zeng, *Org. Biomol. Chem.* **2014**, *12*, 5866–5875.
[11] D. Li, N. Xu, Y. Zhang, L. Wang, *Chem. Commun.* **2014**, *50*, 14862–14865.
[12] S.-G. Lee, *J. Chem. Soc.* **1993**, *2*, 1361-1372.
[13] G. C. Flowers, J. E. Leffler, *J. Org. Chem.* **1985**, *50*, 4406-4408.
[14] C. G. Little, G. B. Schuster, *J. Org. Chem.* **1986**, *11*, 2050-2055.
[15] I. S. Voloshanovskii, Yu. N. Anisimov, S. S. Ivanchev, *Zhournal Obshchei Khimii* **1968**, *48*, 2364–2368.
[16] N.-D. H. Gamage, B. Stiasny, J. Stierstorfer, P. D. Martin, T. M. Klapötke, C. H. Winter, *Chem. Eur. J.* **2016**, *22*, 2582-2585.
[17] *Römp Online*, Thieme, Stuttgart, Germany, version 2.3.15
[18] *GESTIS Database,* www.dguv.de, accessed 13th June 2016.
[19] A. Syed, P. Umrigar, E. D. Stevens, G. W. Griffin, *Acta Cryst.* **1984**, *C40*, 1458–1460.
[20] W. R. Busing, H. A. Levy, *J. Chem. Phys.* **1965**, *42*, 3054–3059.
[21] D. Izsak, T. M. Klapötke, A. Preimesser, J. Stierstorfer, *Z. Anorg. Allg. Chem.* **2016**, *642*, *(1)*, 48–55.
[22] T. M. Klapötke, T. G. Witkowski, *ChemPlusChem.* **2016**, *81*, 357-360.
[23] T. M. Klapötke, *Chemistry of High-Energy Materials*, de Gruyter, Berlin/Boston, 2nd edition, **2012**.
[24] T. M. Klapötke, *Chemie der Hochenergetischen Materialien*, de Gruyter, Berlin, 1. Auflage, **2009**.

Submitted: August 10, 2016
Accepted: August 16, 2016

Supplementary Information

Table of Contents

1. Experimental details

CAUTION! All investigated compounds are potentially explosive materials, although no hazards were observed during preparation and handling these compounds. Nevertheless, this necessitates additional meticulous safety precautions (earthed equipment, Kevlar gloves, Kevlar sleeves, face shield, leather coat, and ear plugs).

General: All chemicals were received from Sigma–Aldrich and used without further purification. Sensitivity measurements were performed on a BAM-drophammer, a BAM friction tester and OZM ESD- tester. Infrared spectra were recorded on a Perkin–Elmer One FT-IR Spectrum BX II with a Smith ATR Dura Sample IRII. NMR spectra were recorded on a Bruker 400 MHz-spectrometer

operating at 400 MHz for proton spectra. Melting points and decomposition points were recorded on an OZM Research DTA 552-Ex instrument.

Acyl chlorides were prepared starting from the corresponding acids by reacting them with thionyl chloride and catalytic amounts of dimethylformamide at reflux conditions and subsequent removal of the excessive thionyl chloride. Peracids were prepared by procedures given in the literature. [S1], [S2]

Bis-4-nitrobenzoyl peroxide (1) 1.000 g 4-nitrobenzoyl chloride (5.380 mmol) is dissolved in 10 mL diethyl ether and 0.32 mL of a 30% H_2O_2 solution (0.38 g, 3.34 mmol) are added. This is followed by the drop wise addition of a solution of 0.26 g NaOH (6.61 mmol) in 5 mL water. The reaction mixture is stirred at 0 °C for 30 minutes. A white precipitate is formed which is filtered off, washed with water and diethyl ether and air dried. Yield: 0.670 g (37%). $T_{dec.}$(onset/ 5 °C/min) = 158 °C. IR (ATR) $\tilde{\nu}$ (cm^{-1}) = 3109 (w), 3084 (w), 3052 (w), 2361 (w), 1950 (w), 1793 (m), 1777 (s), 1606 (m), 1522 (s), 1491 (m), 1414 (w), 1405 (m), 1347 (s), 1319 (m), 1303 (w), 1220 (s), 1181 (m), 1133 (w), 1115 (w), 1108 (w), 1077 (w), 1026 (m), 1005(s), 924 (w), 869 (m), 857 (s), 771 (w), 703 (s), 667 (w). Raman (1064 nm, $\tilde{\nu}$ (cm^{-1}) =

3090 (26), 1792 (70), 1601 (98), 1545 (15), 1352 (100), 1302 (5), 1280 (3), 1111 (44), 1050 (7), 920 (6), 895 (15), 750 (5), 682 (6), 626 (23), 98 (95). ^{1}H NMR (Aceton-d^{6}, 298 K, 400 MHz) δ (ppm) = 8.39 (d, ^{3}J=12 Hz, 4H), 8.50 (d, ^{3}J=12 Hz, 4H), ^{13}C NMR (Aceton-d^{6}, 298 K, 100 MHz) δ (ppm) = 125.2 (*C*CCH), 131.4 (*C*CCH), 132.0 (*C*CCC), 152.6 (*C*CC(NO$_2$)), 162.2 ($C_{carb.}$), EA found (calcd.) N 8.45 (8.69), C 50.63 (50.61), H 2.47 (2.43). IS: 3 J, FS: 240 N, ESD: 0.300 J.

Bis-3-nitrobenzoyl peroxide (2) 1.000 g 3-nitrobenzoyl chloride (5.380 mmol) are dissolved in 10 mL diethyl ether and 0.32 mL of a 30% H_2O_2 solution (0.38 g, 3.34 mmol) are added. This is followed by the drop wise addition of a solution of 0.26 g NaOH (6.61 mmol) in 5 mL water. The reaction mixture is stirred at 0 °C for 30 minutes. A white precipitate forms which is filtered off, washed with water and diethyl ether and air dried. Yield: 0.462 g (26%). $T_{dec.}$(onset/ 5 °C/min) = 140 °C. IR (ATR) $\tilde{\nu}$ (cm^{-1}) = 3099 (w), 3079 (w), 2361 (w), 1865 (w), 1764 (s), 1733 (w), 1614 (m), 1584 (w), 1528 (s), 1476 (w) 1439 (m), 1349 (s), 1321 (m), 1285 (w), 1222 (s), 1092 (s), 1061 (s), 1000 (m), 934 (m), 881 (w), 813 (m), 797 (m), 758 (w), 703 (s), 660 (w). Raman (1064 nm, $\tilde{\nu}$ (cm^{-1}) = 3120 (10), 1798 (22), 1615 (6), 1554 (18), 1538 (18), 1349 (100), 1450 (3), 1003 (48), 970 (5), 610 (7), 86 (51). ^{1}H NMR (Aceton-d^{6}, 298 K, 400 MHz) δ (ppm) = 8.00 (m, 2H), 8.53 (m, 2H), 8.68 (m, 2H), 8.83 (m, 2H). ^{13}C NMR (Aceton-d^{6}, 298 K, 100 MHz) δ (ppm) = 125.1 (*C*CCH), 127.6 (*C*CCH), 130.1 (*C*CCH), 132.1 (*C*CCH), 136.2 (*C*CCC), 149.6 (*C*CCN), 162.0 ($C_{carb.}$). EA found (calcd.) N 8.42 (8.42), 50.44 (50.61), H 2.42 (2.43). IS: 3 J, FS: 360 N, ESD: 0.180 J.

Bis-3,5-dinitrobenzoyl peroxide (3) 2.000 g 3,5-ninitrobenzoylchloride (8.675 mmol) are dissolved in 20 mL acetonitrile. To this solution 0.533 mL of a 30% H_2O_2-solution (0.178 g, 5.22 mmol) is added followed by the drop wise addition of a solution of 0.48 g NaOH (12.0 mmol) in 15 mL water. The reaction mixture is stirred at 0 °C for 30 minutes. A white precipitate forms. This is filtered off, washed with water and dried on air. Yield: 0.470 g (13%). T_{dec} (onset/ 5 °C/min) = 164 °C. IR (ATR) $\tilde{\nu}$ (cm^{-1}) = 3015 (m), 3089 (m), 2889 (w), 2361 (w), 1860 (w), 1766 (s), 1738 (m), 1627 (m), 1598 (m), 1541 (s), 1458 (m), 1346 (s), 1325 (m), 1245 (s), 1131 (s), 1076 (s), 1001 (w), 932 (m), 923 (m), 898 (m), 802 (m), 729 (s), 713 (s), 701 (s). Raman (1064 nm, $\tilde{\nu}$ (cm^{-1}) = 3126 (14), 1804 (36), 1715 (12), 1600 (20), 1521 (43), 1365 (100) 1212 (11), 1100 (9), 1004 (80), 914 (22), 872 (9), 327 (30), 93 (84). ^{1}H NMR (DMSO-d^{6}, 298 K, 400 MHz) δ (ppm) = 9.02 (s, 4H), 8.90 (s, 2H), ^{13}C NMR (DMSO-d^{6}, 298 K, 100 MHz) δ (ppm) = 122.1 (*C*CCH), 128.9 (*C*CCH), 134.0 (*C*CCC), 148.4 (*C*CCN), 164.0 ($C_{carb.}$). EA found (calcd.) N 13.31 (13.26), C 39.88 (39.82), H 1.64 (1.44). IS: 1.5 J, FS: 240 N, ESD: 0.300 J.

3-Nitrobenzoyl-4-nitrobenzoyl peroxide (4) 0.250 g 4-nitroperbenzoic acid (1.365 mmol) and 0.253 g 3-nitrobenzoyl chloride (1.365 mmol) are dissolved in 10 mL diethyl ether and cooled to 0 °C. A solution of 0.056 g NaOH (1.400 mmol) in 5 mL water is added drop wisely and the solution is stirred at 0 °C for 30 minutes. The white precipitate is filtered off, washed with water and diethyl ether and air dried. Yield: 0.263 g (58%). T_{dec} (onset/ 5 °C/min) = 125 °C. IR (ATR) $\tilde{\nu}$ (cm^{-1}) = 3113 (w), 3092 (w), 2874 (w), 2361 (w), 1791 (m), 1765 (s), 1617 (m), 1538 (s), 1479 (w), 1437 (w), 1419 (w), 1348 (s), 1318 (m), 1302 (w), 1290 (w), 1223 (s), 1098 (m), 1020 (m), 1006 (s), 995 (s), 928 (m), 903 (m), 861 (m), 825 (m), 771 (w), 760 (w), 733 (w), 706 8s), 664 (w). Raman (1064 nm, $\tilde{\nu}$ (cm^{-1}) = 3115 (19), 1723 (17), 1590 (23), 1524 (5), 1351 (100), 1287 (6), 1120 (17), 1003 (22), 884 (15), 627 (6), 91 (10), 80 (73). ^{1}H NMR (DMSO-d^{6}, 298 K, 400 MHz) δ (ppm) = 7.81 (dd, ^{3}J = 8 Hz, 1H), 8.17 (d, ^{3}J = 8 Hz, 2H), 8.33 (m, 3H), 8.46 (m, 1H), 8.62 (s, 1H). ^{13}C NMR (DMSO-d^{6}, 298 K, 100 MHz) δ (ppm) = 123.6(7) (*C*CCH), 123.7 (*C*CCH), 127.3 (*C*CCH), 130.5 (*C*CCH), 130.7 (*C*CCH), 132.5

(*C*CCH), 135.4 (*C*CCC), 136.4 (*C*CCC), 147.9 (*C*CCN), 150.0 (*C*CCN), 165.5 ($C_{carb.}$), 165.8 ($C_{carb.}$). EA found (calcd.) N 8.37 (8.43), C 50.57 (50.61), H 2.47 (2.43), IS: 5 J, FS: 360 N, ESD: 0.15 J.

3,5-Dinitrobenzoyl-3-nitrobenzoyl peroxide (5) 0.260 g 3,5-dinitroperbenzoic acid are dissolved (1.140 mmol) and 0.202 g 3-nitrobenzoyl chloride (1.090 mmol) are dissolved in 10 mL diethyl ether and cooled to 0 °C. To this reaction mixture a solution of 0.050 g NaOH (1.250 mmol) are added drop wisely. This solution is stirred at 0 °C for 30 minutes. The white precipitate is filtered off, washed with water and diethyl ether and dried on air. Yield: 0.219 g (53 %), $T_{dec.}$ (onset/ 5 °C/min) = 143 °. IR (ATR) $\tilde{\nu}$ (cm^{-1}) = 3083 (w), 2361 (w), 1798 (m), 1771 (s), 1616 (m), 1542 (s), 1530 (s), 1477 (w), 1440 (w), 1343 (s), 1285 (w), 1222 (s), 1130 (m), 1091 (m), 1071 (m), 1033 (s), 999 (m) 934 (m), 924 (m), 888 (w), 868 (w), 846 (w), 820 (w), 797 (w), 742 (m), 729 (m), 717 (s), 706 (s), 659 (w). Raman (1064 nm, $\tilde{\nu}$ (cm^{-1}) = 3118 (22), 1800 (31), 1615 (10), 1572 (27), 1560 (28), 1350 (100), 1414 (5), 1002 (60), 823 (11), 796 (19), 606 (7), 1023 (22), 87 (80). ^{1}H NMR (DMSO-d^6, 298 K, 400 MHz) δ (ppm) = 7.82 (m, 1H), 8.35 (m, 1H), 8.46 (m, 1H), 8.62 (s, 1H), 8.90 (s, 2H), 9.02 (s, 1H). ^{13}C NMR (DMSO-d^6, 298 K, 100 MHz) δ (ppm) = 122.1 (*C*CCH), 123.7 (*C*CCH), 127.4 (*C*CCH), 128.9 (*C*CCH), 130.6 (*C*CCH), 132.5 (*C*CCH), 134.0 (*C*CCC), 135.4 (*C*CCC), 147.9 (*C*CCN), 148.4 (*C*CCN), 164.0 ($C_{carb.}$), 165.5 ($C_{carb.}$), EA found (calcd.) N 10.93 (11.13), C 45.11 (44.57), H 2.10 (1.87). IS: 4 J, FS: 360 N, ESD: 0.150 J.

3,5-Dinitrobenzoyl-4-nitrobenzoyl peroxide (6) 0.300 g 3,5-dinitrobenzoyl chloride (1.301 mmol) and 0.238 g 4-nitroperbonzoic acid (1.299 mmol) are dissolved in 10 mL diethyl ether and cooled to 0 °C. Afterwards a solution of 0.056 g NaOH (1.400 mmol) in 5 mL water are added drop wisely. The mixture is stirred at 0 °C for 30 minutes. The white precipitate formed is filtered off, washed with water and diethyl ether and dried on air. Yield: 0.301 g (61%), $T_{dec.}$ (onset/ 5 °C/min) = 141 °C. IR (ATR) $\tilde{\nu}$ (cm^{-1}) = 3085 (m), 2362 (w), 1799 (m), 1769 (m), 1639 (m), 1607 (m), 1548 (s), 1528 (s), 1458 (w), 1411 (w), 1347 (w), 1327 (m), 1395 (m), 1229 (s), 1182 (m), 1127 (m), 1089 (w), 1070 (m), 1030 (s), 1010 (s), 932 (m), 923 (m), 864 (m), 846 (m), 827 (m), 773 (w), 729 (m), 712 (s), 667 (w). Raman (1064 nm, $\tilde{\nu}$ (cm^{-1}) = 3123 (27), 1823 (31), 1599 (76), 1554 (29), 1361 (100), 1250 (5), 1106 (34), 1001 (52), 880 (25), 603 (7), 530 (10), 400 (8), 105 (96). ^{1}H NMR (DMSO-d^6, 298 K, 400 MHz) δ (ppm) = 8.18 (d, 8 Hz, 2H), 8.31 (d, 8 Hz, 2H), 8.90 (s, 2H), 9.01 (s, 1H). ^{13}C NMR (DMSO-d^6, 298 K, 100 MHz) δ (ppm) = 122.0 (*C*CCH), 123.7 (*C*CCH), 128.9 (*C*CCH), 130.7 (*C*CCH), 134.2 (*C*CCC), 136.4 (*C*CCC), 148.4 (*C*CCN), 150.1 (*C*CCN), 164.0 ($C_{carb.}$), 165.8 ($C_{carb.}$). EA found (calcd.) N 10.95 (11.13), C 44.28 (44.57), H 2.10 (1.87). IS: 4 J, FS: 360 N, ESD: 0.100 J.

Bis-4-nitrobenzoyl-terephthaloyl peroxide (7) 0.300 g terephthaloyl chloride (1.478 mmol) and 0.595 g 4-nitroperbenzoic acid (3.249 mmol) are dissolved in 15 mL diethyl ether and cooled to 0 °C. Afterwards a solution of 0.132 g NaOH (3.300 mmol) in 5 mL water is added drop wisely. The reaction mixture is stirred at 0 °C for 30 minutes. The resulting precipitate is filtered off, washed with water and diethyl ether and dried on air. Yield: 0.254 g (35 %), $T_{dec.}$ (onset/ 5 °C/min) = 164 °C. IR (ATR) $\tilde{\nu}$ (cm^{-1}) = 3121 (w), 2361 (w), 2341 (w), 1744 (s), 1607 (m), 1525 (s), 1407 (m), 1346 (m), 1320 (m), 1229 (s), 1180 (w), 1115 (w), 1047 (s), 1009 (s), 870 (m), 851 (m), 783 (m), 704 (s9, 668 (w). Raman (1064 nm, $\tilde{\nu}$ (cm^{-1}) = 3135 (26), 1786 (100), 1600 (78), 1532 (8), 1348 (85), 1109 (19), 1080 (7), 950 (28), 860 (18), 723 (21), 600 (19), 122 (89), 97 (92). ^{1}H NMR (DMSO-d^6, 298 K, 400 MHz) δ (ppm) = 8.04 (s, 4H),

8.17 (d, 12 Hz, 4H), 8.32 (d, 12 Hz, 4H). ^{13}C NMR (DMSO-d^6, 298 K, 100 MHz) δ (ppm) = 123.8 (*C*CCH), 129.5 (*C*CCH), 130.7 (*C*CCH), 134.4 (*C*CCC), 136.4 (*C*CCC), 150.1 (*C*CCN), 165.8 ($C_{carb.}$), 166.7 ($C_{carb.}$), EA found (calcd.) N 5.43 (5.64), C 53.19 (53.23), H 2.73 (2.44). IS: 1 J, FS: 8 N, ESD: 0.056 J.

Bis-3,5-dinitrobenzoyl-terephthaloyl peroxide (8) 0.300 g terephthaloyl chloride (1.478 mmol) and 0.736 g 3,5-dinitroperbenzoic acid (3.227 mmol) are dissolved in 20 mL diethyl ether and cooled to 0 °C. Afterwards a solution of 0.132 g NaOH (3.300 mmol) in 5 mL water is added drop wisely. The reaction mixture is stirred at 0 °C for 30 minutes. The resulting precipitate is filtered off, washed with water and diethyl ether and dried on air. Yield: 0.120 g (14%). $T_{dec.}$ (onset/ 5 °C/min) = 163 °C. IR (ATR) $\tilde{\nu}$ (cm^{-1}) = 3097 (w), 2361 (w), 1789 (m), 1767 (s), 1699 /m), 1629 (m), 1598 (w), 1547 (s), 1460 (w), 1419 (m), 1345 (s), 1251 (m), 1223 (m), 1131 (m), 1071 (m), 1036 (m), 1009 (m), 1000 (m), 923 (m), 869 (m9, 824 (w), 729 (s), 713 (s), 705 (s). Raman (1064 nm, $\tilde{\nu}$ (cm^{-1}) = 3136 (19), 1803 (40), 1690 (43), 1573 (40), 1386 (98), 1208 (12), 1187 (13) 1005 (53), 883 (24), 110 (27), 93 (100). ^{1}H NMR (DMSO-d^6, 298 K, 400 MHz) δ (ppm) = 8.03 (s, 4H), 8.90 (s, 4H), 9.02 (s, 2H). ^{13}C NMR (DMSO-d^6, 298 K, 100 MHz) δ (ppm) = 122.1 (*C*CCH), 128.9 (*C*CCH), 129.4 (*C*CCH), 134.0 (*C*CCC), 134.4 (*C*CCC), 148.4 (*C*CCN), 163.9 ($C_{carb.}$), 166.6 ($C_{carb.}$), EA found (calcd.) N 8.79 (9.55), C 45.73 (45.06), H 2.04 (1.72. IS: 1 J, FS: 18 N, ESD: 0.064 J.

Bis-3-nitrobenzoyl terephthaloyl peroxide (9) 0.300 g terephthaloyl chloride (1.478 mmol) and 0.595 g 3-nitroperbenzoic acid (3.249 mmol) are dissolved in 15 mL diethyl ether and cooled to 0 °C. Afterwards a solution of 0.132 g NaOH (3.300 mmol) in 5 mL water is added drop wisely. The reaction mixture is stirred at 0 °C for 30 minutes. The resulting precipitate is filtered off, washed with water and diethyl ether and dried on air. Yield: 0.292 g (40%). $T_{dec.}$ (onset/ 5 °C/min) = 169 °C. IR (ATR) $\tilde{\nu}$ (cm^{-1}) = 3090 (w), 1791 (s), 1766 (s), 1694 (m), 1617 (m), 1537 (m), 1479 (w), 1408 (m), 1350 (s), 1322 (w), 1292 (m), 1219 (s), 1093 (m), 1029 (m), 1004 (s), 992 (s), 930 (m),903 (m), 862 (m), 846 (m), 825 (m), 761 (w), 712 (s), 701 (s). Raman (1064 nm, $\tilde{\nu}$ (cm^{-1}) = 3136 (40), 1810 (44), 1611 (47), 1593 (32), 1524 (12), 1352 (100), 1403 (17), 1356 (12), 1298 (10), 1005 (48), 883 (13), 790 (14), 601 (13), 590 (8), 89 (92). ^{1}H NMR (DMSO-d^6, 298 K, 400 MHz) δ (ppm) = 7.81 (m, 2H), 8.04 (s, 4H), 8.35 (m, 2H), 8.47 (m, 2H), 8.62 (s, 2H). ^{13}C NMR (DMSO-d^6, 298 K, 100 MHz) δ (ppm) = 123.7 (*C*CCH), 127.4 (*C*CCH), 129.4 (*C*CCH), 130.6 (*C*CCH), 132.5 (*C*CCH), 134.4 (*C*CCC), 135.4 (*C*CCC), 147.9 (*C*CCN), 165.5 ($C_{carb.}$), 166.7 ($C_{carb.}$), EA found (calcd.) N 4.52 (5.64), C 53.54 (53.23), H 2.57 (2.44). IS: 1 J, FS: 9 N, ESD: 0.050 J.

2. NMR-spectroscopy

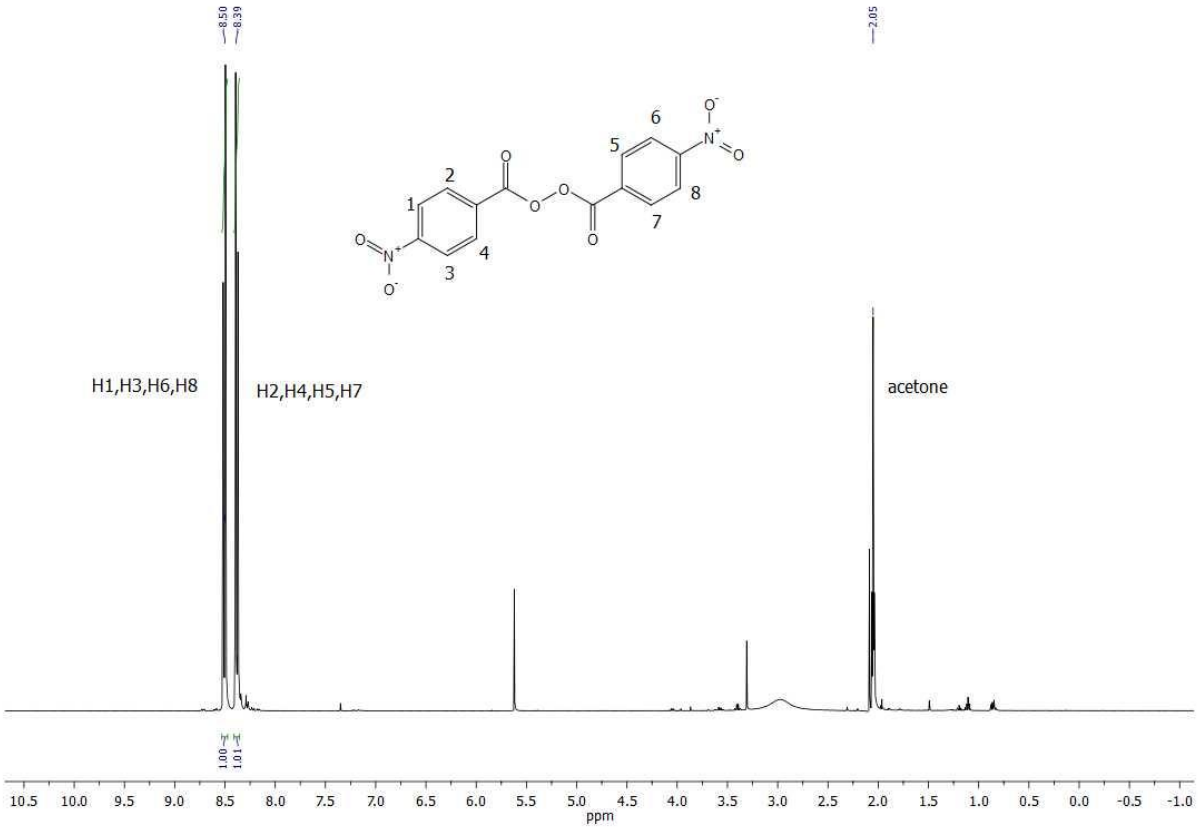

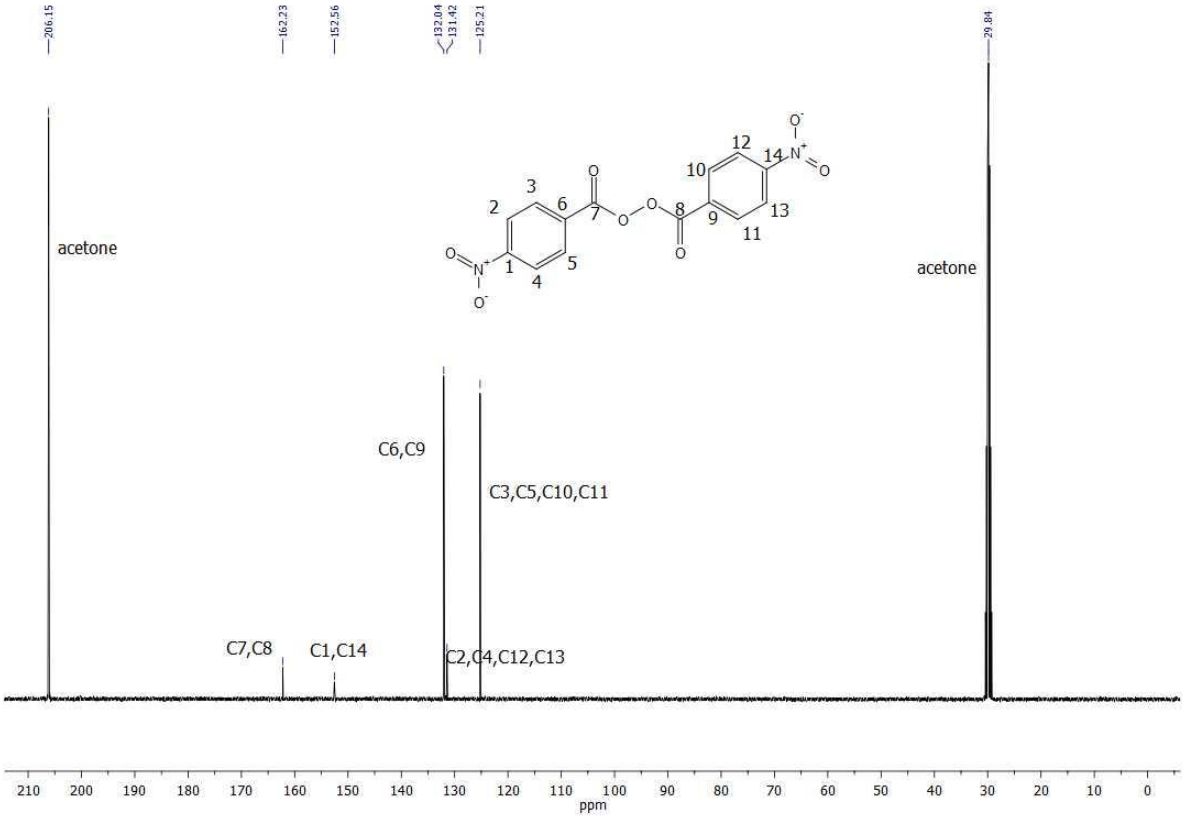

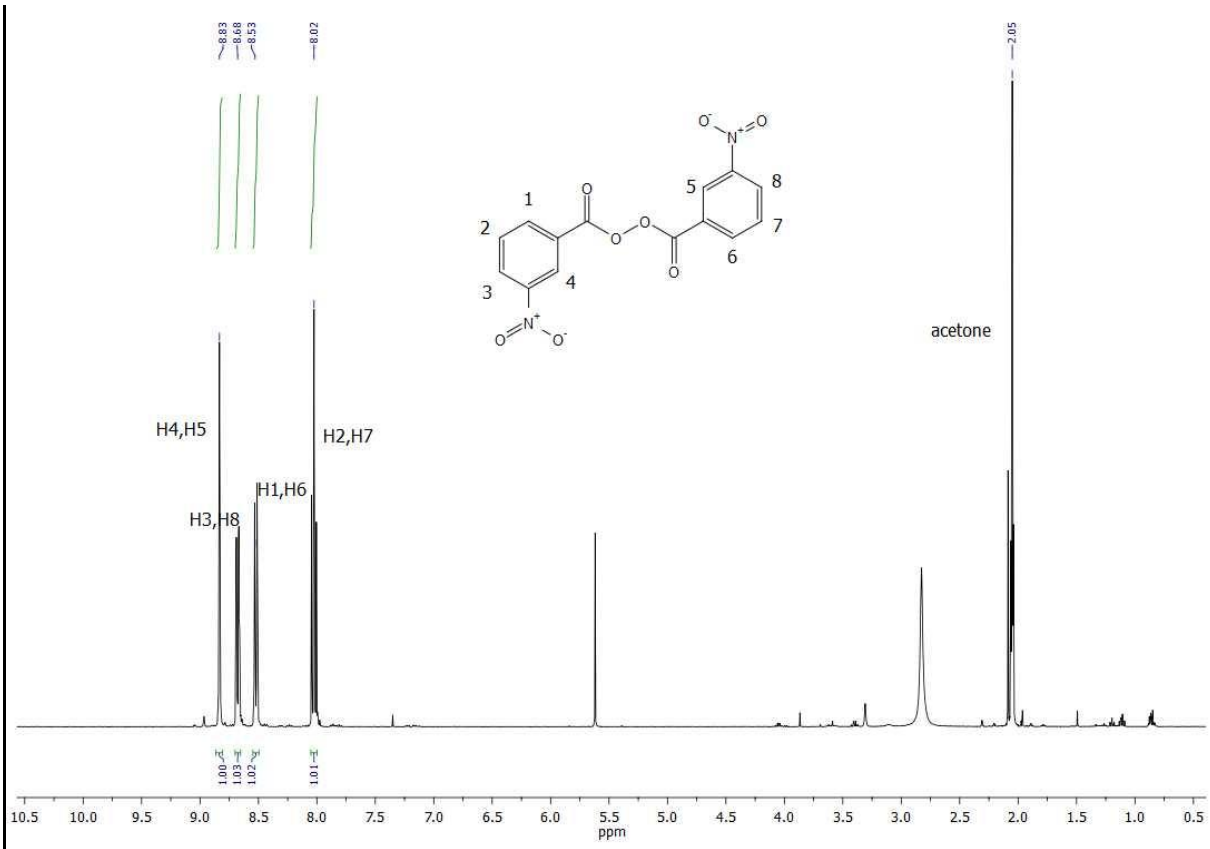
8.83
8.68
8.53
8.02
2.05
1.00
1.03
1.02
1.01
H4,H5
H3,H8
H1,H6
H2,H7
acetone
ppm

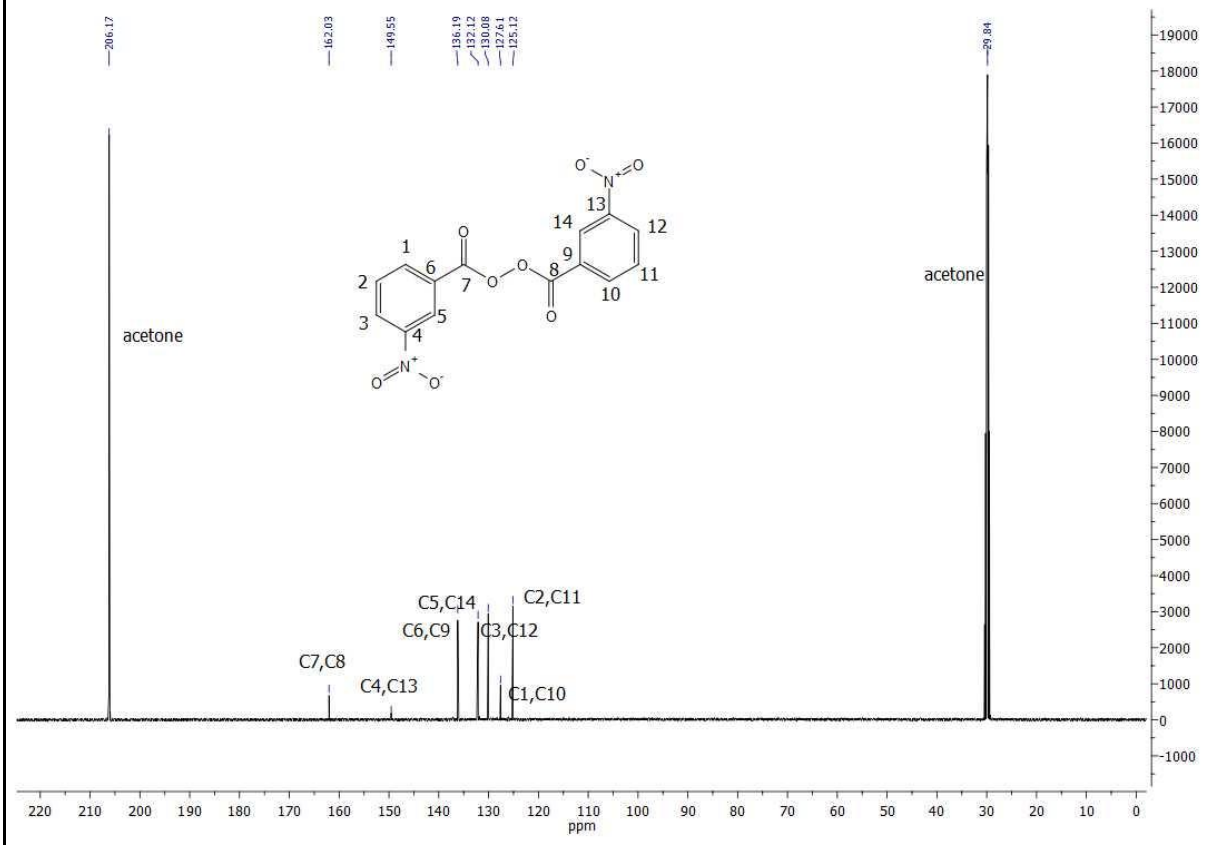
206.17
162.03
149.55
136.19
132.12
130.08
127.61
125.12
29.84
acetone
acetone
C5,C14
C6,C9
C3,C12
C2,C11
C7,C8
C4,C13
C1,C10
ppm

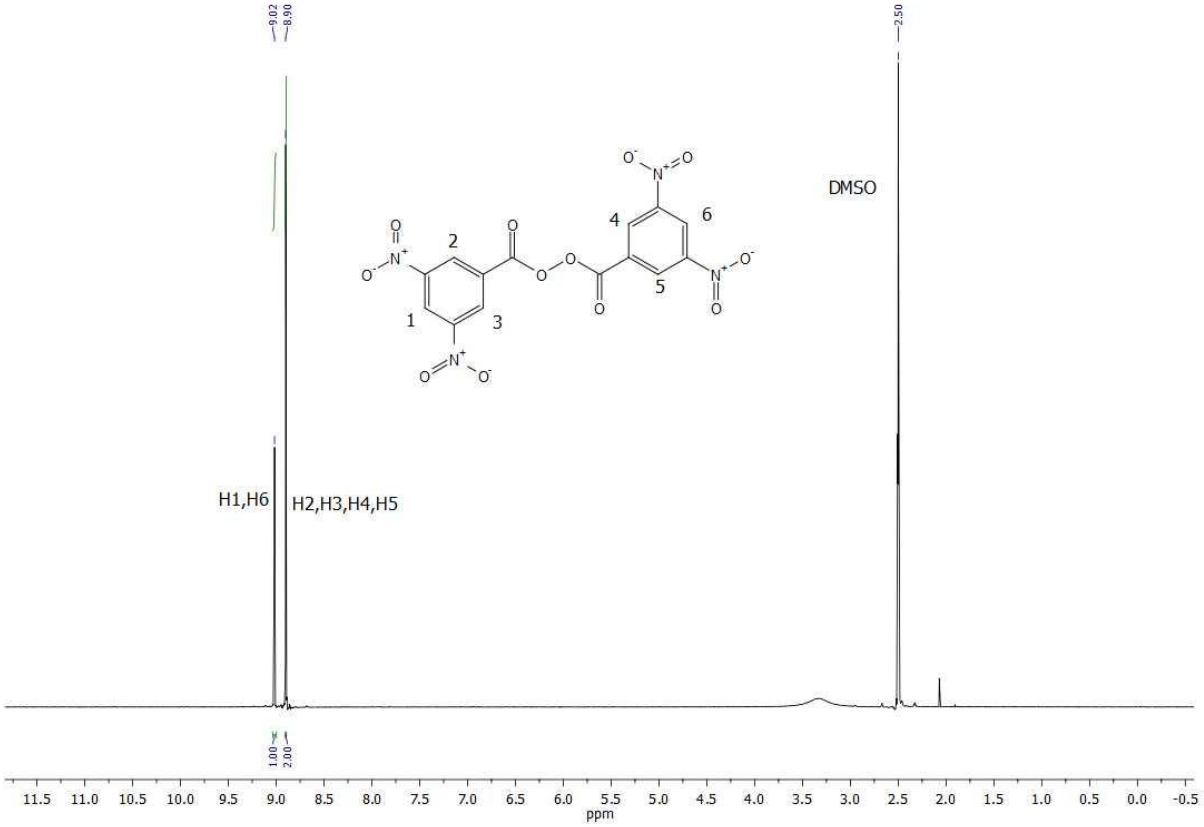
9.02
8.90
2.50
DMSO
H1,H6
H2,H3,H4,H5
1.00
2.00
ppm

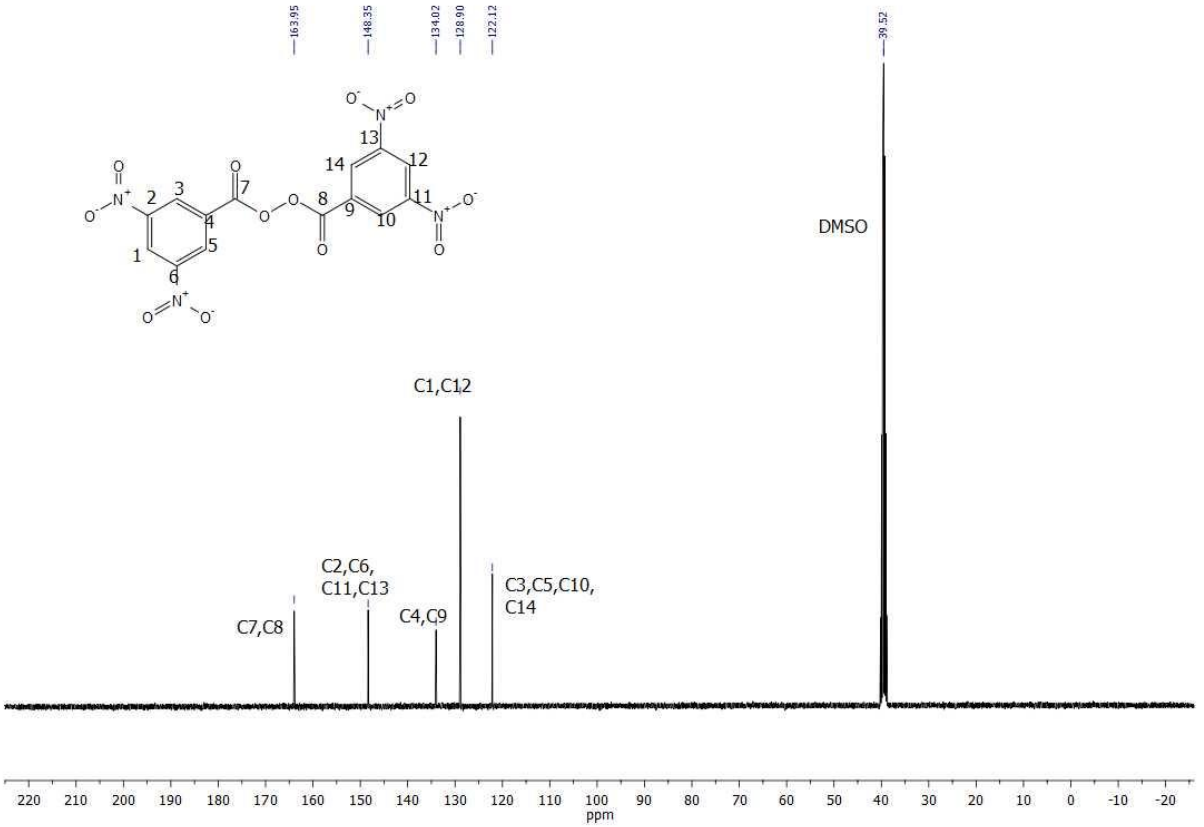
163.95
148.35
134.02
128.90
122.12
39.52
DMSO
C1,C12
C2,C6,
C11,C13
C3,C5,C10,
C14
C4,C9
C7,C8
ppm

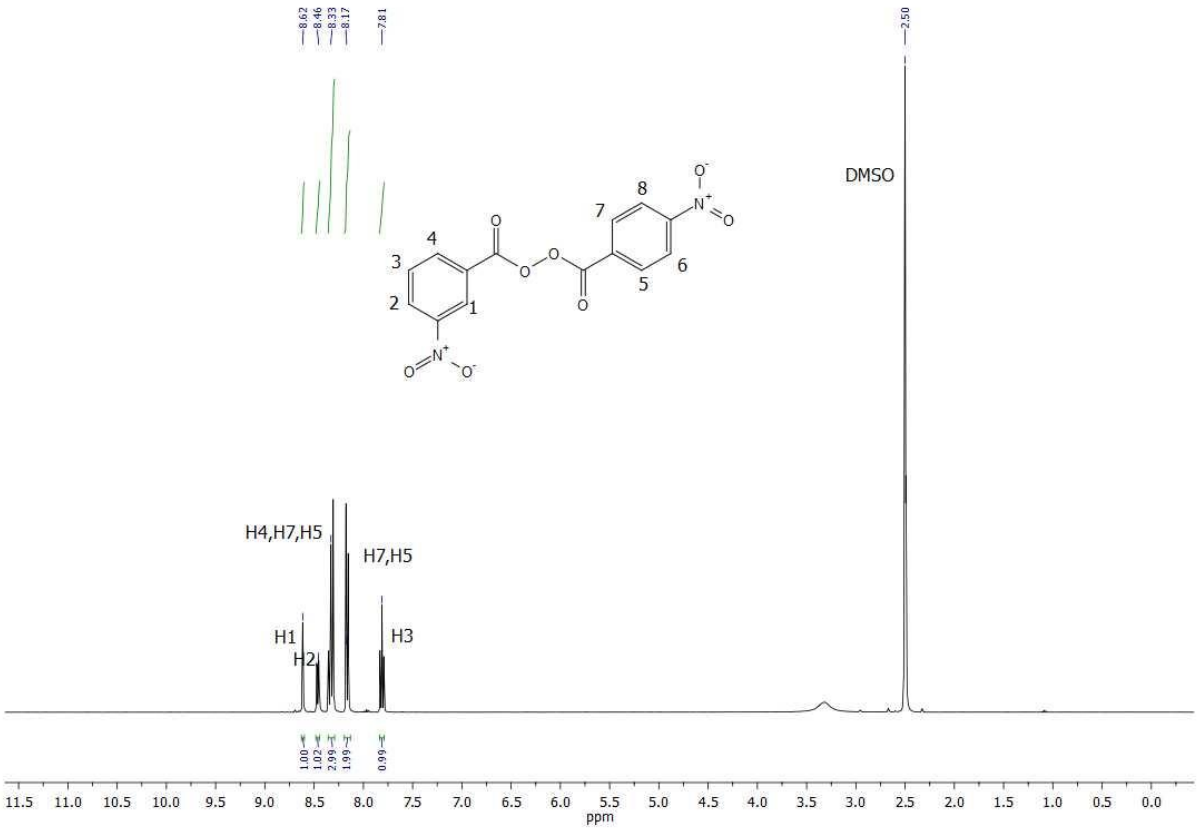
8.62
8.46
8.33
8.17
7.81
2.50
DMSO
H4,H7,H5
H7,H5
H1
H2
H3
1.00
1.02
2.99
1.99
0.99
ppm

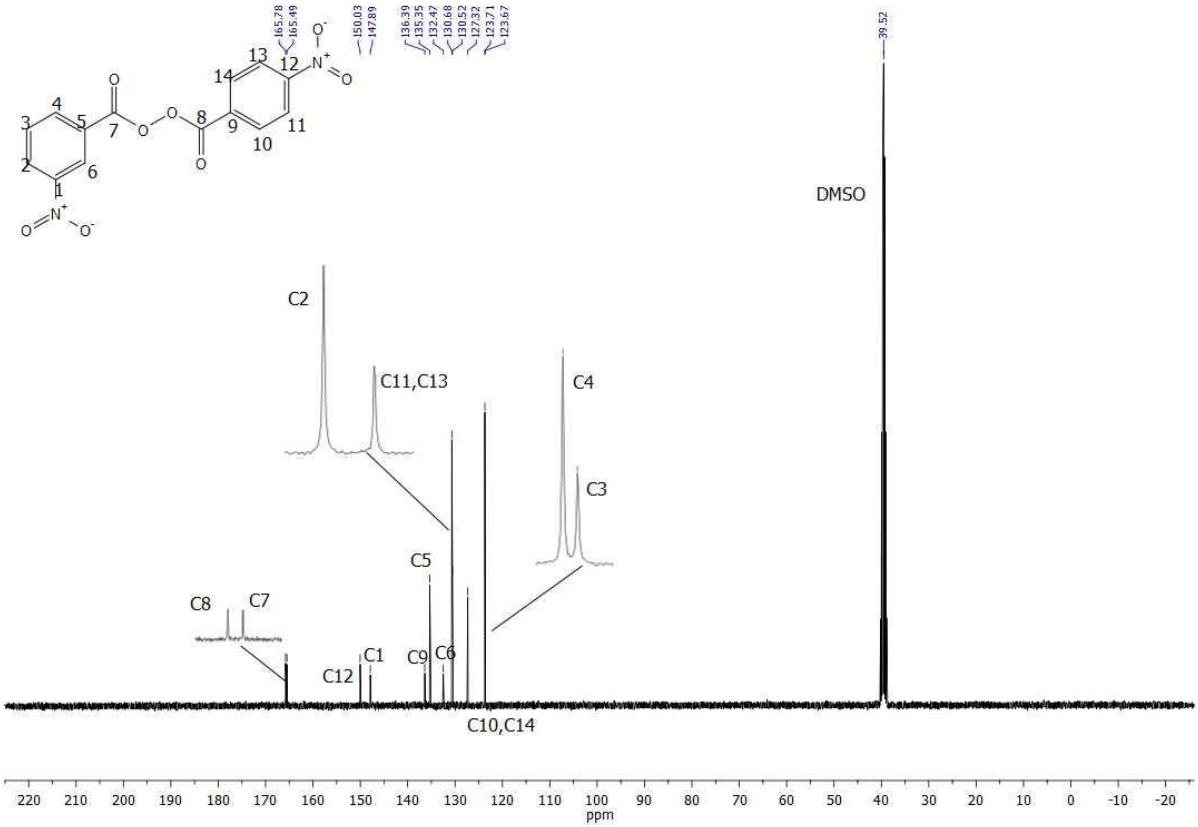
165.78
165.49
150.03
147.89
136.39
135.35
132.47
130.68
130.52
127.32
123.71
123.67
39.52
DMSO
C2
C11,C13
C4
C3
C5
C8
C7
C12
C1
C9
C6
C10,C14
ppm

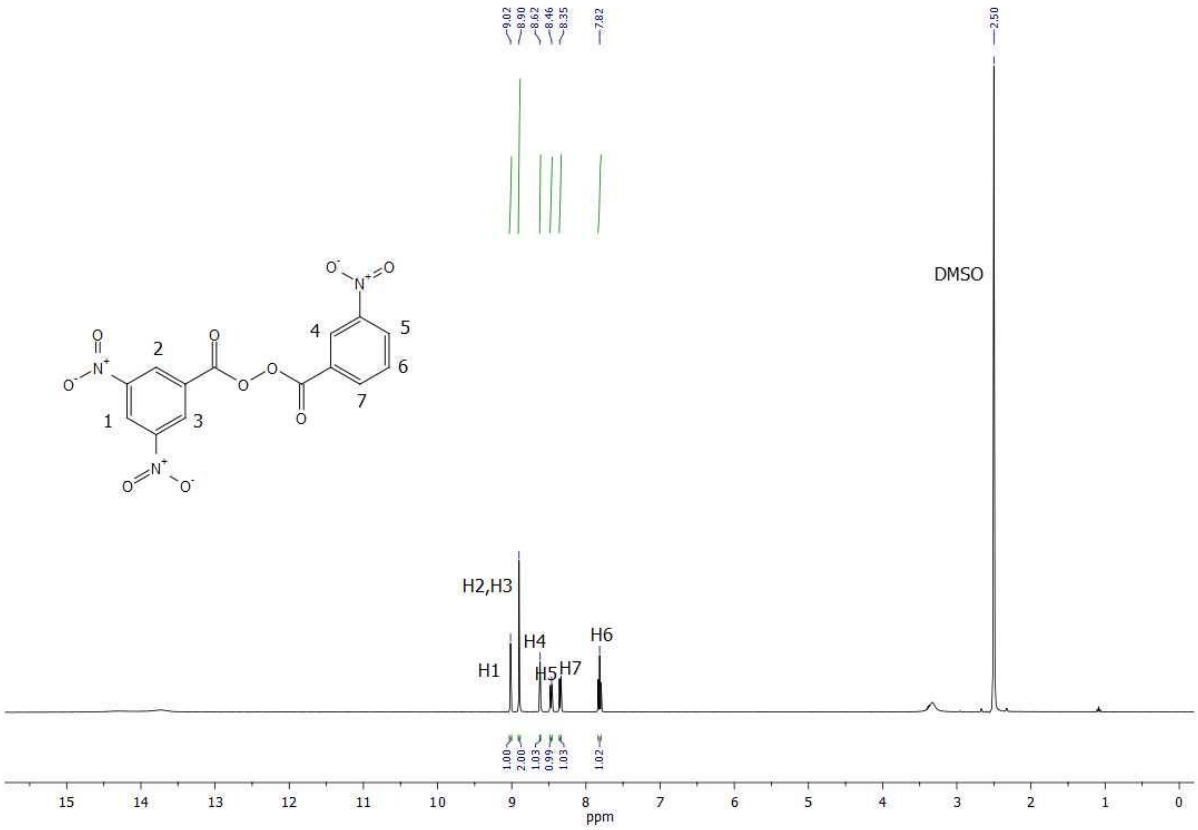
9.02
8.90
8.62
8.46
8.35
7.82
2.50
DMSO
H2,H3
H4
H6
H1
H5
H7
1.00
2.00
1.03
0.99
1.03
1.02
ppm

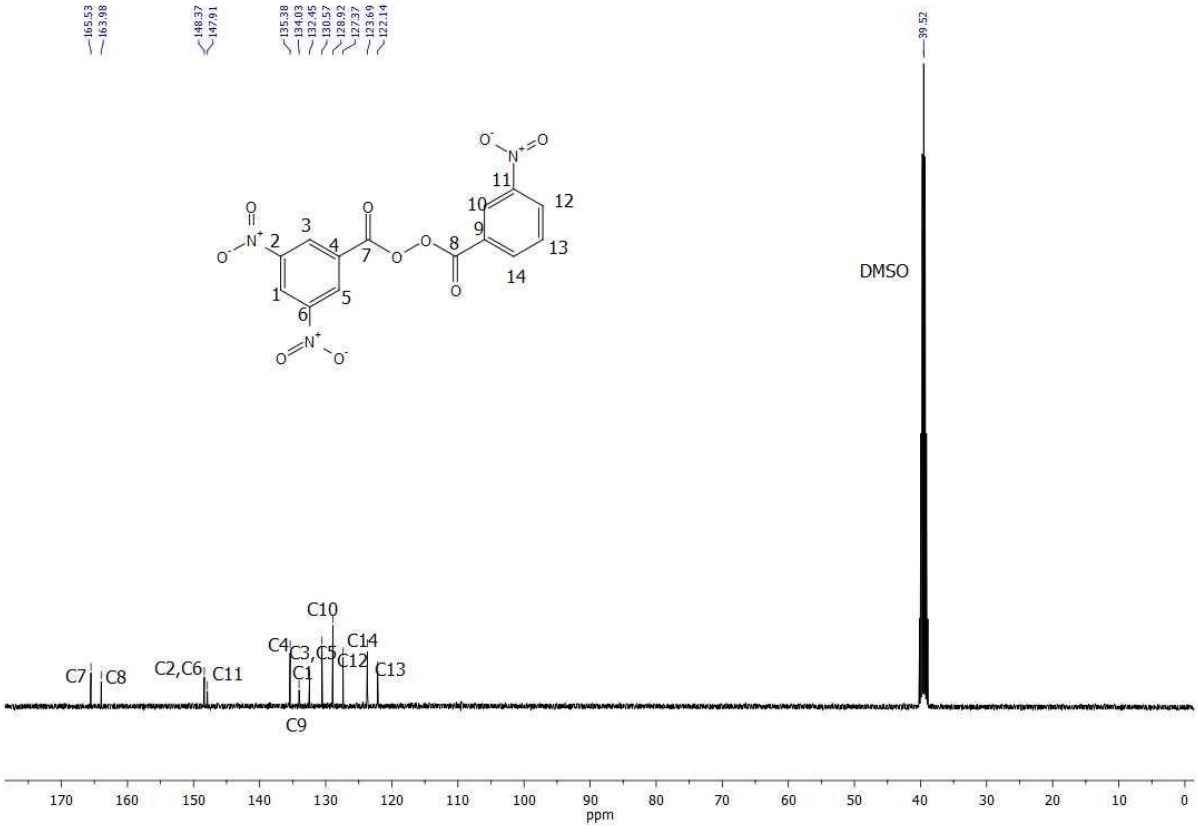
165.53
163.98
148.37
147.91
135.38
134.03
132.45
130.57
128.92
127.37
123.69
122.14
39.52
DMSO
C10
C4
C3,C5
C14
C7
C8
C2,C6
C11
C1
C12
C13
C9
ppm

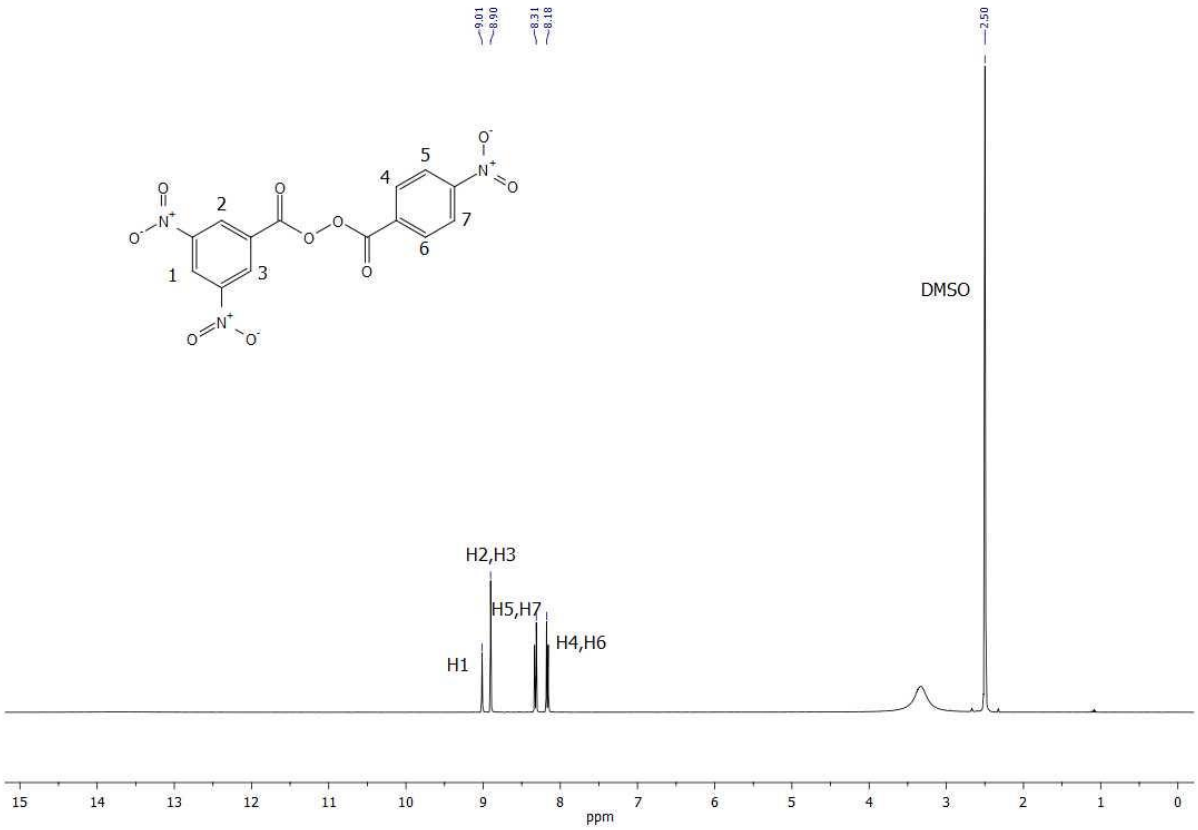
9.01
8.90
8.31
8.18
2.50
DMSO
H2,H3
H5,H7
H4,H6
H1
ppm

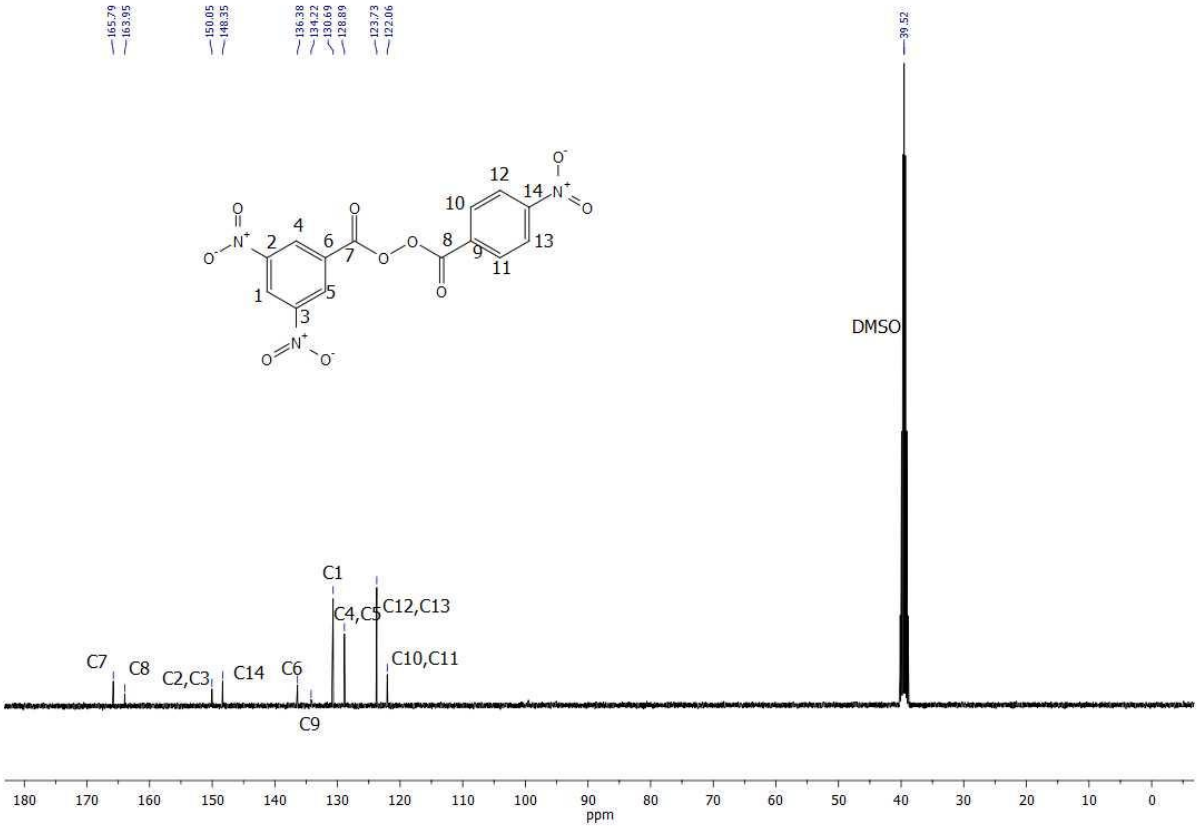
165.79
163.95
150.05
148.35
136.38
134.22
130.69
128.89
123.73
122.06
39.52
DMSO
C1
C4,C5
C12,C13
C7
C8
C2,C3
C14
C6
C10,C11
C9
ppm

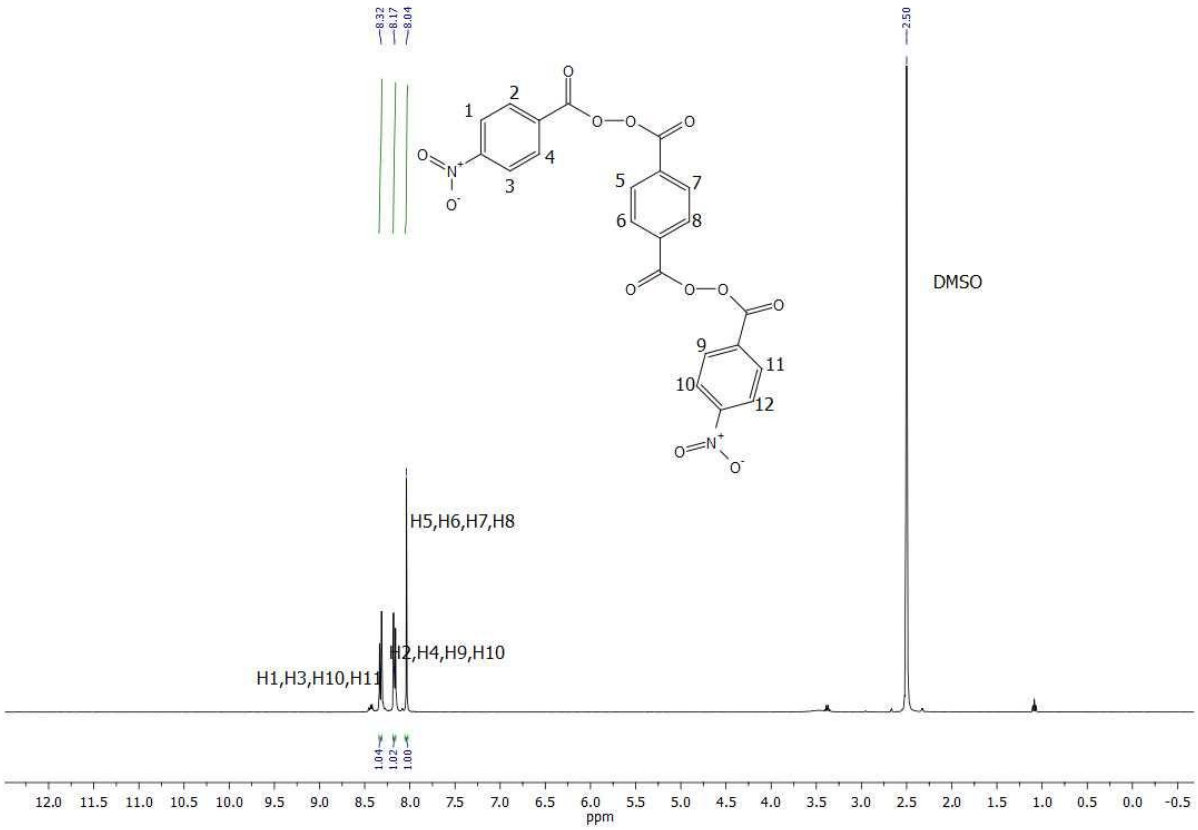
8.32
8.17
8.04
2.50
DMSO
H5,H6,H7,H8
H2,H4,H9,H10
H1,H3,H10,H11
1.04
1.02
1.00
ppm

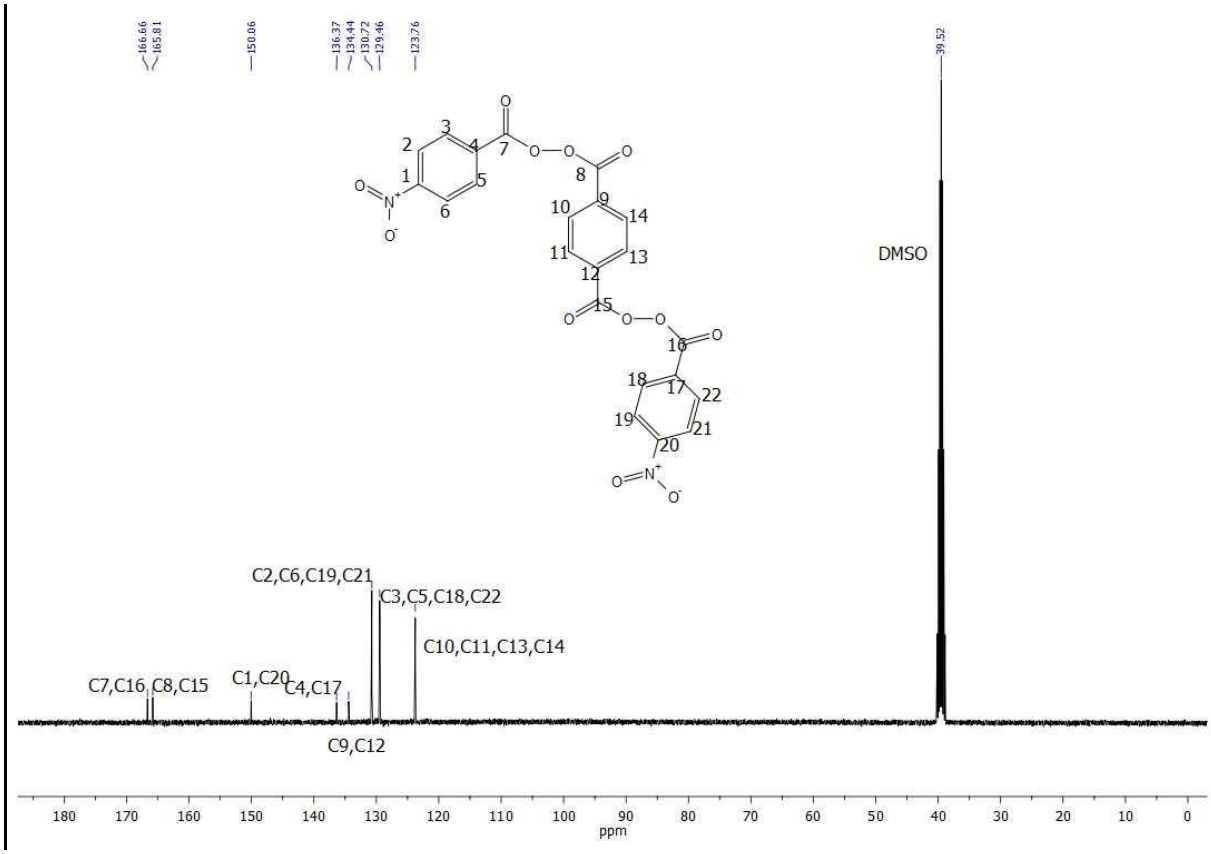
166.66
165.81
150.06
136.37
134.44
130.72
129.46
123.76
39.52
DMSO
C2,C6,C19,C21
C3,C5,C18,C22
C10,C11,C13,C14
C7,C16
C8,C15
C1,C20
C4,C17
C9,C12
ppm

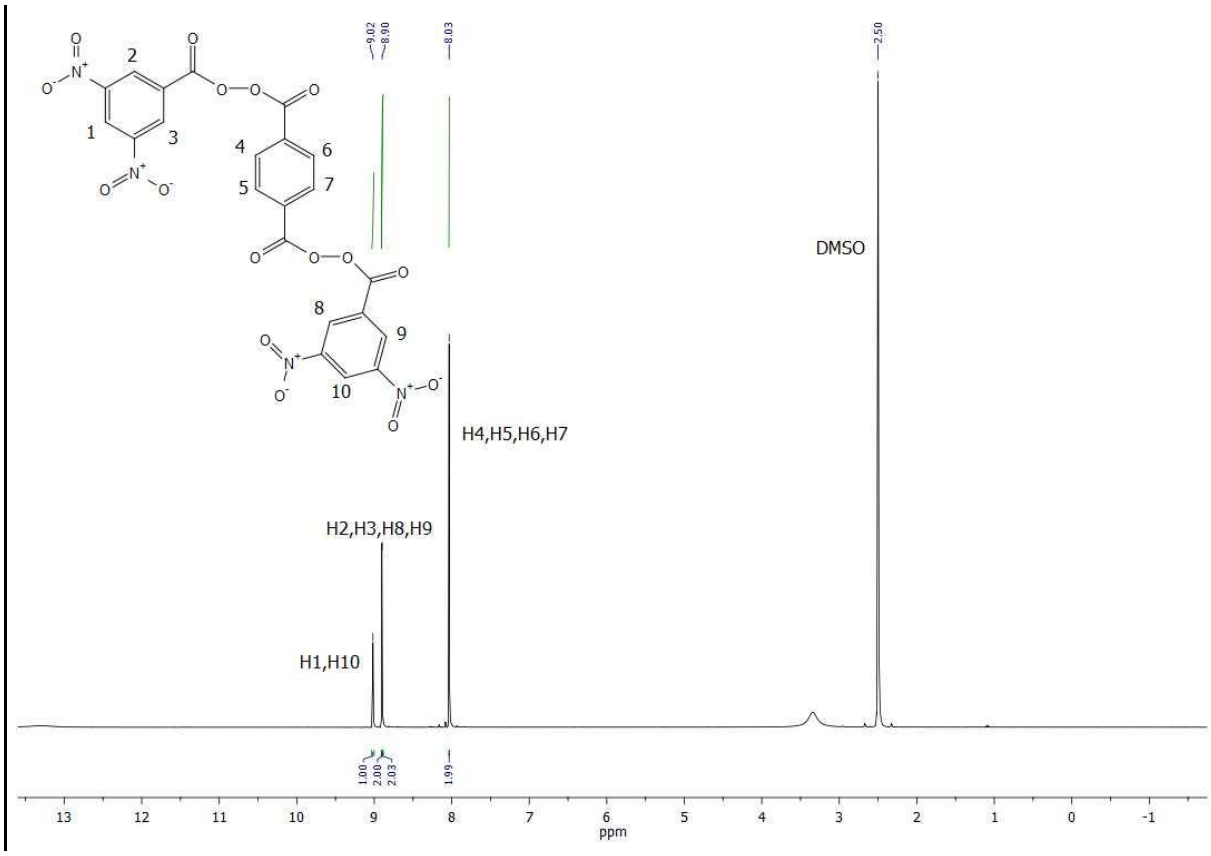
9.02
8.90
8.03
2.50
DMSO
H4,H5,H6,H7
H2,H3,H8,H9
H1,H10
1.00
2.00
2.03
1.99
ppm

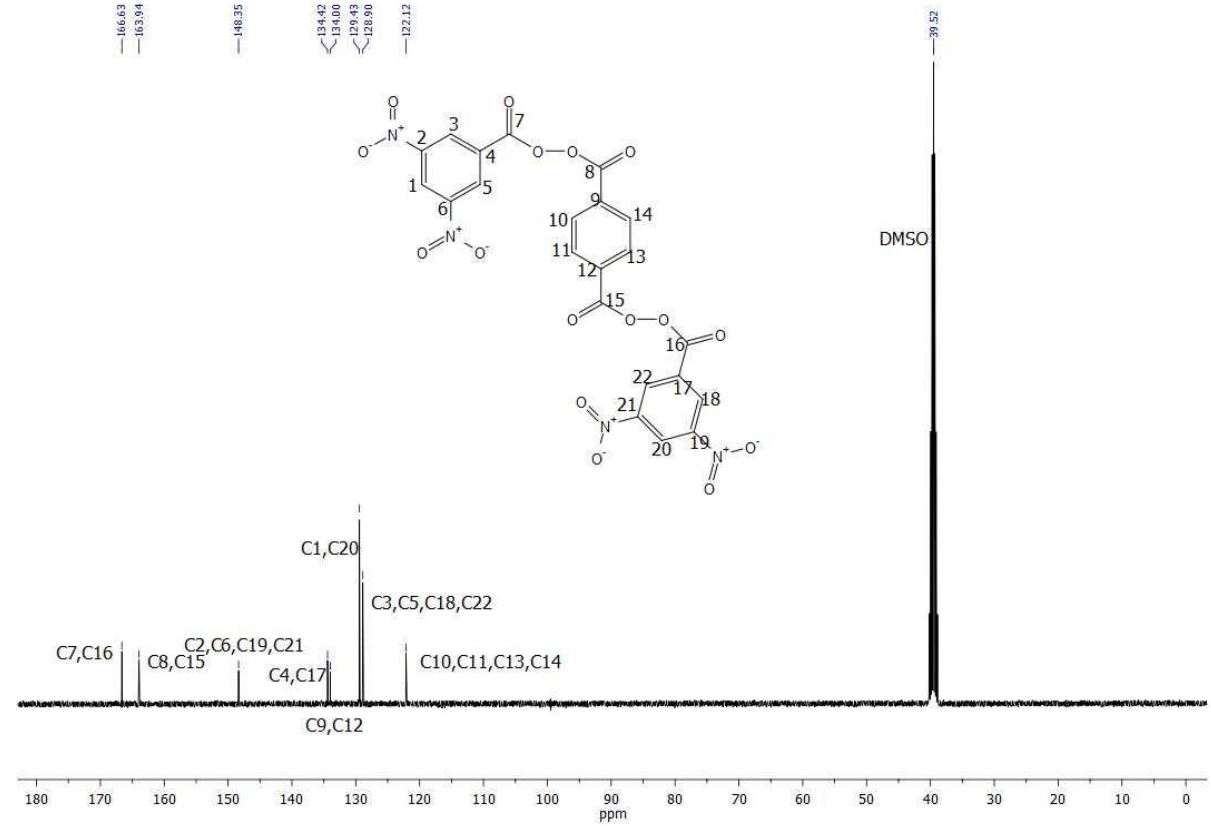
166.63
163.94
148.35
134.42
134.00
129.43
128.90
122.12
39.52
DMSO
C1,C20
C3,C5,C18,C22
C7,C16
C8,C15
C2,C6,C19,C21
C4,C17
C10,C11,C13,C14
C9,C12
ppm

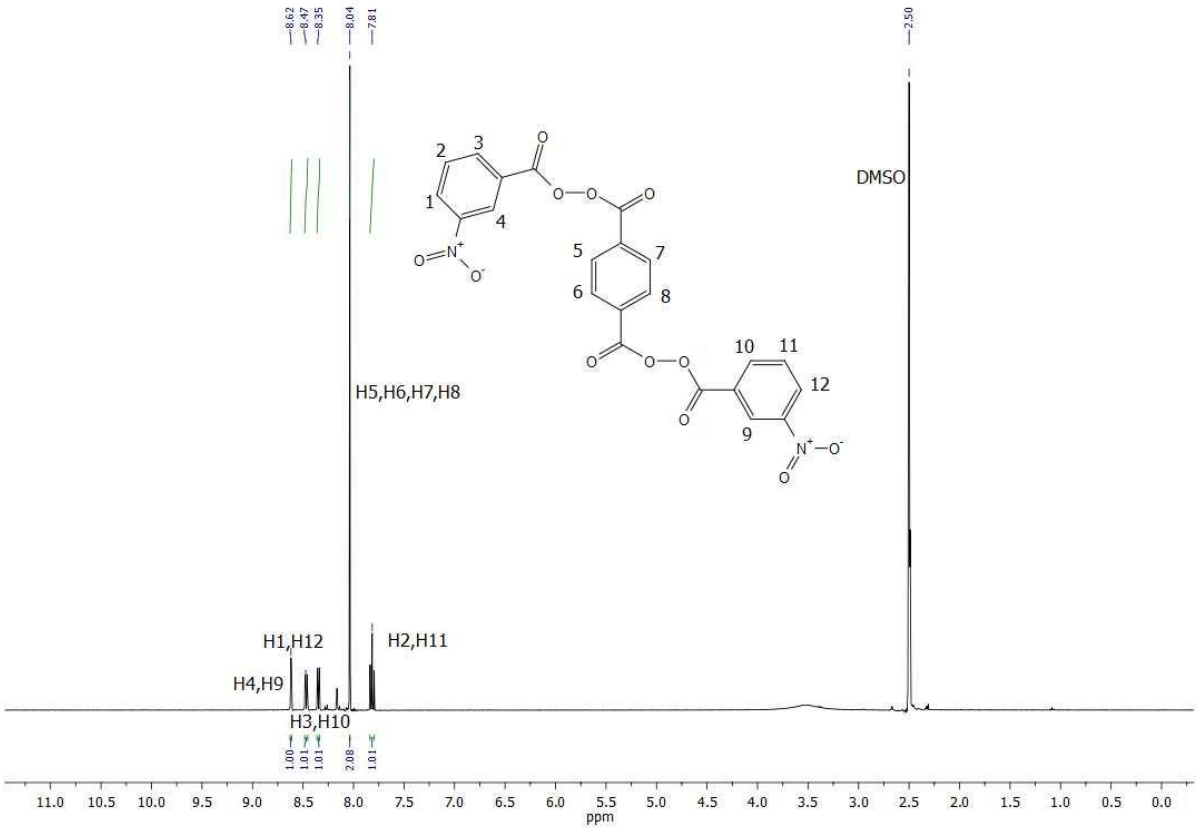
8.62
8.47
8.35
8.04
7.81
2.50
DMSO
H5,H6,H7,H8
H1,H12
H2,H11
H4,H9
H3,H10
1.00
1.01
1.01
2.08
1.01
11.0 10.5 10.0 9.5 9.0 8.5 8.0 7.5 7.0 6.5 6.0 5.5 5.0 4.5 4.0 3.5 3.0 2.5 2.0 1.5 1.0 0.5 0.0
ppm

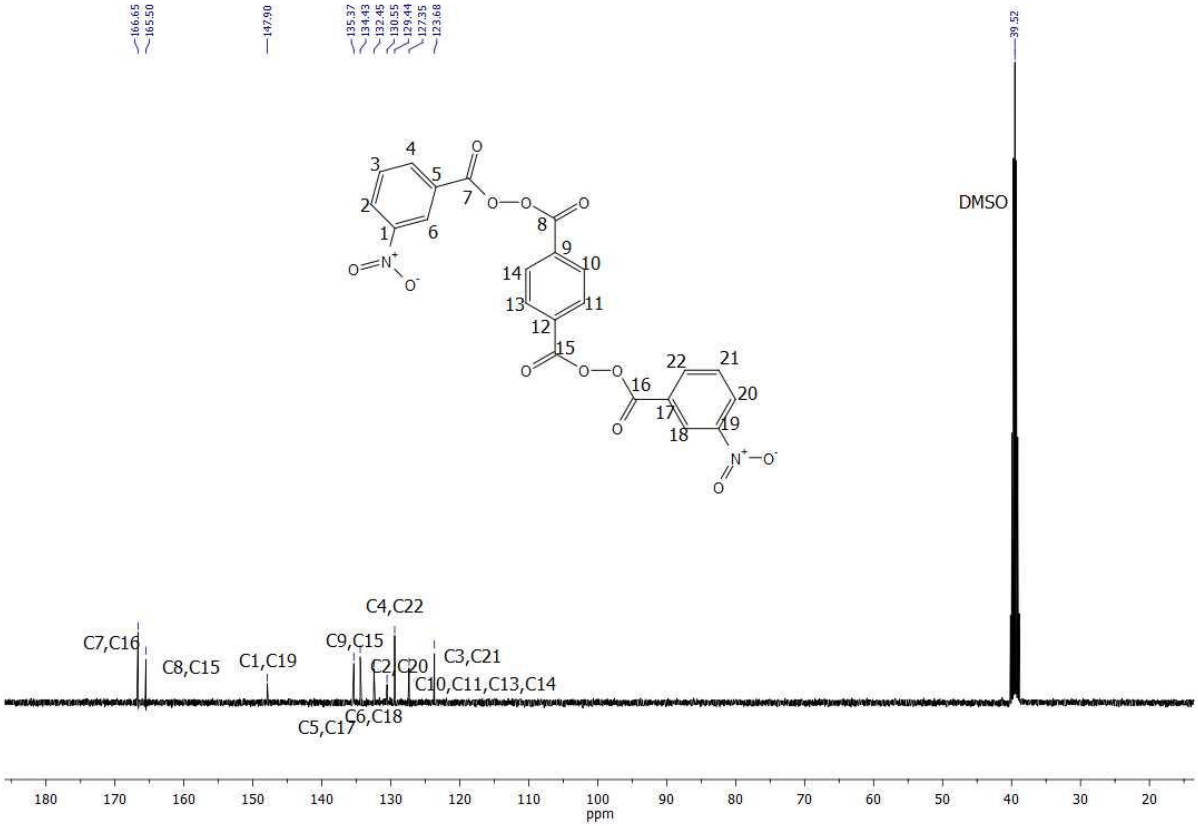
166.65
165.50
147.90
135.37
134.43
132.45
130.55
129.44
127.35
123.68
39.52
DMSO
C4,C22
C7,C16
C9,C15
C8,C15
C1,C19
C2,C20
C3,C21
C10,C11,C13,C14
C5,C17
C6,C18
180 170 160 150 140 130 120 110 100 90 80 70 60 50 40 30 20
ppm

3. X-ray diffraction

For both compounds, an Oxford Xcalibur3 diffractometer with a CCD area detector was employed for data collection using Mo-Kα radiation (λ = 0.71073 Å). By using the Crystalispro software[S3] the data collection and reduction was performed. The structures were solved by SIR-92[S4] and refined by fullmatrix least-squares on *F*2 (SHELXL [S5]) and finally checked by using the PLATON software [S6] integrated in the WinGX software suite. The non-hydrogen atoms were refined anisotropically and the hydrogen atoms were located and freely refined. The absorptions were corrected by a SCALE3 ABSPACK multiscan method [S7]. All DIAMOND2 plots are shown with thermal ellipsoids at 50% probability level and hydrogen atoms are shown as small spheres of arbitrary radius.

	2	**3**
Formula	$C_{14}H_8N_2O_8$	$C_{14}H_6N_4O_{12}$
FW [g/mol]	332.22	422.23
Crystal system	triclinic	monoclinic
Space Group	*P*−1 (No. 2)	*C*2/*c* (No.15)
Color / Habit	Colorless plate	Colorless plate
Size [mm]	0.32 x 0.08 x 0.01	0.2 x 0.15 x 0.02
a [Å]	3.7130(9)	24.7537(19)
b [Å]	7.4052(9)	5.3382(4)
c [Å]	12.464(2)	12.2617(7)
α [°]	99.774(13)	90
β [°]	97.336(18)	98.54(1)
γ [°]	92.642(15)	90
V [Å^3]	334.16(11)	1602.29(19)
Z	1	4
$\rho_{calc.}$ [g cm^{-3}]	1.651	1.750
μ [mm^{-1}]	0.139	0.158
F (000)	170	856
$\lambda_{MoK\alpha}$ [Å]	0.71073	0.71073
T [K]	123	123
ϑ min max [°]	4.7, 26.0	4.2, 26.0
Dataset h; k; l	−4:4;−9:9;−15:15	−30:29;−6:6;−11:15
Reflect. coll.	4612	5657
Independ. refl.	1304	1570
R_{Int}	0.068	0.039
Reflection obs.	1304	1570
No. parameters	109	148
R_1 obs.	0.0569	0.0402
wR_2 (all data)	0.1534	0.0908
S	1.02	1.07
Resd. Dens. [e Å^{-3}]	−0.28;0.28	−0.22;0.22
Device type	Oxford Xcalibur3 CCD	Oxford Xcalibur3 CCD
Solution	SIR-92	SIR-92
Refinement	SHELXL-2013	SHELXL-2013
Absorption corr.	multi-scan	multi-scan
CCDC	1490207	1490206

4. Heat of formation calculations

All calculations were carried out using the Gaussian G09W (revision A.02) program package.[S8] The enthalpies (H), listed in Table S3, were calculated using the complete basis set (CBS) method of Petersson and coworkers in order to obtain accurate energies. The CBS models uses the known asymptotic convergence of pair natural orbital expressions to extrapolate from calculations using a finite basis set to the estimated complete basis set limit. CBS-4 begins with a HF/3-21G(d) structure optimization and the zero point energy is computed at the same level. Subsequently it uses a large basis set SCF calculation as a base energy, and a MP2/6-31+G calculation with a CBS extrapolation to correct the energy through second order. A MP4(SDQ)/6-31+(d,p) calculation is used to approximate higher order contributions. In this paper we applied the modified CBS-4M method (M referring to the use of Minimal Population localization) which is a re-parameterized version of the original CBS-4 method and also includes some additional empirical corrections.[S9] The gas-phase enthalpies of species M were computed according to the atomization energy method (eq.1).

$$\Delta_f H^\circ_{(g,\,M,\,298)} = H_{(Molecule,\,298)} - \Sigma H^\circ_{(Atoms,\,298)} + \Sigma \Delta_f H^\circ_{(Atoms,\,298)} \quad \textbf{(1)}$$

$H^0_{Atoms,298}$ for the corresponding Atoms were determined experimentally and are reported in the literature. ${}_fH^0_{(Atoms,298)}$ are calculated theoretically.[S10]

Atom	$\Delta_f H^0_{g,Atom}$ [kcal·mol^{-1}]	$H^0_{g,Atom}$ [Hartree·atom^{-1}]
H	52.103	−0.500991
C	171.29	−37.786156
N	112.97	−54.522462
O	59.56	−74.991202

Standard molar enthalpies of formation were calculated using $\Delta_f H^0_{g,Atom}$ and the standard molar enthalpies of sublimation (estimated by applying Trouton´s rule).[S12]

$$\Delta_f H^0_M = \Delta_f H^0_{(g,M,298)} - \Delta_{sub} H^0_M = \Delta_f H^0_{(g,M,298K)} - 188 \cdot T \left[\frac{J}{mol}\right]$$

Where T [K] is either the melting point or the decomposition temperature (if the compounds do not melt before they decompose)

Detonation parameters

The Chapman-Jouguet (C-J) characteristics, (i.e. heat of detonation, $\Delta_E U^0$, detonation temperature T_{C-J}, detonation pressure P_{C-J}, detonation velocity V_{C-J}) based on the calculated $\Delta_f H^0_M$ values and the theoretical maximum densities were computed using the EXPLO5 V6.02 thermochemical computer code.[S11] Calculations for explosives assume ideal behavior. The estimation of the detonation parameters is based on the chemical equilibrium steady-state detonation model. The Beckler-Kistiakowsky-Wilson equation of state (BKWEOS) with the following sets of constants: $\alpha = 0.5, \beta = 0.38, \kappa = 9.4, and\ \Theta = 4120$ for gaseous detonation products and the Murnaghan equation of state for condensed products (compressible solids and liquids) were applied. The calculation of the equilibrium composition of the detonation products uses modified White, Johnson and Dantzig´sfree energy minimization technique.
The specific energies of explosives(f) were calculated according to the equation for ideal gases where isochronic condition were assumed.

$$f = p_e \cdot V = n \cdot R \cdot T_0 \left[\frac{kJ}{kg}\right]$$

Where p_e is the maximum pressure through the explosion, V is the volume of detonation gases ($m^3 \cdot kg^{-1}$), n is the number of moles of gas formed by the explosion per kilogram of explosive (*Volume of Explosive Gases*), R is the ideal gas constant and T_C is the absolute temperature of the explosion. [S12], [S13]

5. References

[S1] N.-D. H. Gamage, B. Stiasny, J. Stierstorfer, P. D. Martin, T. M. Klapötke, C. H. Winter, *Chem. Eur. J.* **2015**, *21*, 1-5.

[S2] D. G. Hamann, A. Ramachandran, M. Gracanin, S. J. Blanksby, *J. Org. Chem.* **2006**, *21*, 7996-8005.

[S3] *CrysAlisPro*, Oxford Diffraction Ltd., version 171.33.41, **2009**.

[S4] *SIR-92*, *A program for crystal structure solution*: A. Altomare, G. Cascarano, C. Giacovazzo, A. Guagliardi, *J. Appl. Crystallogr.* **1993**, *26*, 343.

[S5] a) G. M. Sheldrick, *SHELX-97*, University of Göttingen, Göttingen, Germany, **1997**; b) G. M. Sheldrick, *Acta Crystallogr., Sect. A* **2008**, *64*, 112–122.

[S6] A. L. Spek, *PLATON*, *A Multipurpose Crystallographic Tool*, Utrecht University, The Netherlands, **1999**.

[S7] *SCALE3 ABSPACK – An Oxford Diffraction program* (1.0.4, gui: 1.0.3), Oxford Diffraction Ltd., **2005**.

[S8] Gaussian 09, M. J. Frisch, G. W. Trucks, H. B. Schlegel, G. E. Scuseria, M. A. Robb, J. R. Cheeseman, G. Scalmani, V. Barone, B. Mennucci, G. A. Petersson, H. Nakatsuji, M. Caricato, X. Li, H. P. Hratchian, A. F. Izmaylov, J. Bloino, G. Zheng, J. L. Sonnenberg, M. Hada, M. Ehara, K. Toyota, R. Fukuda, J. Hasegawa, M. Ishida, T. Nakajima, Y. Honda, O. Kitao, H. Nakai, T. Vreven, J. A. Montgomery, Jr., J. E. Peralta, F. Ogliaro, M. Bearpark, J. J. Heyd, E. Brothers, K. N. Kudin, V. N. Staroverov, R. Kobayashi, J. Normand, K. Raghavachari, A. Rendell, J. C. Burant, S. S. Iyengar, J. Tomasi, M. Cossi, N. Rega, J. M. Millam, M. Klene, J. E. Knox, J. B. Cross, V. Bakken, C. Adamo, J. Jaramillo, R. Gomperts, R. E. Stratmann, O. Yazyev, A. J. Austin, R. Cammi, C. Pomelli, J. W. Ochterski, R. L. Martin, K. Morokuma, V. G. Zakrzewski, G. A. Voth, P. Salvador, J. J. Dannenberg, S. Dapprich, A. D. Daniels, Ö. Farkas, J. B. Foresman, J. V. Ortiz, J. Cioslowski, and D. J. Fox, Gaussian, Inc., Wallingford CT, 2009.

[S9] a) J. W. Ochterski, G. A. Petersson, J. A. Montgomery, *J. Chem. Phys*. **1996**, *104*, 2598–2619; b) J. A. Montgomery, M. J. Frisch, J. W. Ochterski, G. A. Petersson, *J. Chem. Phys.* 2**000**, *12*, 6532–6542.

[S10] P. J. Linstorm, W. G. Mallard, *National Institute of Standards and Tehcnology*, Gaithersburg, MD, 20899.

[S11] a)F. Trouton, *Philos. Mag. (1876-1900)* **1884**, *18*, 54-57; b) M. S. Westwell, M. S. Searle, D. J. Wales, D. H. Willimas, *J. Am. Chem. Soc.* **1995**, *117*, 5013-5015.

[S12] M. Suceska, *Explo5 Version Users´s Guide*, January **2013**.

[S13] a)R. Meyer, J. Köhler, A. Homburg, *Explosives*, 6thedn. , Wiley, Weinheim, **2007**, p. 291-292;
b)T. M. Klapötke, *Chemistry of High-Energy Materials*, de Gruyter, Berlin, **2015**

Journal of Inorganic and General Chemistry
ZAAC
Zeitschrift für anorganische und allgemeine Chemie
www.zaac.wiley-vch.de
ARTICLE

DOI: 10.1002/zaac.201600389

Synthesis and Investigation of 1,3-Bis(5-nitraminotetrazol-1-yl)propan-2-ol and its Salts

Thomas M. Klapötke,*[a] Benedikt Stiasny,[a] and Jörg Stierstorfer[a]

Keywords: Nitrogen-rich molecules; Salt formation; X-ray diffraction; Structure elucidation

Abstract. 1,3-Bis(5-nitraminotetrazol-1-yl)propan-2-ol (**5**) was prepared by the reaction of 5-aminotetrazole and 1,3-dichloroisopropanol under basic conditions. Obtained 1,3-bis(5-aminotetrazol-1-yl)propan-2-ol (**3**) was nitrated with 100 % nitric acid. In this context in situ hydrolysis of the nitrate ester was studied. Metal and nitrogen-rich salts of the neutral compound **5** were prepared and analyzed. Crystal structures of three salts and the sensitivities toward impact, friction and electrostatic discharge were determined as well. The performance values of the compounds were calculated using the EXPLO5 program. A detailed comparison of the different salts is also enclosed.

Introduction

Traditional explosives gain their explosive power from the oxidation of a carbon backbone by oxidizing groups present in the same molecule.[1] Most popular is the carbon connected nitro-group, which for example is applied in 2,4,6-trinitrotoluene (TNT) and almost all high-temperature stable explosives like hexanitrostilbene (HNS) and 1,3,5-triamino-2,4,6-trinitrobenzene (TATB) and most recently TKX-55.[2] A more recent approach to design explosives is to use nitrogen containing heterocycles, which form molecular dinitrogen as the main detonation product.[1] For example tetrazoles have a high enthalpy of formation [$\Delta_f H^0$(*5H*-tetrazole) = +237.2 kJ·mol^{-1}][3] and contain more energy as for example triazoles.[4] Pentazoles carry an even larger amount of internal energy but they are very difficult to prepare and to handle.[5] The tetrazole ring can be substituted with different organic residues to vary its properties, for example lower the sensitivity.[6] Deprotonation and salt formation is also a well known strategy to decrease the sensitivity of energetic materials.[7,8] One molecular building block in order to get potential explosives is the nitrimino group. It is obtained via the reaction of an amino group with e.g. 100 % nitric acid. Hydroxy groups, which are present in the same molecule are reacted to nitric acid esters under the mentioned conditions,[4,9] which is one of the reasons why molecules containing a hydroxy group and a nitrimino group at the same time are only barely known today.[6,10] On the one hand this is advantageous because of the higher oxygen balance and higher enthalpy of formation introduced by the O–NO_2– group. But on the other hand the alcohol cannot be used for further different derivatizations. Further, transition metal complexes for application as laser ignitable primary explosives are of great interest today.[11,12] The hydroxyl group can serve as a further coordination site for the central metal and therefore form more stable complexes.

In this study we would like to report on the formation of 1,3-bis(5-nitraminotetrazol-1-yl)propan-2-ol, a molecule carrying a hydroxy and a nitrimino group at the same time and give an insight in the formation of selected metal and nitrogen containing salts. The salts with nitrogen containing cations can serve as potential new secondary explosives. The lithium salt is not hygroscopic and can therefore find application in new, environmentally benign red flare compositions.[13] The strontium and the barium salt can serve as color producing agents in red and green pyrotechnics. The sodium salt was prepared to give a crystallographic proof of the structure and the potassium salt can serve as ingredient for infrared pyrotechnical compositions.[14,15]

Results and Discussion

Synthesis

The synthesis of (1,3-di-5-nitraminotetrazolyl)propan-2-ol (**5**) starts with the formation of 1,3-bis(5-amino-tetrazol-1-yl) propan-2-ol (**3**). 1,3-Dichloroisopropanol (**2**) and two equivalents of 5-aminotetrazol (**1**) are reacted under basic NaOH conditions in aqueous solution overnight. During the reaction time of 10 h, compound **3** precipitates as a colorless solid in a yield of 16 %. The ^{13}C NMR spectrum of the precipitate shows exclusively the signals of the 1,1′-substituted isomer **3** (δ = 48.3, 67.0, 156.0 ppm). This compound was already prepared by *Shreeve* et al.[16] In their study the possible formation of isomers is avoided by the use of cyanogen-azide, which is a highly useful but extremely dangerous reagent at the same time. The low yield in our study can be explained by the ad-

* Prof. Dr. T. M. Klapötke
E-Mail: tmk@cup.uni-muenchen.de
www.hedm.cup.uni-muenchen.de
[a] Department of Chemistry
Ludwig-Maximilian University
81377 Munich, Germany
Supporting information for this article is available on the WWW under **http://dx.doi.org/10.1002/zaac.201600389** or from the author.

ditional formation of the 1,2′- and 2,2′-substituted isomers. The formation of those compounds was proven by NMR investigations of the dried reaction mixture showing also the respective signals (over 160 ppm in [D$_6$]DMSO for ring carbon atom of a 2-substituted tetrazole). However, those compounds do not precipitate. Since 1,1′-substituted compounds are normally superior with respect to performance and thermal stability,[17,18] and a 1,1′-subsitution pattern normally is beneficial for complexation,[19,20] we choose to limit our investigations to this isomer.

Compound **3** is further reacted with 100 % nitric acid overnight to form the dinitrimino compound **4**. During addition of solid **3** to HNO_3, the mixture was cooled in an ice-water bath. It slowly reached room temperature over the reaction time. The reaction is quenched by pouring the mixture on an excessive amount of crushed ice whereupon no precipitate forms. The nitrate ester compound is already known.[4] In this publication, the compounds were worked up by pouring the reaction mixtures on ice and stirring them for 3 h during which time the products precipitated. We wanted to investigate whether the nitrate ester can be cleaved under acidic reaction conditions, since this is a well investigated[21] and also well known process even in reactions on industrial scale.[22] For this, the amount of ice used for quenching the reaction was tripled and no precipitate was formed initially. The mixture was cooled to 5 °C and the formed precipitate was isolated and analyzed by ^{13}C NMR spectroscopy. The observed signals appeared at 45.5, 76.8, and 151.0 ppm. The clear solution is left in the (compared to 100 % nitric acid) now relatively slight acidic mixture (pH about 2) at room temperature for crystallization for around four weeks, which causes the formation of small needle like crystals of **5** in 62 % yield. The formation of **5** is proven by ^{13}C NMR spectroscopy again. The signals can be observed at 50.0, 64.8, and 151.1 ppm. The NMR shifts of the C atoms are therefore significantly different for compounds **4** and **5**. The ^{13}C NMR spectra of the two compounds are displayed in the Supporting Information. The synthetic pathway of the performed reactions is depicted in Scheme 1. In further approaches towards the product, the crystallization time was reduced to 6 d, which proved, to be long enough for obtaining the desired compound in the same yields. The successful formation of **5** supports our theory that the nitrated compound **4** is formed as an intermediate product and the nitric acid ester is hydrolyzed over time.

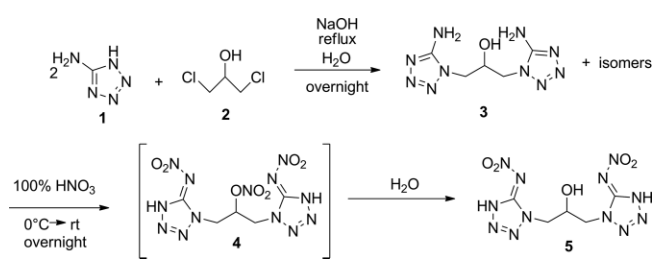

Scheme 1. Reaction pathway of the performed reactions.

The reaction of **5** with different metal hydroxides and N-bases resulted in the formation of salts containing the following cations: lithium (**6**), sodium (**7**), potassium (**8**), strontium (**9**), barium (**10**), ammonium (**11**), hydrazinium (**12**), hydroxylammonium (**13**), guanidinium (**14**), and aminoguanidinium (**15**). Details regarding the hydration state and the yields related on the hydrates can be drawn from Scheme 2. The water content of the hydrates was calculated from the elemental analysis values.

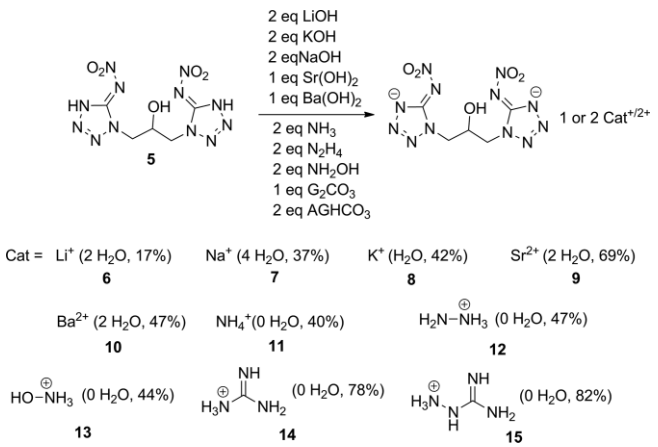

Scheme 2. Synthetic pathway for the synthesis of the salts **6**–**15**.

In this context it is conspicuous, that only the metal salts are formed as hydrates, the nitrogen containing salts all are isolated free of water. A reason for this might be that water coordinates on the metal ions with the oxygen atom. This is not possible in the nitrogen containing salts.

The isolated products however are stable. The diamino-molecule **3** contains basic nitrogen atoms, which allows for the formation of salts with strong acids. This is also a widely known strategy for the synthesis of novel energetic materials.[23,24] In this context we synthesized **16** to give a crystallographic proof for the 1,1′-substitution of **3**. The nitrate salt **16** was prepared by dissolving **3** in an excess of 65 % HNO_3 (Scheme 3).

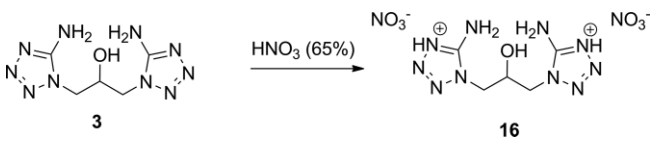

Scheme 3. Synthetic pathway for the synthesis of the nitrate salt **16**.

The compound precipitates after a reaction time of around 5 min as a flaked colorless solid in a yield of 51 %.

Single Crystal X-ray Analysis

The structures of **7**·3H_2O, **14**, and **16** were determined by low temperature X-ray diffraction analysis. Single crystals of **6**·3H_2O and **14** were grown from water, single crystals of **16** from 65 % HNO_3. Compound **6** was isolated as a tetrahydrate when the procedure given in the Experimental Section was applied. However the crystal that was isolated from the mother liqueur was clearly trihydrate, which is most likely a result of the recrystallization process. Compound **7**·3H_2O crystallizes in

the orthorhombic space group $P2_12_12_1$ with a density of 1.816 g•cm^{-3} (100 K). The molecular structure is displayed in Figure 1.

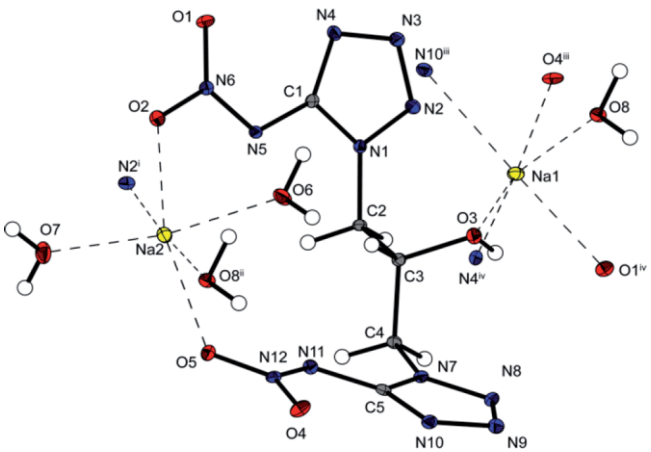

Figure 1. Extended molecular structure of the sodium salt **7** and its labeling scheme. Ellipsoids in all structures represent the 50% probability level. Symmetry codes: (i) 1.5–*x*, 2–*y*, –0.5+*z*; (ii) 1+*x*, *y*, *z*; (iii) 1–*x*, 0.5+*y*, 1.5–*z*; (iv) 1–*x*, –0.5+*y*, 1.5–*z*.

The bond lengths and bond angles of the tetrazole rings are roughly in the range of 129–136 pm and 108–111°, and therefore in a usual range.[25] Also the bond length of the N–O and N–N bonds of the nitrimine (values in the range of 124.7–127.0 pm and 131.6–132.1 pm, respectively), and the corresponding N–N–O bond angles with values between 115.4 and 124.5° are in an expected range.[25,26] The nitrimines are slightly twisted with torsion angles of 3.4 and 4.4°. The sodium atom Na1 is coordinated by one water molecule, the OH group, two O atoms of different nitrimino groups, and two ring nitrogen atoms of the different tetrazole rings. The sodium atom Na2 is octahedrally coordinated. The plane of the octahedron is formed by two O atoms of different nitrimino groups and two water molecules. Additional coordinating bonds are formed by a further water molecule and by one N atom of the tetrazole ring.

In addition, it was possible to determine the X-ray crystal structure of the guanidinium salt **14**. The compound crystallizes in the triclinic space group $P\bar{1}$ with a density of 1.661 g•cm^{-3} (100 K). The molecular structure is displayed in Figure 2. The bond lengths and bond angles of the tetrazole rings are again roughly in the range of 129–136 pm and 105–116°, and therefore in the normal range for tetrazoles.[19] The N–N bond length of the nitrimine has a value in the range of 131.63–132.81 pm and is therefore in the normal range for nitrimines.[25,26] The N–O bond lengths are between 124.46 and 126.79 pm and therefore also normal for nitrimines. The same applies for the bond angles, which for the N–N–O angles are between 115.02 and 124.62° and for O–N–O between 119.88 and 120.62°. One nitrimino group is slightly twisted with a torsion angle of 5.05°, whereas the other is practically planar with a torsion angle of 0.7°. A huge number of hydrogen bonds are formed between the hydrogen atoms of the guanidinium cation and the NO_2 oxygen atoms as well as nitrogen atoms of the tetrazole ring.

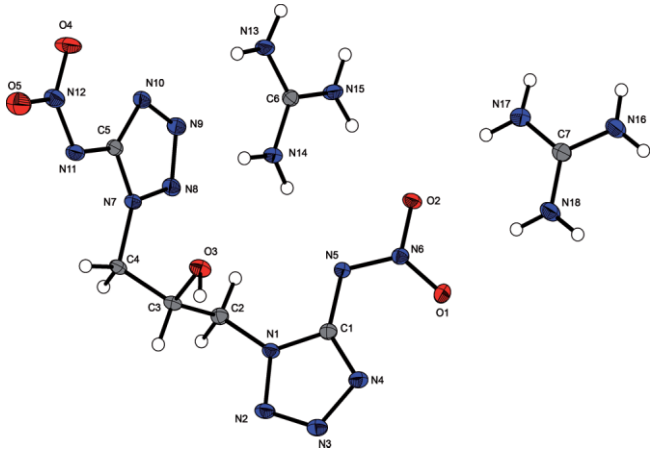

Figure 2. Molecular structure of the guanidinium salt **14** and its labeling scheme. Ellipsoids in all structures represent the 50% probability level.

The nitrate salt **16** crystallizes in the monoclinic space group $P2_1/c$ with a density of 1.709 g•cm^{-3} (100 K). Figure 3 displays the molecular structure.

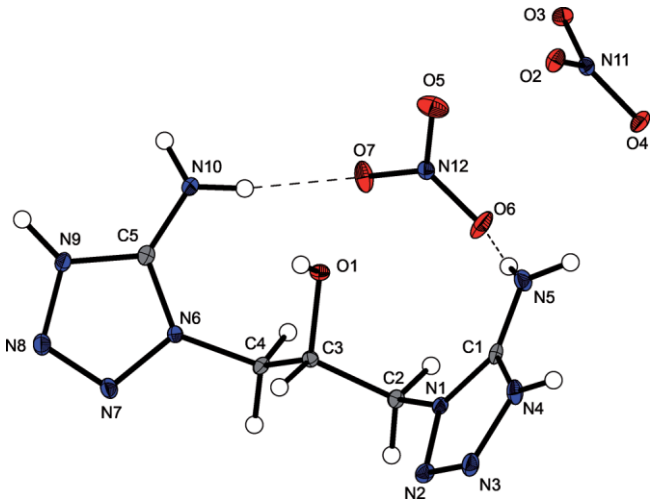

Figure 3. Molecular structure of the nitrate salt **16** and its labeling scheme. Ellipsoids in all structures represent the 50% probability level.

The N–O bond lengths of the nitrate ion are between 124 and 125 pm and are therefore in the normal range for nitrate salts of tetrazole containing compounds.[27] The same applies for the O–N–O angle, which is in the range of 120°. The bond lengths between the ring atoms and the corresponding bond angles are in the area of 140 pm and 109° and therefore in the comparable range with other tetrazole based energetic materials.[5,9,21] The nitrate ions are participating in hydrogen bonds. The interactions are formed between the oxygen atoms of the nitrate ions and the hydrogen atoms of the amino-group, the hydroxylic hydrogen atom and of the hydrogen atoms linked to N4 and N9, respectively. Moreover the structure proves that the protonation takes place at the ring nitrogen atoms and not on the amino groups.

Additional information about the data collection and refinement are given in the Supporting Information.

Table 1. Energetic properties of the diamino compound **3** and the metal salts **6**–**10**.

	3	**6**	**7**	**8**	**9**	**10**
Formula	$C_5H_{10}N_{10}O$	$Li_2C_5H_6N_{12}O_5{\cdot}2H_2O$	$Na_2C_5H_6N_{12}O_5{\cdot}4H_2O$	$K_2C_5H_6N_{12}O_5{\cdot}H_2O$	$SrC_5H_6N_{12}O_5{\cdot}2H_2O$	$BaC_5H_6N_{12}O_5{\cdot}2H_2O$
F_W /g·mol^{-1}	226.15	327.99	360.11	392.29	401.73	451.44
IS[a] /J	>40	>40	>40	>40	>40	>40
FS[b]/N	>360	>360	>360	>360	>360	>360
ESD[c]/J	>1.5	>1.5	>1.5	>1.5	>1.5	>1.5
T_{dec}[d]	352	160	245	271	299	166

a) Impact sensitivity according to BAM drophammer (method 1 of 6) (100 ≥ g.s. ≥ 50 µm). b) Friction sensitivity according to BAM friction tester (method 1 of 6) (100 ≥ g.s. ≥ 50 µm). c) Electrostatic discharge sensitivity (OZM ESD tester) (100 ≥ g.s. ≥ 50 µm). d) Temperature of decomposition according to DTA (onset temperatures at a heating rate of 5 K·min^{-1}).

Energetic Properties

Table 1 gathers the sensitivity properties of **3** and the metal salts of **5**. All compounds are insensitive toward impact and friction with values > 40 J for impact and > 360 N for friction sensitivity. In case of compound **3** this is explained by the absence of energetic groups. For the different metal salts the low sensitivity can be explained by the containment of crystal water. The values for decomposition points of the metal salts range from 160 °C (Li salt **6**) to 299 °C (Sr salt **9**) and are therefore in the normal range for nitrimino compounds.[8]

Table 2 gathers the energetic properties of **5**, the nitrogen containing salts **11** to **15** and the nitrate salt **16**. The neutral dinitrimine **5** has an impact sensitivity of 4 J and a friction sensitivity of 240 N, which accounts for a classification as sensitive. All salts of the nitrogen rich cations are insensitive toward impact and friction with values of > 40 J and > 360 N, which results from the deprotonation and accompanied decrease of the sensitivities. The nitrate salt **16** however must again be classified as sensitive with values of 25 J impact and 288 N friction sensitivity. Since the performance of an energetic material is strongly dependent on the amount of gases formed per molecule during detonation and therefore on the composition of the material, we choose to limit our investigations of the energetic performance to neutral **5**, the non metal salts, and the nitrate salt **16**.

The performance data of the compounds were calculated using the EXPLO5 program in version 6.02. Heats of formation were calculated with the atomization method based on CBS-4M electronic enthalpies. Exact values are given in Table 2. Calculated detonation velocities and detonation pressures for the nitrogen-rich salts have values between 8024–8475 m·s^{-1} and 21–25 GPa. This means they perform better than the standard explosive TNT (6950 m·s^{-1}, 21 GPa) but still weaker than RDX (hexogen) (8750 m·s^{-1}, 35 GPa).[1] The compound with the highest calculated detonation velocity is the aminoguanidinium salt **15** (8475 m·s^{-1}), the compound with the highest calculated detonation pressure is the ammonium salt **11** (25 GPa). While correlating the calculated values with the densities no general trend can be observed, all in all the compounds perform more or less similar. Thermal decomposition points for the non metal salts are between 207 °C (aminoguanidinium salt **15**) and 236 °C (guanidinium salt **14**) and therefore significantly higher than for neutral **5**, which is a direct result of the deprotonation.

Conclusions

We succeed in the synthesis of 1,3-bis(5-nitraminotetrazol-1-yl)propan-2-ol (**5**), a new highly energetic ditetrazole derivative containing a hydroxyl and a nitrimino group at the same time and a number of its salts. The neutral compound can serve as a tridentate ligand for energetic transition metal complexes. The lithium-, strontium- and barium salt could have interest as colorants in pyrotechnical compositions and the potassium salt in IR range pyrotechnics. We were also able to synthesize the sodium salt **7** and to determine the corresponding crystal structure, which proves the exclusive formation of the 1,1′-isomer crystallographically. In addition it was possible to prepare nitrogen-rich salts for the possible application as secondary explosives and we determined the crystal structure of the guanidinium salt **14**. Those compounds show reduced sensitivity to outer stimuli compared to the neutral compound and in fact can be classified as insensitive materials. Also their thermal stability are significantly higher than for the neutral compound **5** and decomposition temperatures are all above 200 °C. The calculated detonation parameters are higher than those of TNT, but still lower than those of RDX. Moreover we discovered a saver route to 1,1′-substituted **3** since no cyanogen azide is applied.

Experimental Section

CAUTION! All investigated compounds are potentially explosive energetic materials, although no hazards were observed during preparation and handling these compounds. Nevertheless, this necessitates additional meticulous safety precautions (earthed equipment, Kevlar gloves, Kevlar sleeves, face shield, leather coat, and earplugs.)

General Part: All chemicals were received from Sigma-Aldrich or ABCR and used without further purification. Sensitivity-measurements were performed on a BAM drophammer, a BAM friction tester and an OZM-ESD tester. Infrared-spectra were recorded with a Perkin-Elmer One FT-IR Spectrum BX II with a Smith ATR Dura Sample IRII. Raman spectra were determined with a Bruker MULTIRAM 1064 2000R NIR-FT Raman spectrometer. NMR spectra were recorded with a Bruker 400 MHz-spectrometer operating at 400 MHz for proton spectra. Determination of melting points and decomposition points were performed in covered Al-containers containing a hole in the lid and a nitrogen flow of 20 mL per minute with a Linseis PT 10 DSC calibrated with standard pure indium and zinc at a heating rate of 5 K·min^{-1}.

Table 2. Energetic properties of **4**, the nitrogen containing salts **11**–**15** and the nitrate salt **16**.

	5	**11**	**12**	**13**	**14**	**15**	**16**
Formula	$C_5H_8N_{12}O_5$	$(NH_4)_2\ C_5H_6N_{12}O_5$	$(N_2H_5)_2C_5H_6N_{12}O_5$	$(NH_3OH)_2C_5H_6N_{12}O_5$	$(CN_3H_7)_2C_5H_6N_{12}O_5$	$(CH_8N_4)_2C_5H_6N_{12}O_5$	$C_5H_{12}N_{10}O(NO_3)_2$
F_W /g·mol^{-1}	316.13	350.19	380.21	382.19	458.84	464.27	352.17
IS[a] /J	5	>40	>40	>40	>40	>40	25
FS[b] /N	240	>360	>360	>360	>360	>360	288
ESD[c] /J	0.7	1.5	1.5	1.5	1.5	1.5	1.5
Ω_{CO2}[d] /%	–45.55	–54.83	–54.71	–41.86	–73.23	–79.26	–40.89
T_{dec}[e] /°C	156	218	213	212	236	207	180
ρ[f] /g·cm^{-3}	1.60 pyc.	1.62 pyc.	1.52 pyc.	1.55 pyc.	1.530	1.59 pyc.	1.660
$\Delta_f H_m^{0}$[g] /kJ·mol^{-1}	467	370	669	492	350	584	–172
$\Delta_f U^{0}$[h] /kJ·kg^{-1}	1574	1055	1758	1288	806	1258	–490
EXPLO5 6.02 values							
$-\Delta_{ex}U$[i] /kJ·kg^{-1}	5470	4716	5181	5584	–969	4286	4157
T_{det}[j] /K	3691	3040	3264	3625	2610	2708	2896
P_{CJ}[k] /GPa	24	25	24	24	21	24	25
V_{Det}[l] /m·s^{-1}	8024	8462	8318	8166	8054	8475	8213
V^{0}[m] /L·kg^{-1}	816	905	935	905	912	925	864

a) Impact sensitivity according to BAM drophammer (method 1 of 6) (100 ≥ g.s. ≥ 50 µm). b) Friction sensitivity according to BAM friction tester (method 1 of 6) (100 ≥ g.s. ≥ 50 µm). c) Electrostatic discharge sensitivity (OZM ESD tester) (100 ≥ g.s. ≥ 50 µm). d) Oxygen balance. e) Temperature of decomposition according to DTA (onset temperatures at a heating rate of 5 K·min^{-1}). f) Room temperature X-ray densities. Those were calculated by the low temperature X-ray values using the equation $\{\rho 298\ K = \rho T/[1 + \alpha V(298 - T0)]$; $\alpha V = 1.5\ 10^{-4}\ K^{-1}\}$. g) Calculated heat of formation using the atomization method and CBS-4M electronic enthalpies. h) Calculated energy of formation. i) Energy of detonation. j) Temperature of detonation. k) Detonation pressure. l) Detonation velocity. m) Volume of gas after detonation.

1,3-Bis(5-amino-1*H*-tetrazol-1-yl)propan-2-ol (3): 5-Aminotetrazole (17.0 g, 0.200 mol) was suspended in water (50 mL). To this suspension NaOH (8.40 g, 0.210 mol) was added and the reaction mixture was stirred at room temperature until all solid had dissolved. Afterwards, 1,3-dichloroisopropanole (7.19 mL, 10.00 g, 0.08 mol) was added drop wisely and the mixture was heated at reflux overnight. During this time, a colorless solid precipitated, which was filtered off and washed with water. The compound was dried in an oven at 60 °C for 10 h to yield 2.81 g (16%) of the final product. $T_{dec.}$ (onset)/(5 K·min^{-1}) > 352 °C. **IR** (ATR) $\tilde{\nu}$ = 3419 (m), 3368 (m), 3241 (m), 3176 (m), 2348 (w), 1655 (s), 1646 (s), 1582 (s), 1551 (m), 1485 (m), 1446 (m), 1427 (m), 1384 (m), 1328 (m), 1280 (m), 1162 (m), 1126 (s), 1100 (s), 978 (m), 870 (m), 835 (m), 740 (m), 682 (m) cm^{-1}. **Raman** (1064 nm): $\tilde{\nu}$ = 3121 (5), 2985 (5), 1750 (3), 1263 (7), 972 (8), 880 (10), 732 (8), 89 (100) cm^{-1}. **^{1}H NMR** ([D$_6$]DMSO, 400 MHz, 298 K): δ = 4.05–4.31 (m, 4 H), 5.59 (d, 1 H, ^3J = 8 Hz), 6.62 (s, 4 H). **^{13}C NMR** ([D$_6$]DMSO, 100 MHz, 298 K): δ = 48.3 (*C*H$_2$), 67.0 (*C*HO), 156.0 ($C_{arom.}$) ppm. **MS** (DEI$^+$): *m*/*z*: 226.1 [M]$^+$. $C_5H_{10}N_{10}O$ (226.15 g·mol^{-1}) found (calcd.): N 61.51 (61.90), C 26.70 (26.55), H 4.30 (4.47)%. IS: 40 J. FS: 360 N. ESD: 1.5 J (100 ≥ g.s. ≥50 µm).

1,3-Bis(5-nitraminotetrazol-1-yl)propan-2-ol (5): Compound **3** (1.250 g, 5.527·10^{-3} mol) was portion wise put into 100% nitric acid (30 mL) at 0 °C. This solution was stirred overnight whereupon it slowly reached room temperature. The next day, the mixture was poured onto ca. 400 g of crushed ice. This solution was left at air for the solvent to evaporate. After 4 d, the product was filtered off as a colorless solid, washed excessively with water, and dried on air to yield 1.090 g (62%) of the pure product as a colorless solid. $T_{dec.}$ (onset)/(5 K·min^{-1}) = 156 °C. **IR** (ATR) $\tilde{\nu}$ = 2361 (s), 2342 (s), 1576 (m), 1207 (m), 1028 (w) cm^{-1}. **Raman** (1064 nm): $\tilde{\nu}$ = 3052 (5), 2948 (10), 1612 (24), 1522 (100), 1476 (23), 1210 (11), 1165 (46), 971 (10), 858 (6), 712 (11), 500 (8), 301 (12), 298 (11) cm^{-1}. **^{1}H NMR** ([D$_6$]DMSO, 400 MHz, 298 K): δ = 3.92–4.65 (m, 6 H). **^{13}C NMR** ([D$_6$]DMSO, 100 MHz, 298 K): δ = 50.0 (*C*H$_2$), 64.8 (*C*HO), 151.1 ($C_{arom.}$) ppm. **MS** (DEI$^+$): *m*/*z*: 340.1 [M]$^+$. $C_5H_8N_{12}O_5$ (316.13 g·mol^{-1}) found (calcd): N 52.83 (53.14), C 18.70 (19.00), H 2.43 (2.56) %. IS: 5 J. FS: 240 N. ESD: 0.7 J.

Lithium (1,3-Bis(5-nitraminotetrazol-1-ylate)propan-2-ol·2H$_2$O (6): Compound **5** (0.100 g, 3.16×10^{-4} mol) was suspended in water (10 mL). Afterwards a LiOH solution (0.317 mL, 2 M, 0.0152 g, 6.33×10^{-4} mol) was added and the mixture was heated to reflux for 10 min. The solvent was removed in vacuo. After this, the crude product was recrystallized form hot ethanol under the dropwise addition of water to yield 0.0200 g (17%) of the final product as a colorless solid. $T_{dec.}$ (onset)/(5 K·min^{-1}) = 160 °C. **IR** (ATR) $\tilde{\nu}$ = 3424 (w), 2286 (w), 1640 (w), 1575 (m), 1514 (m), 1487 (m), 1462 (m), 1307 (s), 1242 (s), 1212 (s), 1106 (m), 1032 (m), 976 (w), 885 (w), 777 (w), 740 (w), 723 (w), 693 (w) cm^{-1}. **Raman** (1064 nm): $\tilde{\nu}$ = 3051 (5), 2945 (10), 1612 (24), 1523 (100), 1473 (23), 1213 (11), 1163 (46), 971 (10), 853 (6), 714 (11), 502 (8), 303 (12), 298 (11) cm^{-1}. **^{1}H NMR** (D$_2$O, 400 MHz, 298 K): δ = 4.42–4.69 (m, 5 H). ^{13}C NMR (D$_2$O, 100 MHz, 298 K): δ = 49.3 (*C*H$_2$), 66.7 (*C*OH), 155.6 (C_{arom}). **^{14}N NMR** (D$_2$O, 29 MHz, 298 K): δ = –18 (*N*O$_2$) ppm. **MS** (FAB$^-$): *m*/*z*: 315.4 ($C_5H_7N_{12}O_5^-$). $Li_2C_5H_6N_{12}O_5{\cdot}2H_2O$ (364.03 g·mol^{-1}) found (calcd.): N 44.92 (46.15), C 16.70 (16.50), H 3.16 (2.78)%. IS: 40 J. FS: 360 N. ESD: 1.5 J (100 ≥ g.s. ≥ 50 µm).

Sodium 1,3-Bis(5-nitraminotetrazol-1-ylate)propan-2-ol·4H$_2$O (7): Compound **5** (0.200 g, 6.33×10^{-4} mol) was suspended in water (10 mL). To this solution a NaOH solution (0.635 mL, 2 M, 0.0508 g, 1.27×10^{-3} mol) was added drop wisely. After all solid has dissolved, the reaction mixture was heated under reflux for 10 min. Afterwards, the solvent was removed in vacuo. After this, the crude product was recrystallized form hot ethanol under the dropwise addition of water to yield 0.101 g (37%) of the final product as a colorless solid. $T_{dec.}$ (onset)/(5 K·min^{-1}) = 245 °C. **IR** (ATR) $\tilde{\nu}$ = 3853 (w), 3745 (w), 3649 (w), 3410 (m), 1653 (m), 1540 (m), 1506 (s), 1457 (s), 1429 (m), 1388 (s), 1338 (s), 1108 (m), 1042 (m), 900 (m), 867 (m), 789 (m), 739 (m) cm^{-1}. **Raman** (1064 nm): $\tilde{\nu}$ = 3050 (5), 2986 (6), 2975 (5), 1511 (100), 1412 (8), 1395 (14), 1213 (6), 1045 (45), 982 (3), 912 (4), 895 (5), 723 (8), 501 (8), 302 (3), 298 (6), 283 (6) cm^{-1}. **^{1}H NMR**

(D_2O, 400 MHz, 298 K): δ = 4.40–4.60 (m, 5 H). **^{13}C NMR** (D_2O, 100 MHz, 298 K): δ = 49.2 (CH_2), 66.9 (COH), 156.4 (C_{arom}). **^{14}N NMR** (D_2O, 29 MHz, 298 K): δ = –18 (NO_2) ppm. **MS** (FAB$^-$): *m/z*: 315.4 ($C_5H_7N_{12}O_5^-$). $Na_2C_5H_6N_{12}O_5{\cdot}4H_2O$ (432.19 g·mol^{-1}) found (calcd.): N 37.54 (38.87), C 14.08 (13.89), H 2.97 (3.26)%. IS: 40 J. FS: 360 N. ESD: 1.5 J (100 ≥ g.s. ≥ 50 µm).

Potassium 1,3-Bis(5-nitraminotetrazol-1-ylate)propan-2-ol·H$_2$O (8): Compound **5** (0.100 g, 3.16×10^{-4} mol) was suspended in water (10 mL). To this solution a KOH solution (0.317 mL, 2 M, 0.0355 g, 6.33×10^{-4} mol) was added drop wisely. After all solid has dissolved, the reaction mixture was heated under reflux for 10 min. Afterwards the solvent was removed in vacuo. After this, the crude product was recrystallized form hot ethanol under the dropwise addition of water to yield 0.0523 g (42%) of the final product as a colorless solid. $T_{dec.}$ (onset)/(5 K·min^{-1}) = 271 °C. **IR** (ATR) $\tilde{\nu}$ = 3356 (w), 1725 (w), 1503 (m), 1451 (m), 1296 (s), 1104 (m), 1033 (m), 884 (w), 776 (m), 739 (w), 693 (w) cm^{-1}. **Raman** (1064 nm): $\tilde{\nu}$ = 2984 (8), 1513 (100), 1320 (14), 1210 (7), 1040 (48), 820 (5), 752 (8), 501 (5) cm^{-1}. **^{1}H NMR** (D_2O, 400 MHz, 298 K): δ = 4.39–4.64 (m, 5 H). **^{13}C NMR** (D_2O, 100 MHz, 298 K): δ = 49.2 (CH_2), 66.9 (COH), 156.4 (C_{arom}). **^{14}N NMR** (D_2O, 29 MHz, 298 K): δ = –18 (NO_2) ppm. **MS** (FAB$^-$): *m/z*: 315.4 ($C_5H_7N_{12}O_5^-$). $K_2C_5H_6N_{12}O_5{\cdot}H_2O$ (394.13 g·mol^{-1}) found (calcd): N 40.15 (40.94), C 15.12 (14.63), H 2.25 (1.97)%. IS: 40 J. FS: 360 N. ESD: 1.5 J (100 ≥ g.s. ≥ 50 µm).

Strontium 1,3-Bis(5-nitraminotetrazol-1-ylate)propan-2-ol·2H$_2$O (9): Compound **5** (0.100 g, 3.16×10^{-4} mol) was suspended in water (10 mL). To this solution strontiumhydroxide octahydrate (0.0840 g, 3.16×10^{-4} mol) was added and the resulting clear solution was heated under reflux conditions for 10 min. Afterwards the solvent was removed in vacuo. After this, the crude product was recrystallized form hot ethanol under the dropwise addition of water to yield 0.0815 g (69%) of the product as a colorless solid. $T_{dec.}$ (onset)/(5 K·min^{-1}) = 299 °C. **IR** (ATR) $\tilde{\nu}$ = 3459 (w), 1604 (w), 1509 (m) 1456 (m), 1364 (s), 1333(s), 1324 (s), 1303 (s), 1276 (m), 1245 (m), 1148 (w), 1107 (w), 1083 (w), 1038 (m), 1004 (w), 964 (w), 905 (w), 887 (w), 856 (w), 787 (w), 770 (w), 759 (w), 746 (w), 735 (w), 702 (w) cm^{-1}. **Raman** (1064 nm): $\tilde{\nu}$ = 2985 (9), 1511 (100), 1323 (12), 1043 (32), 502 (5) cm^{-1}. **^{1}H NMR** (D_2O, 400 MHz, 298 K): δ = 4.34–4.54 (m, 5 H). **^{13}C NMR** (D_2O, 100 MHz, 298 K): δ = 49.2 (CH_2), 66.9 (COH), 155.6 (C_{arom}). **^{14}N NMR** (D_2O, 29 MHz, 298 K): δ = –18 (NO_2). **MS** (FAB$^-$): *m/z*: 315.4 ($C_5H_7N_{12}O_5^-$). $SrC_5H_6N_{12}O_5{\cdot}2H_2O$ (373.77 g·mol^{-1}) found (calcd.): N 36.86 (38.38), 13.65 (13.72), 2.56 (2.31)%. IS: 40 J. FS: 360 N. ESD: 1.5 J (100 ≥ g.s. ≥ 50 µm).

Barium 1,3-Bis(5-nitraminotetrazol-1-ylate)propan-2-ol·2H$_2$O (10): Compound **5** (0.100 g, 3.16×10^{-4} mol) was suspended in water (10 mL). To this solution bariumhydroxide octahydrate (0.0943 g, 3.16×10^{-4} mol) was added and the resulting clear solution was heated under reflux conditions for 10 min. Afterwards the solvent was removed in vacuo. After this, the crude product was recrystallized form hot ethanol under the dropwise addition of water to yield 0.0722 g (47%) of the product as a colorless solid. $T_{dec.}$ (onset)/(5 K·min^{-1}) = 166 °C. **IR** (ATR) $\tilde{\nu}$ = 2361 (s), 2341 (s), 1596 (m), 1307 (m), 1243 (m), 1032 (w) cm^{-1}. **Raman** (1064 nm): = 2984 (5), 1506 (100), 1349 (28), 1115 (12), 1025 (26), 942 (5), 753 (12), 502 (4), 295 (3) cm^{-1}. **^{1}H NMR** (D_2O, 400 MHz, 298 K): δ = 4.32–4.58 (m, 5 H). **^{13}C NMR** (D_2O, 100 MHz, 298 K): δ = 49.3 (CH_2), 66.7 (COH), 155.7 (C_{arom}). **^{14}N NMR** (D_2O, 29 MHz, 298 K): δ = –18 (NO_2) ppm. **MS** (FAB$^-$): *m/z*: 315.4 ($C_5H_7N_{12}O_5^-$). $BaC_5H_6N_{12}O_5{\cdot}2H_2O$ (487.48 g·mol^{-1}) found (calcd.): N 34.42 (34.46), C 13.23 (12.31), H 2.38 (2.07)%. IS: 40 J. FS: 360 N. ESD: 1.5 J (100 ≥ g.s. ≥ 50 µm).

Ammonium 1,3-Bis(5-nitraminotetrazol-1-ylate)propan-2-ol (11): Compound **5** (0.499 g, 1.58×10^{-3} mol) was suspended in a 25% aqueous ammonia solution (49 mL, 0.0540 g, 3.16×10^{-3} mol) at room temperature. The clear solution was stored in an open vessel for evaporation to yield 0.223 g (40%) of the product as a colorless solid. $T_{dec.}$ (onset)/(5 K·min^{-1}) = 218 °C. **IR** (ATR) $\tilde{\nu}$ = 3209 (m), 2361 (m), 2341 (m), 1635 (w), 1500 (m), 1418 (s), 1374 (s), 1302 (s), 1284 (s), 1169 (m), 1112 (m), 1035 (m), 919 (w), 886 (m), 861 (s), 792 (w), 773 (m), 755 (w), 738 (m), 684 (w) cm^{-1}. **Raman** (1064 nm): $\tilde{\nu}$ = 2985 (6), 1515 (100), 1505 (98), 1431 (11), 1409 (29), 1198 (12), 1037 (82), 962 (5), 812 (6), 713 (8), 501 (5), 296 (7) cm^{-1}. **^{1}H NMR** (D_2O, 400 MHz, 298 K): δ = 4.37–4.57 (m, 5 H). **^{13}C NMR** (D_2O, 100 MHz, 298 K): δ = 49.2 (CH_2), 66.9 (COH), 156.3 (C_{arom}). **^{14}N NMR** (D_2O, 29 MHz, 298 K): δ = –18 (NO_2), 365 (NH_4). **MS** (FAB$^-$): *m/z*: 315.4 ($C_5H_7N_{12}O_5^-$), (FAB$^+$): *m/z*: 18.0 (NH_4^+). $C_5H_{14}N_{14}O_5$ (350.19 g·mol^{-1}) found (calcd.): N 52.23 (55.97), C 16.70 (17.15), H 4.42 (4.04)%. IS: 40 J. FS: 360 N. ESD: 1.5 J (100 ≥ g.s. ≥ 50 µm).

Hydrazinium 1,3-Bis(5-nitraminotetrazol-1-ylate)propan-2-ol (12): Compound **5** (0.200 g, 6.33×10^{-4} mol) was suspended in water (10 mL). Afterwards hydrazinhydrate (100%) (0.0611 mL, 1.26×10^{-3} mol, 0.0631 g) was added and the solution was stirred at room temperature until it turns completely clear. Afterwards the solvent was evaporated. After this, the crude product was recrystallized form hot ethanol under the dropwise addition of water to yield 0.113 g (47%) of the product as a colorless solid. $T_{dec.}$ (onset)/(5 K·min^{-1}) = 213 °C. **IR** (ATR) $\tilde{\nu}$ = 3331 (m), 3089 (m), 2044 (w), 1605 (m), 1502 (s), 1450 (m), 1425 (m), 1366 (m), 1290 (s), 1172 (m), 1095 (s), 11031 (m), 948 (m), 884 (m), 773 (m), 751 (w), 736 (m), 716 (w), 690 (w) cm^{-1}. **Raman** (1064 nm): $\tilde{\nu}$ = 2988 (8), 1502 (100), 1315 (9), 1231 (5), 1224 (28), 752 (5), 503 (4) cm^{-1}. **^{1}H NMR** (D_2O, 400 MHz, 298 K): δ = 4.38–4.63 (m, 5 H). **^{13}C NMR** (D_2O, 100 MHz, 298 K): δ = 49.2 (CH_2), 67.0 (COH), 156.4 (C_{arom}). **^{14}N NMR** (D_2O, 29 MHz, 298 K): δ = –13 (NO_2), 332 (N_2H_4) ppm. **MS** (FAB$^-$): *m/z*: 315.4 ($C_5H_7N_{12}O_5^-$), (FAB$^+$): *m/z*: 33.1 ($N_2H_5^+$). $C_5H_{16}N_{16}O_5$ (380.21 g·mol^{-1}) found (calcd.): N 56.08 (58.93), C 15.87 (15.79), H 4.58 (4.24)%. IS: 40 J. FS: 360 N. ESD: 1.5 J (100 ≥ g.s. ≥ 50 µm).

Hydroxylammonium 1,3-Bis(5-nitraminotetrazol-1-ylate)propan-2-ol (13): Compound **5** (0.200 g, $6.33.10^{-4}$ mol) was suspended in water (10 mL). Afterwards hydroxylamine in water (0.0798 mL, 50 wt%, 0.0430 g, 1.30×10^{-3} mol) was added and the solution was stirred at room temperature until it turns completely clear. Afterwards the solvent was evaporated. After this, the crude product was recrystallized form hot ethanol under the dropwise addition of water to yield 0.105 g (44%) of the product as a colorless solid. $T_{dec.}$ (onset)/(5 K·min^{-1}) = 212 °C. **IR** (ATR) $\tilde{\nu}$ = 3979 (w), 3789 (w), 2950 (m), 2713 (m), 1587 (w), 1548 (w), 1510 (m), 1502 (m), 1451 (m), 1426 (m), 1295 (s), 1165 (m), 1106 (m), 1032 (m), 1000 (m), 874 (w), 773 (m), 739 (w), 692 (w) cm^{-1}. **Raman** (1064 nm): $\tilde{\nu}$ = 2986 (8), 1505 (100), 1311 (9), 1231 (5), 1223 (28), 753 (5), 501 (4) cm^{-1}. **^{1}H NMR** (D_2O, 400 MHz, 298 K): δ = 4.40–4.62 (m, 5 H). **^{13}C NMR** (D_2O, 100 MHz, 298 K): δ = 49.3 (CH_2), 67.2 (COH), 156.6 (C_{arom}). **^{14}N NMR** (D_2O, 29 MHz, 298 K): δ = –13 (NO_2) ppm. **MS** (FAB$^-$): *m/z*: 315.4 ($C_5H_7N_{12}O_5^-$), (FAB$^+$): *m/z*: 34.0 (NH_3OH^+). $C_5H_{14}N_{14}O_7$ (382.19 g·mol^{-1}) found (calcd.): N 48.85 (51.28), C 15.47 (15.71), H 4.01 (3.70)%. IS: 40 J. FS: 360 N. ESD: 1.5 J (100 ≥ g.s. ≥ 50 µm).

Guanidinium 1,3-Bis(5-nitraminotetrazol-1-ylate)propan-2-ol (14): Compound **5** (0.200 g, 6.33×10^{-4} mol) was suspended in water (10 mL). Afterwards guanidinium carbonate (0.114 g, 6.33×10^{-4} mol) was added and the mixture was heated until a clear solution remains. Afterwards the solvent was evaporated. After this, the crude product was recrystallized form hot ethanol under the dropwise addition of

water to yield 0.214 g (78 %) of the final product as a colorless solid. $T_{dec.}$ (onset)/(5 K·min^{-1}) = 236 °C. **IR** (ATR) $\tilde{\nu}$ = 3745 (w), 3356 (m), 1653 (s), 1506 (s), 1456 (m), 1312 (s), 1284 (m), 1112 (m), 1052 (m), 863 (w), 769 (w) cm^{-1}. **Raman** (1064 nm): $\tilde{\nu}$ = 2991 (11), 2523 (12), 1510 (100), 1499 (97), 1432 (33), 1103 (13), 1039 (72), 1062 (15), 823 (5), 720 (13), 503 (5) cm^{-1}. **^{1}H NMR** (D_2O, 400 MHz, 298 K): δ = 4.38–4.62 (m, 5 H). **^{13}C NMR** (D_2O, 100 MHz, 298 K): δ = 49.2 (CH_2), 66.9 (*C*OH), 156.3 (C_{arom}). **^{14}N NMR** (D_2O, 29 MHz, 298 K): δ = –18 (NO_2), –313 (NH_2) ppm. **MS** (FAB$^-$): *m/z*: 315.4 ($C_5H_7N_{12}O_5^-$), (FAB$^+$): *m/z*: 60.1 ($CN_3H_6^+$). $C_7H_{18}N_{18}O_5$ (434.25 g·mol^{-1}) found (calcd.): N 57.12 (58.03), C 19.86 (19.36), H 4.17 (4.19) %. IS: 40 J. FS: 360 N. ESD: 1.5 J (100 ≥ g.s. ≥ 50 µm).

Aminoguanidinium 1,3-Bis(5-nitraminotetrazol-1-ylate)propan-2-ol (15): Compound **5** (0.100 g, 3.16×10^{-4} mol) was suspended in water (5 mL) and heated under reflux conditions. Afterwards a solution of aminoguanidinium hydrogen carbonate (0.0854 g, 6.27×10^{-4} mol) was added and the heating was continued for additional 30 min. The solvent was evaporated. After this, the crude product was recrystallized form hot ethanol under the dropwise addition of water to yield 0.120 g (82 %) of the final product as a colorless solid. $T_{dec.}$ (onset)/(5 K·min^{-1}) = 207 °C. **IR** (ATR) $\tilde{\nu}$ = 3334 (m), 3173 (m), 2361 (m), 2342 (m), 1661 (s), 1595 (m), 1507 (s), 1450 (m), 1315 (s), 1273 (s), 1106 (s), 1033 (m), 885 (m), 773 (m), 737 (w), 716 (w), 694 (w) cm^{-1}. **Raman** (1064 nm): $\tilde{\nu}$ = 3252 (3), 1782 (2), 1509 (100), 1385 (16), 1132 (14), 1033 (42), 978 (7), 898 (5), 762 (5), 661 (3), 502 (7), 107 (48) cm^{-1}. **^{1}H NMR** (D_2O, 400 MHz, 398 K): δ = 4.42–4.65. **^{13}C NMR** (D_2O, 100 MHz, 398 K): δ = 49.8 (CH_2), 67.0 (*C*HO), 158.2 ($C_{arom.}$), 160.0 [$C(NH_2)_2NHNH_2$]. **^{14}N NMR** (D_2O, 29 MHz, 298 K): δ = –13 (NO_2) ppm. **MS** (FAB$^-$): *m/z*: 315.4 ($C_5H_7N_{12}O_5^-$), (FAB$^+$): *m/z*: 75.1 ($CN_4H_7^+$). $C_7H_{20}N_{20}O_5$ (464.27 g·mol^{-1}) found (calcd.): N 56.77 (60.31), C 18.41 (18.11), H 4.05 (4.35) %. IS: 40 J. FS: 360 N. ESD: 1.5 J (100 ≥ g.s. ≥ 50 µm).

1,3-Bis(5-amino-1*H*-tetrazol-1-yl)propan-2-ol nitrate (16): Compound **3** (0.453 g, 2.00×10^{-3} mol) was suspended in water (5 mL). To this suspension 65 % HNO_3 (5.00 mL, 4.52 g, 0.0717 mol) was added. After the short formation of a clear solution a colorless, flaked precipitate forms. This solid was filtered off, washed with water and subsequently diethyl ether to yield 0.360 g (51 %) of the final product as a colorless solid after air drying. $T_{dec.}$ (onset)/(5 K·min^{-1}) = 180 °C. **IR** (ATR)$\tilde{\nu}$ = 3852 (w), 3745 (w), 3254 (m), 3117 (m), 1733 (w), 1683 (s), 1507 (w), 1329 (s), 1253 (s),1150 (m), 1093 (m), 11035 (m), 993 (m), 972 (m), 875 (m), 818 (m), 780 (w), 724 (w), 711 (m) cm^{-1}. **Raman** (1064 nm):$\tilde{\nu}$ = 3952 (11), 3286 (5), 3042 (7), 2986 (10), 1983 (13), 1523 (14), 1724 (12), 1403 (11), 1210 (13), 1052 (100), 820 (9), 803 (12), 782 (13), 502 (6) cm^{-1}. **^{1}H NMR** ([D_6]DMSO, 400 MHz, 398 K): δ = 4.03–4.34 (m, 5 H), 5.89 (s). **^{13}C NMR** ([D_6]DMSO, 100 MHz, 398 K): δ = 48.4 (CH_2), 66.4 (*C*HO), 155.7 ($C_{arom.}$). **MS** (FAB$^-$): *m/z*: 62 (NO_3^-), (FAB$^+$): *m/z*: 229 ($C_5H_{13}N_{10}O^+$). $C_5H_{12}N_{12}O_7$ (352.17 g·mol^{-1}) found (calcd.): N 47.26 (47.72), C 17.31 (17.05), H 3.41 (3.60) %. IS: 25 J. FS: 288 N. ES: 1.5 J (100 ≥ g.s. ≥ 50 µm).

Supporting Information (see footnote on the first page of this article): a) crystallographic data and parameters; b) theoretical calculations.

Acknowledgements

Financial support of this work by the Ludwig-Maximilian University of Munich (LMU) and the Office of Naval Research (ONR) under grant no. ONR.N00014–12–1-0538 is gratefully acknowledged. The authors acknowledge collaborations with *Dr. Mila Krupka* (OZM Research, Czech Republic) in the development of new testing and evaluation methods for energetic materials and with *Dr. Muhamed Suceska* (Brodarski Institute, Croatia) in the development of new computational codes to predict the detonation and propulsion parameters of novel explosives. The authors thank *Mr. Stefan Huber* for sensitivity measurements.

References

[1] T. M. Klapötke *Chemistry of High Energy Density Materials*, Walter de Gruyter, 3rd ed., Berlin, **2015**.
[2] T. M. Klapötke, T. G. Witkowski, *ChemPlusChem* **2016**, *81*, 357–360.
[3] V. A. Ostrovskii, M. S. Pevzner, T. M. Kofman, I. V. Tselinskii, *Targets Heterocycl. System* **1999**, *3*, 467–526.
[4] Y.-H. Joo, J. M. Shreeve, *Angew. Chem. Int. Ed.* **2009**, *48*, 564–567.
[5] X. Zhang, X. Gong, *J. Mol. Model.* **2015**, *21*, 318–324.
[6] N. Fischer, T. M. Klapötke, J. Stierstorfer, *Eur. J. Inorg. Chem.* **2011**, *28*, 4471–4480.
[7] T. M. Klapötke, M. Leroux, P. C. Schmid, J. Stierstorfer, *Chem. Asian J.* **2016**, *11*, 844–851.
[8] N. Fischer, D. Izsak, T. M. Klapötke, J. Stierstorfer, *Chem. Eur. J.* **2013**, *19*, 8948–8957.
[9] N. Fischer, T. M. Klapötke, J. Stierstorfer, K. R. Tarantik, *13th Seminar New Trends in Research of Energetic Materials*, Pardubice, Czech Republic, Apr. 21–23, **2010**, Pt. 2, 455–467.
[10] J. Stierstorfer, K. R. Tarantik, T. M. Klapötke, *Chem. Eur. J.* **2009**, *15*, 5775–5792.
[11] M. Joas, T. M. Klapötke, *Propellants Explos. Pyrotech.* **2015**, *2*, 246–252.
[12] N. Fischer, M. Joas, T. M. Klapötke, J. Stierstorfer, *Inorg. Chem.* **2013**, *52*, 13791–13802.
[13] E. C. Koch, *Propellants Explos. Pyrotech.* **2004**, *29*, 67–80.
[14] S. Scheutzow, *Dissertation* **2012**, LMU Munich.
[15] B. Stiasny, *Master's Thesis* **2013**, TU Munich.
[16] Y.-H. Joo, J. M. Shreeve, *Org. Lett.* **2008**, *10*, 4665–4667.
[17] J. Stierstorfer, private communication.
[18] K. Hafner, T. M. Klapötke, P. C. Schmid, J. Stierstorfer, *Eur. J. Inorg. Chem.* **2015**, 2794–2803.
[19] P. J. van Koningsbruggen, Y. Garcia, O. Kahn, L. Fournès, H. Kooijman, A. L. Spek, J. G. Haasnoot, J. Moscovici, K. Provost, A. Michalowicz, F. Renz, P. Gütlich, *Inorg. Chem.* **2000**, *39*, 1891–1900.
[20] P. J. van Koningsbruggen, Y. Garcia, G. Brevic, D. Chesseau, O. Kahn, *Inorg. Chim. Acta* **2001**, *326*, 101–105.
[21] J. W. Baker, A. J. Neale, *J. Chem. Soc.* **1955**, 608–615.
[22] E. Camera, G. Modena, B. Zotti, *Propellants Explos. Pyrotech.* **1983**, *8*, 70–73.
[23] K. Karaghiosoff, T. M. Klapötke, P. Mayer, C. M. Sabate, A. Penger, J. M. Welch, *Inorg. Chem.* **2008**, *47*, 1007–1019.
[24] N. Fischer, T. M. Klapötke, J. Stierstorfer, *Propellants Explos. Pyrotech.* **2011**, *36*, 225–232.
[25] N. Fischer, T. M. Klapötke, D. G. Piercey, J. Stierstorfer, *Z. Anorg. Allg. Chem.* **2012**, *2*, 302–310.
[26] J. Stierstorfer, K. R. Tarantik, T. M. Klapötke, *Chem. Eur. J.* **2009**, *15*, 5775–5792.
[27] M. v. Denffer, T. M. Klapötke, G. Kramer, G. Spieß, J. M. Welch, *Propellants Explos. Pyrotech.* **2005**, *30*, 191–195.

Received: October 10, 2016
Published Online: ■

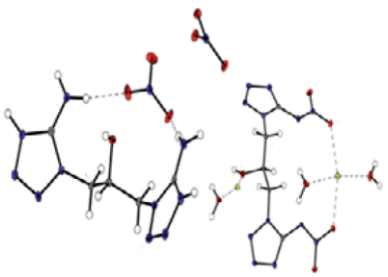

Z. Anorg. Allg. Chem. **2016** · ISSN 0044–2313

SUPPORTING INFORMATION

Title: Synthesis and Investigation of 1,3-Bis(5-nitraminotetrazol-1-yl)propan-2-ol and its Salts
Author(s): T. M. Klapötke,* B. Stiasny, J. Stierstorfer
Ref. No.: z201600389

Supporting Information

Table of contents

1.X-ray diffraction

For all compounds, an Oxford Xcalibur3 diffractometer with a CCD area detector was employed for data collection using Mo-Kα radiation (λ = 0.71073 Å). By using the Crystalispro software[S1] the data collection and reduction were performed. The structures were solved by direct methods (SIR-92[S2], SIR-97[S3] and SHELXS-97[S4]) and refined by fullmatrix least-squares on *F*2 (SHELXL [S4]) and finally checked by using the PLATON software [S5] integrated in the WinGX software suite. The non-hydrogen atoms were refined anisotropically and the hydrogen atoms were located and freely refined. The absorptions were corrected by a SCALE3 ABSPACK multiscan method [S6]. All DIAMOND2 plots are shown with thermal ellipsoids at 50% probability level and hydrogen atoms are shown as small spheres of arbitrary radius.

Table S1. X-ray data of compounds **6**, **13** and **17**.

Compound	**6**	**13**	**17**
Formula	$Na_2C_5H_{12}N_{12}O_8$	$(CH_6N_3)_2C_5H_6N_{12}O_5$	$C_5H_{12}N_{10}O\ (NO_3)_2$
FW [g/mol]	414.25	434.39	352.27
Crystal system	orthorhombic	triclinic	monoclinic
Space Group	$P2_12_12_1$	$P\bar{1}$	$P2_1/c$
Color / Habit	Colorless plate	Colorless plate	Colorless plate
Size [mm]	0.05 x 0.20 x 0.18	0.12 x 0.16 x 0.20	0.05 x 0.09 x 0.19
a [Å]	8.2263(4)	6.4582(3)	5.5668(5)
b [Å]	12.3460(5)	9.9563(4)	9.7479(9)
c [Å]	14.9228(6)	13.7821(5)	25.3527(19)
α [°]	90	94.765(3)	90
β [°]	90	98.026(3)	95.670(2)
γ [°]	90	95.835(3)	90
V [Å^3]	1515.59(11)	868.69(6)	1369.0(2)
Z	4	2	4
$\rho_{calc.}$ [g cm^{-3}]	1.816	1.661	1.709
μ [mm^{-1}]	0.209	0.140	0.154
F (000)	848	452	728
$\lambda_{MoK\alpha}$ [Å]	0.71073	0.71073	0.71073
T [K]	100	123	100
ϑ min max [°]	4.1, 27.0	4.3, 26.5	2.2, 26.5
Dataset h; k; l	−10:10; −15:15; −19:18	−8:8; −12:12; −17:17	−6:6; −11:12;−29:31
Reflect. coll.	12826	13085	20089
Independ. refl.	1892	3585	2822
R_{Int}	0.046	0.023	0.037
Reflection obs.	1692	3585	2344
No. parameters	272	339	265
R_1 obs.	0.0275	0.0343	0.0363
wR_2 (all data)	0.0657	0.0890	0.0848
S	1.06	1.04	1.06
Resd. Dens. [e Å^{-3}]	−0.19;0.37	−0.25:0.56	−25;0.36
Device type	Oxford Xcalibur3 CCD	Oxford Xcalibur3 CCD	Oxford Xcalibur3 CCD
Solution	SIR-92	SIR-92	SIR-92
Refinement	SHELXL-2013	SHELXL-2013	SHELXL-2013
Absorption corr.	multi-scan	multi-scan	multi-scan
CCDC	1505422	1505421	1505420

2.NMR-spectroscopy

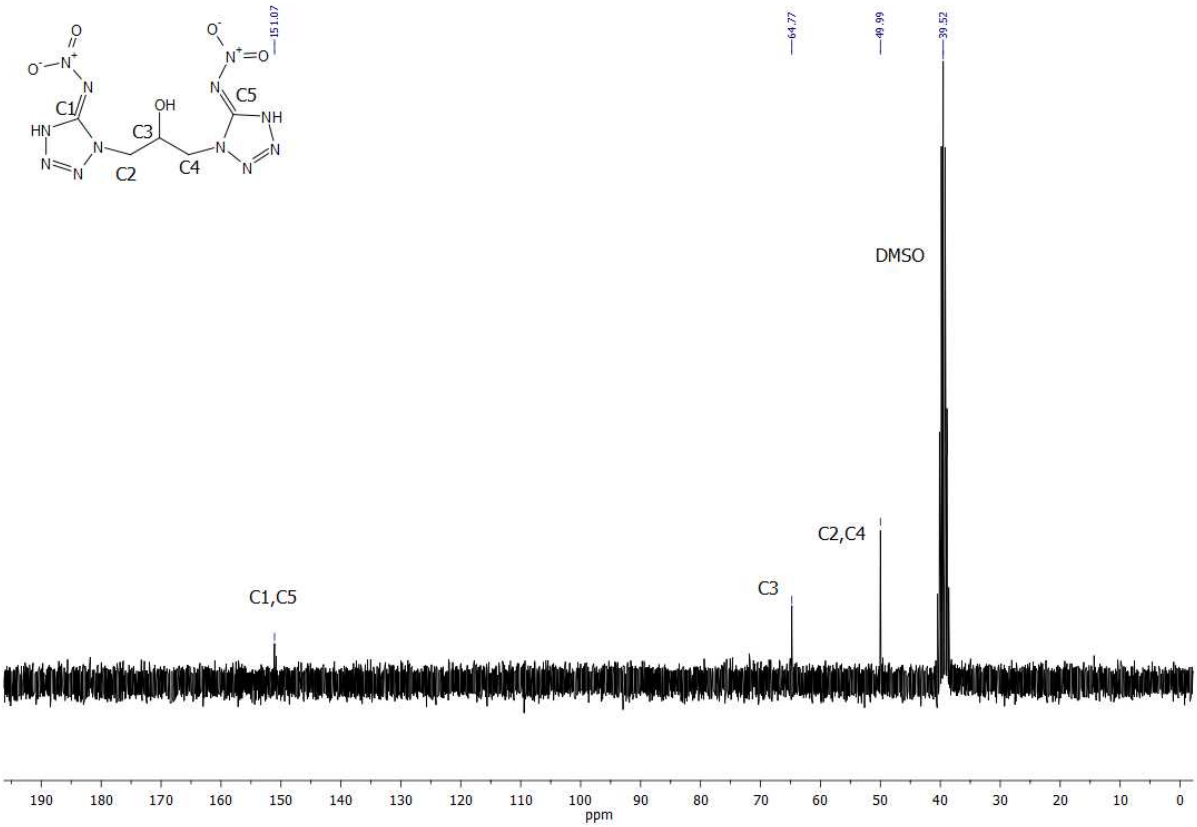

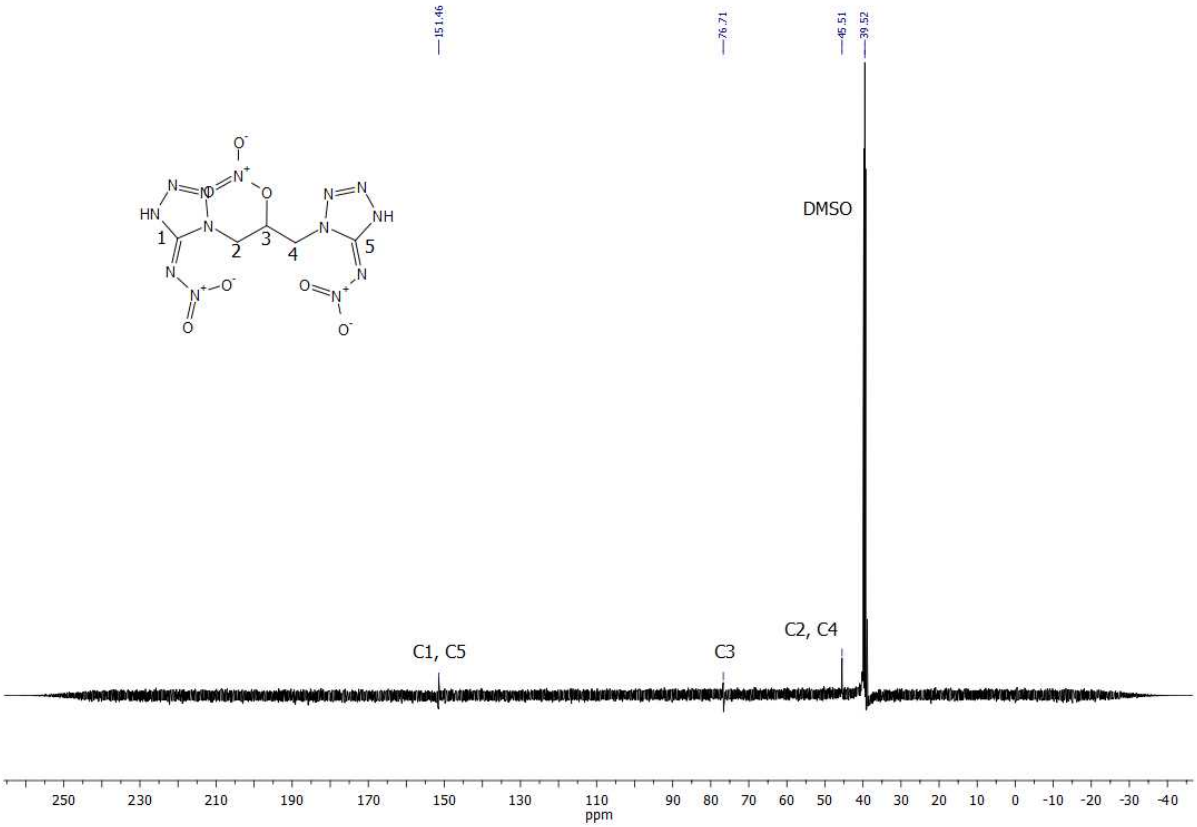

3.Heats of formation calculations

All calculations were carried out using the Gaussian G09W (revision A.02) program package. The enthalpies (H) and free energies (G) were calculated using the complete basis set (CBS) method of Petersson and coworkers in order to obtain very accurate energies. The CBS models use the known asymptotic convergence of pair natural orbital expressions to extrapolate from calculations using a finite basis set to the estimated complete basis set limit. CBS-4 begins with a HF/3-21G(d) geometry optimization; the zero point energy is computed at the same level. It then uses a large basis set SCF calculation as a base energy, and a MP2/6-31+G calculation with a CBS extrapolation to correct the energy through second order. A MP4(SDQ)/6-31+(d,p) calculation is used to approximate higher order contributions. In this study we applied the modified CBS-4M method (M referring to the use of Minimal Population localization) which is a re-parametrized version of the original CBS-4 method and also includes some additional empirical corrections.[S7] The enthalpies of the gas-phase species M were computed according to the atomization energy method (eq.1).

$$\Delta_f H^\circ_{(g,\,M,\,298)} = H_{(Molecule,\,298)} - \sum H^\circ_{(Atoms,\,298)} + \sum \Delta_f H^\circ_{(Atoms,\,298)} \quad (1)$$

Table S2. CBS-4M results and calculated gas-phase enthalpies

	M	$-H^{298}$ / a.u.	$\Delta_f H°$(g,M) / kcal mol^{-1}
5	316.13	1226.61983	128.9
5^{2-}	314.11	1225.55226	68.3
11	350.19	1339.145476	372.1
NH_4^+	18.04	56.796608	151.9
12	380.21	1449.613306	438.1
$N_2H_5^+$	33.05	112.030523	184.9
13	382.19	1489.278758	396.6
NH_4O^+	34.04	131.863249	164.1
14	458.84	1636.458644	341.5
G^+	60.07	205.453192	136.6
15	464.47	1746.955864	389.2
AG^+	75.08	260.701802	160.4
16	352.17	1378.844201	309.6
3^{2+}	228.17	818.683309	459.4
NO_3^-	62.00	280.080446	−74.9

Table S3 CBS-4M values and literature values for atomic $\Delta H°_f^{298}$ / kcal mol^{-1}

	$-H^{298}$ / a.u.	NIST [S8]
H	0.500991	52.1
C	37.786156	171.3
N	54.522462	113.0
O	74.991202	59.6

In the case of the ionic compounds, the lattice energy (U_L) and lattice enthalpy (ΔH_L) were calculated from the corresponding X-ray molecular volumes according to the equations provided by Jenkins and Glasser. With the calculated lattice enthalpy (Table 8) the gas-phase enthalpy of formation (Table 7) was converted into the solid state (standard conditions) enthalpy of formation (Table 8). These molar standard enthalpies of formation (ΔH_m) were used to calculate the molar solid state energies of formation (ΔU_m) according to equation 2.

$$\Delta U_m = \Delta H_m - \Delta n\, RT \quad \textbf{(2)}$$

(Δn being the change of moles of gaseous components)

Table S4. Calculated gas phase heat of formation, molecular volumes, lattice energies and lattice enthalpies of **1**-**4** as well as **16**-**18**.

	$\Delta_f H°$(g,M) / kcal mol^{-1}	V_M / nm^3	U_L / kJ mol^{-1}	ΔH_L / kJ mol^{-1}
5	128.9	-	-	-
5^{2-}	68.3	0.31575	-	-
11	372.1	0.35775	1218.3	1229.2
NH$_4^+$	151.9	0.021	-	-
12	438.1	0.37175	1200.5	1211.5
N$_2$H$_5^+$	184.9	0.028	-	-
13	396.6	0.37175	1200.5	1211.5
NH$_4$O$^+$	164.1	0.028	-	-
14	341.5	0.44575	1119.6	1130.5
G$^+$	136.6	0.065	-	-
15	389.2	0.47775	1089.9	1100.8
AG$^+$	160.4	0.081	-	-
16	309.6	0.35241	1499.9	1507.4
3^{2+}	459.4	0.0649	-	-
NO$_3^-$	−74.9	0.064	-	-

Table S5. Solid state energies of formation ($\Delta_f U°$)

	$\Delta_f H°$(s) / kcal mol^{-1}	$\Delta_f H°$(s) / kJ mol^{-1}	Δn	$\Delta_f U°$(s) / kJ mol^{-1}	M / g mol^{-1}	$\Delta_f U°$(s) / kJ kg^{-1}
5	128.9	458.9	12.5	489.9	316.12	1549.6
11	78.5	328.6	16.5	369.5	350.33	1054.7
12	148.8	623.0	18.5	668.8	380.37	1758.4
13	107.2	449.0	17.5	492.4	382.33	1288.0
14	71.5	299.5	20.5	350.3	434.43	806.4
15	126.2	528.6	22.5	584.3	464.47	1258.1
16	−50.4	−210.9	15.5	−172.5	352.26	−489.7

Notes: Δn being the change of moles of gaseous components when formed.

4.References

[S1] *CrysAlisPro*, Oxford Diffraction Ltd., version 171.33.41, **2009**.

[S2] *SIR-92*, *A program for crystal structure solution*: A. Altomare, G. Cascarano, C. Giacovazzo, A. Guagliardi, *J. Appl. Crystallogr.* **1993**, *26*, 343.

[S3] a) A. Altomare, G. Cascarano, C. Giacovazzo, A. Guagliardi, A. G. G. Moliterni, M. C. Burla, G. Polidori, M. Camalli, R. Spagna, *SIR97*, **1997**; b) A. Altomare, M. C. Burla, M. Camalli, G. L. Cascarano, C. Giacovazzo, A. Guagliardi, A. G. G. Moliterni, G. Polidori, R. Spagna, *J. Appl. Crystallogr.* **1999**, *32*, 115–119.

[S4] a) G. M. Sheldrick, *SHELX-97*, University of Göttingen, Göttingen, Germany, **1997**; b) G. M. Sheldrick, *Acta Crystallogr., Sect. A* **2008**, *64*, 112–122.

[S5] A. L. Spek, *PLATON*, *A Multipurpose Crystallographic Tool*, Utrecht University, The Netherlands, **1999**.

[S6] *SCALE3 ABSPACK – An Oxford Diffraction program* (1.0.4, gui: 1.0.3), Oxford Diffraction Ltd., **2005**.

[S7] Gaussian 09, M. J. Frisch, G. W. Trucks, H. B. Schlegel, G. E. Scuseria, M. A. Robb, J. R. Cheeseman, G. Scalmani, V. Barone, B. Mennucci, G. A. Petersson, H. Nakatsuji, M. Caricato, X. Li, H. P. Hratchian, A. F. Izmaylov, J. Bloino, G. Zheng, J.
L. Sonnenberg, M. Hada, M. Ehara, K. Toyota, R. Fukuda, J. Hasegawa, M. Ishida, T. Nakajima,

Y. Honda, O. Kitao, H. Nakai, T. Vreven, J. A. Montgomery, Jr., J. E. Peralta, F. Ogliaro, M. Bearpark, J. J. Heyd, E. Brothers, K. N. Kudin, V. N. Staroverov, R. Kobayashi, J. Normand, K. Raghavachari, A. Rendell, J. C. Burant, S. S. Iyengar, J. Tomasi, M. Cossi, N. Rega, J. M. Millam, M. Klene, J. E. Knox, J. B. Cross, V. Bakken, C. Adamo, J. Jaramillo, R. Gomperts, R. E. Stratmann, O. Yazyev, A. J. Austin, R. Cammi, C. Pomelli, J. W. Ochterski, R. L. Martin, K. Morokuma, V. G. Zakrzewski, G. A. Voth, P. Salvador, J. J. Dannenberg, S. Dapprich, A. D. Daniels, Ö. Farkas, J. B. Foresman, J. V. Ortiz, J. Cioslowski, and D. J. Fox, Gaussian, Inc., Wallingford CT, 2009.

Gas-phase concentration of Triacetone Triperoxide (TATP) and Diacetone Diperoxide (DADP)

Martin A. C. Härtel[a], Thomas M. Klapötke*[a], Benedikt Stiasny[a] and Jörg Stierstorfer[a]

Dedicated to the late Alexander Shulgin.

Abstract: The investigation deals with the determination of the gas phase concentration parameters of the medium performance explosive triacetone triperoxide TATP **1** and diacetone diperoxide DADP **2**, which are frequently used in improvised explosive devices. According to calculations with EXPLO5 the energetic performance of both explosives is similar but decreased in comparison to 2,4,6-trinitrotoluene. The enthalpy of sublimation $\Delta_{cr}^{g}H_{m}^{\circ}$ (298.15K) (**1**: 76.7 ± 0.7 kJ mol^{-1}; **2**: 75.0 ± 0.5 kJ mol-1); and vapor pressures p_{sat}(298.15 K) (**1**: 6.7 Pa, **2**: 26.6 Pa) of both compounds have been studied using the transpiration method in the ambient temperature range of 274 – 314 K. The results obtained in this work were compared critically with the existing literature values. Whilst for DADP **2** the agreement with literature data is satisfying the comparison of the TATP **1** data obtained in this work with the literature data available revealed insufficient agreement of all sets of data available, which might be explained by the rich polymorphism of TATP **1**. The saturation and diffusion equilibrium concentration of both analytes was calculated at 298.15 K. In comparison to the saturation equilibrium concentration measured in this work (**1**: 600 µg L^{-1}, **2**: 1589 µg L^{-1}) the corresponding diffusion condition air concentrations (**1**: 3.1 ng L^{-1}, **2**: 10 ng L^{-1}, for a surface of 200 cm²) are lower by five orders of magnitude.

Introduction

Triacetone triperoxide **1**, also known as TATP or APEX, is the condensation product of hydrogen peroxide with acetone and was discovered accidentally by *Wolffenstein* [1] in 1895.
Due to its high volatility and sensitivity towards external stimuli the medium performance explosive is not applied in neither the civil nor the military sector. With respect to the free availability of its precursors and its readiness for detonation initiation the compound is popular in the amateur chemist and terrorist scene as demonstrated by the recent TATP **1** related incident in Oberursel (Germany, 2015, [2]) and the ISIS terror attack in Paris (France,2015, [3]). A 17 year old teenager (Germany, 2006, [4]) was arrested for hoarding 2 kg of TATP **1**, which underlines the ease of TATP **1** synthesis. *Oxley* et al. investigated the factors influencing the formation of TATP **1** and its sideproduct DADP **2** [5] as well as the destruction of TATP **1** [6]. *Lubczyk* et al. [7] recently published a method for desensitizing TATP **1** for training and testing purposes in an ionic liquid matrix and pointed out that resublimed TATP **1** with a BAM impact and friction sensitivity of 0.1 J and 0.05 N is more sensitive than the crude product from an aqueous synthesis (0.5 J, 0.2 N) that is stabilized by trace amounts of water. The resublimation of TATP **1** during storage enhances the risk of unintended detonation. With respect to this and the relatively new trend of the gas phase detection of explosives [8] one of the most interesting parameters of TATP **1** and its potential, more volatile, side product DADP **2** is the vapor pressure of the material. The sublimation behavior of both peroxides **1** and **2** was measured in this work with the transpiration method and compared critically with the existing literature data to give recommendations for the ambient condition (298.15 K) vapor pressure, saturation and diffusion equilibrium air concentration and enthalpy of sublimation.

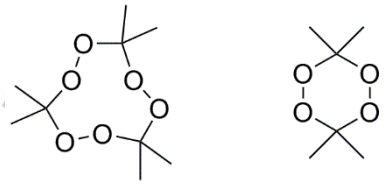

1 **2**

Figure 1. Chemical Structures of TATP **1** and DADP **2**.

Results and Discussion

TATP **1** was synthesized according to *Milas* et al. [9]. DADP **2** was synthesized according to *Landenberger* et al. [10]. The complete chemical characterization of both compounds can be found in the experimental section. With respect to the six possible solid state polymorphs of TATP **1** reported with crystal structures by *Reany at al.* [11] the TATP **1** synthesized in this

[a] Martin A.C. Härtel, Thomas M. Klapötke, Benedikt Stiasny, Jörg Stierstorfer
Department of Chemistry
University of Munich
Butenandtstr. 9, 81377 Munich, Germany
*e-mail: tmk@cup.uni-muenchen.de

work was analyzed with powder X-Ray diffraction to determine its polymorphic composition. (see Figure 2) It could be found that the TATP **1** synthesized in this work consisted mainly of the main polymorph reported for TATP crude products (Cif-File #241973 ,[11-12]). The discrepancies between observed and calculated diffractogram can be explained by the presence of further unknown polymorphs.

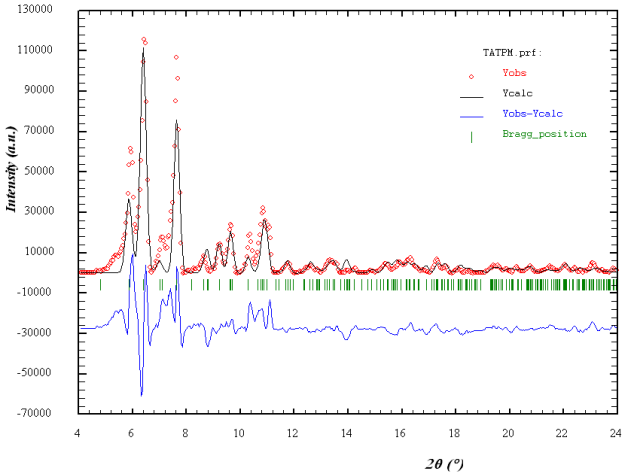

Figure 2. Powder diffractogram of the TATP 1 synthesized in this work after Rietveld Refinement in comparison with the calculated diffractogram of the major polymorph (Cif-File #241973, [11-12]) found in TATP crude products. Red: observed reflexes, blue calculated reflexes, blue: difference of observed and calculated reflexes.

Sensitivities and Energetic Properties

Table 1 gives an overview about the energetic properties and other selected parameters of TATP **1**, DADP **2** synthesized in this work and the medium performance explosive 2,4,6-trinitrotoluene (TNT) for comparison. TATP **1** is very sensitive and DADP **2** less sensitive towards impact. Both peroxides are extremely sensitive towards friction. [13] The sensitivity values for TATP **1** are slightly higher than the values stated by *Lubczyk* et al. [7], yet the friction sensitivity measured in this work is at the lower limit of the measurement range of the testing device used (5 N). Both compounds have a 200 mJ sensitivity towards electrostatic discharge, which is above the 50 mJ discharge that can be generated by human interaction. With a room temperature density of 1.25 g cm^{-3} the nine-membered ring system TATP **1** is less dense than the six-membered DADP **2** (1.31 g cm^{-3}). The denser crystal packing in DADP **2** results in the higher melting range (5 °C min^{-1}) of 132–133 °C in comparison to 97-98 °C for TATP **1**. The exothermic enthalpies of formation of both compounds (**1**: -640 kJ mol^{-1}; **2**: -435 kJ mol^{-1}) were calculated on a CBS-4M level using the *Gaussian 09* [14] software. Based on these values and the theoretical maximum density at 298 K the energetic characteristics were calculated using EXPLO5 v6.03. Both peroxides have a similar detonation pressure $p_{C\text{-}J}$ (**1**: 114 kbar, **2**: 131 kbar), detonation velocity v_{DET} (**1**: 6322 m s^{-1}, **2**: 6246 m s^{-1}) and have a decreased, but similar performance in comparison to TNT ($p_{C\text{-}J}$: 191 kbar, v_{DET}: 6906 m s^{-1}).

Table 1. Selected Energetic Parameters and relevant properties of TATP 1 and DADP 2 synthesized in this work.

	TATP **1**	DADP **2**	TNT
Formula	$C_9H_{18}O_6$	$C_6H_{12}O_4$	$C_7H_5N_3O_6$
MW / g mol−1	222.24	148.16	227.13
IS[a] / J	1.5	5	15
FS[b] / N	<5	5	>360
ESD[c] / mJ	0.2	0.2	0.7
Grain Size / µm	<100	<100	100-500
O[d] / %	43.19	43.19	42.26
Ω_{CO}; Ω_{CO2} / %	-86.4; -151.2	-86.4; -151.2	-24.7; -74.0
Tmelt[f]. / °C	97-98	132-133	(81.1)
ρ[g] / g cm^{-3}	1.27 [180 K][15] 1.25 [298 K]*	1.33 [208 K][16] 1.31 [298 K]*	1.71 [100 K] 1.66*
ΔfH°[h] / kJ mol^{-1}	-640	-435	-54
ΔfU°[i] / kJ kg^{-1}	-2744	-2802	-163
EXPLO6.03 values:			
$-\Delta_{ex}U^{o}$[j] / kJ kg^{-1}	3420	3194	4425
P_{CJ}[k] / kbar	114	131	191
V_{det}[l] / m s^{-1}	6322	6246	6906
V_0[m] / L kg^{-1}	821	815	642

[a] impact sensitivity, BAM drophammer (method 1 of 6); [b] friction sensitivity, BAM friction tester (method 1 of 6); [c] sensitivity towards electrostatic discharge; [d] oxygen content; [e] oxygen balance; [f] melting range (5 °C min^{-1}, glass capillary) [h] densities (*values at 298 K calculated using the equation ($\rho_{298K} = \rho_T / (1+\alpha_V(298-T_0)$; $\alpha_V = 1.5\ 10^{-4}\ K^{-1}$; [i] calculated heat of formation (CBS-4M); [h] calculated energy of formation (CBS-4M); [i] heat of detonation; [j] detonation pressure; [k] detonation velocity; [l] volume of gases after detonation.

VO-GC/MS Gas Chromatography of Peroxides

TATP **1** and DADP **2** were analyzed using vacuum outlet gas chromatography as established by *de Zeeuw et al.* [17] using a Shimadzu GC/MS QP2010 SE device equipped with an Atas Optic 4 injector and a Shimadzu AOC-20i autosampler. The necessary restriction (10.1 mm length, 0.05 mm inner diameter, Restek® cat. # 10098) was connected to a Restek® RTX TNT 1 column (cat. #12998) with a SGE Siltite® µ-Union (cat. #073562)

inside the injector. Due to the incompatibility of the inner diameter of the commercially available Atas liners a custom V2A stainless steel liner (10 mm length, 5 mm outer diameter, 0.5 mm wall thickness, split notches at bottom end) was used. Both the liner and the µ-union were inertized with a Silconert® 2000 coating. The injector was operated at 175 °C in the constant pressure mode with a head pressure of 90 kPa Helium 5.0 carrier gas and a split ratio of 150 in combination with a virtual column (100 m length, 0.25 µm film thickness, 0.20 mm diameter) for the LabSolutions GCMS Solution Software. The injection volume was 1 µL. The GC oven program start temperature was 30 °C with a hold time of 6 seconds followed by a temperature ramp to 204 °C with 60 °C min^{-1}. The temperature of the MS-Interface and the ion source was 200 °C. The mass spectrometer was operated in the single ion monitoring mode with an event time of 0.10 s and a micro scan width of 0.1 amu. From 0.50 to 2.00 min the mass channels 43, 59, 58 and 75 were monitored for the detection of the peroxides **1** and **2**. From 2.00 to 3.00 min the mass channels 57, 43, 71 and 85 were monitored for the detection of *n*-docecane C-12 as analytical standard in quantification applications.

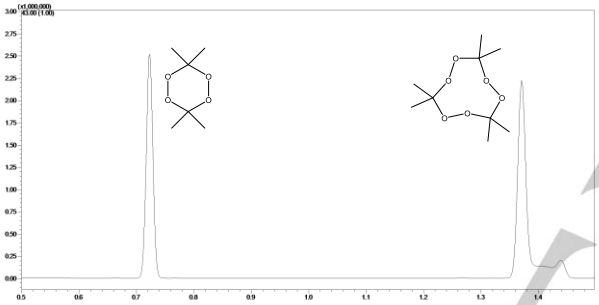

Figure 3. SIM mode (m/z 43) GC/MS chromatogram of TATP **1** and DADP **2**.

Figure 3 shows a chromatogram of TATP **1** and DADP **2** in *tert*-butyl methyl ether using the method stated before. DADP **2** elutes after 0.72 min at 67 °C as a single peak whilst one TATP **1** conformer A elutes after 1.37 min at 106 °C and a second TATP **1** conformer B elutes after 1.44 min at 110 °C. The augmented baseline between both conformers indicates the conversion of conformer A to the more stable conformer B during the GC/MS analysis. The solid state polymorphism of TATP **1** has been reported before [11] and two isomers of TATP have been separated by LC-NMR [18]. The activation barrier of an exothermic TATP **1** polymorph interconversion has been calculated to be 110 kJ mol^{-1} [19]. With respect to this the GC/MS behavior of TATP **1** observed in this work can be justified. Both TATP **1** (R^2 = 0.99995) and DADP **2** (R^2 = 0.9998) could be quantified excellently in concentrations of 20 to 60 µg/mL with an internal standard (C-12) method using the GC/MS configuration detailed above.

Vapor Pressure Measurement

Since the vapor pressure of a compound is the key parameter for its gas phase detectability the vapor pressure of TATP **1** and DADP **2** was measured in this work using the transpiration method. The transpiration method setup adapted in this work has been established by *Verevkin et al.* [20]. For the experiments in this work nitrogen (99.999 % purity) was used as carrier gas. The flow-rate ranging from 1-3 L h^{-1} was adjusted and kept constant using a mass flow controller (Natec Sensors MC-100 CCM). The gas flow is conducted through the saturator, which is a glass vessel surrounding a U-shaped tube (8 mm inner diameter, 50 cm length) and containing a thermofluid, which is pumped through the saturator vessel with a circulation thermostat (Huber Ministat 230 with external class A PT-100 temperature sensor inside the saturator vessel). The peroxide is coated on glass beads and filled into the saturator tube. For the coating of the glass beads with the sensitive peroxide explosives they were dispersed in a minimum amount of n-pentane and the resulting slurry filled into the saturator tube followed by removal of the n-pentane by application of the carrier gas stream at room temperature. After leaving the saturator and reaching the saturation equilibrium with the analyte the carrier gas stream is conducted through a condenser tube, which is positioned in a dewar vessel containing *iso*-propanol that is cooled to -30 °C by an immersion cooler (Huber TC45E). The exact carrier gas flow-rate is measured with a soap film flowmeter (Hewlett Packard No.: 0101-0113) and the ambient temperature is recorded for the volume measurement (Greisinger GFTB 200) for each datapoint. The time span from insertion of the condenser tube into the saturator to its removal was measured for the calculation of the total volume of carrier gas. After its removal from the saturator the condenser tube was closed at both ends and *tert*-butyl methyl ether solvent was filled into it containing a known amount of *n*-dodecane as internal standard for the subsequent GC/MS quantification. With the temperature of the saturator T_{exp}, the mass of the analyte in trapped in the condenser tube m_a, the ambient temperature T_{amb} and the volume of carrier gas measured at ambient conditions V_{amb} the vapor pressure p_{sat} of the analyte can be calculated. The calculation of the vapor pressure relies on the Ideal Gas Law, the Dalton's Law of partial pressures and the assumption that the volume of the gaseous analyte is negligibly small in comparison to that of the carrier gas:

$$p_{sat}(T_{exp}) = \frac{m_a \mathrm{R} T_{amb}}{\mathrm{M} V_{amb}} \qquad (1)$$

p_{sat}: vapor pressure of the analyte [Pa] , T_{exp}: temperature of the saturator [K], m_a: mass of analyte [kg], T_{amb}: ambient temperature [K], V_{amb}: volume of carrier gas at ambient conditions [m^3], M: molecular weight of the analyte [kg mol^{-1}], R: universal gas constant: 8.3145 J mol^{-1} K^{-1}

The obtained values of the experimental vapor pressure p_{sat} at the saturator temperature T_{exp} are processed mathematically with a fitting function that is based on the *Clarke-Glew* equation [21]:

$$ln\ {}^{p_{\mathrm{sat}}}/_{p^{\mathrm{o}}} - \frac{\Delta^{\mathrm{g}}_{\mathrm{cr}} C^{\mathrm{o}}_{p,m}}{R} ln \frac{T}{T_0} = A - \frac{B}{T} \qquad (2)$$

p^{o}: reference pressure (1 Pa), $\Delta^{\mathrm{g}}_{\mathrm{cr}} C^{\mathrm{o}}_{p,m}$: heat capacity difference from crystalline to gaseous state [J mol^{-1} K^{-1}], T: temperature [K], T_0: reference temperature [K], A/B: fitting coefficients [ ].

The enthalpy of sublimation at the temperature T calculated by:

$$\Delta^{g}_{cr}H^{o}_{m}(T) = RB + \Delta^{g}_{cr}C^{o}_{p,m}T \quad (3)$$

$\Delta^{g}_{cr}H^{o}_{m}(T)$: molar enthalpy of sublimation at temperature T.

The experimental heat capacities $C^{o}_{p,m}$ of both peroxides at room temperature were reported by *Pilar et al.* [22] and are in good agreement with the values calculated by the empiric elemental composition approach by *Hurst et al.* [23] ($C^{o}_{p,m}$ (cr, 298.15 (calculated/experimental) [J mol^{-1} K^{-1}], **1**: 314.6/271.8, **2**: 209.7/223.4). In this work the experimental values were used and the corresponding heat capacity differences $\Delta^{g}_{cr}C^{\circ}_{p,m}$ calculated according to *Chickos et al.* [24]. The method for the calculation of the sublimation enthalpy is described elsewhere [20b]. The available literature vapor pressure data for TATP **1** and DADP **2** was also collected. In some works the sublimation enthalpy was not derived from the vapor pressures or it was carried out in a different manner. In this work the literature vapor pressures were treated with equations (2) and (3) and the corresponding uncertainties were estimated according to [20b]. The obtained enthalpies of sublimation and vapor pressures at 298.15 K are compiled in comparison with our results in Table 3. For TATP **1** a value for $\Delta^{g}_{cr}H^{o}_{m}(298.15\,K)$ of 76.7 ± 0.7 kJ mol^{-1} and a vapor pressure p_{sat}(298.15 K) of 6.7 Pa and for DADP **2** a value for $\Delta^{g}_{cr}H^{o}_{m}(298.15\,K)$ of 75.0 ± 0.5 kJ mol^{-1} and a vapor pressure p_{sat}(298.15 K) of 26.6 Pa was derived from the data obtained with the transpiration method in this work. (cf. Table 1)

The sublimation behavior of TATP **1** was studied in this work in the temperature range from 274.3 – 314.1 K. The absolute vapor pressures p_{sat} and thermodynamic properties of sublimation obtained by the transpiration method in this work for TATP **1** are compiled in Table 1. A comparison of own data with literature experiments regarding the enthalpies of sublimation is compiled in Table 3, Figure 4 shows a Clausius-Clapeyron plot of the own and literature p-T data for the sublimation of TATP **1**. Available p-T literature data for comparison are four headspace gas chromatography measurements by *Mbah* et al. [25] and *Oxley* et al. [26], three thermogravimetric measurements by *Mbah* et al. [27], *Oxley* et al. [28] and *River* et al.[29], one static method measurement by *Egorshev* et al.[30], a Knudsen-effusion measurement by *Damour* et al.[31] and a Quantum Cascade Laser Photoacoustic Spectroscopy measurement by *Dunayevskiy* et al. [32]. The thermogravimetric analysis (TGA) measurements may result in correct enthalpies of sublimation, yet they need to be calibrated with a reference material for the derivation of correct pressure values from the data measured. It has not been proven that this reference material calibration is suitable for precise measurements of vapor pressures. Therefore TGA measurements will be disregarded in the discussion of absolute vapor pressures. The data published by *Dunayevskiy* et al. [32] has been scaled to a measurement by Oxley et al. [26b]. *Dunayevskiy* et al. [32] published solely a p-T-equation of their data combined with that of *Oxley* et al. [26b] and no discrete pressure analog-tempature values which would allow fitting to other sets of data. Additionally it was mentioned by *Damour* et al.[31] that the dataset provided by *Dunayevskiy* at al. [32] seems to be systematically erroneous in the low temperature regime and needs to be cut. Therefore the data published by *Dunayevskiy* et al. [32] is excluded from the calculation of average values. *Mbah* et al. [25] measured TATP **1** crude products that were synthesized under acid catalysis with hydrochloric and sulfuric acid. The crude product synthesized with sulfuric acid contained a large fraction of a DADP **2** impurity and therefore its measurement is disregarded in the calculation of average values and the discussion of measurement results.

Regarding the enthalpies of sublimation $\Delta^{g}_{cr}H^{\circ}_{m}$ that were adjusted to 298.15 K (cf. Table 3) it becomes obvious that the values spread from 68.0±6.3 kJ mol^{-1} derived from the data reported by *Mbah* et al. [27] to 103.8±6.4 kJ mol^{-1} derived from the data reported by *Oxley* et al. [26b] The scattering of the measurement values may be explained by the polymorphism of TATP **1** reported by Reany at al. [11]. It was demonstrated that crude products of TATP **1** contain one major and two minor mass fraction polymorphs of TATP **1** and three additional polymorphs can be synthesized by recrystallization in organic solvents (hexane, tetrachloromethane, ethanol). Four of these polymorphs were analyzed by differential scanning calorimetry with reported sublimation enthalpies ranging from 14.6 kJ mol^{-1} at 93.6 °C onset temperature to 77.2 kJ mol^{-1} at 91.6 °C onset temperature. A sublimation enthalpy of 14.6 kJ mol-1 is unrealistically low for the TATP **1** molecule (cf. Table 3). Therefore these values have to be considered erroneous. Despite that it cannot be neglected that polymorphism influences the sublimation behavior of TATP **1**. It cannot be excluded that all measurements discussed in this work were measurements of polymorph mixtures or different pure polymorphs of **1**. The relevant information about the synthesis of the TATP **1** used in this work and in literature publications is summarized in Table 2. In many cases no sufficient data about the details of sample synthesis have been provided, whilst samples that have been recrystallized from methanol were reported with different sublimation characteristics regarding the enthalpy of sublimation at 298.15 K. In this work the crude product was extracted from the reaction mixture with pentane. The data published by *Mbah* et al. [25] for the crude product of synthesis under hydrochloric acid catalysis is in fair agreement with the data obtained in this work. (cf. Table 3, Figure 4) For TATP **1** an average uncertainty-weighted value for $\Delta^{g}_{l}H^{\circ}_{m}$(298.15 K) of 80.8 ± 0.5 kJ mol-1 is calculated considering all available sets of data. This value is not in agreement with the one obtained in this work (76.7 ± 0.7 kJ mol-1), which is supposedly caused by the polymorphism of TATP **1** and different methods of synthesis in all measurements. The vapor pressures of TATP 1 at 298.15 K that were calculated from each individual complete dataset are compiled in Table 3. The mean value of 6.9 Pa can be considered as a recommendation for the ambient condition vapor pressure of TATP.

The sublimation behavior of DADP **2** was studied in this work in the temperature range from 274.7 – 314.1 K. The absolute vapor pressures p_{sat} and thermodynamic properties of sublimation obtained by the transpiration method in this work for DADP **2** are compiled in Table 1. A comparison of own data with literature experiments regarding the enthalpies of sublimation is compiled in Table 3. Figure 5 shows a *Clausius-Clapeyron* plot of the own and literature p-T data for the sublimation of DADP **2**.

Available p-T literature measurement data for comparison are provided by *Egorshev* et al. [30] (static method), *Brady* et al. [33] (thermogravimetry), *Damour et al.* [31] (Knudsen effusion), and *Oxley et al.* [26a] (headspace). The thermogravimetric analysis measurement by Brady *et al.* is excluded from data comparison

Table 1 - TATP: absolute vapor pressures p_{sat} and thermodynamic properties of sublimation obtained by the transpiration method in this work

TATP 1: $\Delta^{g}_{cr}H^{\circ}_{m}$ (298.15 K) = 76.7 ± 0.7 kJ mol-1

$$\ln p_{sat}/p^{\circ} = \frac{317.7}{R} - \frac{89091.1}{RT} + \frac{41.5}{R} ln \frac{T}{298.15K}$$

T_{exp}a	mb	V_{N2}c	T_{amb}d	Gasflow	p_{sat}e	u(p_{sat}) f	$\Delta^{g}_{cr}H^{\circ}_{m}$	$\Delta^{g}_{cr}S^{\circ}_{m}$
[K]	[mg]	[dm³]	[K]	[dm³ h-1]	[Pa]	[Pa]	[kJ mol-1]	[J mol-1 K-1]
274.3	0.11	2.80	296.6	2.58	0.43	0.02	77.71	180.6
274.4	0.09	2.43	296.5	1.62	0.44	0.02	77.71	180.6
278.3	0.11	1.65	296.5	1.62	0.74	0.02	77.54	180.4
283.2	0.11	0.926	296.4	2.14	1.4	0.0	77.34	179.9
288.2	0.24	1.16	296.9	2.17	2.3	0.1	77.13	178.9
293.2	0.23	0.610	296.5	2.15	4.2	0.1	76.92	178.7
293.2	0.23	0.611	297.1	2.16	4.1	0.1	76.92	178.4
298.2	0.57	0.898	297.0	2.15	7.1	0.2	76.72	177.9
293.2	0.20	0.613	296.5	2.16	3.7	0.1	76.92	177.5
303.1	0.53	0.538	296.8	2.15	10.9	0.3	76.51	176.5
308.1	1.25	0.751	296.3	2.15	18.4	0.5	76.30	176.1
314.1	1.55	0.540	296.7	2.16	31.8	0.8	76.06	175.2
314.1	1.54	0.538	296.3	2.15	31.7	0.8	76.06	175.2
314.1	1.53	0.539	296.7	2.16	31.5	0.8	76.06	175.1

DADP 2: $\Delta^{g}_{cr}H^{\circ}_{m}$ (298.15 K) = 75.0 ± 0.5 kJ mol-1

$$\ln p_{sat}/p^{\circ} = \frac{313.2}{R} - \frac{85244.0}{RT} + \frac{34.3}{R} ln \frac{T}{298.15K}$$

T_{exp}a	mb	V_{N2}c	T_{amb}d	Gasflow	p_{sat}e	u(p_{sat}) f	$\Delta^{g}_{cr}H^{\circ}_{m}$	$\Delta^{g}_{cr}S^{\circ}_{m}$
[K]	[mg]	[dm³]	[K]	[dm³ h-1]	[Pa]	[Pa]	[kJ mol-1]	[J mol-1 K-1]
274.7	0.16	1.38	296.6	2.02	1.98	0.05	75.82	186.0
274.7	0.15	1.27	296.6	1.52	1.95	0.05	75.82	185.8
278.5	0.16	0.862	296.6	1.52	3.13	0.08	75.69	185.6
288.3	0.38	0.635	296.4	2.01	9.95	0.27	75.36	184.8
283.4	0.34	1.07	296.5	2.01	5.36	0.16	75.52	184.8
293.3	0.74	0.740	296.8	2.02	16.6	0.44	75.18	184.0
293.3	0.72	0.740	296.3	2.02	16.3	0.43	75.19	183.9
293.3	0.69	0.741	296.6	2.02	15.6	0.42	75.19	183.5
298.2	1.33	0.805	296.9	2.01	27.6	0.71	75.02	183.4
293.3	0.68	0.739	297.1	2.02	15.4	0.41	75.19	183.4
303.2	1.29	0.501	297.2	2.00	43.0	1.10	74.85	182.4
308.1	3.78	0.871	297.5	2.01	72.4	1.84	74.68	182.2
314.1	3.70	0.499	296.5	1.99	123	3.11	74.47	181.4
314.1	3.45	0.467	297.0	2.00	123	3.11	74.47	181.4
314.1	3.59	0.500	296.7	2.00	120	3.02	74.47	181.2

[a] Saturation temperature ($u(T)$ = 0.1 K). [b] Mass of transferred sample condensed at T = 243 K [c] Volume of nitrogen ($u(V)$ = 0.005 dm^3) used to transfer m ($u(m)$ = 0.0001 g) of the sample. [d] T_a is the temperature of the soap bubble meter used for measurement of the gas flow. [e] Vapor pressure at temperature T, calculated from the m and the residual vapor pressure at the condensation temperature calculated by an iteration procedure; p°=1 Pa. [f] Standard uncertainty in p was calculated with $u(p/\text{Pa})$ = 0.005+0.025(p/Pa) for p < 5 Pa and $u(p/\text{Pa})$ = 0.025+0.025(p/Pa) for p > 5 to 3000 Pa.

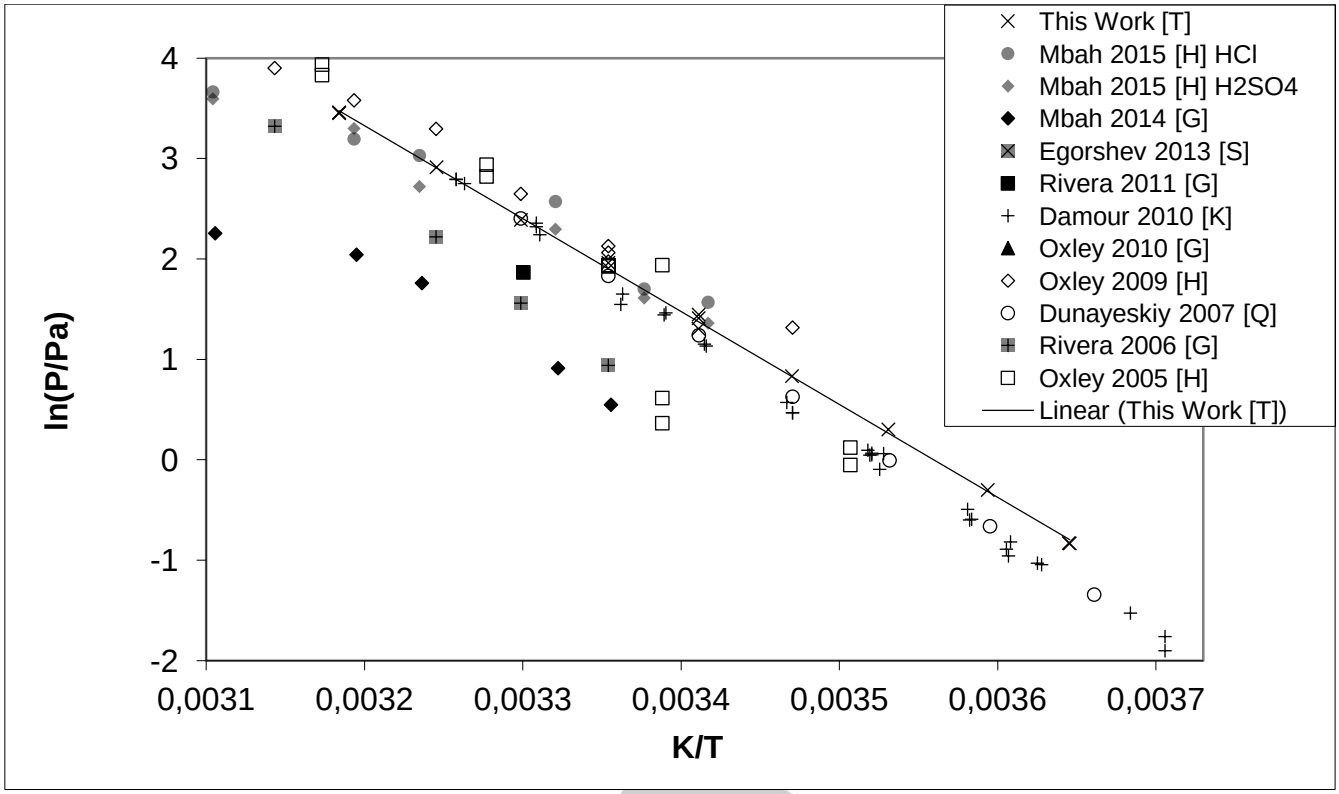

Figure 4. Experimental vapor pressure of TATP in comparison with literature values. ×: this work, ● [25] (HCl), ♦ [25] (H_2SO_4), ♦ [27], ⊠ [30], ■ [34], + [31], ▲ [28], ◊ [26a], ○ [32], ⊞ [29], □ [26b]. Linear regression line for this work.

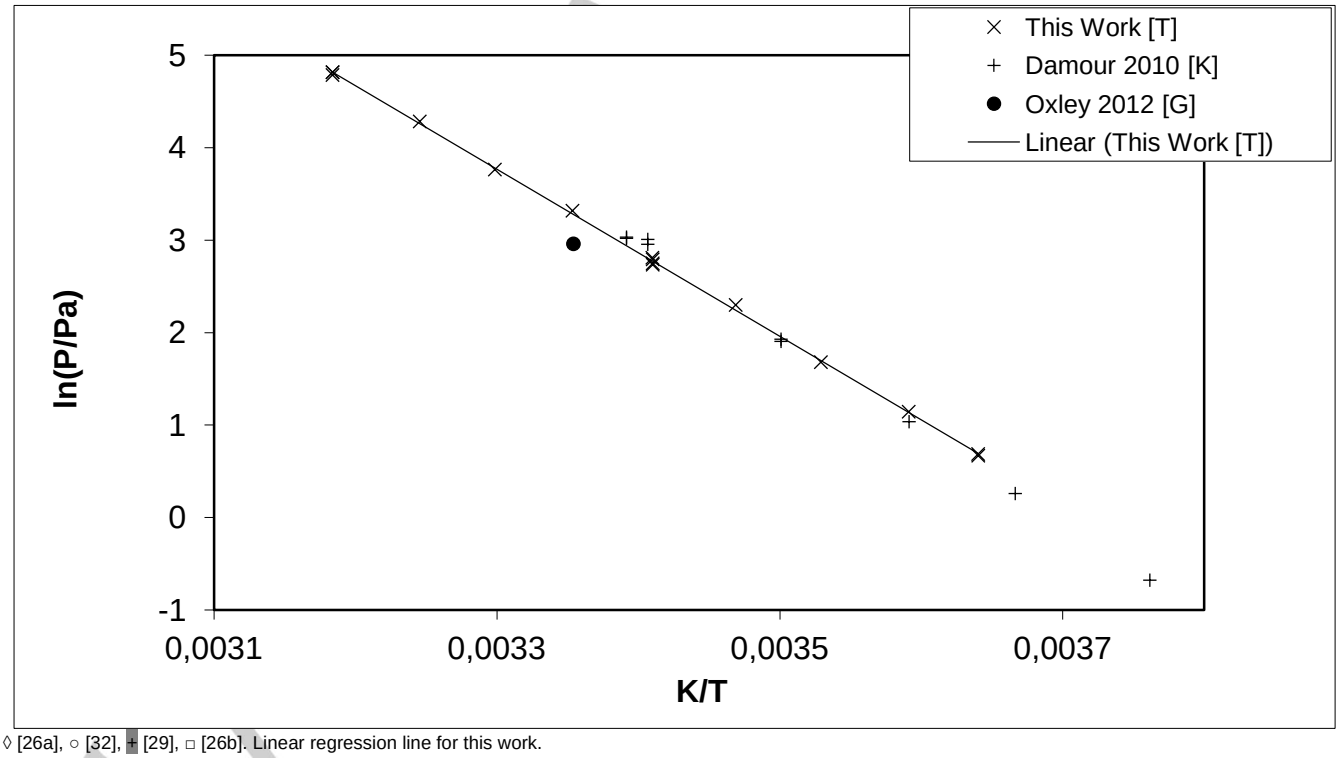

Figure 5. Experimental vapor pressure of DADP 1 in comparison with literature values. ×: this work, +[31], ●[33]. Linear regression line for this work.

Table 2 – Details of TATP synthesis in this work and in literature references.

Experiment[a]	Acid[b]	Solvent	Purity	Melting Range	$\Delta_{cr}^{g}H_{m}^{\circ}$(298.15K)[d]
				° C	kJ mol^{-1}
This Work	H_2SO_4	Pentane	99.9 %	97-98	76.7±0.7
Mbah 2015 HCl [25]	HCl	-	-	-	71.6±6.9
Mbah 2015 H_2SO4 [25]	H_2SO_4	-	impure	-	66.6±3.8
Mbah 2014 [27]	-	-	-	86	68.0±6.3
Egorshev 2013 [30]	HCl	-	-	95 – 97	98.7±7.7
Rivera 2011 [34]	-	-	-	-	(73.0)
Damour 2010 [31]	CAR[c]	Methanol	-	94.2 – 95.2	85.7±0.9
Oxley 2010 [28]	H_2SO_4	Methanol	"good"	-	92.8±2.7
Oxley 2009 [26a]	-	-	-	-	72.0±3.3
Dunayevskiy 2007 [32]	-	-	-	-	(85.4)
Rivera 2006 [29]	-	-	-	95.9	86.8±2.2
Oxley 2005 [26b]	H_2SO_4	Methanol	"good"	-	103.8±6.4

[a] First author and year of publication, [b] Acid catalyst used in synthesis, [c] CAR: Cationic Acid Resin [d] Molar Enthalpy of Sublimation at 298.15 K.

Table 3. Compilation of data on the enthalpy of sublimation and vapor pressures obtained in this work and from literature values for TATP **1** and DADP **2**.

Experiment[a]	Method[b]	T-Range	T_{avg}	$\Delta_{cr}^{g}H_{m}^{\circ}(T_{avg})$	$\Delta_{cr}^{g}H_{m}^{\circ}$(298.15K)[c]	p_{sat}[d]
		K	K	kJ mol^{-1}	kJ mol^{-1}	Pa
TATP **1**						
This Work	T	274.3 – 314.1	294.3	76.9±0.6	76.7±0.7	6.7
Mbah 2015 HCl [25]	H	292.7 – 327.2	310.3	71.1±6.9	71.6±6.9	7.6
Mbah 2015 H_2SO_4 [25]	H	292.7 – 327.2	310.3	66.1±3.7	(66.6±3.8)	(6.5)
Mbah 2014 [27]	G	298.0 – 327.0	313.2	67.4±6.2	68.0±6.3	(1.9)
Egorshev 2013 [30]	S	348.2 – 367.2	357.9	96.2±7.6	98.7±7.7	(1.6)
Rivera 2011 [34]	G,O	303.0 – 338.0	320.5	72.1	(73.0)	-
Damour 2010 [31]	K	269.9 – 307.0	287.0	86.6±0.8	85.7±0.9	5.9
Oxley 2010 [28]	G	313.9 – 332.5	321.9	91.7±2.5	92.8±2.7	(24.4)
Oxley 2009 [26a]	H	288.2 – 323.2	305.0	71.7±3.2	72.0±3.3	8.7
Dunayevskiy 2007 [32]	Q,O	243.2 – 331.2	285.5	86.0	(85.4)	(6.3)
Rivera 2006 [29]	G	298.2 – 348.2	319.4	85.8±2.2	86.8±2.2	(2.8)
Oxley 2005 [26b]	H	285.2 – 331.2	305.3	103.4±6.4	103.8±6.4	5.8
					80.8±0.5[e]	6.9[f]

Table 4. continued

DADP 2						
This Work	T	274.7 – 314.1	294.4	75.2±0.4	75.0±0.5	26.6
Egorshev 2013 [30]	S	340.7 – 393.0	358.5	74.3±1.5	76.6±1.5	25.6
Brady 2012 [33]	G,O	333.2 – 369.2	351.2	73	(74.8)	(19.3)
Damour 2010 [31]	K	265.9 – 294.9	284.7	84.6±1.1	84.0±1.2	31.2
Oxley 2009 [26a]	H	288.2 – 323.2	305.0	79.4±3.4	79.6±3.4	18.6
					76.4±0.4[e]	25.5[f]

[a] First author and year of publication, [b] Methods: T: Transpiration, H: Headspace, S: Static Method, G: Thermogravimetric Analysis, K: Knudsen-Effusion, Q: Quantum-Cascade Laser Photoacoustic Spectroscopy, O: Equation Only [c] Enthalpies of vaporization were adjusted according to *Chickos et al.* [24] with the values for $\Delta_{cr}^{g}C_{p,m}^{\circ}$ and $C_{p,m}^{\circ}$(cr) stated in §. [d] Vapor pressure at 298.15 K, calculated according to equation in §. [e] Weighted average value, calculated using the uncertainty as the weighing factor. [f] Average value. Values in brackets were excluded from average value calculation.

Table 5. Calculation of Molar Heat Capacity Differences at T = 298.15 K

compound	$C_{p,m}^{o}$(l)	$C_{p,m}^{o}$(cr)	$C_{p,m}^{o}$(l)	$C_{p,m}^{o}$(cr)	$\Delta_{l}^{g}C_{p,m}^{o}$	$\Delta_{cr}^{g}C_{p,m}^{o}$
	calc.	calc.	lit.	lit.		
	[J mol^{-1} K^{-1}]	[J mol^{-1} K^{-1}]	[J mol^{-1} K^{-1}]	[J mol^{-1} K^{-1}]	[J mol^{-1} K^{-1}]	[J mol^{-1} K^{-1}]
TATP **1**	379.3[a]	(314.6)[a]	n.a.	271.8 [22]	-109.2	-41.5
DADP **2**	252.9[a]	(209.7)[a]	n.a.	223.4 [22]	-76.3	-34.3

Bracketed values not used for calculation of heat capacity differences. n.a.: not available a) calculated according to the increment method and data by Hurst et al. [23] b) calculated by $\Delta_{l}^{g}C_{p,m}^{o} = 10.58 + C_{p,m}^{o}(\mathrm{l}) \times 0.26$ according to [24] c) calculated by $\Delta_{cr}^{g}C_{p,m}^{o} = 0.75 + C_{p,m}^{o}(\mathrm{cr}) \times 0.15$ according to [24]

and average value calculation since solely a p-T-equation and a vapor pressure extrapolation to 298.15 K was published.

For DADP 2 an average uncertainty-weighted value for $\Delta_{cr}^{g}H_{m}^{\circ}$ (298.15 K) of 76.4 ± 0.4 kJ mol-1 is recommended considering all available sets of data. This value is in fair agreement with the one obtained in this work (75.0 ± 0.5 kJ mol^{-1}). The vapor pressures of DADP **2** at 298.15 K that were calculated from each individual complete dataset are compiled in Table 3. The mean value of 25.5 Pa can be considered as a recommendation for the ambient condition vapor pressure of DADP 2.

Air Concentration of Peroxides 1 and 2

Vapor pressures are measured under ideal saturation conditions. In a real case scenario the saturation equilibrium of the explosive will not be reached and diffusion processes will dictate the air concentration of the explosive. *Dravnicks* et al. [35] have stated a mathematical model for the estimation of the non-equilibrium air concentration of an explosive, which shall be applied to TATP **1** and DADP **2** in the following using the equations and values provided by Bird et al. [36]

Fick's Law of Diffusion provides a suitable approximation for the rate of molecular vapor emission per cm² J:

$$J = A \times D_{AB} \times \frac{n_c - n_a}{d} \qquad (4)$$

J:emission flux [molecules s^{-1}], A: area of explosive exposed to air [cm²], D_{AB}: diffusivity of explosive vapor in air [cm^2 s^{-1}], n_c: concentration of explosive under saturation conditions [molecules cm^{-3}], n_a : concentration of the explosive in air [molecules cm^{-3}], d: thickness of non-turbulent layer air [cm]

The concentration of the explosive in the air is considered to be negligibly small (→ n_a = 0) and the thickness of the non-turbulent layer of air surrounding the explosive is considered to be 0.2 cm [35].

The diffusivity D_{AB} can be calculated by the following formula:

$$D_{AB} = 0.0018583 \sqrt{T^3 \left(\frac{1}{M_A} + \frac{1}{M_B}\right)} \frac{1}{p\sigma_{AB}^2 \Omega_{D,AB}} \qquad (5)$$

T: Temperature [K] (298.15 K), M_A: Molecular Mass of Explosive [g mol^{-1}], M_B: Molecular Mass of Air [g mol^{-1}] (28.97 g mol^{-1}), p: total pressure [atm] (1 atm), σ_{AB}: combined collision diameter [Å], $\Omega_{D,AB}$: collision integral for diffusion [ ]

$$\sigma_{AB} = 1/2(\sigma_A + \sigma_B) \qquad (6)$$

σ_A: collision diameter of explosive [Å], σ_B: collision diameter of air [Å] (3.617 Å) [36]

$$\varepsilon_{AB} = \sqrt{\varepsilon_A \varepsilon_B} \qquad (7)$$

ε_A: characteristic energy of explosive [J], ε_B: characteristic energy of air [J]

Whilst the collision diameter of σ_B (3.617 Å) [36] and the characteristic energy ε_B (ε_B/κ = 97.0 K) [36] of air is known, the collision diameter of the explosive σ_A and its characteristic energy ε_A have to be estimated. These values may be estimated from the fluid at the critical point (c), the liquid at the boiling point (b) and the solid at the melting point (m):

$$\varepsilon/\kappa = 0.77T_c; \quad \sigma = 0.841\sqrt[3]{V_c} \text{ or } \sigma = 2.44\sqrt[3]{T_c/p_c} \quad (8)$$
$$\varepsilon/\kappa = 1.15T_b; \quad \sigma = 1.166\sqrt[3]{V_b} \quad (9)$$
$$\varepsilon/\kappa = 1.92T_m; \quad \sigma = 1.222\sqrt[3]{V_m} \quad (10)$$

T_c: critical temperature [K], T_b: boiling point [K], T_m: melting point [K], V_c: critical volume [cm³ mol^{-1}], V_b: volume of the liquid at the boiling point [cm³ mol^{-1}], V_m: volume of the solid at the melting point [cm^3 mol^{-1}], p_c: critical pressue [atm], κ: Boltzmann's constant (1.38066 × 10^{-23} J K^{-1})The concentration of the explosive in the air is considered to be negligibly small ($\rightarrow n_a = 0$) and the thickness of the non-turbulent layer of air surrounding the explosive is considered to be 0.2 cm [35].

The diffusivity D_{AB} can be calculated by the following formula:

$$D_{AB} = 0.0018583\sqrt{T^3\left(\frac{1}{M_A}+\frac{1}{M_B}\right)}\frac{1}{p\sigma_{AB}^2\Omega_{D,AB}} \quad (11)$$

T: Temperature [K] (298.15 K), M_A: Molecular Mass of Explosive [g mol^{-1}], M_B: Molecular Mass of Air [g mol^{-1}] (28.97 g mol^{-1}), p: total pressure [atm] (1 atm), σ_{AB}: combined collision diameter [Å], $\Omega_{D,AB}$: collision integral for diffusion

$$\sigma_{AB} = 1/2(\sigma_A + \sigma_B) \quad (12)$$

σ_A: collision diameter of explosive [Å], σ_B: collision diameter of air [Å] (3.617 Å) [36]

$$\varepsilon_{AB} = \sqrt{\varepsilon_A\varepsilon_B} \quad (13)$$

ε_A: characteristic energy of explosive [J], ε_B: characteristic energy of air [J]

With ε_{AB} the collision integral for diffusion $\Omega_{D,AB}$ can be calculated according to:

$$\Omega_{D,AB} = \frac{1.16145}{T^{*0.15610}} + \frac{0.19300}{\exp(0.47635T^*)} + \frac{1.03587}{\exp(1.52996T^*)} + \frac{1.76474}{\exp(3.89411T^*)} \quad (14)$$

$$T^* = \kappa T/\varepsilon_{AB} \quad (15)$$

In case of TATP **1** and DADP **2** the diffusion coefficient can be calculated from their melting point (eq. (7)). The needed molar volume V_m can be approximated from the crystal structure density at the temperature T_{XRD}:. The density can be adjusted to the melting point by the following equation [37]:

$$\rho_m = \rho_{XRD}/(1 + 0.00015(T_m - T_{XRD}) \quad (16)$$

ρ_m: density at melting point [g cm^{-3}], ρ_{XRD}: density from X-Ray diffraction [g cm^{-3}], T_{XRD}: temperature of XRD-experiment [K]

The molar volume at the melting point can be calculated by:

$$V_m = M/\rho_m \quad (17)$$

With equations 1 to 17 the diffusion coefficient of a solid explosive in air can be approximated when solely its melting point and a density are known and equation (1) can be used to calculate the mass flux of material from the explosive to the air:

$$J = A \times D_{AB} \times \frac{n_c - n_a}{d} \quad (4)$$

With A = 1 cm², n_a= 0 and d = 0.2 cm it can be written:

$$J = \frac{D_{AB}}{0.2} \times n_c \quad (18)$$

If the concentration n_c is converted to partial pressure (n_c = 3.3×10^{16}p, p: vapor pressure [Torr]) and the emission flux is converted into a mass flux (unit conversion factor: M/N_A) the mass flux can be calculated:

$$Q = \frac{D_{AB}}{0.2} \times 3.3\times10^{16} p \times (M/N_A) \quad (19)$$

Q: emission flux of explosive [g s^{-1} cm^{-2}], N_A: Avogadro Constant (6.022 × 10^{23} mol^{-1})

An example pf this calculation can be found for TATP **1** and DADP **2** in Table 6:

Table 6. Example of Calculation for the emission flux of explosive Q for TATP and DADP at STP conditions (298.2 K, 1 atm)

	TATP	DATP	Unit
T_m	370.2[a]	405.2[a]	K
ρ_{XRD}	1.27[b]	1.33[b]	g cm^{-3}
T_{XRD}	180[b]	208[b]	K
ρ_m	1.24	1.292	g cm^{-3}
M	222.237	148.158	g mol^{-1}
V_m	179.981	114.691	cm^3 mol^{-1}
σ_A	6.899	5.937	Å
ε_B	710.688	777.888	K
σ_{AB}	5.258	4.777	Å
ε_{AB}	262.558	274.691	J
κT/ε_{AB}	1.136	1.085	[]
$\Omega_{D,AB}$	1.355	1.385	[]
D_{AB}	0.050	0.062	cm^2 s^{-1}
p_{sat}	6.7[a]	26.6[a]	Pa
p_{sat}	0.050[a]	0.200[a]	mmHg
Q	0.154	0.497	µg/cm² s

[a] value obtained in this work, [b] values obtained from the literature for TATP[15] and DADP[16].

With the emission flux Q in hands the concentration of the explosive in air at the diffusion equilibrium state can be calculated:

$$c_{dif} = S \times Q \times r \quad (20)$$

c: concentration of explosive in air at diffusion equilibrium, S: surface of explosive exposed to air, r: attenuation factor (10^{-4})

The attenuation factor r has been established in the study by *Dravnicks et al.* [35] For a surface of 200 cm² the following values for c_{dif} can be obtained: TATP **1**: 3.1 ng L^{-1}, DADP **2**: 10 ng L^{-1}. These values must be regarded as the maximum concentrations of explosive that can be present for detection since further diffusion barriers like foil wrapped around the explosive are highly probable. c_{dif} is directly proportional to the exposed surface of the explosive (Equation 20) and was calculated in this work for an exemplary surface of 200 cm².

Using the Ideal gas equation the saturation concentration of an explosive can be calculated:

$$c_{sat} = \frac{p_{sat} \times M}{R \times T} \quad (21)$$

c_{sat}: saturation concentration [mg L^{-1}], R: ideal gas constant (8.314 J mol^{-1} K^{-1}), T: temperature [K]

For TATP a value of 600 µg L^{-1} and for DADP a value of 1589 µg L^{-1} can be calculated using the vapor pressures stated in Table 6. This indicates that the diffusion phenomenon discussed lowers the gas phase concentration of the explosive by about five orders of magnitude (10^5).

Conclusions

TATP **1** and its sideproduct DADP **2** have been demonstrated to be medium performance explosives that are easily accessible from freely available chemicals. Whilst for DADP **2** the p-T-values obtained in this work are in agreement with literature values the p-T-values obtained for TATP **1** are not in agreement with literature values. This might be due to the rich polymorphism of TATP **1** elucidated by *Reany et al.* [11]. It would be recommendable to carry out future vapor pressure measurements of **1** with the synthetic procedure detailed in this work for the reason of comparability. The saturation equilibrium concentrations of TATP **1** (600 µg L^{-1}) and DADP **2** (1589 µg L^{-1}) are about five magnitudes higher than at the diffusion equilibrium state (**1**: 31 ng L^{-1}, **2**: 100 ng L^{-1}). The latter concentrations correspond to a ppt-concentration level and are valuable for the conception of gas phase detection devices.

Experimental:

All reagents and solvents were used as received (Sigma-Aldrich, Fluka, Acros Organics, ACBR). NMR spectra were measured with a *JEOL* ECX-400 and a *Bruker* AVANCE 400 MHz NMR instrument. The chemical shift of the solvent peaks were adjusted according to literature values [38]. Infrared spectra were measured with a *Perkin-Elmer* FT-IR Spektrum BXII instrument equipped with a Smith Dura SampIIR II ATR unit. Transmittance values are described as “strong” (s), “medium” (m), and “weak” (w). Raman spectra were recorded on a *Bruker RAM II* device (1064 nm, 300 mW). Relative peak intensities are given in brackets. Elemental analyses (EA) were performed with a *Netsch* STA 429 simultaneous thermal analyzer. Sensitivity data were determined using a BAM drophammer and a BAM friction tester. The electrostatic sensitivity tests were carried out using an Electric Spark Tester ESD 2010 EN (*OZM Research*) operating with the “Winspark 1.15” software package. The particle sizes stated are valid for all sensitivity measurements. Melting points were measured with a *Buechi B-540* melting point apparatus using a heating rate of 5 °C min^{-1}. For the powder diffraction experiment on TATP **1** the analytes was filled into a 0.5 mm Lindemann capillary. The material was then investigated on a Huber G644 Guinier diffractometer with the angle calibrated using electronic grade germanium (a = 5.6575 Å). Measurements with $MoK_{\alpha 1}$ radition were made over the 2θ range 2 - 12 ° with an increment of 0.02 ° and a counting time of 20 seconds per increment at 25 °C.

*CAUTION! TATP **1** and DADP **2** are energetic materials with sensitivity to various stimuli. While we encountered no issues in the handling of these materials, proper protective measures (face shield, ear protection, body armor, Kevlar gloves, and earthened equipment) should be used during the handling of both compounds at all times including vapor pressure measurements.*

TATP **1**: 3.14 mL 50% aqueous H_2O_2 solution (3.76 g, 0.11 mol) and 0.86 mL conc. H_2SO_4 (1.58 g, 0.016 mol) are mixed and cooled to 0 °C. 4.90 mL acetone (3.87 g, 0.07 mol) are added dropwise. After stirring the mixture at 0 °C for 3 h, it is extracted with 70 mL pentane. The pentane mixture is washed two times with 20 mL saturated ammonium sulfate solution and afterwards three times with 20 mL of water. The organic phase is dried over magnesium sulfate. After evaporation of the solvent a colorless solid is isolated. (2.07 g, 40%) [9]

^{1}H NMR ($CDCl_3$, 400 MHz, 300 K): **δ=** 1.45 (18 H). **^{13}C NMR** ($CDCl_3$, 100 MHz, 300 K): **δ=** 21.5 (*CH_3*), 107.7 (*C*). **IR (ATR)**: $\tilde{\nu}$ (cm^{-1}) =3005 (w), 2945 (w), 1600 (w), 1461 (w), 1376 (m), 1361 (m), 1274 (w), 1232 (m), 1200 (m), 1178 (s), 997 (w), 945 (m), 937 (m), 884 (s), 842 (m), 784 (m), 615 (m). **Raman** (1064 nm) $\tilde{\nu}$ (cm^{-1}) = 3012 (55), 3001 (54), 2948 (100), 10450 (30), 1372 (5), 1338 (6), 962 (48), 913 (50), 864 (60), 856 (48), 653 (7), 555 (61), 452 (28), 434 (30), 412 (28), 380 (8). **EA** found (calcd.): C 48.73 (48.63), H: 8.26 (8.18). **IS**: 1.5 J, **FS**: <5 N, **ESD**: 0.2 J (<100 µm).

DADP **2**: 10 mL dichloromethane are cooled in an ice bath. 2.00 mL acetone (1.58 g, 0.03 mol) and 4.00 mL 30% aqueous H_2O_2 solution (4.44 g, 0.04 mol) are added. 4.00 mL concentrated perchloric acid (7.08 g, 0.07 mol) are added drop wisely and the mixture was stirred at 0 °C for 1 h. Afterwards the mixture is stored for three days at room temperature to allow complete conversion of TATP to DADP. The formed colorless precipitate is filtered off, washed with water and recrystallized from methanol. (0.23 g, 10%). [10]

^{1}H NMR ($CDCl_3$, 400 MHz, 300 K): **δ=** 1.35 (s, 6H), 1.79 (s, 6H). **^{13}C NMR** ($CDCl_3$, 100 MHz, 300 K): **δ=** 20.7 (*CH_3*), 22.5 (*CH_3*), 107.7 (*C*). **IR (ATR)**: $\tilde{\nu}$ (cm^{-1}) = 3031 (w), 3000 (w), 2955 (w), 1603 (w), 1452 (w), 1374 (m), 1367 (m), 1284 (w), 1268 (m), 1198 (s), 1006 (w), 943 (m), 930 (m), 858 (m), 839 (w), 814 (m), 686 (m). **Raman** (1064 nm) $\tilde{\nu}$ (cm^{-1}) =3053 (25), 3004 (100), 2980 (62), 1450 (18), 1417 (21), 1260 (17), 940 (23), 917 (19), 863 (64), 720 (65), 512 (8), 501 (58), 491 (22), 452 (10), 447 (9), 428 (17), 382 (53). **EA** found (calcd.): C 48.24 (48.63), H: 8.13 (8.18), **IS**: 5 J, **FS**: 5 N, **ESD**: 0.2 J (<100 µm).

Acknowledgements

Financial support of this work by the Ludwig-Maximilian University of Munich (LMU), the Office of Naval Research (ONR) under grant no. ONR.N00014-16-1-2062, and the Bundeswehr –

Wehrtechnische Dienststelle für Waffen und Munition (WTD 91) under grant no. E/E91S/FC015/CF049 and the German Ministry of Education and Research (BMBF) under grant no. 13N12583 is gratefully acknowledged. The authors acknowledge collaborations with Dr. Mila Krupka (OZM Research, Czech Republic) in the development of new testing and evaluation methods for energetic materials and with Dr. Muhamed Suceska (Brodarski Institute, Croatia) in the development of new computational codes to predict the detonation and propulsion parameters of novel explosives. We are indebted to and thank Drs. Betsy M. Rice, Jesse Sabatini and Brad Forch (ARL, Aberdeen, Proving Ground, MD) for many inspired discussions.

[1] R. Wolffenstein, Ueber die Einwirkung von Wasserstoffsuperoxyd auf Aceton und Mesityloxyd, *Ber. Dtsch. Chem. Ges.* **1895**, 28, 2265-2269.

[2] http://news.nationalpost.com/news/world/german-police-seize-bomb-firearm-in-raid-that-foiled-imminent-boston-marathon-style-terror-attack

[3] http://www.nydailynews.com/news/world/paris-suicide-bombers-tatp-homemade-explosive-article-1.2435082.

[4] http://www.n-tv.de/panorama/17-Jaehriger-hortete-Sprengstoff-article334469.html

[5] [5a] J. C. Oxley, J. L. Smith, L. Steinkamp, G. Zhang, Factors Influencing Triacetone Triperoxide (TATP) and Diacetone Diperoxide (DADP) Formation: Part 2, *Propellants, Explos., Pyrotech.* **2013**, 38, 841-851; bJ. C. Oxley, J. L. Smith, P. R. Bowden, R. C. Rettinger, Factors Influencing Triacetone Triperoxide (TATP) and Diacetone Diperoxide (DADP) Formation: Part I, *Propellants, Explos., Pyrotech.* **2013**, 38, 244-254.

[6] J. C. Oxley, J. L. Smith, J. E. Brady, L. Steinkamp, Factors Influencing Destruction of Triacetone Triperoxide (TATP), *Propellants, Explos., Pyrotech.* **2014**, 39, 289-298.

[7] D. Lubczyk, A. Hahma, M. Brutschy, C. Siering, S. R. Waldvogel, A New Reference Material and Safe Sampling of Terrorists Peroxide Explosives by a Non-Volatile Matrix, *Propellants, Explos., Pyrotech.* **2015**, 40, 590-594.

[8] [8a] R.-M. Räsänen, M. Nousiainen, K. Peräkorpi, M. Sillanpää, L. Polari, O. Anttalainen, M. Utriainen, Determination of gas phase triacetone triperoxide with aspiration ion mobility spectrometry and gas chromatography–mass spectrometry, *Anal. Chim. Acta* **2008**, 623, 59-65; [8b] J. L. Anderson, A. A. Cantu, A. W. Chow, P. S. Fussell, R. G. Nuzzo, J. E. Parmeter, G. S. Sayler, J. n. M. Shreeve, R. E. Slusher, M. Story, W. Trogler, V. Venkatasubramaniam, L. A. Waller, J. Young, C. F. Zukoski, Existing and Potential Standoff Explosives Detection Techniques, National Academies Press, Washington, DC, **2004**; [8c] C. L. Rhykerd, D. W. Hannum, D. W. Murray, J. E. Parmeter, Guide for the Selection of Commercial Explosives Detection Systems for Law Enforcement Applications, National Institute of Justice Office of Science and Technology, Washington, DC, **1999**; [8d] J. Cabalo, R. Sausa, Trace detection of explosives with low vapor emissions by laser surface photofragmentation–fragment detection spectroscopy with an improved ionization probe*, Appl. Opt.* **2005**, 44, 1084-1091; [8e] J. I. Steinfeld, J. Wormhoudt, Explosives Detection: A Challenge for Physical Chemistry, *Ann. Rev. Phys. Chem.* **1998**, 49, 203-232; [8f] G. Bunte, J. Hürttlen, H. Pontius, K. Hartlieb, H. Krause, Gas phase detection of explosives such as 2,4,6-trinitrotoluene by molecularly imprinted polymers, *Anal. Chim. Acta* **2007**, 591, 49-56; [8g] http://www.sedet.com/Technology.html

[9] N. A. Milas, A. Golubovic, Studies in Organic Peroxides. XXVI. Organic Peroxides Derived from Acetone and Hydrogen Peroxide, *J. Am. Chem. Soc.* **1959**, 81, 6461-6462.

[10] K. B. Landenberger, O. Bolton, A. J. Matzger, ., Two Isostructural Explosive Cocrystals with Significantly Different Thermodynamic Stabilities, *Angew. Chem., Int. Ed.* **2013**, 52, 6468-6471.

[11] O. Reany, M. Kapon, M. Botoshansky, E. Keinan, Rich Polymorphism in Triacetone-Triperoxide, *Cryst. Growth Des.* **2009**, 9, 3661-3670.

[12] C. R. Groom, I. J. Bruno, M. P. Lightfoot, S. C. Ward, The Cambridge Structural Database, *Acta Crystallogr., Sect. B: Struct. Sci., Cryst. Eng. Mater.* **2016**, 72, 171-179.

[13] Impact: Insensitive > 40 J, less sensitive ≥ 35 J, sensitive ≥ 4 J, very sensitive ≤ 3 J; Friction: Insensitive > 360 N, less sensitive = 360 N, sensitive < 360 N and > 80 N, very sensitive ≤ 80 N, extremely sensitive ≤ 10 N. According to the UN Recommendations on the Transport of Dangerous Goods.

[14] M. J. Frisch, G. W. Trucks, H. B. Schlegel, G. E. Scuseria, M. A. Robb, J. R. Cheeseman, G. Scalmani, V. Barone, B. Mennucci, G. A. Petersson, H. Nakatsuji, M. Caricato, X. Li, H. P. Hratchian, A. F. Izmaylov, J. Bloino, G. Zheng, J. L. Sonnenberg, M. Hada, M. Ehara, K. Toyota, R. Fukuda, J. Hasegawa, M. Ishida, T. Nakajima, Y. Honda, O. Kitao, H. Nakai, T. Vreven, J. A. Montgomery Jr., J. E. Peralta, F. Ogliaro, M. J. Bearpark, J. Heyd, E. N. Brothers, K. N. Kudin, V. N. Staroverov, R. Kobayashi, J. Normand, K. Raghavachari, A. P. Rendell, J. C. Burant, S. S. Iyengar, J. Tomasi, M. Cossi, N. Rega, N. J. Millam, M. Klene, J. E. Knox, J. B. Cross, V. Bakken, C. Adamo, J. Jaramillo, R. Gomperts, R. E. Stratmann, O. Yazyev, A. J. Austin, R. Cammi, C. Pomelli, J. W. Ochterski, R. L. Martin, K. Morokuma, V. G. Zakrzewski, G. A. Voth, P. Salvador, J. J. Dannenberg, S. Dapprich, A. D. Daniels, Ö. Farkas, J. B. Foresman, J. V. Ortiz, J. Cioslowski, D. J. Fox, Gaussian, Inc., Wallingford, CT, USA, **2009**.

[15] F. Dubnikova, R. Kosloff, J. Almog, Y. Zeiri, R. Boese, H. Itzhaky, A. Alt, E. Keinan, Decomposition of Triacetone Triperoxide Is an Entropic Explosion, *J. Am. Chem. Soc.* **2005**, 127, 1146-1159.

[16] F. G. Gelalcha, B. Schulze, P. Lonnecke, ., 3,3,6,6-Tetramethyl-1,2,4,5-tetroxane: a twinned crystal structure, *Acta Crystallogr., Sect. C: Struct. Chem.* **2004**, 60, o180-o182.

[17] J. de Zeeuw, S. Reese, J. Cochran, S. Grossman, T. Kane, C. English, Simplifying the setup for vacuum-outlet GC: Using a restriction inside the injection port, *J. Sep. Sci.* **2009**, 32, 1849-1857.

[18] N. Haroune, A. Crowson, B. Campbell, Characterisation of triacetone triperoxide (TATP) conformers using LC-NMR, *Sci. Justice* **2011**, 51, 50-56.

[19] C. Denekamp, L. Gottlieb, T. Tamiri, A. Tsoglin, R. Shilav, M. Kapon, Two Separable Conformers of TATP and Analogues Exist at Room Temperature, *Org. Lett.* **2005**, 7, 2461-2464.

[20] [20a] V. N. Emel'yanenko, S. P. Verevkin, Benchmark thermodynamic properties of 1,3-propanediol: Comprehensive experimental and theoretical study, *J. Chem. Thermodyn.* **2015**, 85, 111-119; [20b] S. P. Verevkin, A. Y. Sazonova, V. N. Emel'yanenko, D. H. Zaitsau, M. A. Varfolomeev, B. N. Solomonov, K. V. Zherikova, Thermochemistry of Halogen-Substituted Methylbenzenes, *J. Chem. Eng. Data* **2015**, 60, 89-103; [20c] S. P. Verevkin, Experimental Thermodynamics, Volume 7 (Eds.: R. D. Weir, T. W. D. Loos), Elsevier, **2005**, pp. 5-30.

[21] E. C. W. Clarke, D. N. Glew, Evaluation of thermodynamic functions from equilibrium constants, *Trans. Faraday Soc.* **1966**, 62, 539-547.

[22] R. Pilar, J. Pachman, R. Matyáš, P. Honcová, D. Honc, Comparison of heat capacity of solid explosives by DSC and group contribution methods, *J. Therm. Anal. Calorim.* **2015**, 121, 683-689.

[23] J. E. Hurst, B. Keith Harrison, Estimation of Liquid and Solid Heat Capacities Using a Modified Kopps' Rule, *Chem. Eng. Commun.* **1992**, 112, 21-30.

[24] W. Acree, J. S. Chickos, Phase Transition Enthalpy Measurementsof Organic and Organometallic Compounds. Sublimation, Vaporizationand Fusion Enthalpies From 1880 to 2010, *J. Phys. Chem. Ref. Data* **2010**, 39, 043101.

[25] J. Mbah, D. Knott, S. Steward, D. Cornett, Vapor Pressure and Sublimation Enthalpy of Triacetone Triperoxide by a Gas Chromatography Headspace Approach, *Int. J. Energ. Mater. Chem. Propul.* **2015**, 14, 321-329.

[26] J. C. Oxley, J. L. Smith, W. Luo, J. Brady, Determining the Vapor Pressures of Diacetone Diperoxide (DADP) and Hexamethylene Triperoxide Diamine (HMTD), *Propellants, Explos., Pyrotech.* **2009**, 34, 539-543.

[27] J. Mbah, D. Knott, S. Steward, Thermogravimetric study of vapor pressure of TATP synthesized without recrystallization, *Talanta* **2014**, 129, 586-593.

[28] J. Oxley, J. L. Smith, J. Brady, S. Naik, Determination of Urea Nitrate and Guanidine Nitrate Vapor Pressures by Isothermal Thermogravimetry, *Propellants, Explos., Pyrotech.* **2010**, 35, 278-283.

[29] M. L. Ramírez, L. C. Pacheco-Londoño, Á. J. Peña, S. P. Hernández-Rivera, *Characterization of peroxide-based explosives by thermal analysis, Proc. SPIE*, **2006**, 6201, 62012B1-62012B10.

[30] V. Y. Egorshev, V. P. Sinditskii, S. P. Smirnov, A comparative study on two explosive acetone peroxides, *Thermochim. Acta* **2013**, 574, 154-161.

[31] P. L. Damour, A. Freedman, J. Wormhoudt, Knudsen Effusion Measurement of Organic Peroxide Vapor Pressures, *Propellants, Explos., Pyrotech.* **2010**, 35, 514-520.

[32] I. Dunayevskiy, A. Tsekoun, M. Prasanna, R. Go, C. K. N. Patel, High-sensitivity detection of triacetone triperoxide (TATP) and its precursor acetone, *Appl. Opt.* **2007**, 46, 6397-6404.

[33] J. C. Oxley, J. L. Smith, K. Shinde, J. Moran, Determination of the Vapor Density of Triacetone Triperoxide (TATP) Using a Gas Chromatography Headspace Technique, *Propellants, Explos., Pyrotech.* **2005**, 30, 127-130.

[34] J. E. Brady, J. L. Smith, C. E. Hart, J. Oxley, ., Estimating Ambient Vapor Pressures of Low Volatility Explosives by Rising-Temperature Thermogravimetry, *Propellants, Explos., Pyrotech.* **2012**, 37, 215-222.

[35] H. Félix-Rivera, M. L. Ramírez-Cedeño, R. A. Sánchez-Cuprill, S. P. Hernández-Rivera, Triacetone triperoxide thermogravimetric study of vapor pressure and enthalpy of sublimation in 303–338 K temperature range, *Thermochim. Acta* **2011**, 514, 37-43.

[36] A. Dravnicks, R. Brabets, T. A. Stanley, Evaluating Sensitivity Requirements of Explosive Vapor Detector Systems, IIT Research Institute Technology Center, Chicago Illinois, **1972**.

[37] R. B. Bird, W. E. Stewart, E. N. Lightfoot, Transport Phenomena, Second Edition, John Wiley & Sons, Inc., New Jork, **2002**.

[38] C. Xue, J. Sun, B. Kang, Y. Liu, X. Liu, G. Song, Q. Xue, ., The β-δ-Phase Transition and Thermal Expansion of Octahydro-1,3,5,7-Tetranitro-1,3,5,7-Tetrazocine, *Propellants, Explos., Pyrotech.* **2010**, 35, 333-338.

[39] G. R. Fulmer, A. J. M. Miller, N. H. Sherden, H. E. Gottlieb, A. Nudelman, B. M. Stoltz, J. E. Bercaw, K. I. Goldberg, NMR Chemical Shifts of Trace Impurities: Common Laboratory Solvents, Organics, and Gases in Deuterated Solvents Relevant to the Organometallic Chemist, *Organometallics* **2010**, 29, 2176-2179.